

UC Santa Barbara

UC Santa Barbara Electronic Theses and Dissertations

Title

Transition Metal Catalyzed Cross-Couplings in Water

Permalink

<https://escholarship.org/uc/item/3df4n443>

Author

Hu, Yuting

Publication Date

2024

Peer reviewed|Thesis/dissertation

UNIVERSITY OF CALIFORNIA

Santa Barbara

Transition Metal Catalyzed Cross-Couplings in Water

A dissertation submitted in partial satisfaction of the
requirements for the degree Doctor of Philosophy
in Chemistry

by

Yuting Hu

Committee in charge:

Professor Bruce Lipshutz, Chair

Professor Liming Zhang

Professor Yang Yang

Professor Vojtech Vlcek

March 2024

The dissertation of Yuting Hu is approved.

Liming Zhang

Yang Yang

Vojtech Vlcek

Bruce Lipshutz, Committee Chair

December 2023

Transition Metal Catalyzed Cross-Couplings in Water

Copyright © 2023

by

Yuting Hu

ACKNOWLEDGEMENTS

Firstly, I want to give my sincere acknowledgement to Professor Bruce Lipshutz. In research, he is a wise professor with deep understanding of both organic chemistry and green chemistry. He has a passion and enthusiasm to chemistry research, and he is dedicated to evaluating the organic chemistry to a greener way. With those characters, he not only guides me through my Ph.D. studies from a naïve undergraduate student, but also sets up a model for my future research. Beyond research, he is the most supportive professor I could image. He genuinely cares about his students, making efforts to guide us towards becoming professional Ph.D. student and helping us lead easier lives. As an international student, I encountered a lot of problems about visa, culture, and languages. I could not have completed my Ph.D. program without his support. I still remember the times when he interviewed me, when he introduced the research to me, when he emailed me about his crazy idea, and when we argued about chemistry in his office. Now I am ready to defense my degree in two weeks. I want to say, thank you, Bruce. You are the greatest professor.

I would also like to express my warm acknowledge to my parents. Although they wish me to stay closer to home, they have wholeheartedly supported my decision to study abroad in the U.S. Their unconditional love has been a constant in my life, regardless of my location or the achievements I have attained. I deeply appreciate their understanding and miss them.

Moreover, I would like to thank Xiaohan Li, who joined our group a year after me. Our labs are adjacent, and as fellow night workers, we have spent countless hours together. Over the past five years, we have supported each other through hard times, helped each other out of troubles, and inspired one another to become better people. Interestingly, although we are

from the same university, we never met until we arrived at UCSB. It is my luck to meet you here. Fortunately, we got the chance to work in the same company, as we planned. I am grateful for the opportunity to continue our journey together in the future.

Furthermore, I would like to thank all the great members of the Lipshutz group. This is the most friendly and warm place to be. As an international student, it feels like my second home. Haobo Pang, my mentor in the group, has a rigorous and innovative scientific attitude. I learned the nanoparticle technology from him, modified it to a more general version, and passed it along. Joseph, Vani, and Julie, as my peers in the group, all are great scientists. We started the same time from taking classes five years ago to industrial jobs now. Bala and Ruchi, as my co-workers and mentors in the TPG-lite project, gave me lots of suggestions and taught me techniques. Maddy, as my co-worker in the Negishi project, is always smart and cheerful. Thanks for bringing joy and happiness to the group. Juan, as my co-worker in the BMGF project, is a reliable and productive teammate. Thank you and Cristina for hosting the thanksgiving parties. It is warm to spend the night with everyone. Karthik, as my co-worker in the amination project, is an ambitious and excellent scientist. Katie, thanks for sharing another lifestyle to us and being kindhearted. Rohan is both professional and outgoing at the same time, thanks for the joy and suggestions. Please keep the enzymatic presentation shorter or make more bread... I want to thank Dr. Ruhel Kavthe. He is super productive with numerous experiences. Thanks for your suggestions in research and support in job searching. I also want to give my special thanks to Dr. Yuzo Abe. He is a genius chemist. We spent seven months together and shared the same room. Thanks for sharing thoughts about research and inspire me to become a process chemist. Erfan, Chandler, and John Micheal, thank you all for the advice and fun times.

Lastly, I would like to thank the past members and incoming members of the group. And all my friends here at UCSB. And all my friends in the Ice in Paradise rink. Rose, Mirka, Katie, Coleen, Greg, Karla, Ildi, Kestrel, Sam, Sabina, and Lindsay, thank you guys so much for the most fun time on ice. And my coaches, Frank, Nadia, Breanne, Summer, and Ashley. Thank you for the patient instruction. I agree with you Ashley, skating is sometimes extremely hard for Ph.D., because we overthink. But I will continue skating for the rest of my life. Thank you everyone for your help and for the great time we shared!

VITA OF YUTING HU
September 2023

EDUCATION

Bachelor of Science, Nankai University, June 2018

Doctor of Philosophy in Organic Chemistry, University of California, Santa Barbara,
November, 2023 (expected)

PROFESSIONAL EMPLOYMENT

2018-2023: Teaching Assistant, Department of Chemistry and Biochemistry, University of
California, Santa Barbara

PUBLICATIONS

- 1 Zhang X.; Lu G.; Sun M.; Mahankali M.; Ma Y.; Zhang M.; Hua W.; **Hu Y.**; Wang Q.; Chen J.; He G.; Qi X.; Shen W.; Liu P. and Chen G. A General Strategy for Synthesis of Cyclophane- Braced Peptide Macrocycles via Palladium-Catalyzed Intramolecular sp³ C-H Arylation. *Nat. Chem.* **2018**, *10*, 540-548.
- 2 Thakore, R. R.; Takale, B. S.; **Hu, Y.**; Kostal, J.; Gallou, F.; Lipshutz, B. H. “TPG-lite”: a new, simplified “designer” surfactant for general use in synthesis under micellar catalysis conditions in recyclable water. *Tetrahedron* **2021**, *87*, 132090.
- 3 Pang, H.; **Hu, Y.**; Yu, J.; Gallou, F.; Lipshutz, B. H. Water-Sculpting of a Heterogeneous Nanoparticle Pre-catalyst for Mizoroki-Heck Couplings Under Aqueous Micellar Catalysis Conditions. *J. Am. Chem. Soc.* **2021**, *143*, 3373.
- 4 **Hu, Y.**; Wong, M. J.; Lipshutz, B. H. ppm Pd-Containing Nanoparticles as Catalysts for Negishi Couplings. . . in Water. *Angew. Chem., Int. Ed.* **2022**, *61*, e202209784.
- 5 **Hu, Y.**; Li, X.; Jin, G.; and Lipshutz, B. H. Simplified Preparation of ppm Pd-Containing Nanoparticles as Catalysts for Chemistry in Water. *ACS Catal.* **2023**, *13*, 3179.
- 6 Li, X.; **Hu, Y.**; Bailey, D. J.; and Lipshutz, B. H. Impact of Nonionic Surfactants on Reactions of IREDS. Applications to One-Pot Chemoenzymatic Sequences in Water. *Org. Lett.* asap DOI: 10.1021/acs.orglett.3c02790
- 7 Iyer, K.; Kavthe R.; **Hu. Y.**; and Lipshutz, B. H. Nanoparticles as heterogeneous catalysts for ppm Pd-catalyzed aminations in water. in revision.
- 8 Caravez, J. C.; **Hu. Y.**; Oftadeh, E.; Mamo, K. T.; and Lipshutz, B. H. Preparation of a key intermediate en route to the anti-HIV drug lenacapavir. Submitted

ABSTRACT

Fe/ppm Pd Nanoparticle as an Effective Catalytic System for Cross-Couplings in Water

by

Yuting Hu

I. A greener and sustainable technology for Negishi coupling reactions in water is reported. This work demonstrates the efficacy of palladium-containing nanoparticles (NPs) with low palladium loadings, typically ca. 2500 ppm (0.25 mol %), as robust catalysts that operate in water under remarkably mild conditions. The water serves not only as a green reaction medium but is also recyclable, further reinforcing the green aspects of this methodology. A broad substrate scope of highly functionalized aromatic and heteroaromatic bromides, including select examples from the Merck Informer Library, readily underwent coupling, thereby underscoring the excellent functional group tolerance associated with this approach. Furthermore, residual palladium levels in the resulting products are found to be particularly low, as confirmed by Inductively Coupled Plasma Mass Spectrometry (ICP-MS). Comprehensive characterization of these catalytically active nanoparticles has been carried out using techniques such as Dynamic Light Scattering (DLS), Transmission Electron Microscopy (TEM), cryogenic-TEM (cryo-TEM), and Energy-Dispersive X-ray Spectroscopy (EDX).

II. An optimized methodology had been developed that not only streamlines the preparation of nanoparticles (NPs) featuring ppm levels of palladium loading but also ensures reliable outcomes in cross-coupling reactions due to the utilization of freshly added ligand and palladium catalyst. The scope of this research encompasses four types of coupling reactions: Suzuki–Miyaura, Sonogashira, Mizoroki–Heck, and Negishi, all executed under aqueous micellar conditions. The novelty of this approach lies in the initial generation of storable, shelf-stable nanoparticles that, without either palladium or ligand can be subsequently converted to active NPs. This conversion involves the simple addition of precise quantities of palladium salt and the corresponding ligand, tailored to catalyze the specific type of coupling reaction being targeted, all in an aqueous medium.

III. Ketones plays an important role in the field of organic chemistry. They are present in various molecules like pharmaceuticals, fragrances, and polymers. Moreover, they serve as precursors in synthesizing heterocycles and natural products. Traditional ketone synthesis methods, such as oxidation of alcohols or Friedel-Crafts acylation, have limitations like low regioselectivity and environmental concerns. The Fukuyama reaction, noted for its chemoselectivity and mild conditions, still faces challenges like the need for intermediate thioester synthesis, organozinc reagent synthesis and the use of odorous ethanethiol. Our group developed a new reagent, dipyridyldithiocarbonate (DPDTC), for converting carboxylic acids into thioesters, offering odorless alternatives. We also pioneered a Negishi reaction in water using organozinc reagents, overcoming their typical sensitivity to water. This development paves the way for a more sustainable, efficient Fukuyama reaction approach.

TABLE OF CONTENTS

1. ppm Pd-Containing Nanoparticles as Catalysts for Negishi Couplings... in Water	1
1.1 Background Introduction.....	2
1.2 Results and discussion.....	13
Optimization of the synthesis of nanoparticles (NPs).....	13
Optimization of reaction conditions.....	17
Characterization of the nanoparticles.....	19
Substrate scope in Negishi reactions.....	25
Gram scale reaction.....	30
Recycle study.....	30
Residual metal analysis.....	32
Direct comparisons with literature.....	34
E Factor evaluation.....	35
One-pot Synthetic sequence.....	36
Conclusion.....	38
Reference.....	39
1.3 Appendix.....	46
General Information.....	46
Optimization of the preparation of Fe/ppm Pd NPs.....	48
Optimization of reagents addition sequence.....	52
Optimization of surfactants.....	54
Titration of MeMgCl in THF solution with LiCl/I ₂	55

Final Optimized Procedure for the Preparation of Fe/ppm Pd Nanoparticles	56
General procedure for Negishi coupling reactions	57
Analyses of nanoparticles (NPs).....	58
E Factor evaluation	64
Residual metal as measured by ICP-MS	65
Recycle study.....	68
Gram scale reaction	71
1-Pot sequence of reactions	72
Analytical data.....	74
References.....	101
NMR spectra.....	103
2. Simplified Preparation of ppm Pd-Containing Nanoparticles as Heterogeneous Catalysts for Chemistry in Water	138
2.1 Background Introduction.....	139
2.2 Results and discussion	154
Optimization of reaction conditions and use in synthesis	154
Substrate scope	159
Characterization of the nanoparticles	165
Direct comparison between new and original procedure	166
Application of air-stable ferrocene-based ligand in NPs catalysis	167
E Factor evaluation	169
Gram-scale reaction	169
Recycle study.....	170

One-pot reaction sequence.....	171
Other reactions tested	173
Conclusion.....	174
References.....	175
2.3 Appendix.....	181
General Information.....	181
Procedures to synthesize different NPs	183
Optimization on ferrocene-based ligands on four different reactions	185
Titration of MeMgCl in THF with LiCl/I ₂	186
General procedure for Suzuki-Miyaura coupling reactions.....	187
General procedure for Sonogashira coupling reactions.....	187
General procedure for Mizoroki-Heck coupling reactions	188
General procedure for Negishi coupling reactions	189
STEM-EDS images for new Fe NPs with SPhos in 2 wt % TPGS-750-M/H ₂ O solution	189
STEM-EDS images for original NPs with SPhos in 2 wt % TPGS-750-M/H ₂ O solution	192
E Factor evaluation	194
Gram Scale Reaction	195
Recycling reactions.....	196
One-pot sequence of reactions.....	199
Analytical data.....	201
References.....	226

NMR spectra.....	228
3. Efforts towards using Dipyridyldithiocarbonate (DPDTC) as an Environmentally Responsible Reagent for Ketone Synthesis via Fukuyama Reactions in Water.....	265
3.1 Background Introduction.....	266
3.2 Results and discussion.....	277
DPDTC synthesis and purification.....	277
Thioester formation.....	279
Optimization of Fukuyama reaction conditions.....	281
Substrate scope.....	284
One-pot reaction test.....	286
Conclusion.....	286
References.....	287
3.3 Appendix.....	291
General Information.....	291
DPDTC synthesis and purification.....	292
Thioester formation.....	293
Fukuyama reaction optimization.....	294
General procedure for the Fukuyama reaction.....	295
Analytical data.....	295
NMR spectra.....	306

1. ppm Pd-Containing Nanoparticles as Catalysts for Negishi Couplings... in Water

Reproduced with permission from
Hu, Y.; Wong, M. J.; Lipshutz, B. H. ppm Pd-Containing Nanoparticles as Catalysts for
Negishi Couplings... in Water. *Angew. Chem., Int. Ed.*, **2022**, e202209784
Copyright 2022 Wiley-VCH

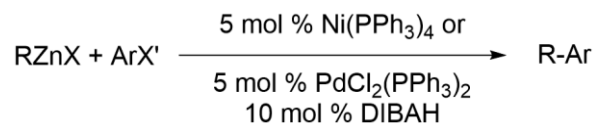
1.1 Background Introduction

Palladium-catalyzed cross-coupling reactions between aromatic halides or pseudohalides and organometallic compounds have found extensive applications across a range of industries, including pharmaceuticals, fine chemicals, agrochemicals, dyes, and polymers.^{1,2,3} The Negishi reaction, involving the coupling of aromatic halides or pseudohalides with organozinc reagents, stands out for its rapid transmetalation rates⁴ and excellent functional group tolerance.^{5,6} Furthermore, the Negishi reaction's capacity to build carbon-carbon bonds between sp^2 and sp^3 carbons enhances its importance in pharmaceutical chemistry.⁷ The introduction of sp^3 carbons is particularly valuable as it imparts lipophilicity, rotational bonds, and offers the potential for chiral centers, all of which are crucial for the potency of drug candidates.⁸ In contrast, Suzuki reactions involving alkyl boranes often show reduced reactivity due to undesirable side reactions, such as deboration and β -hydride elimination.⁹ Similarly, the Kumada reaction is usually constrained by the inherent basicity of Grignard reagents, limiting its functional group tolerance. Applications of Stille reactions, on the other hand, are limited due to the toxicity of organostannane compounds, causing a significant environmental and health risk.¹⁰

In 1977, Eiichi Negishi first reported the cross-coupling reaction between organozinc reagents and halides, marking a pivotal development in organic chemistry (Scheme 1).¹¹ Prior to this breakthrough, Negishi and his team focused on cross-coupling reactions using organoaluminium reagents and halides. The research direction shifted towards organozinc reagents to improve reactivity and enhance chemoselectivity, regioselectivity, and stereoselectivity. THF was selected as the solvent for these experiments, conducted at room

temperature. Subsequent studies and advancements have continually refined the Negishi reaction, leading to the optimized reaction conditions that are widely employed in today.

Scheme 1. Eiichi Negishi's first Negishi reaction



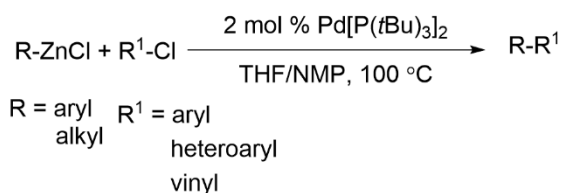
Since the 1990s, there has been a significant push to develop palladium-based catalytic systems for cross-coupling reactions. While a variety of methods have been established for classic coupling processes such as Suzuki, Heck, and Stille reactions, it wasn't until 2001 that Gregory C. Fu's group introduced the first general protocol for Negishi cross-coupling of inactive and deactivated aryl chlorides.¹² This method utilized the electron rich complex Pd[P(*t*Bu)₃]₂ as the precatalyst. Employing standard conditions—2 mol % Pd[P(*t*Bu)₃]₂ in THF at 100 °C—this approach enabled the synthesis of a range of sterically hindered biaryls with excellent yields. The catalyst system, often referred to as the 'Fu catalyst', has demonstrated exceptional efficacy in Negishi reactions and other palladium-catalyzed processes.

In 2005, Fu's group reported the use of nickel and Pybox ligands in catalyzing asymmetric Negishi cross-couplings of secondary α -bromo amides with organozinc reagents.¹³ These Ni/(*i*-Pr)-Pybox-catalyzed reactions exhibited a high tolerance for various functional groups and generally yielded products with both high enantiomeric excess and good overall yield. Building on this foundational work, Fu's team subsequently expanded the application of the asymmetric Negishi reaction to include alkylation of secondary propargylic electrophiles, secondary allylic chlorides, secondary benzylic halides, α -

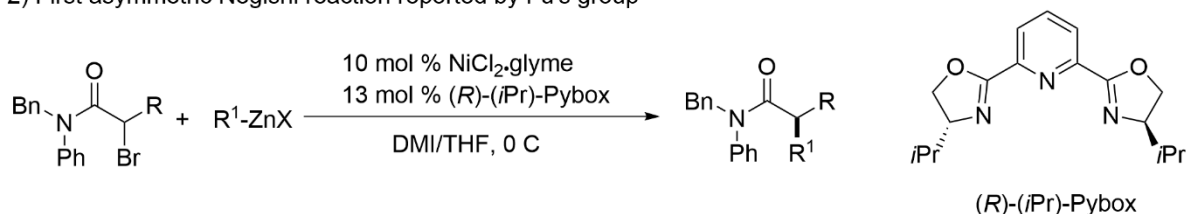
bromonitriles, *N*-Boc-pyrrolidine, and further extended it to arylations of secondary benzylic electrophiles and CF₃ alkyls. Although in 2014, Fu's group suggested that these nickel-catalyzed reactions might proceed via a radical mechanism, instead of only traditional Negishi reaction pathway,¹⁴ the asymmetric Negishi reaction still is a pivotal benchmark in the field of asymmetric cross-coupling reactions. It also inspires ongoing advancements in the development of cross-electrophile couplings.

Scheme 2. Fu catalyst used in Negishi reaction of aryl chlorides.

1) First general condition for Negishi reaction



2) First asymmetric Negishi reaction reported by Fu's group

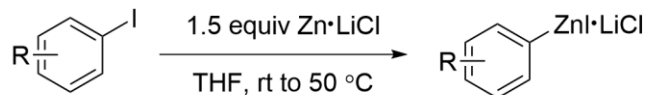


Research into cross-coupling reactions began to gain prominence in the 1970s. However, the Negishi reaction initially attracted considerably less attention, primarily due to the ionic nature of the C–Zn bond. This characteristic makes the organozinc reagent inherently basic and nucleophilic. Reports on gentler and more efficient synthetic methods for organozinc reagents has since revealed a remarkable tolerance for what was once believed to be incompatible functionality. In 2006, the work of the Knochel group employing LiCl¹⁵ and the Uchiyama group's use of *t*Bu₄ZnLi₂¹⁶ to synthesize functionalized organozinc reagents,

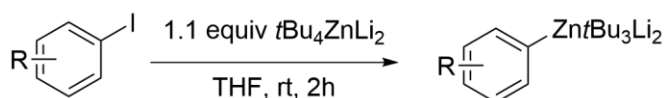
have redefined perspectives on organozinc compounds. These developments have reignited interest in organozinc chemistry and, moreover, in the Negishi reaction.

Scheme 3. Knochel group's work and Uchiyama group's work to synthesize organozinc reagent.

Knochel group's work:



Uchiyama group's work:

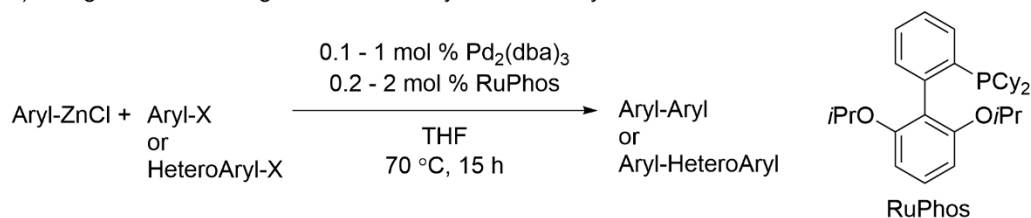


Research has consistently demonstrated the critical role of supporting ligands in palladium-catalyzed reactions. As cross-coupling increasingly finds application in industrial and synthetic chemistry, the demand for novel ligands has intensified. In 2004, the Buchwald group introduced a groundbreaking ligand known as 'SPhos' for the Suzuki reaction, facilitating the formation of functionalized biaryls. Following this, in 2005, a ligand specifically tailored for the Negishi reaction, 'RuPhos', was developed to catalyze the palladium-catalyzed cross-coupling of organozinc reagents with aryl halides.¹⁷ Employing RuPhos as the ligand, a diverse array of biaryls has been synthesized via the Negishi reaction using only 0.1 – 1 mol % Pd, with THF as the solvent. In 2009, the Buchwald group introduced 'CPhos,' a novel ligand, for the Negishi coupling of aryl halides with secondary alkyl zinc halides.¹⁸ This innovation established an efficient catalyst system, employing just 1 mol % of Pd(OAc)₂ and 2 mol % CPhos, for a wide range of aryl bromides and activated

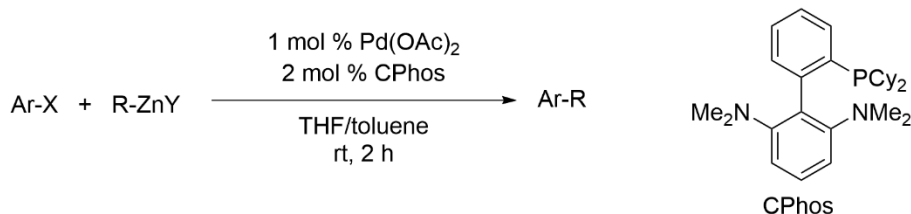
chlorides. Significantly, this system effectively suppresses the undesirable hydride elimination pathway. Expanding beyond the traditional Pd/ligand framework, in 2013, the Buchwald group further enhanced the field by reporting mild and general conditions for Negishi cross-coupling using palladacycle precatalysts (XPhos Pd G3).¹⁹ This approach, utilizing 0.025 – 2 mol % of the palladacycle, proved effective for a diverse array of substrates, including heteroaryl halides, pseudohalides, and other challenging types, under the specified conditions.

Scheme 4. Buchwald group's catalyst system of Negishi reaction

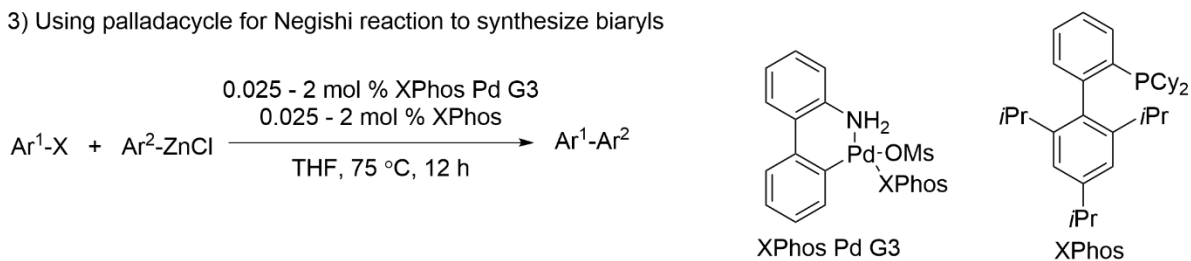
1) Using RuPhos for Negishi reaction to synthesize biaryls



2) Using CPhos for Negishi reaction of secondary alkylzinc halides and aryl halides



3) Using palladacycle for Negishi reaction to synthesize biaryls



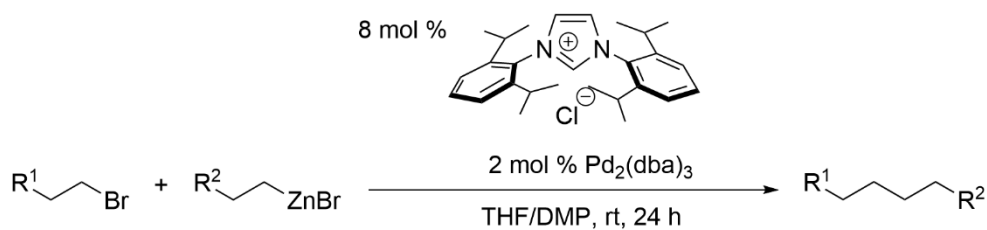
Although phosphine ligands have been pivotal in cross-coupling reactions, N-heterocyclic carbene (NHC) ligands have also been integral in numerous catalytic systems. The synthesis of the first stable, isolated NHC by Arduengo in 1991 marked a paradigm shift in organometallic chemistry.²⁰ Although classically, NHCs were viewed as simple tertiary phosphine mimics, NHCs have since been recognized for their unique properties. In 2005, the Organ group reported the pioneering use of a Pd–NHC catalyst in the Negishi coupling of two alkyl centers.²¹ Employing 2 mol % Pd₂(dba)₃ and 8 mol % of the NHC ligand IPr·HCl, they successfully achieved C–C bond formation between two sp³ carbons via Negishi reaction, minimizing β-hydride elimination.

The Organ group's innovations extended beyond sp³–sp³ cross-coupling. In 2006, they introduced PEPPSI-IPr (pyridine-enhanced precatalyst preparation, stabilization, and initiation; IPr = diisopropylphenylimidazolium derivative), a readily synthesized, air-stable, highly active, well-defined precatalyst.²² This represented the first user-friendly, general catalyst for the Negishi reaction. The combination of the highly active NHC ligand and the stabilizing pyridine ligand enabled a versatile catalyst system for forming sp³–sp³, sp³–sp², sp²–sp³, or sp²–sp² C–C bonds, effective across various halo/pseudohalo groups with just 1 mol % catalyst.

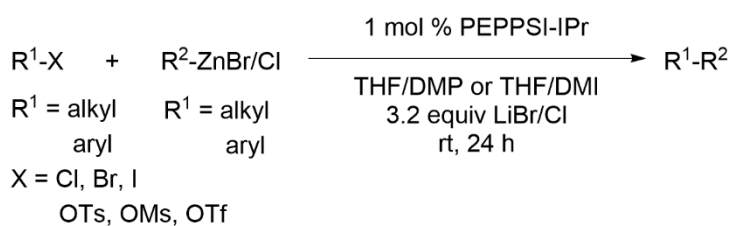
Further advancements by the Organ group included the 2010 introduction of Pd-PEPPSI-IPent, a modified PEPPSI catalyst for synthesizing tetra-ortho-substituted biaryls,²³ and the 2012 development of Pd-PEPPSI-IPent^{Cl} for coupling aryl halides with secondary alkyl zinc reagents.²⁴ Over time, a series of Pd-PEPPSI complexes with diverse substitutions on the NHC backbone have been developed, showcasing exceptional selectivity and reactivity in Negishi cross-coupling reactions.

Scheme 5. Organ group's PEPPSI catalyst system for Negishi reaction

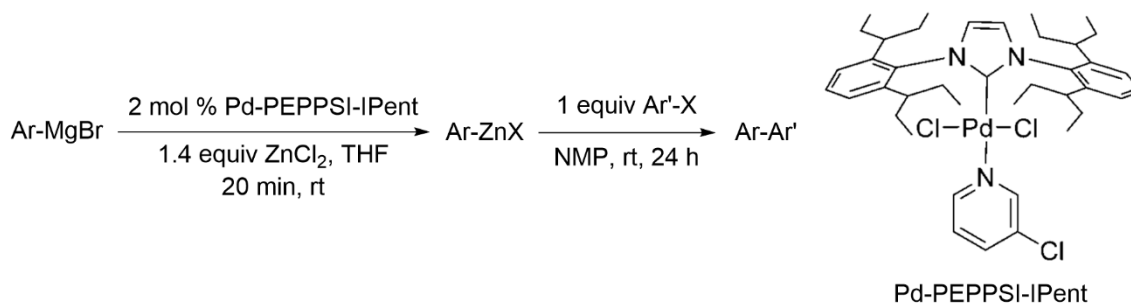
1) Pd-NHC system catalyzed Negishi reaction of two sp^3 carbons



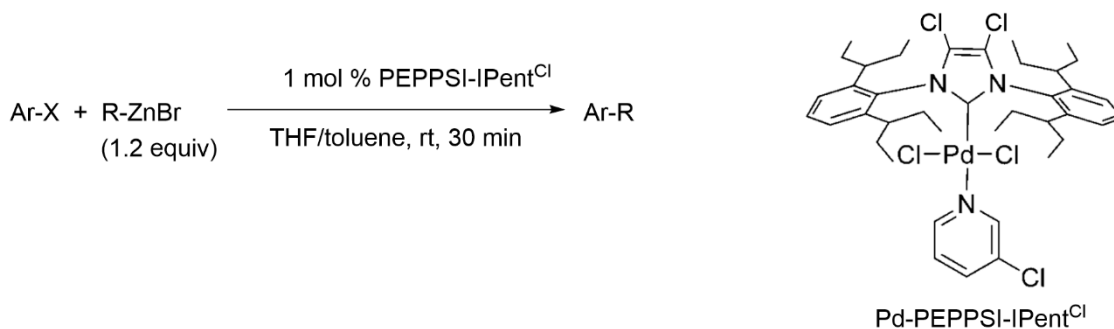
2) PEPPSI-IPr catalyzed Negishi reaction



3) Pd-PEPPSI-IPent catalyzed Negishi reaction for the preparation of tetra-ortho-substituted biaryls



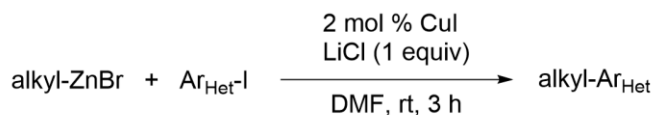
4) Pd-PEPPSI-IPent^{Cl} catalyzed Negishi reaction of aryl halides and secondary zinc nucleophiles



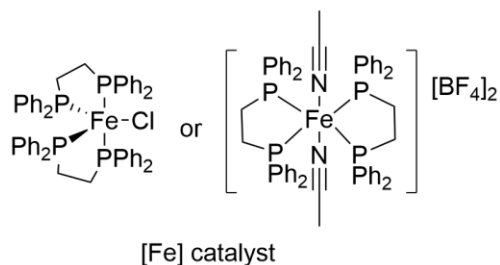
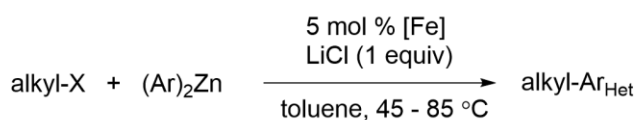
While palladium and nickel are the predominant metal catalysts for Negishi cross-couplings, recent studies have shown the efficiency of other metallic salts, including copper, iron, and cobalt derivatives, in catalyzing these reactions. Notably, Giri has reported a versatile Negishi cross-coupling method that effectively combines alkyl-, aryl-, and alkynyl-zinc reagents with various heteroaryl iodides.²⁵ Although limited to electronic deficient substrates, the condition is particularly interesting due to its simple commercially available catalyst without ligand. Also noteworthy is the iron(I)-catalyzed cross-coupling process developed by Bedford.²⁶ This method employs an easily accessible catalyst to facilitate the smooth cross-coupling of alkyl halides and diarylzinc reagents, yielding the coupled product in quantitative measure.

Scheme 6. Other transition metals catalyzed Negishi reactions.

1) Giri's work using CuI to catalyze Negishi reaction

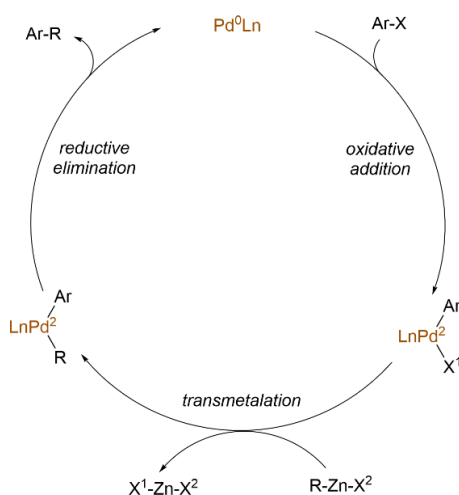


2) Bedford's work using Fe(I) to catalyze Negishi reaction



Despite these advantages associated with Negishi reactions, it has not achieved prominence in its frequency of usage, as indicated by statistical data reported by Brown and Bostrom.²⁷ A primary limitation is the moisture sensitivity of organozinc reagents, which readily protio-quench to form inactive organic byproducts and zinc(II) salts.^{28,29} Consequently, the reaction requires not only an oxygen-free environment to maintain catalytic activity of palladium, but also a moisture-free environment to prevent the quenching of organozinc reagents. Both requirements often need additional precautions and procedures. The reaction mechanism is shown in Scheme 7.

Scheme 7. Proposed mechanism for Negishi reactions



In addition, the palladium loadings for Negishi cross-couplings generally range between 2-5 mol % relative to the cross-coupling partner.^{12,30} Although instances exist wherein catalysts for the Negishi reaction use palladium at parts-per-million³¹ or parts-per-billion³² amounts, the molecule synthesized through these catalysts frequently lack complexity. Meanwhile the target molecules of interest in medicinal chemistry are often heterocyclic and functionalized in nature.^{33,34} Additionally, the increasing cost of palladium over the past several decades suggests an eventual shortage of this precious metal.³⁵ In fact, a report from

the ACS Green Chemistry Institute indicates that palladium,³⁶ recognized as the most reactive and commonly used catalyst for cross-coupling reactions, is at increasing risk of depletion.

To address the challenges above, two methodologies were strategically combined. Previous investigations within our research group have demonstrated that the combination of TMEDA and zinc powder in the designer surfactant solutions, such as with PTS or TPGS-750-M,³⁷ effectively enable formation of organozinc reagents from alkyl iodides in water.³⁸ In this system, the newly formed organozinc reagents are transferred into micelles, thereby affording protection against quenching while enabling reaction with the ligated palladium species present within the same micellar environment. Notably, this innovation accomplishes two novel objectives: it provides the possibility for the Negishi reaction in aqueous media and substantially enhances the accessibility of organozinc reagents. This is particularly valuable given the limited commercial availability of organozinc compounds compared to organoboronic acids.³⁹

As one approach to minimizing use of endangered palladium resources, Fe/ppm Pd nanoparticles, synthesized from commercially available FeCl₃, have been demonstrated to serve as effective catalysts in various cross-coupling reactions.⁴⁰ Originating from work in 2015, these nanoparticles were obtained by reducing a suspension of FeCl₃, Pd(OAc)₂, and SPhos in tetrahydrofuran (THF) using commercially available MeMgCl. After removal of solvent, the isolated nanoparticles displayed noteworthy catalytic activity for use in Suzuki reactions under mild conditions in aqueous micellar solutions, with only 320 ppm of palladium.⁴¹ Following this pioneering work, novel nanoparticles were made using Pd(OAc)₂ with XPhos to catalyze Sonogashira reactions with 500 ppm Pd,⁴² while

$\text{Pd}(\text{PtBu}_3)_2\text{Cl}_2$ paired with PtBu_3 for the Heck reaction could be accomplished with 1000 to 2500 ppm Pd.⁴³ The nanoparticles' enhanced reactivity is hypothesized to stem from several factors: electronic interactions between the reduced iron and palladium atoms, finely dispersed palladium particles, and the "nano-to-nano" effect.^{44,45} This impressive catalytic performance, coupled with the in-situ-generated organozinc reagents, opens the door for the development of Negishi reactions catalyzed by palladium at ppm levels... in water.

1.2 Results and discussion

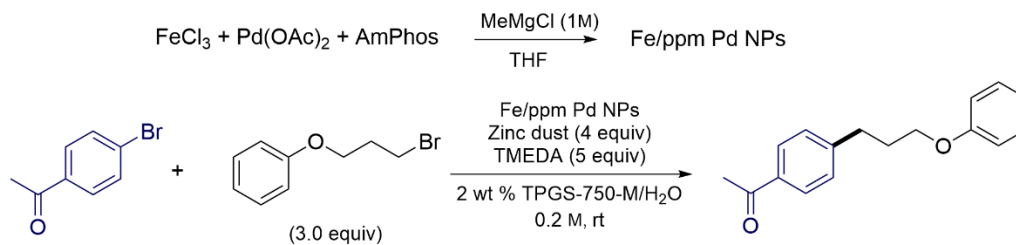
Optimization of the synthesis of nanoparticles (NPs)

To test the preliminary feasibility of the Fe/Pd nanoparticles as catalysts, nanoparticles were made by dissolving 10 mol % FeCl₃, 4 mol % AmPhos, and 2 mol % Pd(OAc)₂ in 0.04 mL of anhydrous tetrahydrofuran (THF). This mixture was stirred for 15 minutes, after which 0.04 mL of 1 M MeMgCl was added into the vial. After an additional 15 minutes of stirring, the black nanoparticles were formed. Subsequently, 0.2 mmol of 4-bromoacetophenone and 0.6 mmol of (3-bromopropoxy)benzene were added into the reaction mixture, followed by the addition of three equivalents of zinc dust and five equivalents of tetramethylethylenediamine (TMEDA). These nanoparticles demonstrated their ability to effectively catalyze the Negishi reaction between 4-bromoacetophenone and (3-bromopropoxy)benzene, with the organozinc reagent generated in-situ made using zinc powder. This initial trial resulted in an isolated yield of 63%. Despite the success of this preliminary experiment, the focus for subsequent efforts was to reduce the palladium loading to the ppm level. Table 1 reveals that diminishing palladium loading correlated with decreased yields; for example, using nanoparticles with 0.25 mol % palladium acetate yielded only 33% product on GC-MS analysis.

To achieve optimal catalytic reactivity, the composition of the nanoparticles was investigated by varying the amounts of FeCl₃, AmPhos, and MeMgCl. As shown in Table 1, reducing the level of MeMgCl (1.0 equivalent relative to FeCl₃) failed to facilitate nanoparticle formation; rather, a viscous, non-isolable sludge was generated. Conversely, more MeMgCl (4.0 equivalents relative to FeCl₃) led to nanoparticles that exhibited better

catalytic activity, achieving a 46% yield. An increase in the amount of FeCl₃ led to diminished reactivity of the nanoparticles, possibly due to reduced exposure of palladium on the nanoparticle surface.

Table 1. Initial Optimization of amount of FeCl₃, AmPhos, and MeMgCl



Entry ^a	FeCl ₃ / mol %	Pd(OAc) ₂ / mol %	AmPhos / mol %	MeMgCl (equiv) ^b	Yield(%) ^c
1	FeCl ₃ / 5	Pd(OAc) ₂ / 1.0	5	2.0	62
2	FeCl ₃ / 5	Pd(OAc) ₂ / 0.5	5	2.0	50
3	FeCl ₃ / 5	Pd(OAc) ₂ / 0.25	5	2.0	33
4	FeCl ₃ / 5	Pd(OAc) ₂ / 0.1	5	2.0	15
5	FeCl ₃ / 5	Pd(OAc) ₂ / 0.25	5	1.0	NR ^d
6	FeCl ₃ / 5	Pd(OAc) ₂ / 0.25	5	4.0	46
7	FeCl ₃ / 10	Pd(OAc) ₂ / 0.25	5	4.0	38
8	FeCl ₃ / 15	Pd(OAc) ₂ / 0.25	5	4.0	17
9	FeCl ₃ / 20	Pd(OAc) ₂ / 0.25	5	4.0	8
10	FeCl ₃ / 25	Pd(OAc) ₂ / 0.25	5	4.0	4
11	FeCl ₃ / 10	Pd(OAc) ₂ / 0.25	10	4.0	24
12	FeCl ₃ / 15	Pd(OAc) ₂ / 0.25	15	4.0	14
13	FeCl ₃ / 20	Pd(OAc) ₂ / 0.25	20	4.0	16

^a Conditions: 4-bromoacetophenone (0.2 mmol), 3-phenoxypropyl bromide (0.6 mmol), zinc dust (0.8 mmol), Fe/ppm Pd NPs, TMEDA (1.0 mmol), 2 wt % TPGS-750-M/H₂O (1.0 mL), rt, 16 h

^b Amount relative to FeCl₃

^c Yield determined by GC-MS; naphthalene as standard, NR = no reaction;

^d Nanoparticles not formed

Subsequently, a variety of ligands and palladium sources were evaluated to optimize catalytic reactivity. Ligands with different denticities, electron densities, coordinating atoms, and ligand cone angles were screened. As shown in Table 2, bidentate ligands, as well as ligands with electron deficiency, significantly impacted the yield. Among all the ligands tested, AmPhos emerged as the most reactive, possibly due to its electron-donating capabilities and its unique amino group.

Table 2. Initial Optimization of ligands

$\text{FeCl}_3 + \text{Pd}(\text{OAc})_2 + \text{Ligand} \xrightarrow[\text{THF}]{\text{MeMgCl (1M)}} \text{Fe/ppm Pd NPs}$

$\text{4-bromoacetophenone} + \text{3-phenoxypropyl bromide (3.0 equiv)} \xrightarrow[\text{0.2 M, rt}]{\text{Fe/ppm Pd NPs, Zinc dust (4 equiv), TMEDA (5 equiv), 2 wt \% TPGS-750-M/H}_2\text{O}} \text{Product}$

Entry ^a	FeCl ₃ / mol %	Pd(OAc) ₂ / mol %	L / mol %	MeMgCl (equiv) ^b	Yield(%) ^c
1	FeCl ₃ / 5	Pd(OAc) ₂ / 0.25	AmPhos / 5	4.0	46
2	FeCl ₃ / 5	Pd(OAc) ₂ / 0.25	SPhos / 5	4.0	15
3	FeCl ₃ / 5	Pd(OAc) ₂ / 0.25	cBRIDP / 5	4.0	7
4	FeCl ₃ / 5	Pd(OAc) ₂ / 0.25	vBRIDP / 5	4.0	11
5	FeCl ₃ / 5	Pd(OAc) ₂ / 0.25	PPh ₃ / 5	4.0	3
6	FeCl ₃ / 5	Pd(OAc) ₂ / 0.25	P(C ₆ F ₅) ₃ / 5	4.0	NR
7	FeCl ₃ / 5	Pd(OAc) ₂ / 0.25	DPPE / 5	4.0	9
8	FeCl ₃ / 5	Pd(OAc) ₂ / 0.25	DPPF / 5	4.0	8
9	FeCl ₃ / 5	Pd(OAc) ₂ / 0.25	XantPhos / 5	4.0	NR
10	FeCl ₃ / 5	Pd(OAc) ₂ / 0.25	Pt-Bu ₃ / 5	4.0	22
11	FeCl ₃ / 5	Pd(OAc) ₂ / 0.25	L1 / 5	4.0	5
12	FeCl ₃ / 5	Pd(OAc) ₂ / 0.25	L2 / 5	4.0	7
13	FeCl ₃ / 5	Pd(OAc) ₂ / 0.25	L3 / 5	4.0	26

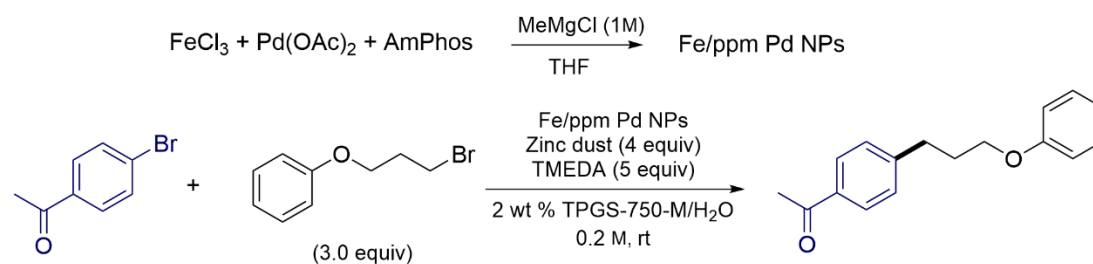
^a Conditions: 4-bromoacetophenone (0.2 mmol), 3-phenoxypropyl bromide (0.6 mmol), zinc dust (0.8 mmol), Fe/ppm Pd NPs, TMEDA (1.0 mmol), 2 wt % TPGS-750-M/H₂O (1.0 mL), rt, 16 h

^b Amount relative to FeCl₃;

^c Yield determined by GC-MS; naphthalene as standard, NR = no reaction

Changing the source of palladium was found to have no effect on yield (see Supplementary Table). Interestingly, the quantity of Grignard reagent is found to be crucial in optimizing nanoparticle reactivity. As illustrated in Table 3, carefully controlled addition of MeMgCl to 2.9 equivalents relative to FeCl₃ yielded nanoparticles that catalyzed the Negishi reaction in an aqueous medium, achieving an impressive 86% yield.

Table 3. Optimization of Grignard amount



Entry ^a	FeCl ₃ / mol %	Pd(OAc) ₂ / mol %	AmPhos / mol %	MeMgCl (equiv) ^b	Yield(%) ^c
1	5	0.25	5	4.0	46
2	5	0.25	5	3.0	61
3	5	0.25	5	2.9	86
4	5	0.25	5	2.8	50
5	5	0.25	5	2.7	45
6	5	0.25	5	2.5	16
7	5	0.25	5	2.0	15

^a Conditions: 4-bromoacetophenone (0.2 mmol), 3-phenoxypropyl bromide (0.6 mmol), zinc dust (0.8 mmol), Fe/ppm Pd NPs TMEDA (1.0 mmol), 2 wt % TPGS-750-M/H₂O (1.0 mL), rt, 16 h

^b Amount relative to FeCl₃;

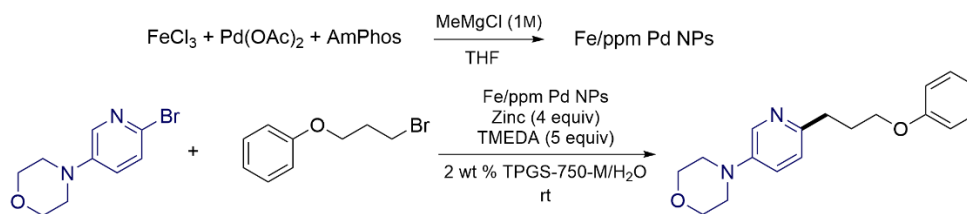
^c Yield determined by GC-MS; naphthalene as standard, NR = no reaction

Optimization of reaction conditions

Although the synthesized nanoparticles exhibited excellent catalytic reactivity in Negishi reactions with basic hydrocarbon compounds, the study further aimed to extend its applicability to more complex substrates. These substrates were chosen specifically because biologically active molecules frequently feature heterocyclic structures containing several nitrogen atoms.¹⁸ For instance, when utilizing nanoparticles to catalyze the Negishi reaction between 4-(6-bromopyridin-3-yl)morpholine and (3-bromopropoxy)benzene, the yield was 17%, as shown in Table 4. Efforts to improve this yield, such as modulating the equivalent of alkyl bromide, global concentration or introducing various additives, did not significantly help the observed results.

Motivated by results from a previous project that revealed the morphology change of nanoparticle under aqueous conditions, this study assessed the impact of the different sequences in which the catalyst, cross-coupling partners, zinc, and base were introduced into the reaction medium (THF). As shown in Table 4, three different Sequences (A, B, and C) were evaluated. Of these, Sequence C proved to be the most effective, yielding an 85% isolated yield of product. This protocol commenced with a one hour stirring of the nanoparticles in a 2 wt % TPGS-750-M solution, followed by the addition of zinc powder and aromatic bromide. After a further 15 minutes of stirring, the alkyl bromide and TMEDA were introduced into the reaction mixture. Subsequent stirring at room temperature for 16 hours yielded optimal results. This sequence's superior catalytic performance could be attributed to specific morphological changes that the nanoparticles undergo in aqueous solution, resulting in 100-200 nm nanorods that act as the actual catalytic species.

Table 4. Further optimization of reaction conditions



Sequence A: Fe/ppm Pd NPs + solvent + Zinc + Aryl bromide $\xrightarrow{15 \text{ min}}$ TMEDA + alkyl bromide

Sequence B: Fe/ppm Pd NPs + solvent $\xrightarrow{15 \text{ min}}$ aryl bromide + alkyl bromide $\xrightarrow{15 \text{ min}}$ TMEDA + Zinc

Sequence C: Fe/ppm Pd NPs + solvent $\xrightarrow{\text{time}}$ Zinc + aryl bromide $\xrightarrow{15 \text{ min}}$ TMEDA + alkyl bromide

Entry ^a	Equiv of alkyl bromide	Zinc source	Global Concentration	Sequence to add reagents	time in sequence C	Yield(%)
1	2	Zinc dust	0.2 M	A	-	8 ^b
2	3	Zinc dust	0.2 M	A	-	17 ^b
3	4	Zinc dust	0.2 M	A	-	36 ^b
4	5	Zinc dust	0.2 M	A	-	38 ^b
5	4	Zinc nanopowder	0.2 M	A	-	15 ^b
6	4	Zinc powder	0.2 M	A	-	44 ^b
7	2	Zinc powder	0.1 M	A	-	35 ^c
8	3	Zinc powder	0.33 M	A	-	31 ^c
9	4	Zinc powder	0.4 M	A	-	39 ^c
10	5	Zinc powder	0.5 M	A	-	33 ^c
11	4	Zinc powder	0.75 M	A	-	25 ^c
12	4	Zinc powder	1.0 M	A	-	22 ^c
13	4	Zinc powder	0.2 M	B	-	53 ^b
14	4	Zinc powder	0.2 M	C	15 min	68 ^b
15	4	Zinc powder	0.2 M	C	5 min	46 ^b
16	4	Zinc powder	0.2 M	C	30 min	78 ^b
17	4	Zinc powder	0.2 M	C	1 hour	85 ^b

^a Conditions: 4-(6-bromopyridin-3-yl)morpholine (0.2 mmol), 3-phenoxypropyl bromide (0.4 - 1.0 mmol) Fe/ppm Pd NPs (15.5 mg, containing 0.25 mol % Pd), zinc (0.8 mmol), TMEDA (1.0 mmol), 2 wt % TPGS-750-M/H₂O, rt, 16 h

^b Isolated yield.

^c Yield determined by GC-MS; naphthalene as standard

Characterization of the nanoparticles

Subsequent studies were conducted to characterize these nanoparticles, employing an array of analytical techniques including scanning transmission electron microscopy - electron dispersive spectroscopy (STEM-EDX), dynamic light scattering (DLS), cryogenic electron microscopy (cryo-EM), and elemental mapping. STEM was utilized to disclose the morphological and structural attributes of the nanoparticles in various conditions: as a dry powder, in aqueous solution, and in micellar solution. Electron dispersive spectroscopy (EDX) was used to determine the elementary composition of the nanoparticles, and elemental mapping was used to reveal the physical distribution of different elements. DLS was applied to measure the sizes of both nanomicelles and nanoparticles, while the cryo-EM was applied to investigate the interaction between nanoparticles and nanomicelles.

As shown in Figure 1A, the dry powder form of the nanoparticles, obtained after evaporation of THF, exhibited a spherical shape with a diameter of approximately 10 nm. Remarkably, when the nanoparticles were stirred in water for one hour, a significant morphological change was observed; the particles transformed from 10 nm spheres into ca. 200 nm nanorods, as illustrated in Figure 1B. The underlying mechanisms for this morphological change remain to be fully understood but may be related to the dissolution of magnesium, chlorine, and phosphine in water, as well as the potential quenching of methylmagnesium chloride by water. Figure 1C shows the nanoparticle structure after a one-hour stirring in the presence of 2 wt % TPGS-750-M solution. Notably, in comparison to their structure in pure water, the nanoparticles in the micellar solution displayed a more uniform size distribution, averaging around 100 nm. This suggests that the micellar environment may be conducive to the generation of the active catalytic species.

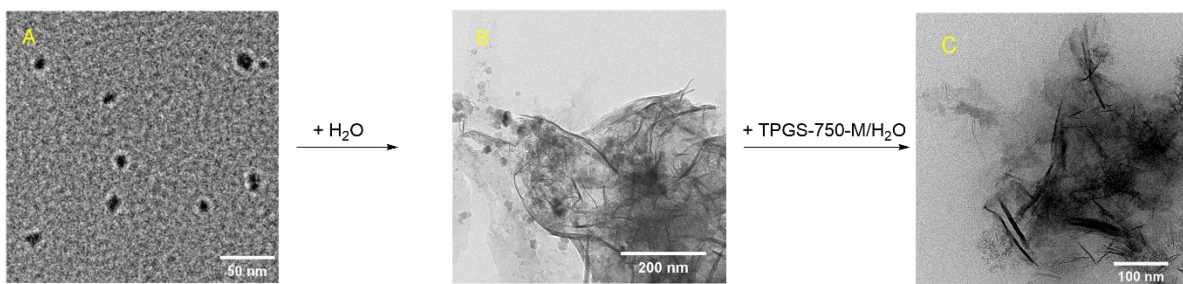


Figure 1. Bright field transmission electron microscopy images of A) spherical dry Fe/ppm Pd NPs under 50 nm scale; B) long needle like Fe/ppm Pd nanomaterials in degassed water under 200 nm scale; C) Fe/ppm Pd nanorod in 2 wt % TPGS-750-M/H₂O under 100 nm scale.

Elementary mapping was employed to illustrate the elemental distribution within STEM images. As shown in Figure 2, a sample of nanoparticles after stirring in a 2 wt % TPGS-750-M solution for one hour was imaged utilizing High-Angle Annular Dark-Field (HAADF) microscopy. Elemental analyses for Fe, O, P, N, Cl, and C were conducted on this same image.

In the HAADF image, nanorod structures with 100 nm length were distinctly observed, which align with the results previously shown in Figure 1. Most of the iron was localized within these nanorods, suggesting that the major composition of the nanorods is composed of reduced iron. The distribution of oxygen closely mirrored that of iron, likely due to the oxidation of iron upon exposure to air prior to imaging. The phosphorus and nitrogen were found to be dispersed throughout the image, suggesting that the ligands in the nanoparticles were dissolved in solution. Similarly, chloride appeared to be evenly distributed across the image, indicative of its dissolution in water. As for carbon, its presence in the mapping is much less valuable due to the fact that the grid supporting the sample is composed of both copper and carbon.

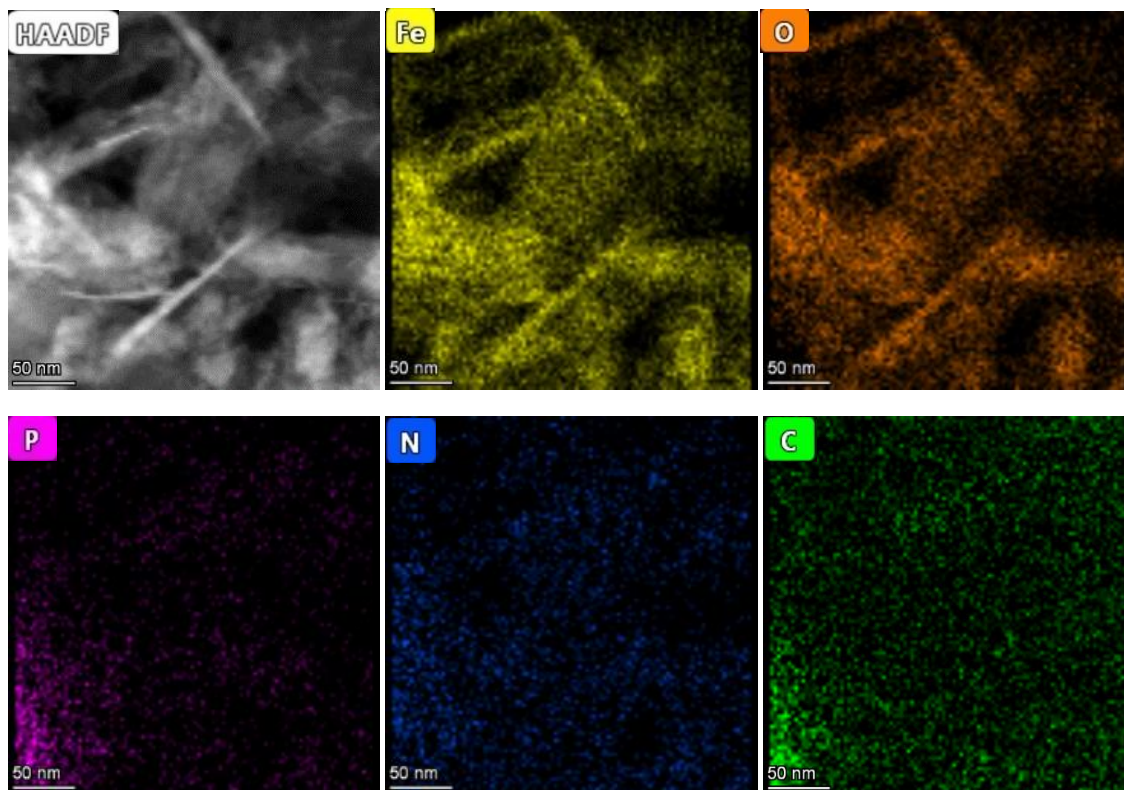


Figure 2. HAADF-STEM elemental mapping of Fe/pptm Pd nanorods in 2 wt % TPGS-750-M/H₂O.

EDX was employed to determine the elemental composition of the nanoparticles. As shown in Figure 3A, within the HAADF image, an area containing a moderate density of nanorods was specifically chosen for analysis. An 80-second energy dispersion was conducted over this selected area. The resulting qualitative spectrum and quantitative table are presented in Figures 3B and 3C. The spectrum revealed the presence of elements such as Cl, P, N, Fe, Mg, thereby confirming that the "nanorods" observed in the image was transformed from the nanoparticles. In the quantitative table, excluding carbon and copper from the background, it was determined that the principal ingredients of the nanoparticles are iron and oxygen, with approximately 13% and 14%, respectively.

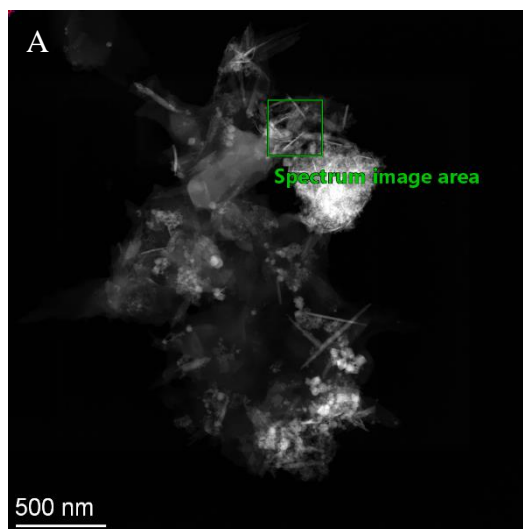


Figure 3A. HAADF image of nanorod in 2 wt % aqueous TPGS-750-M solution

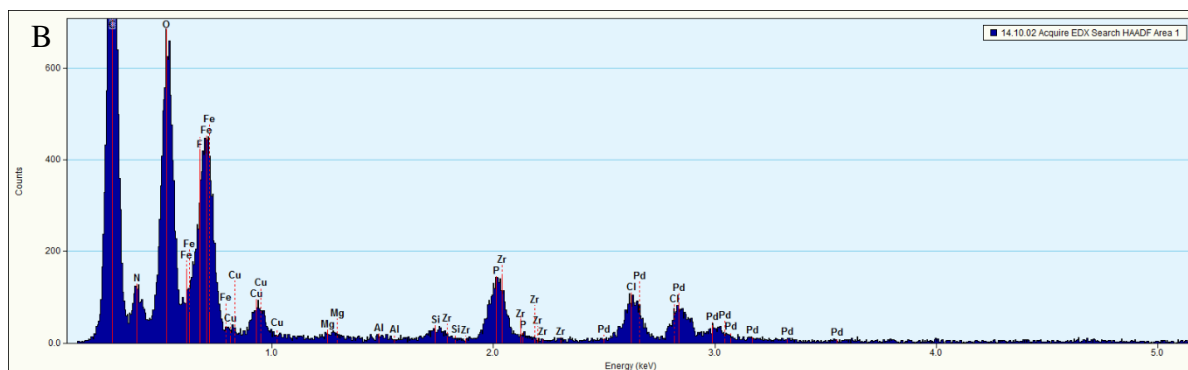


Figure 3B, EDX analysis spectrum of area 1 in Figure 3A

C ***Quantification Results***

Correction method: None

Element	Weight %	Atomic %	Uncert. %	Detector Correction	k-Factor
C(K)	39.04	60.47	0.44	0.28	3.601
N(K)	4.03	5.35	0.14	0.28	3.466
O(K)	14.32	16.65	0.18	0.51	1.889
F(K)	5.64	5.52	0.14	0.63	1.573
Mg(K)	0.08	0.06	0.01	0.88	1.050
P(K)	2.68	1.61	0.07	0.90	1.067
S(K)	0.00	0.00	NaN.00	0.93	1.021
Cl(K)	1.64	0.86	0.04	0.95	1.063
Fe(K)	13.18	4.38	0.13	0.99	1.401
Cu(K)	13.92	4.07	0.15	0.99	1.663
Zr(K)	1.17	0.24	0.04	0.99	3.728
Pd(L)	4.25	0.74	0.07	0.95	2.596

Figure 3C. quantitative EDX analysis of area 1 in Figure 3A

Other characterization techniques such as cryo-EM and DLS were employed to further reveal the relationship between the nanorods and nanomicelles. As shown in Figure 4A, DLS analysis of a sample of nanoparticles suspended in a 2 wt % aqueous TPGS-750-M solution revealed the presence of nanomicelle aggregates with an average radius of 35.1 nm. Additionally, the nanocatalyst exhibited an average radius of 162.8 nm. The discrepancy between the nanocatalyst's radius observed through DLS and that observed through STEM imaging may be due to the aggregation of nanorod around the nanomicelles, consequently resulting in larger particle sizes noted in the DLS measurements.

This phenomenon, which we refer to as the “nano-to-nano” effect,⁴⁴ is further observed by cryo-EM imaging, as seen in Figure 4B. Although several isolated nanorods and nanomicelles were observed, the majority of nanorods were found in close proximity to the nanomicelles. This specific relationship is important for understanding the superior catalytic activity of these nanoparticles. The cross-coupling partners, as organic molecules, are mainly soluble in the nanomicelles, while the active catalytic nanorods are situated around these nanomicelles. This unique relationship significantly enhances the chance of the cross-coupling partners interacting with the catalyst, thereby leading to the remarkable reactivity of these NPs in micellar solutions.

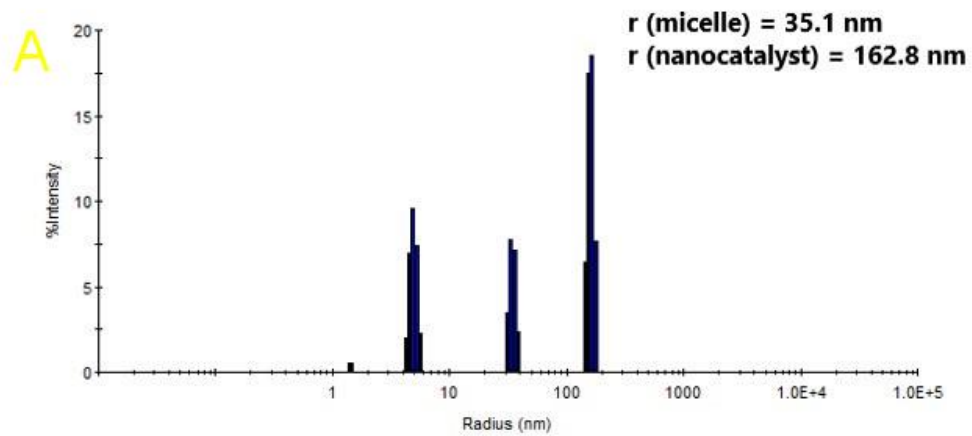


Figure 4A. DLS analysis of nanoparticles in 2 wt % TPGS-750-M solution

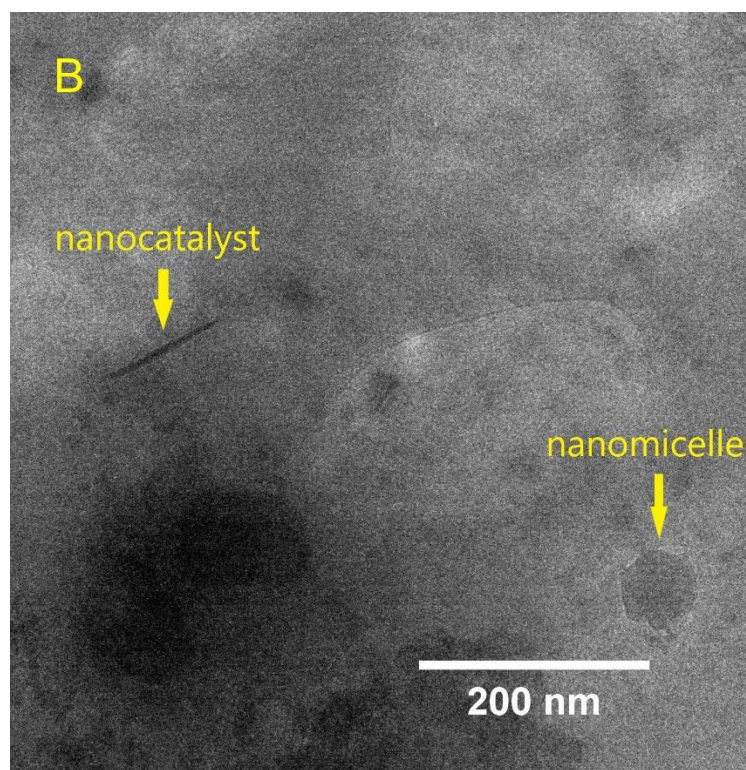


Figure 4B, cryo-EM image of nanoparticles in 2 wt % TPGS-750-M solution

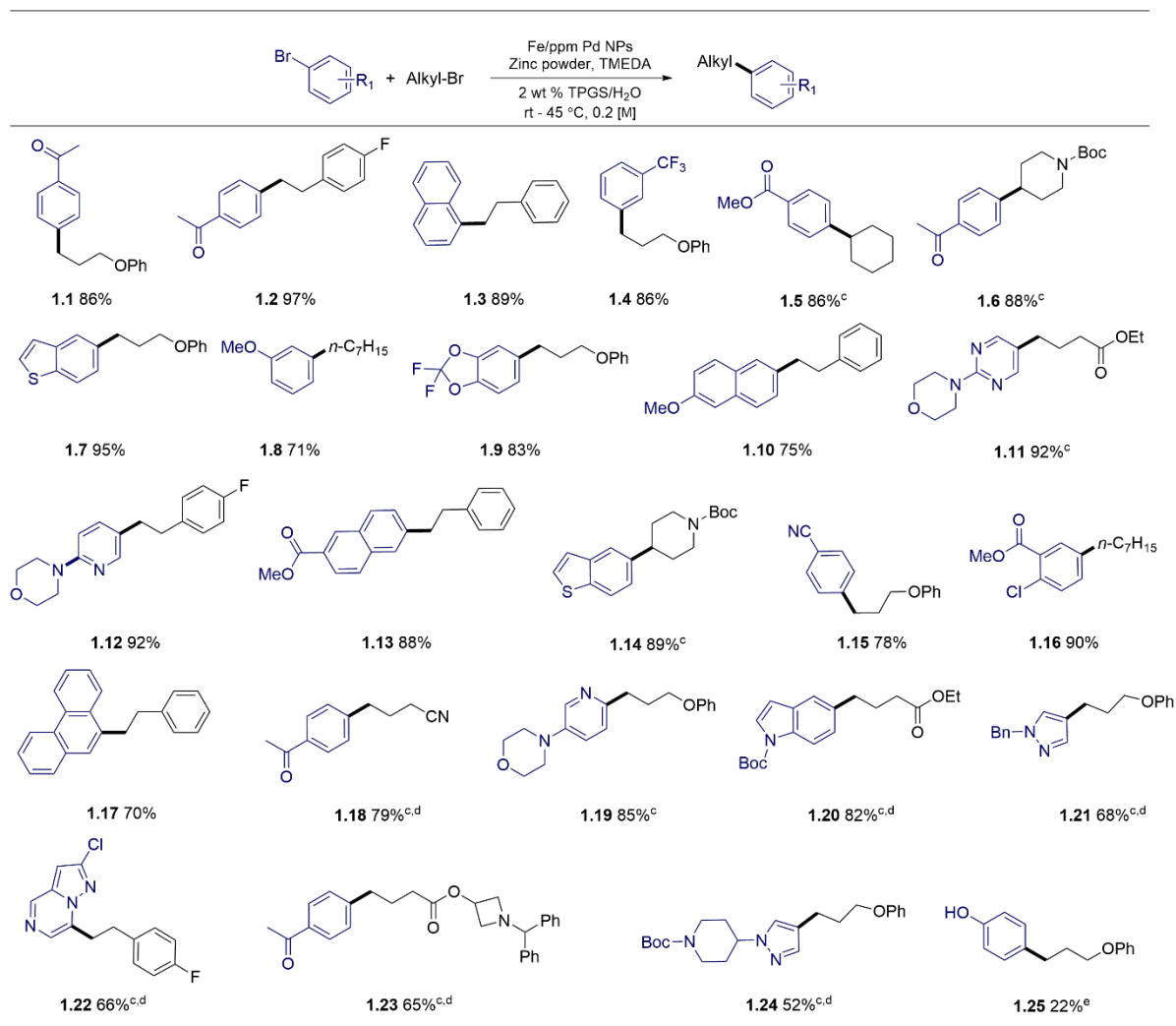
Substrate scope in Negishi reactions

With the nanoparticle synthesis, reaction conditions, and addition sequence thoroughly optimized, other coupling partners were evaluated, particularly those featuring functional groups and heterocycles. Variations within the aryl and alkyl bromides with diverse functional groups were tested in these couplings, yielding products in moderate-to-high yields. Functional groups such as ketone-containing products (**1.1**, **1.2**, **1.6**, **1.18**, **1.23**), products containing an ether (**1.1**, **1.4**, **1.7**, **1.9**, **1.15**, **1.19**, **1.21**, **1.24**), fluorides (**1.2**, **1.9**, **1.12**, **1.22**), trifluoromethyl groups (**1.4**), esters (**1.5**, **1.11**, **1.13**, **1.16**, **1.20**, **1.23**), methoxy groups (**1.8**, **1.10**), nitriles (**1.15**, **1.18**), and chlorides (**1.16**, **1.22**) were all well-tolerated under the established conditions.

Moreover, heterocyclic-containing substrates, often considered challenging reactants due to their unique electronic densities and potential bonding interactions with the catalyst, were also amenable. Heterocycles such as those products containing piperidine (**1.6**, **1.24**), benzothiophene (**1.7**, **1.14**), pyrimidine (**1.11**), morpholine (**1.11**, **1.12**, **1.19**), pyridine (**1.12**, **1.19**), indole (**1.20**), pyrazole (**1.21**, **1.24**), pyrazolopyrimidine (**1.22**), and azetidine (**1.23**) could be formed in good yields. Importantly, many of these compounds possess functionality found in active ingredients in the agricultural and pharmaceutical industries.

While most of the substrates tested yielded excellent results, a few containing reactive protons underperformed in terms of yield. Specifically, product **1.25**, which has a free hydroxy group, was obtained in only 22% yield, as determined by ¹H NMR analysis. A significant amount of starting material underwent alternative reaction pathways leading to the formation of undesirable side products.

Table 5. Substrate scope table



^a Aryl bromide (0.2 mmol), alkyl bromide (0.6 mmol), zinc powder (0.8 mmol), TMEDA (1.0 mmol) and Fe/ppm Pd NPs (15.5 mg, 0.25 mol % Pd), 2 wt % TPGS-750-M/H₂O (1.0 mL), rt, 16 h.

^b Isolated yield.

^c Used 4 equiv of alkyl bromide.

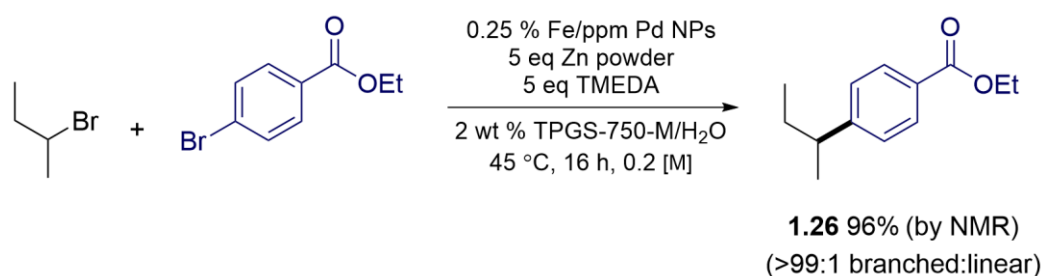
^d Run at 45 °C, for 40 h.

^e Yield from ¹H NMR

Importantly, this methodology is compatible with organozinc reagents derived from both primary and secondary alkyl bromides. The yields obtained using either type of alkyl bromide did not differ significantly under the same reaction conditions. This stands in contrast to traditional Negishi reactions, where primary and secondary organozinc reagents require different reactions conditions, including palladium catalysts, temperature, and solvents.^{18,46}

To further assess the compatibility of secondary alkyl bromides, a specific substrate was evaluated. This effort was made due to literature observations that secondary zinc halide coupling partners may undergo isomerization to their thermodynamically more stable primary forms, thereby resulting in undesired side-product isomers.^{47,48} As shown in Scheme 8, ethyl 4-bromobenzoate and 2-bromobutane were tested under the standard reaction conditions. According to the crude ¹H NMR, the desired branched product, ethyl 4-(sec-butyl)benzoate, was obtained in 96% yield, where the undesirable linear by-product was present only in trace amounts.

Scheme 8. Screening for alkyl group rearrangement (from branched to linear product).

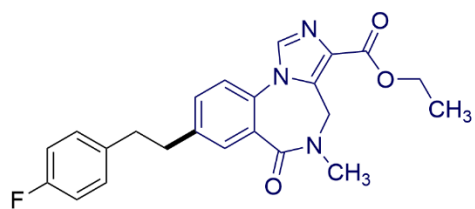


To further assess the generality of Fe/ppm Pd nanoparticle-catalyzed Negishi reaction in forming sp^2 - sp^3 C-C bonds, aryl halides sourced from the Merck Informer Library were tested. These starting materials were proposed by Merck and consist of a group of aryl halides and boronic acids selected for their "drug-like" properties.⁴⁹ These properties include a range of 14 physicochemical factors, such as molecular weight, ring count, hydrogen bond donors and acceptors, sp^3 character fraction, and Alog P values.

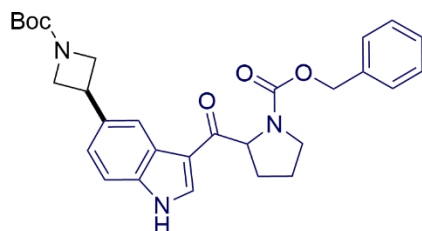
As shown in Scheme 9, three aryl halide precursors from this Library were effectively coupled with different alkyl bromides, with a remarkably low palladium loading of just 0.40 mol %. The reactions gave moderate-to-good product yields, ranging from 47% to 72%. Notably, in most cases, the remaining mass was unreacted starting material. For compound **1.28**, an increase in isolated yield from 58% to 69% was observed with only 0.1 mol % of additional Pd catalyst.

Given the inherent complexity of these aryl halides, coupled with the functionality present in each alkyl bromide, these results are quite promising. They become all the more remarkable when considering the ppm level palladium-containing catalyst involved, the in-situ formation of the zinc reagent, the mild reaction conditions, and the greenness of this method which uses water as the reaction medium.

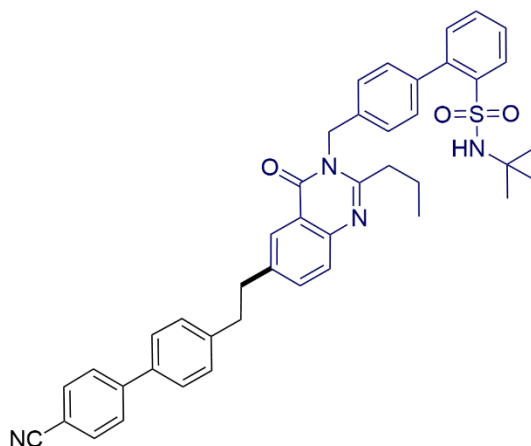
Scheme 9. Fe/ppm Pd NP-catalyzed Negishi couplings involving aryl halides from the Merck Informer Library



1.27 67% (from aryl bromide)



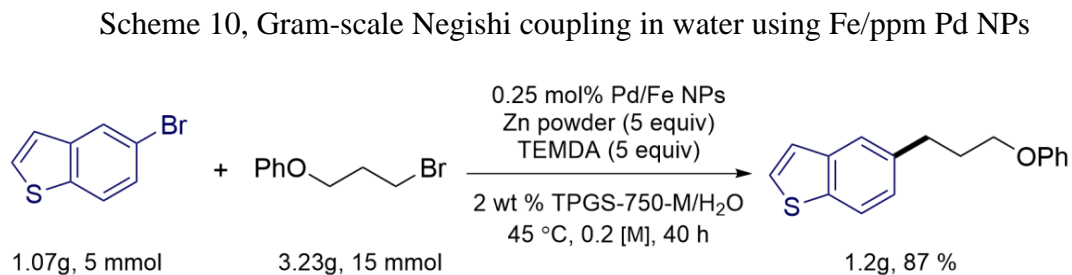
1.28 72 % with 1.0 % Pd/Fe NPs
69 % with 0.5 % Pd/Fe NPs
58 % with 0.4 % Pd/Fe NPs
(from aryl bromide)



1.29 47% (from aryl iodide)

Gram scale reaction

To assess the scalability of this methodology for potential application to large-scale chemical production, an experiment was conducted at the gram scale while maintaining the same catalyst percentage. As shown in Scheme 10, a coupling reaction involving 1.07 g of 5-bromobenzothiophene and 3.23 g of (3-bromopropoxy)benzene was performed under the conditions previously determined. A total mass of 1.2 g of 5-(3-phenoxypropyl)benzothiophene was successfully isolated in 87%. The reaction proceeded readily at this larger scale, showing a freely-stirring silver/white suspension. The success of this gram-scale reaction can be largely attributed to the dilute global concentration. Specifically, at a concentration of 0.2 M, the reaction exhibited no issues related to solid aggregation, overheating, or uneven stirring.



Recycle study

The recycling of both the palladium catalyst and the reaction media is an important feature associated with these coupling reactions. With each recycling of the palladium catalyst, the actual palladium loading required for each reaction is reduced. Meanwhile, the

recyclability of the aqueous reaction media highlights the environmental friendliness of this methodology.

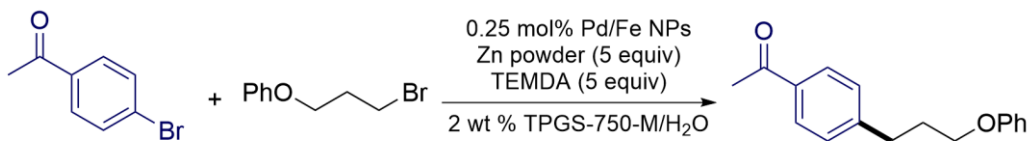
As shown in Table 6, a recycling study was conducted using 1-(4-bromophenyl)ethan-1-one and (3-bromopropoxy)benzene. The initial run was executed under the standard catalytic conditions. Upon completion of the reaction, a minimal amount of methyl *t*-butyl ether (MTBE) was used as the organic phase to extract the target product, leaving the nanoparticles along with the aqueous phase. The product in the organic phase was then purified, resulting in an isolated yield of 86%. For the next run, fresh zinc powder, TEMDA, and ligand were introduced into the recovered aqueous phase containing the nanoparticles. Using this catalytic mixture, the same cross-coupling reaction was initiated. After the reaction, the same extraction procedure was operated, yielding 84% product.

In the third cycle, besides the previously mentioned fresh reagents, an additional 1500 ppm of Pd(OAc)₂ was necessary to maintain catalyst activity. This cycle led to an 80% isolated yield of product. The recharge of fresh reagents is necessary as the zinc powder undergoes continual oxidation. Moreover, TEMDA and the ligand dissociate from the nanoparticles, and are subsequently extracted from the aqueous phase. By the third cycle, supplementary palladium is required. This is because a portion of ligated palladium is dissolved in the aqueous micellar phase during the reaction and was later extracted out by MTBE.

Nonetheless, across three reaction cycles, a total of only 4000 ppm (0.4 mol %) of palladium was utilized, effectively reducing the palladium loading to 1333 ppm (or, 0.133 mol %) per reaction. Notably, the same micellar solution was employed in all three cycles without any decrease in this enabling medium. The recyclability of both the palladium and

the medium highlights the metal economy with respect to palladium loading, and the greenness for minimizing organic waste creation.

Table 6. recycle study



Entry ^a	Recharge (relative to aryl bromide)	Yield ^b
1st run	-	86
2nd run	4 eq zinc powder, 5 eq TEMDA, 5 % ligand	84
3rd run	1500 ppm Pd(OAc) ₂ , 4 eq zinc powder, 5 eq TEMDA, 5 % ligand	80

^a Aryl bromide (0.2 mmol), alkyl bromide (0.8 mmol), zinc powder (1.0 mmol), TEMDA (1.0 mmol) and Fe/ppm Pd NPs (15.5 mg, 0.25 mol % Pd), 2 wt % TPGS-750-M/H₂O (1.0 mL), rt, 8 h.

^b Isolated yield

Residual metal analysis

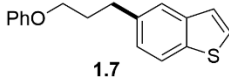
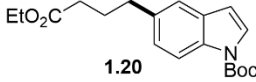
It's also important to consider the residual transition metal residue in the final product, especially since transition metals are widely used in the pharmaceutical industry. The oral daily limitation for palladium is set at 10 ppm per dose by FDA.⁵⁰ If a product exceeds this threshold, pharmaceutical companies must invest additional resources and time to reduce the palladium residue below the permissible limit, potentially incurring considerable financial cost.

While some might point out an alternative approach using nickel to form sp²-sp³ C-C bonds, either through traditional cross-coupling⁵¹ or cross-electrophile coupling,⁵² it's worth noting that the allowable limit for nickel stands at 20 ppm. Yet, typical reactions require a

nickel loading of between 2–10 mol %. Consequently, the final drug product often retains substantial quantities of nickel, presenting potential challenges and concerns.

Two products each synthesized using this technology were sent to UCLA for ICP-MS analysis to assess residual metal concentrations, specifically for Pd, Ni, and Zn. Given the ppm palladium used in the reaction, it was expected that the palladium residue in both compounds would be below the FDA limits. As shown in Table 7, compound **1.7** exhibited a palladium residue of 0.037 ppm. For compound **1.20**, palladium was not detected, indicating that its residue is below the detection threshold of the ICP-MS.

Table 7, Residual metal content in compound 7 and 20, as determined by ICP-MS

sample analyzed	Pd loading used for reaction	weight of sample for analysis (mg)	Pd (ppm)		Mg (ppm)		Zn (ppm)	
			average	STDEV	average	STDEV	average	STDEV
 <p>1.7</p>	2500 ppm	2.61	n/a ^c	n/a	30.014	0.418	0.000	0.000
 <p>1.20</p>	2500 ppm	11.20	0.037	0.005	79.592	0.878	0.000	0.000

^a ICP-MS data was obtained from the UC Center for Environmental Implications of Nanotechnology at UCLA.

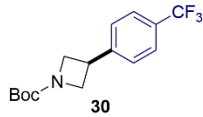
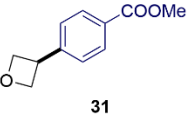
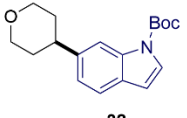
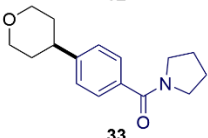
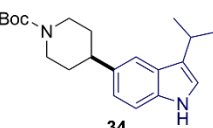
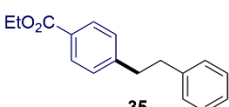
^b Each sample was done in triplicate with background correction.

^c n/a represents a result below the detection limit.

Direct comparisons with literature

A direct comparison was conducted on the formation of sp^2 - sp^3 C-C bonds between using this new methodology with conventional Negishi coupling conditions and cross electrophile coupling catalyzed by precious metals. To synthesize the same compounds, references 53 and 54 require the combined use of iridium and nickel. For a traditional Negishi reaction, 5 mol % of Ni or Pd is required, as outlined in references 55 and 56, respectively. Beyond the sustainability concerns and costs associated with these precious metals, it's noteworthy that most of these reactions are executed by top pharmaceutical corporations using organic solvents. Specifically, solvents with significant environmental impacts were employed, such as water-miscible dioxane (see entries 1 and 2) or the dipolar aprotic solvent DMA (entries 5 and 6). When evaluating both from an economic and environmental perspective, the nanoparticle technology in micellar solution stands out as a far superior approach.

Table 8. Comparison between Fe/ppm Pd NPs and representative recent catalysts used

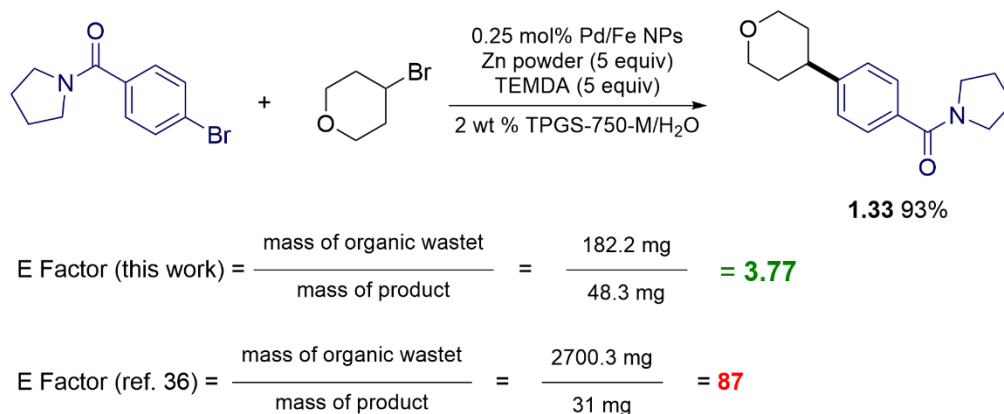
Entry	Product	Lit. Catalyst	Lit. Solvent	Lit. Yield (%)	Yield (%) Fe/ppm Pd NPs ^{a,b}	Lit. Ref.
1	 30	2.5 % [Ir(dF(CF ₃)ppy) ₂ (dtbbpy)]PF ₆ 5 % NiCl ₂ (dtbbpy)	dioxane	53	82	53 (Abbvie)
2	 31	2.5 % [Ir(dF(CF ₃)ppy) ₂ (dtbbpy)]PF ₆ 5 % NiCl ₂ (dtbbpy)	dioxane	29	86	53 (Abbvie)
3	 32	2 % [Ir(dF(CF ₃)ppy) ₂ (TREE-bpy)]PF ₆ 1 % NiCl ₂ (TREE-bpy)	IPAc	63	91	54 (Novartis)
4	 33	2 % [Ir(dF(CF ₃)ppy) ₂ (TREE-bpy)]PF ₆ 1 % NiCl ₂ (TREE-bpy)	IPAc	47	93	54 (Novartis)
5	 34	5 % NiCl ₂ ·6H ₂ O	DMA	79	81	55 (BMS)
6	 35	5 % PdCl ₂ PPh ₃	DMA	53	99	56

E Factor evaluation

Introduced by Sheldon in 1992, the E Factor has become an important tool for evaluating the environmental impact of organic reactions.^{57,58} To further assess the greenness of this method, the E Factor was calculated for one of the compounds above. As shown in Scheme 11, the synthesis of compound **1.33** using nanoparticles in an aqueous micellar solution results in an E Factor of an only 3.77. This low value represents the environmental friendliness of this approach, as only minimal amounts of organic waste are produced. By

contrast, the E Factor to synthesize the same compound using conventional methods stands at 87, according to reference 54. A detailed breakdown of these E Factor calculations is provided in the experimental section.

Scheme 11. E Factor comparison with a typical literature approach

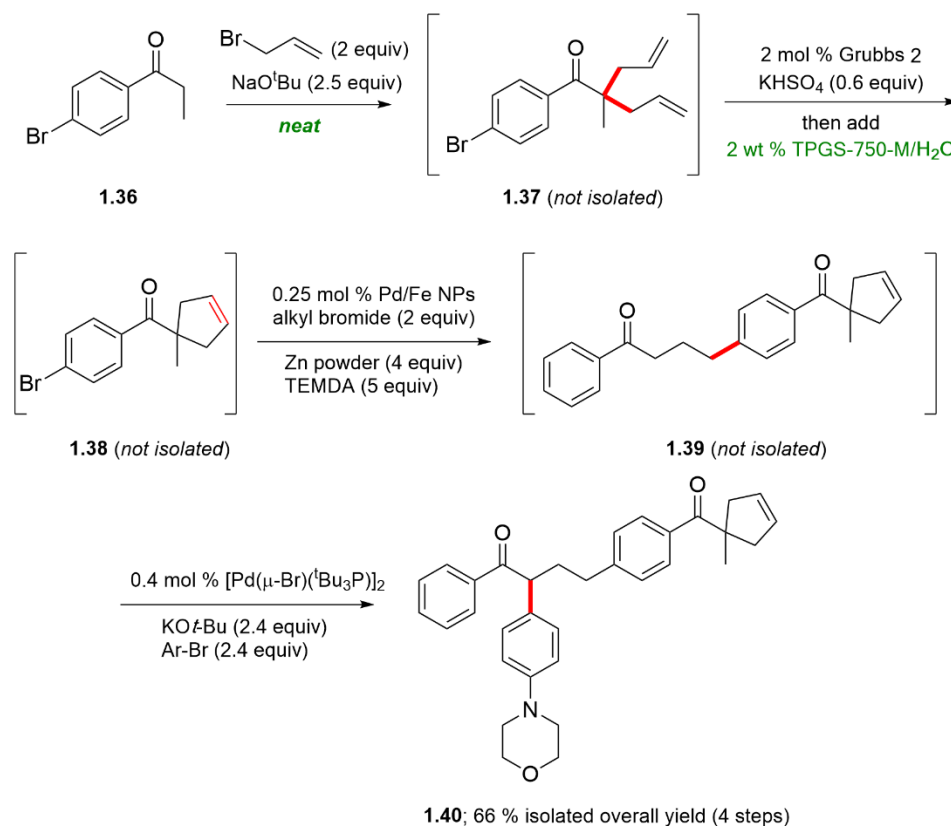


One-pot Synthetic sequence

To further investigate the advantages of reactions in aqueous media, a tandem four-step, one-pot synthetic sequence was executed. Starting with *p*-bromopropiophenone **1.36**, allyl bromide and sodium *t*-butoxide were introduced and stirred in the absence of solvent. Under these solvent-free conditions, the allylation occurred twice at the alpha position of the ketone within minutes,⁵⁹ yielding compound **1.37**. This intermediate was not isolated. Instead, it was directly treated with the Grubbs-2 catalyst, a 2 wt % TPGS-750-M solution as reaction medium, and KHSO₄ to modify the solution's pH. A successful ring-closing metathesis on educt **1.37** led to the cyclopentene-containing ketone,³⁷ compound **1.38**. Again, without isolating compound **1.38**, Fe/ppm Pd nanoparticles were introduced under an argon flow, along with the alkyl bromide and zinc to conduct a Negishi reaction in water. This

produced, compound **1.39** formed in the same pot, was also not isolated. An α -position on the ketone, introduced from the alkyl bromide, underwent a palladium-catalyzed α -arylation,⁶⁰ leading to the final product, compound **1.40**. The overall isolated yield for this four-step, one-pot synthesis is 66%. This sequence not only highlights the time efficiency from eliminating the need for intermediate purification⁶¹ but also showcases the pot economies resulting from avoiding use of several reactors.⁶²

Scheme 12. Tandem, 4-step, 1-pot sequence, neat and in water



Conclusion

In conclusion, new nanoparticles derived from commercially available FeCl_3 have been successfully developed for catalysis of Negishi reactions in water. This technique utilizes ppm levels of ligated palladium and *in situ*-generated organozinc reagents. Various characterization methods, including STEM-EDX, DLS, cryo-EM, and elemental mapping, were employed to better understand the catalytic system. Palladium acetate coupled with the AmPhos ligand were identified as the best combination as catalyst after evaluating multiple palladium sources and ligands. This technology exhibits notable generality, as evidenced by its efficiency with compounds bearing various functional groups and heterocycles. Impressively, complex halides from the Merck Informer Library could be used as examples of "late-stage functionalization." In direct comparisons with cases from existing literature, this approach leads to higher yields, utilizes cost-effective catalysts, uses greener reaction media, and achieves a lower E Factor. Additionally, a four-step, one-pot reaction sequence in water highlights the huge potential and advantages of this important tool in the expanding green chemistry methodology toolbox.

Reference

1. Li, H.; Seechurn J., C. C. C.; Colacot, T. J., Development of Preformed Pd Catalysts for Cross-Coupling Reactions, Beyond the 2010 Nobel Prize. *ACS Catal.* **2012**, *2*, 1147-1164.
2. Devendar, P.; Qu, R.-Y.; Kang, W.-M.; He, B.; Yang, G.-F., Palladium-Catalyzed Cross-Coupling Reactions: A Powerful Tool for the Synthesis of Agrochemicals. *J. Agric. Food Chem.* **2018**, *66*, 8914-8934.
3. Rayadurgam, J.; Sana, S.; Sasikumar, M.; Gu, Q., Palladium catalyzed C–C and C–N bond forming reactions: an update on the synthesis of pharmaceuticals from 2015–2020. *Org. Chem. Front.* **2021**, *8*, 384-414.
4. del Pozo, J.; Salas, G.; Álvarez, R.; Casares, J. A.; Espinet, P., The Negishi Catalysis: Full Study of the Complications in the Transmetalation Step and Consequences for the Coupling Products. *Organometallics* **2016**, *35*, 3604-3611.
5. Haas, D.; Hammann, J. M.; Greiner, R.; Knochel, P., Recent Developments in Negishi Cross-Coupling Reactions. *ACS Catal.* **2016**, *6*, 1540-1552.
6. Heravi, M. M.; Hashemi, E.; Nazari, N., Negishi coupling: an easy progress for C–C bond construction in total synthesis. *Mol. Divers.* **2014**, *18*, 441-472.
7. Dombrowski, A. W.; Gesmundo, N. J.; Aguirre, A. L.; Sarris, K. A.; Young, J. M.; Bogdan, A. R.; Martin, M. C.; Gedeon, S.; Wang, Y., Expanding the Medicinal Chemist Toolbox: Comparing Seven C(sp²)–C(sp³) Cross-Coupling Methods by Library Synthesis. *ACS Med. Chem. Lett.* **2020**, *11*, 597-604.
8. Lovering, F.; Bikker, J.; Humblet, C., Escape from Flatland: Increasing Saturation as an Approach to Improving Clinical Success. *J. Med. Chem.* **2009**, *52*, 6752-6756.
9. Lennox, A. J. J.; Lloyd-Jones, G. C., Selection of boron reagents for Suzuki–Miyaura coupling. *Chem. Soc. Rev.* **2014**, *43*, 412-443.

10. For the NIH toxicity report, see: [Nomination Background: Trichloromethylstannane \(CASRN: 993-16-8\) \(nih.gov\)](#)
11. Negishi, E.; King, A. O.; Okukado, N., Selective carbon-carbon bond formation via transition metal catalysis. 3. A highly selective synthesis of unsymmetrical biaryls and diarylmethanes by the nickel- or palladium-catalyzed reaction of aryl- and benzylzinc derivatives with aryl halides. *J. Org. Chem.* **1977**, *42*, 1821-1823.
12. Dai, C.; Fu, G. C., The First General Method for Palladium-Catalyzed Negishi Cross-Coupling of Aryl and Vinyl Chlorides: Use of Commercially Available Pd(P(t-Bu)₃)₂ as a Catalyst. *J. Am. Chem. Soc.* **2001**, *123*, 2719-2724.
13. Fischer, C.; Fu, G. C., Asymmetric Nickel-Catalyzed Negishi Cross-Couplings of Secondary α -Bromo Amides with Organozinc Reagents. *J. Am. Chem. Soc.* **2005**, *127*, 4594-4595.
14. Schley, N. D.; Fu, G. C., Nickel-Catalyzed Negishi Arylations of Propargylic Bromides: A Mechanistic Investigation. *J. Am. Chem. Soc.* **2014**, *136*, 16588-16593.
15. Krasovskiy, A.; Malakhov, V.; Gavryushin, A.; Knochel, P., Efficient Synthesis of Functionalized Organozinc Compounds by the Direct Insertion of Zinc into Organic Iodides and Bromides. *Angew. Chem., Int. Ed.* **2006**, *45*, 6040-6044.
16. Uchiyama, M.; Furuyama, T.; Kobayashi, M.; Matsumoto, Y.; Tanaka, K., Toward a Protecting-Group-Free Halogen-Metal Exchange Reaction: Practical, Chemoselective Metalation of Functionalized Aromatic Halides Using Dianion-type Zincate, tBu₄ZnLi₂. *J. Am. Chem. Soc.* **2006**, *128*, 8404-8405.
17. Milne, J. E.; Buchwald, S. L., An Extremely Active Catalyst for the Negishi Cross-Coupling Reaction. *J. Am. Chem. Soc.* **2004**, *126*, 13028-13032.
18. Han, C.; Buchwald, S. L., Negishi Coupling of Secondary Alkylzinc Halides with Aryl Bromides and Chlorides. *J. Am. Chem. Soc.* **2009**, *131*, 7532-7533.

19. Yang, Y.; Oldenhuis, N. J.; Buchwald, S. L., Mild and General Conditions for Negishi Cross-Coupling Enabled by the Use of Palladacycle Precatalysts. *Angew, Chem., Int. Ed.* **2013**, *52*, 615-619.
20. Arduengo, A. J., III; Harlow, R. L.; Kline, M., A stable crystalline carbene. *J. Am. Chem. Soc.* **1991**, *113*, 361-363.
21. Hadei, N.; Kantchev, E. A. B.; O'Brien, C. J.; Organ, M. G., The First Negishi Cross-Coupling Reaction of Two Alkyl Centers Utilizing a Pd–N-Heterocyclic Carbene (NHC) Catalyst. *Org. Lett.* **2005**, *7*, 3805-3807.
22. Organ, M. G.; Avola, S.; Dubovyk, I.; Hadei, N.; Kantchev, E. A. B.; O'Brien, C. J.; Valente, C., A User-Friendly, All-Purpose Pd–NHC (NHC=N-Heterocyclic Carbene) Precatalyst for the Negishi Reaction: A Step Towards a Universal Cross-Coupling Catalyst. *Chem. Eur. J.* **2006**, *12*, 4749-4755.
23. Çalimsiz, S.; Sayah, M.; Mallik, D.; Organ, M. G., Pd-PEPPSI-IPent: Low-Temperature Negishi Cross-Coupling for the Preparation of Highly Functionalized, Tetra-ortho-Substituted Biaryls. *Angew, Chem., Int. Ed.* **2010**, *49*, 2014-2017.
24. Pompeo, M.; Froese, R. D. J.; Hadei, N.; Organ, M. G., Pd-PEPPSI-IPent^{Cl}: A Highly Effective Catalyst for the Selective Cross-Coupling of Secondary Organozinc Reagents. *Angew, Chem., Int. Ed.* **2012**, *51*, 11354-11357.
25. Thapa, S.; Kafle, A.; Gurung, S. K.; Montoya, A.; Riedel, P.; Giri, R., Ligand-Free Copper-Catalyzed Negishi Coupling of Alkyl-, Aryl-, and Alkynylzinc Reagents with Heteroaryl Iodides. *Angew, Chem., Int. Ed.* **2015**, *54*, 8236-8240.
26. Bedford, R. B.; Carter, E.; Cogswell, P. M.; Gower, N. J.; Haddow, M. F.; Harvey, J. N.; Murphy, D. M.; Neeve, E. C.; Nunn, J., Simplifying Iron–Phosphine Catalysts for Cross-Coupling Reactions. *Angew, Chem., Int. Ed.* **2013**, *52*, 1285-1288.

27. Brown, D. G.; Boström, J., Analysis of Past and Present Synthetic Methodologies on Medicinal Chemistry: Where Have All the New Reactions Gone? *J. Med. Chem.* **2016**, *59*, 4443-4458.
28. Stathakis, C. I.; Bernhardt, S.; Quint, V.; Knochel, P., Improved Air-Stable Solid Aromatic and Heterocyclic Zinc Reagents by Highly Selective Metalations for Negishi Cross-Couplings. *Angew. Chem., Int. Ed.* **2012**, *51*, 9428-9432.
29. Eckert, P.; Sharif, S.; Organ, M. G., Salt to Taste: The Critical Roles Played by Inorganic Salts in Organozinc Formation and in the Negishi Reaction. *Angew. Chem., Int. Ed.* **2021**, *60*, 12224-12241.
30. Sämann, C.; Haag, B.; Knochel, P., Highly Regioselective Preparation of Heteroaryl–Magnesium Reagents by Using a Br/Mg Exchange. *Chem. Eur. J.* **2012**, *18*, 16145-16152.
31. Kondolff, I.; Feuerstein, M.; Doucet, H.; Santelli, M., Synthesis of all-cis-3-(2-diphenylphosphinoethyl)-1,2,4-tris(diphenylphosphinomethyl)cyclopentane (Ditricyp) from dicyclopentadiene. *Tetrahedron* **2007**, *63*, 9514-9521.
32. Roy, D.; Uozumi, Y., Recent Advances in Palladium-Catalyzed Cross-Coupling Reactions at ppm to ppb Molar Catalyst Loadings. *Adv. Synth. Cat.* **2018**, *360*, 602-625.
33. Heravi, M. M.; Zadsirjan, V., Prescribed drugs containing nitrogen heterocycles: an overview. *RSC Adv.* **2020**, *10*, 44247-44311.
34. Yuan, S.; Shen, D.-D.; Jia, R.; Sun, J.-S.; Song, J.; Liu, H.-M., New drug approvals for 2022: Synthesis and clinical applications. *Med. Res. Rev.* **2023**, *43*, 2352-2391.
35. ‘Palladium Prices – Interactive Historical Chart’, MacroTrends, Seattle, USA: [Palladium Prices - Interactive Historical Chart | MacroTrends](#) (Accessed on 18th October, 2023)
36. See [The Periodic Table of Endangered Elements - American Chemical Society \(acs.org\)](#) (Accessed on 18th October, 2023)

37. Lipshutz, B. H.; Ghorai, S.; Abela, A. R.; Moser, R.; Nishikata, T.; Duplais, C.; Krasovskiy, A.; Gaston, R. D.; Gadwood, R. C., TPGS-750-M: A Second-Generation Amphiphile for Metal-Catalyzed Cross-Couplings in Water at Room Temperature. *J. Org. Chem.* **2011**, *76*, 4379-4391.
38. Krasovskiy, A.; Duplais, C.; Lipshutz, B. H., Zn-Mediated, Pd-Catalyzed Cross-Couplings in Water at Room Temperature Without Prior Formation of Organozinc Reagents. *J. Am. Chem. Soc.* **2009**, *131*, 15592-15593.
39. A search of the Available Chemicals Directory reveals 57000 boronic acids alone, along with 400 boronate esters and 1900 trifluoroboronate salts. The same database only reveals 150 organozinc reagents. eMolecule database, [eMolecules](#) (Accessed on 18th October, 2023).
40. Lipshutz, B. H.; Caravez, J. C.; Iyer, K. S., Nanoparticle-catalyzed green synthetic chemistry ... in water. *Curr. Opin. Green Sustain. Chem.* **2022**, *38*, 100686.
41. Handa, S.; Wang, Y.; Gallou, F.; Lipshutz, B. H., Sustainable Fe-ppm Pd nanoparticle catalysis of Suzuki-Miyaura cross-couplings in water. *Science* **2015**, *349*, 1087-1091.
42. Handa, S.; Jin, B.; Bora, P. P.; Wang, Y.; Zhang, X.; Gallou, F.; Reilly, J.; Lipshutz, B. H., Sonogashira Couplings Catalyzed by Fe Nanoparticles Containing ppm Levels of Reusable Pd, under Mild Aqueous Micellar Conditions. *ACS Catal.* **2019**, *9*, 2423-2431.
43. Pang, H.; Hu, Y.; Yu, J.; Gallou, F.; Lipshutz, B. H., Water-Sculpting of a Heterogeneous Nanoparticle Precatalyst for Mizoroki-Heck Couplings under Aqueous Micellar Catalysis Conditions. *J. Am. Chem. Soc.* **2021**, *143*, 3373-3382.
44. Lipshutz, B. H., The 'Nano-to-Nano' Effect Applied to Organic Synthesis in Water. *Johnson Matthey Technol. Rev.*, **2017**, *61*, 196
45. Van Vaerenbergh, B.; Lauwaert, J.; Vermeir, P.; De Clercq, J.; Thybaut, J. W., Chapter One - Synthesis and support interaction effects on the palladium nanoparticle catalyst characteristics. In *Advances in Catalysis*, Song, C., Ed. Academic Press: 2019; Vol. 65, pp 1-120.

46. Zhou, J.; Fu, G. C., Palladium-Catalyzed Negishi Cross-Coupling Reactions of Unactivated Alkyl Iodides, Bromides, Chlorides, and Tosylates. *J. Am. Chem. Soc.* **2003**, *125*, 12527-12530.
47. Tamao, K.; Kiso, Y.; Sumitani, K.; Kumada, M., Alkyl group isomerization in the cross-coupling reaction of secondary alkyl Grignard reagents with organic halides in the presence of nickel-phosphine complexes as catalysts. *J. Am. Chem. Soc.* **1972**, *94*, 9268-9269.
48. Hayashi, T.; Konishi, M.; Kobori, Y.; Kumada, M.; Higuchi, T.; Hirotsu, K., Dichloro[1,1'-bis(diphenylphosphino)ferrocene]palladium(II): an effective catalyst for cross-coupling of secondary and primary alkyl Grignard and alkylzinc reagents with organic halides. *J. Am. Chem. Soc.* **1984**, *106*, 158-163.
49. Kutchukian, P. S.; Dropinski, J. F.; Dykstra, K. D.; Li, B.; DiRocco, D. A.; Streckfuss, E. C.; Campeau, L.-C.; Cernak, T.; Vachal, P.; Davies, I. W.; Krska, S. W.; Dreher, S. D., Chemistry informer libraries: a chemoinformatics enabled approach to evaluate and advance synthetic methods. *Chem. Sci.* **2016**, *7*, 2604-2613.
50. The FDA allowed dose is 10 mg Pd/day. See F. D. A., Q3D Elemental impurities Guidance for Industry, [Q3D\(R2\) Elemental Impurities: International Council for Harmonisation: Guidance for Industry \(fda.gov\)](https://www.fda.gov/oc/ohrt/q3d-elemental-impurities-guidance-for-industry) (Accessed on 18th October, 2023).
51. Joshi-Pangu, A.; Ganesh, M.; Biscoe, M. R., Nickel-Catalyzed Negishi Cross-Coupling Reactions of Secondary Alkylzinc Halides and Aryl Iodides. *Org. Lett.* **2011**, *13*, 1218-1221.
52. Kim, S.; Goldfogel, M. J.; Gilbert, M. M.; Weix, D. J., Nickel-Catalyzed Cross-Electrophile Coupling of Aryl Chlorides with Primary Alkyl Chlorides. *J. Am. Chem. Soc.* **2020**, *142*, 9902-9907.
53. Borlinghaus, N.; Schönfeld, B.; Heitz, S.; Klee, J.; Vukelić, S.; Braje, W. M.; Jolit, A., Enabling Metallophotoredox Catalysis in Parallel Solution-Phase Synthesis Using Disintegrating Reagent Tablets. *J. Org. Chem.* **2021**, *86*, 16535-16547.

54. Delgado, P.; Glass, R. J.; Geraci, G.; Duvadie, R.; Majumdar, D.; Robinson, R. I.; Elmaarouf, I.; Mikus, M.; Tan, K. L., Use of Green Solvents in Metallaphotoredox Cross-Electrophile Coupling Reactions Utilizing a Lipophilic Modified Dual Ir/Ni Catalyst System. *J. Org. Chem.* **2021**, *86*, 17428-17436.
55. Beutner, G. L.; Simmons, E. M.; Ayers, S.; Bemis, C. Y.; Goldfogel, M. J.; Joe, C. L.; Marshall, J.; Wisniewski, S. R., A Process Chemistry Benchmark for sp^2 - sp^3 Cross Couplings. *J. Org. Chem.* **2021**, *86*, 10380-10396.
56. Shen, Z.-L.; Goh, K. K. K.; Yang, Y.-S.; Lai, Y.-C.; Wong, C. H. A.; Cheong, H.-L.; Loh, T.-P., Direct Synthesis of Water-Tolerant Alkyl Indium Reagents and Their Application in Palladium-Catalyzed Couplings with Aryl Halides. *Angew. Chem., Int. Ed.* **2011**, *50*, 511-514.
57. Sheldon, R. A., The E factor 25 years on: the rise of green chemistry and sustainability. *Green Chem.* **2017**, *19*, 18-43.
58. Sheldon, R. A., Metrics of Green Chemistry and Sustainability: Past, Present, and Future. *ACS Sustainable Chem. Eng.* **2018**, *6*, 32-48.
59. Li, X.; Wood, A. B.; Lee, N. R.; Gallou, F.; Lipshutz, B. H., Allylations of aryl/heteroaryl ketones: neat, clean, and sustainable. Applications to targets in the pharma- and nutraceutical industries. *Green Chem.* **2022**, *24*, 4909-4914.
60. Wood, A. B.; Roa, D. E.; Gallou, F.; Lipshutz, B. H., α -Arylation of (hetero)aryl ketones in aqueous surfactant media. *Green Chem.* **2021**, *23*, 4858-4865.
61. Hayashi, Y., Time Economy in Total Synthesis. *J. Org. Chem.* **2021**, *86*, 1-23.
62. Hayashi, Y., Pot economy and one-pot synthesis. *Chem. Sci.* **2016**, *7*, 866-880.

1.3 Appendix

General Information

All commercial reagents were used without further purification unless otherwise noted. The THF used for the preparation of NPs was taken from a solvent purification system (Pure-Solv 400, Innovative Technology, Inc. (now Inert, Inc.)), or distilled using a sodium benzophenone ketyl system. All other solvents were used as received, such as MeOH, EtOAc, hexanes, and Et₂O, unless otherwise noted, and purchased from Fisher Scientific. FeCl₃ (anhydrous, 98%) was purchased from Alfa Aesar (Lot number: D06Q37) and stored in an argon purged glove box. Zinc powder was purchased from Alfa Aesar (~100 mesh, 99.9%, Lot number: Z21B027) and stored in an argon purged glove box. AmPhos was purchased from Sigma-Aldrich (product number 677264). Palladium acetate was purchased from Johnson Matthey and kept in its solid state within a glove box. All palladium catalysts and ligands were stored in an argon purged glove box. Methylmagnesium chloride was purchased from Sigma-Aldrich (product number: 189901) and was titrated precisely. TMEDA was purchased from Sigma-Aldrich ($\geq 99.5\%$, purified by redistillation, product number 411019). A solution of 2 wt % TPGS-750-M in H₂O was prepared by dissolving TPGS-750-M in degassed HPLC grade water and was stored in Schlenk flask under argon. TPGS-750-M was made as previously described¹ and is available from Sigma-Aldrich (catalog number 733857). A standard 2 wt % aqueous solution of TPGS-750-M was typically prepared on a 100 g scale by dissolving 2 g of the TPGS-750-M wax into 98 g of thoroughly degassed¹ (steady stream of argon, minimum of 12 h bubbling time with stirring and heating) HPLC grade water in a Schlenk flask equipped with a stir bar and allowed to

dissolve overnight with vigorous stirring under argon pressure (NOTE: Do not attempt to degas the aqueous phase with surfactant wax submerged; vigorous foaming to the point of overflowing will occur). The 2 wt % TPGS-750-M/H₂O solution, once prepared, was always kept in a Schlenk flask. Thin layer chromatography (TLC) was done using Silica Gel 60 F254 plates (0.25 mm thick) purchased from Merck. Column chromatography was done in glass columns using Silica gel 60 (EMD, 40-63 μm) or with pre-packed 25-gram KP-Sil Biotage[®] SNAP Cartridges on the Biotage[®] Isolera One autocolumn. GC-MS data was recorded on an Agilent Technologies 7890A GC system coupled with Agilent Technologies 5975C mass spectrometer using HP-5MS column (30 m × 0.250 mm, 0.25 μ) purchased from Agilent Technologies. ¹H, ¹³C, and ¹⁹F NMR spectra were recorded at 25 °C on a Agilent Technologies 400 MHz, a Varian Unity Inova 500 MHz, Varian Unity Inova 600 MHz, Bruker Avance III HD 400 MHz or Bruker Avance NEO 500 MHz spectrometer in CDCl₃ with residual CHCl₃ (¹H = 7.26 ppm, ¹³C = 77.16 ppm) or in DMSO-d₆ with residual (CH₃)₂SO (¹H = 2.50 ppm, ¹³C = 39.52 ppm) as internal standards. Chemical shifts are reported in parts per million (ppm). NMR Data are reported as follows: chemical shift, multiplicity (s = singlet, d = doublet, dd = doublet of doublets, ddd = doublet of doublet of doublets, t = triplet, td = triplet of doublets, q = quartet, quin = quintet, m = multiplet), coupling constant (if applicable), and integration. Chemical shifts in ¹³C NMR spectra are reported in ppm on the δ scale from the central peak of residual CDCl₃ (77.16 ppm) or the central peak of DMSO-d₆ (39.52 ppm). High-resolution mass analyses (HRMS) were recorded on Waters GCT Premier GC TOF or Agilent 6230 TOF LC/MS System. STEM images were obtained using ThermoFisher Talos G2 200X TEM/STEM w/ChemiSTEM EDS. Cryo-TEM images were obtained using FEI Tecnai G2 Sphera 200kV EDX. DLS

analysis was obtained using DynaPro NanoStar™ from Wyatt Technology under 662 nm laser wavelength.

Optimization of the preparation of Fe/ppm Pd NPs

General procedure for preparation of in situ-derived Fe/ppm Pd NPs:

In an oven dried 4 mL microwave reaction vial purged with argon, covered with a rubber septum containing a PTFE-coated magnetic stir bar, 0.1 mL dry THF solution of 0.1 M FeCl₃ (5 mol %, 0.01 mmol), 0.25 mL dry THF solution of 0.002 M Pd(OAc)₂ (0.25 mol %, 0.0005 mmol) and 0.05 mL dry THF solution of 0.2 M AmPhos (5 mol %, 0.01 mmol) were added under a stream of dry argon. While maintaining a dry atmosphere at rt, a 1 M solution of MeMgCl in THF was very slowly (1 drop/2 sec) added to the reaction mixture. After complete addition of the Grignard reagent, the mixture was stirred for an additional 15 min at rt. The NPs formed were collected and need to be stored under argon.

General procedure for Negishi couplings: optimization

4-Bromoacetophenone (39.8 mg, 0.2 mmol, 1 equiv) and zinc (52.0 mg, 0.8 mmol, 4.0 equiv) were added to the vial with the in situ-prepared Fe/ppm Pd NPs under a continuous argon flow. The reaction vial was closed with a septum under argon, followed by sequential addition of an aqueous solution 2 wt % TPGS-750-M in H₂O (1.0 mL), 3-phenoxypropyl bromide (0.13 mL, 0.8 mmol, 4.0 equiv), and TEMDA (0.15 mL, 1.0 mmol, 5.0 equiv) via syringe through the rubber septum. The reaction vial was stirred vigorously at rt for 16 h. After 16 h, EtOAc (3 x 2 mL) was added, and the mixture was gently stirred for 2 min at rt. Stirring was then stopped and the vial with the organic layer was decanted via pipette with

aid of a centrifuge. The organic layer was passed through a very small silica plug in a pipette.

Yields were determined by GCMS using naphthalene as internal standard.

Table S1. Optimization of the source of palladium

Entry ^a	FeCl ₃ / mol %	Pd(OAc) ₂ / mol %	AmPhos / 5 mol %	MeMgCl (equiv) ^b	Yield(%) ^c
1	FeCl ₃ / 5	Pd(OAc) ₂ / 0.25	-	4.0	46
2	FeCl ₃ / 5	Pd(<i>P</i> t-Bu ₃) ₂ / 0.25	-	4.0	17
3	FeCl ₃ / 5	Pd(PPh ₃) ₄ / 0.25	-	4.0	8
4	FeCl ₃ / 5	Pd(DTBPP) ₂ / 0.25	-	4.0	15
5	FeCl ₃ / 5	Pd(<i>dba</i>) ₂ / 0.25	-	4.0	12
6	FeCl ₃ / 5	Pd(AmPhos) ₂ / 0.25	-	4.0	14
7	FeCl ₃ / 5	[Pd(π -allyl)Cl] ₂ / 0.125	-	4.0	16
8	FeCl ₃ / 5	[Pd(π -cinnamyl)Cl] ₂ / 0.125	-	4.0	21
9	FeCl ₃ / 5	PdCl ₂ / 0.25	-	4.0	4
10	FeCl ₃ / 5	Pd(acac) ₂ / 0.25	-	4.0	16
11	FeCl ₃ / 5	Pd(AmPhos) ₂ Cl ₂ / 0.25	-	4.0	25
12	FeCl ₃ / 5	Pd(dppf)Cl ₂	-	4.0	NR
13	FeCl ₃ / 5	PEPPSI-IPr / 0.25	-	4.0	2

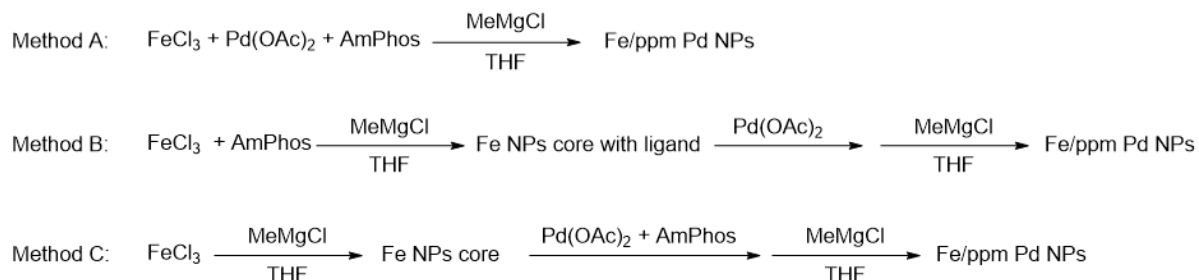
^a Conditions: 4-bromoacetophenone (0.2 mmol), 3-phenoxypropyl bromide (0.6 mmol), zinc dust (0.8 mmol), Fe/ppm Pd NPs, TMEDA (1.0 mmol), 2 wt % TPGS-750-M in H₂O (1.0 mL), rt, 16 h

^b Amount relative to FeCl₃

^c Yield determined by GC-MS; naphthalene as standard, NR = no reaction;

Scheme S1. Optimization of preparation procedure

NPs preparation:



General procedure for preparation of in situ-derived Fe/ppm Pd NPs; Method A

In an oven dried 4 mL microwave reaction vial purged with argon, covered with a rubber septum containing a PTFE-coated magnetic stir bar, 0.1 mL dry THF solution of 0.1 M FeCl_3 (5 mol %, 0.01 mmol), 0.25 mL dry THF solution of 0.002 M $\text{Pd}(\text{OAc})_2$ (0.25 mol %, 0.0005 mmol) and 0.05 mL dry THF solution of 0.2 M AmPhos (5 mol %, 0.01 mmol) were added under dry argon pressure. While maintaining a dry atmosphere at rt, a 1 M solution of MeMgCl in THF was very slowly (1 drop/2 sec) added to the reaction mixture. After complete addition of the Grignard reagent, the mixture was stirred for an additional 15 min at rt. The NPs need to be stored under argon.

General procedure for preparation of in situ-derived Fe/ppm Pd NPs; Method B

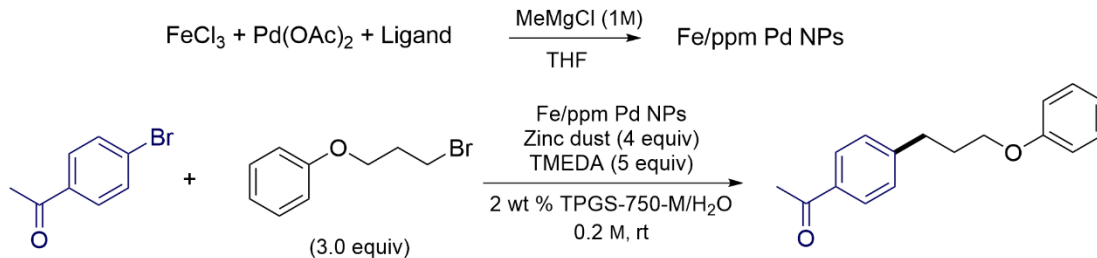
In an oven dried 4 mL microwave reaction vial purged with argon, covered with a rubber septum containing a PTFE-coated magnetic stir bar, 0.1 mL dry THF solution of 0.1 M FeCl_3 (5 mol %, 0.01 mmol), and 0.05 mL dry THF solution of 0.2 M AmPhos (5 mol %, 0.01 mmol) were added under dry argon pressure. While maintaining a dry atmosphere at rt, 0.02 mL 1 M solution of MeMgCl in THF was very slowly (1 drop/2 sec) added to the reaction mixture. Then the mixture was stirred for an additional 1 min at rt. After that time,

0.25 mL dry THF solution of 0.002 M Pd(OAc)₂ (0.25 mol %, 0.0005 mmol) was added to the reaction mixture. After addition, additional 0.02 mL 1 M solution of MeMgCl in THF was very slowly (1 drop/2 sec) added to the reaction mixture. After complete addition of the Grignard reagent, the mixture was stirred for an additional 15 min at rt. The NPs need to be stored under argon.

General procedure for preparation of in situ-derived Fe/ppm Pd NPs; Method C

In an oven dried 4 mL microwave reaction vial purged with argon, covered with a rubber septum containing a PTFE-coated magnetic stir bar, 0.1 mL dry THF solution of 0.1 M FeCl₃ (5 mol %, 0.01 mmol), were added under dry argon pressure. While maintaining a dry atmosphere at rt, 0.02 mL 1 M solution of MeMgCl in THF was very slowly (1 drop/2 sec) added to the reaction mixture. Then the mixture was stirred for an additional 1 min at rt. After that time, 0.25 mL dry THF solution of 0.002 M Pd(OAc)₂ (0.25 mol %, 0.0005 mmol) and 0.05 mL dry THF solution of 0.2 M AmPhos (5 mol %, 0.01 mmol) was added to the reaction mixture. After addition, additional 0.02 mL 1 M solution of MeMgCl in THF was very slowly (1 drop/2 sec) added to the reaction mixture. After complete addition of the Grignard reagent, the mixture was stirred for an additional 15 min at rt. The NPs need to be stored under argon.

Table S4. Optimization of different sequences to make NPs



Entry ^a	Method to make NPs	Yield(%) ^b
1	A	46
2	B	15
3	C	21

^a Conditions: 4-bromoacetophenone (0.2 mmol), 3-phenoxypropyl bromide (0.6 mmol), zinc dust (0.8 mmol), Fe/ppm Pd NPs, TMEDA (1.0 mmol), 2 wt % TPGS-750-M in H₂O (1.0 mL), rt, 16 h

^b Yield determined by GC-MS; naphthalene as standard, NR = no reaction;

Optimization of reagents addition sequence

General procedure for optimization of reaction conditions for a Fe/ppm Pd NPs catalyzed Negishi reaction; **Sequence A**

4-(6-Bromopyridin-3-yl)morpholine (48.6 mg, 0.2 mmol, 1 equiv) and zinc (52 mg, 0.8 mmol, 4 equiv) were added to a oven dried 1-dram vial followed by sequential addition of optimized Fe/ppm NPs (15.5 mg, 0.25 mol % Pd). The reaction vial was sealed with a rubber septum inside of the glovebox. A 2 wt % TPGS-750-M in H₂O solution, 3-phenoxypropyl bromide (0.4–1.0 mmol) and TMEDA (0.15 mL, 1.0 mmol, 5 equiv) were added to the vial by syringe and the mixture was stirred vigorously at rt for 16 h. After 16 h, EtOAc (3 x 2 mL) was added and the mixture stirred gently for 2 min at rt. Stirring was then stopped and the organic layer was decanted via pipette after centrifugation. The organic

layer was passed through a very small silica plug. Yields were determined by GCMS using naphthalene as internal standard or isolated.

Sequence B

To a flame dried 1-dram vial equipped with an oven dried stir bar inside of a glove box was added optimized Fe/ppm NPs (15.5 mg, 0.25 mol % Pd). The vial was then sealed with a rubber septum inside of the glovebox. A 2 wt % TPGS-750-M in H₂O solution was added to the vial by syringe and the mixture was stirred vigorously at rt for indicated time. Then 4-(6-bromopyridin-3-yl)morpholine (48.6 mg, 0.2 mmol, 1 equiv) and 3-phenoxypropyl bromide (0.4–1.0 mmol) were added to the vial under argon flow. The vial was then sealed with rubber septum under argon flow and stirred for 15 min. Then zinc (52 mg, 0.8 mmol, 4 equiv) and TMEDA (0.15 mL, 1.0 mmol, 5 equiv) were added to the vial under argon flow. The vial was then sealed with rubber septum under argon flow and stirred vigorously at rt for 16 h. After 16 h, EtOAc (3 x 2 mL) was added and the mixture stirred gently for 2 min at rt. Stirring was then stopped and the organic layer was decanted via pipette after centrifugation. The organic layer was passed through a very small silica plug. Yields were determined by GCMS using naphthalene as internal standard or isolated.

Sequence C

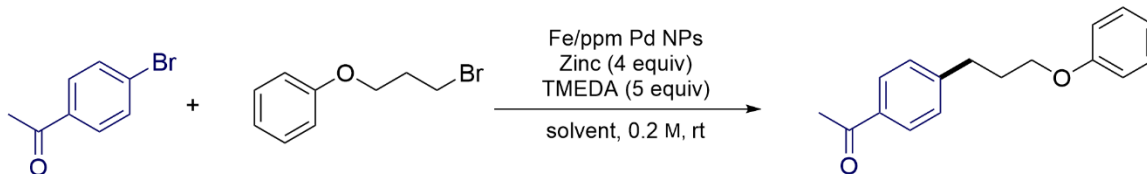
To a flame dried 1-dram vial equipped with an oven dried stir bar inside of a glove box was added optimized Fe/ppm NPs (15.5 mg, 0.25 mol % Pd). The vial was then sealed with a rubber septum inside of the glovebox. A 2 wt % TPGS-750-M/H₂O solution was added to the vial by syringe and the mixture was stirred vigorously at rt for indicated time. Then 4-(6-bromopyridin-3-yl)morpholine (48.6 mg, 0.2 mmol, 1 equiv) and zinc (52 mg, 0.8 mmol, 4

equiv) were added to the vial under argon flow. The vial was then sealed with rubber septum under argon flow and stirred for 15 min. Then 3-phenoxypropyl bromide (0.4–1.0 mmol) and TMEDA (0.15 mL, 1.0 mmol, 5 equiv) were added to the vial via syringe. The vial was then stirred vigorously at rt for 16 h. After 16 h, EtOAc (3 x 2 mL) was added and the mixture stirred gently for 2 min at rt. Stirring was then stopped and the organic layer was decanted via pipette after centrifugation. The organic layer was passed through a very small silica plug. Yields were determined by GCMS using naphthalene as internal standard or isolated.

Optimization of surfactants

To a flame dried 1-dram vial equipped with an oven dried stir bar inside of a glove box was added optimized Fe/ppm NPs (15.5 mg, 0.25 mol % Pd). The vial was then sealed with a rubber septum inside the glovebox. An aqueous surfactant solution was added to the vial by syringe and the mixture was stirred vigorously at rt for 1 h. Then 4-(6-bromopyridin-3-yl)morpholine (48.6 mg, 0.2 mmol, 1 equiv) and zinc (52 mg, 0.8 mmol, 4 equiv) were added to the vial under argon flow. The vial was then sealed with rubber septum under argon flow and stirred for 15 min. Then 3-phenoxypropyl bromide (0.1 mL, 0.6 mmol, 3 equiv) and TMEDA (0.15 mL, 1.0 mmol, 5 equiv) were added to the vial via syringe. The vial was then stirred vigorously at rt for 16 h. After 16 h, EtOAc (3 x 2 mL) was added and the mixture stirred gently for 2 min at rt. Stirring was then stopped and the organic layer was decanted via pipette after centrifugation. The solvent was removed using rotary evaporation. Yields were determined by ¹H NMR using ethylene carbonate as internal standard.

Table S3. Further optimization on reaction conditions



Entry ^a	Solvent	Yield(%) ^b
1	2 wt % TPGS-750-M/H ₂ O	86
2	degassed water	23
3	2 wt % Triton X-100/H ₂ O	61
4	2 wt % TWEEN 40/H ₂ O	66
5	2 wt % MC-1/H ₂ O	39
6	2 wt % Brij 30/H ₂ O	78
7	2 wt % cremorphor/H ₂ O	72
8	4 wt % TPGS-750-M/H ₂ O	83
9	4 wt % Brij 30/H ₂ O	80
10	4 wt % cremorphor/H ₂ O	74

^a Conditions: 4-bromoacetophenone (0.2 mmol), 3-phenoxypropyl bromide (0.6 mmol), Fe/ppm Pd NPs (15.5 mg, containing 0.25 mol % Pd), zinc dust (0.8 mmol), TMEDA (1.0 mmol), solvent (1.0 mL), rt, 16 h

^b Yield determined by ¹H-NMR; ethylene carbonate as internal standard

Titration of MeMgCl in THF solution with LiCl/I₂

To an oven dried 25 mL round bottom flask, anhydrous LiCl (424 mg, 10 mmol) was added under an argon atmosphere in the glovebox. The flask was sealed with a rubber septum, and 20 mL dry THF was added by syringe and the mixture was stirred at rt until the LiCl was completely dissolved, resulting in the formation of a 0.5 M solution of LiCl in THF.

A 10 mL microwave vial equipped with a magnetic stirring bar and a septum was heated with a heat gun under reduced pressure and cooled to rt under an argon atmosphere. In the

glovebox, the dry microwave vial was charged with accurately weighed I₂ (127 mg, 0.5 mmol) and capped with a rubber septum. The saturated solution of LiCl in THF (2 mL) was added and stirring was started. After the iodine was completely dissolved, the resulting brown solution was cooled to 0 °C in an ice bath. Another 5 mL round bottom flask equipped with a magnetic stirring bar and a septum was heated with a heat gun under reduced pressure and cooled to rt under an argon atmosphere. To this round bottom flask, methyl magnesium chloride solution (from Sigma-Aldrich, catalog No. 189901; 3 mL) and dry THF (6 mL) were added by syringe and then stirred. To the vial with I₂, the methyl magnesium chloride solution was added dropwise via a 1.00 mL syringe (0.01 mL graduation) until the brown color disappeared. The amount consumed contains 1 equiv of the methyl magnesium chloride relative to iodine. The MeMgCl solution was titrated five times.

Final Optimized Procedure for the Preparation of Fe/ppm Pd Nanoparticles

In an oven dried round-bottomed flask, FeCl₃ (115.4 mg, 0.71 mmol), AmPhos (189 mg, 0.71 mmol) and Pd(OAc)₂ (8 mg, 0.036 mmol) was added under an atmosphere of argon in glove box. The flask was covered with a septum, and 3.0 mL dry THF was added by syringe. The reaction mixture was stirred for 15 min at rt. While maintaining a dry atmosphere at rt, a 1 M solution of MeMgCl in THF was very slowly (1 drop/2 sec) added to the reaction mixture (2.06 mL, 2.06 mmol). And then, the mixture was stirred for an additional 15 min at rt. (The solution of MeMgCl in THF was titrated by LiCl/I₂, and needs to be added precisely. The NPs are not active if more or less MeMgCl is added during their formation). THF was then evaporated under reduced pressure at rt to provide black

nanomaterial as a powder. The Fe nanoparticles obtained were dried under reduced pressure at rt for 10 min yielding 1.12 g Fe/ppm Pd NPs. These nanoparticles need to be stored under argon in a glovebox. The material was used as such for subsequent reactions under micellar conditions.

General procedure for Negishi coupling reactions

To a flame dried 1-dram vial equipped with an oven dried stir bar inside of a glove box was added optimized Fe/ppm NPs (15.5 mg, 0.25 mol % Pd) in the glovebox. The vial was then sealed with a rubber septum inside of the glovebox. A 2 wt % TPGS-750-M/H₂O solution was added to the vial by syringe and the mixture was stirred vigorously at rt for 1 h. Then aryl bromide (0.2 mmol, 1 equiv) and zinc (52 mg, 0.8 mmol, 4 equiv) were added to the vial under argon flow. The vial was then sealed with rubber septum under argon flow and stirred for 15 min. Then alkyl bromide (0.6–1.0 mmol) and TMEDA (0.15 mL, 1.0 mmol, 5 equiv) were added to the vial via syringe. The vial was then stirred vigorously at rt or 45 °C for indicated time. Then, EtOAc was added and the mixture stirred gently for 2 min at rt. Stirring was then stopped and the organic layer was decanted via pipette after centrifugation. The same extraction procedure was repeated twice. The combined organic extracts were dried under reduced pressure and purified by flash chromatography over silica gel.

Analyses of nanoparticles (NPs)

STEM (BF and HADDF) and EDX for Fe/ppm Pd NP dry powder

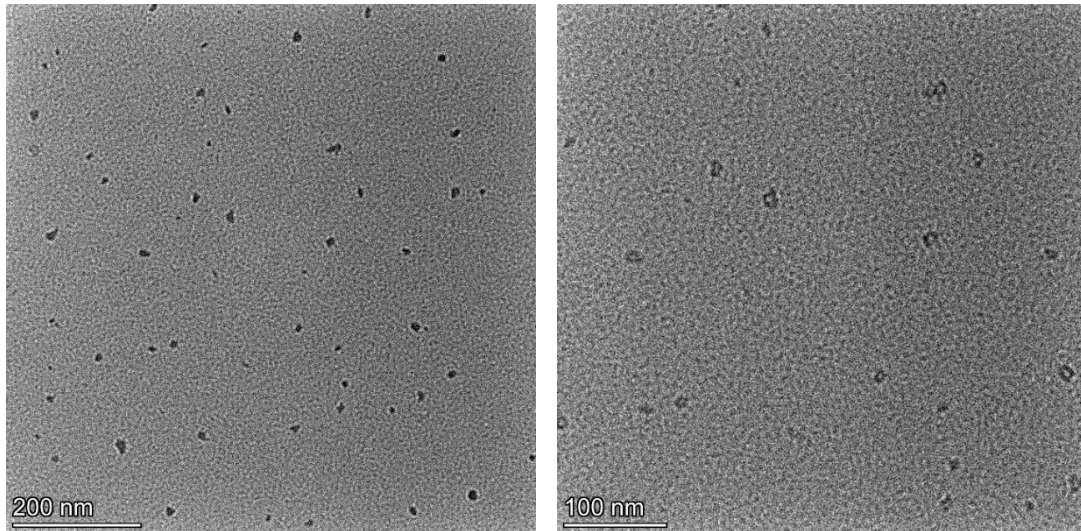
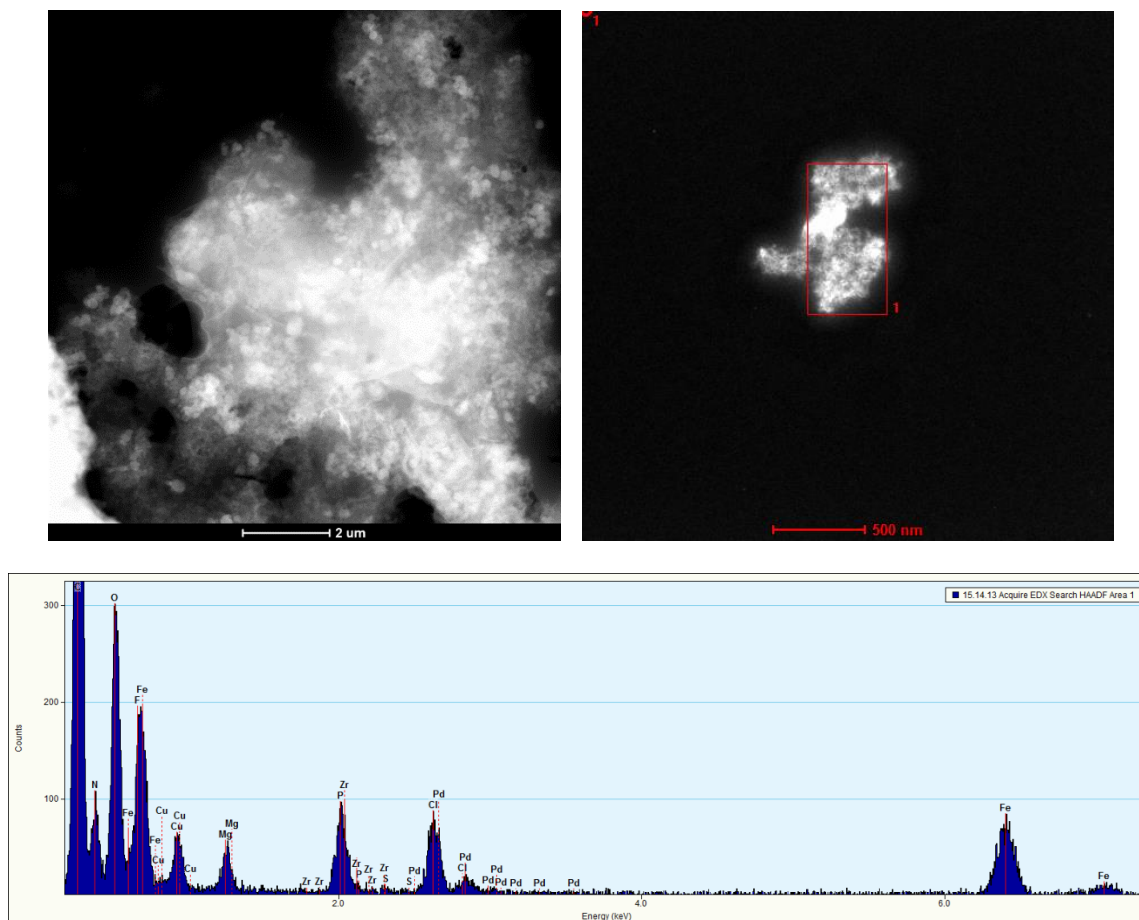


Figure S1. (A) Bright Field TEM image for nanoparticle dry powder on a 200 nm scale. (B) Bright Field TEM image for nanoparticle dry powder on a 100 nm scale.



Quantification Results

Correction method: None

Element	Weight %	Atomic %	Uncert. %	Detector Correction	k-Factor
C(K)	57.23	74.62	0.58	0.28	3.601
N(K)	5.36	5.99	0.17	0.28	3.466
O(K)	9.87	9.66	0.17	0.51	1.889
F(K)	2.74	2.25	0.16	0.63	1.573
Mg(K)	1.01	0.65	0.03	0.88	1.050
P(K)	2.12	1.07	0.06	0.90	1.067
S(K)	0.00	0.00	NaN.00	0.93	1.021
Cl(K)	1.95	0.86	0.05	0.95	1.063
Fe(K)	3.55	0.99	0.07	0.99	1.401
Cu(K)	14.83	3.65	0.17	0.99	1.663
Zr(K)	0.72	0.12	0.06	0.99	3.728
Pd(L)	0.56	0.08	0.04	0.95	2.596

Figure S2. (A) HADDF STEM image for nanoparticle dry powder aggregates on a 2 μm scale. (B) HADDF STEM image for nanoparticle dry powder aggregates on a 500 nm scale. (C) EDX analysis spectrum for nanoparticle dry powder. (D) EDX quantification results for nanoparticle dry powder.

STEM (BF) Fe/ppm Pd nanoparticles in pure degassed water

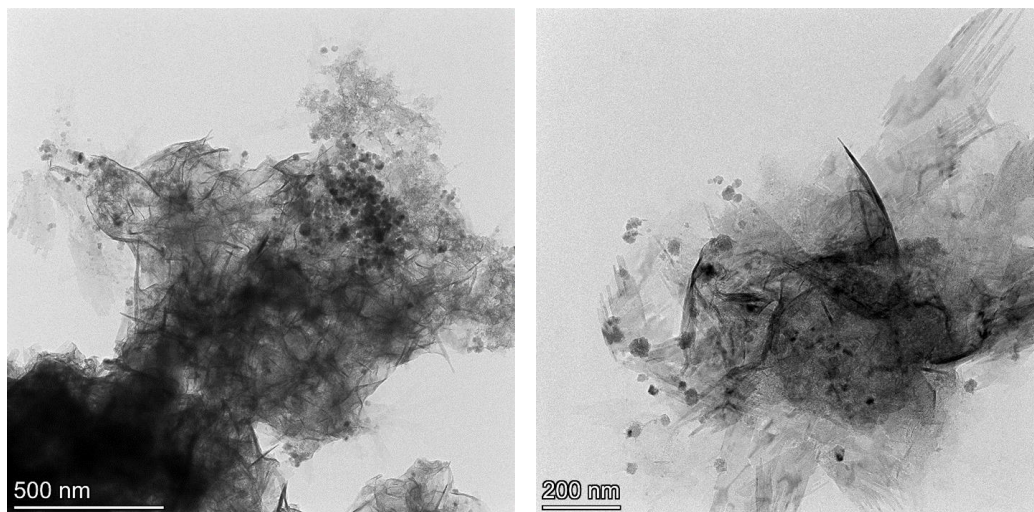


Figure S3. (A) Bright Field TEM image for nanoparticle in degassed water in 500 nm scale. (B) Bright Field TEM image for nanoparticle in degassed water in 200 nm scale.

STEM (BF and HADDF) image and EDX for Fe/ppm Pd nanoparticles in 2 wt % TPGS-750-M/H₂O solution

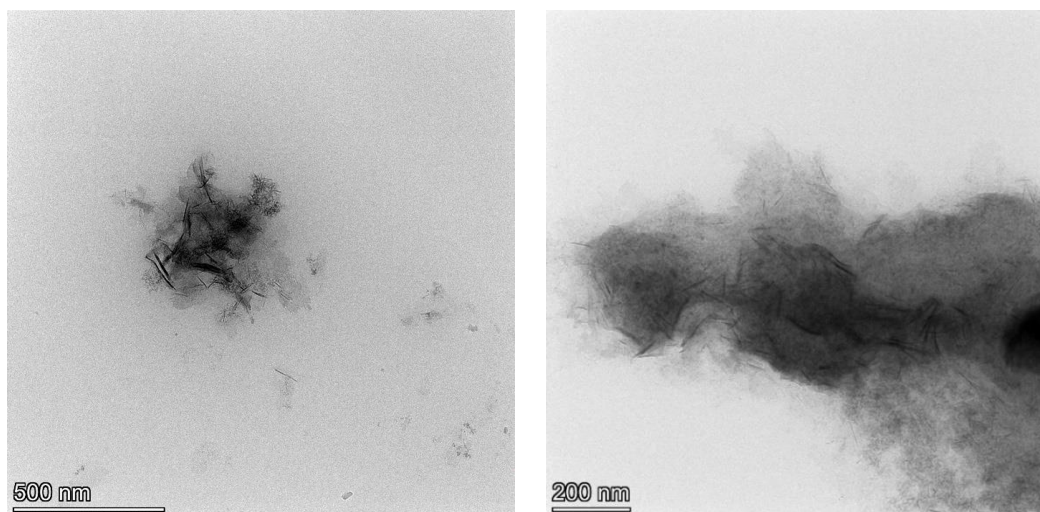
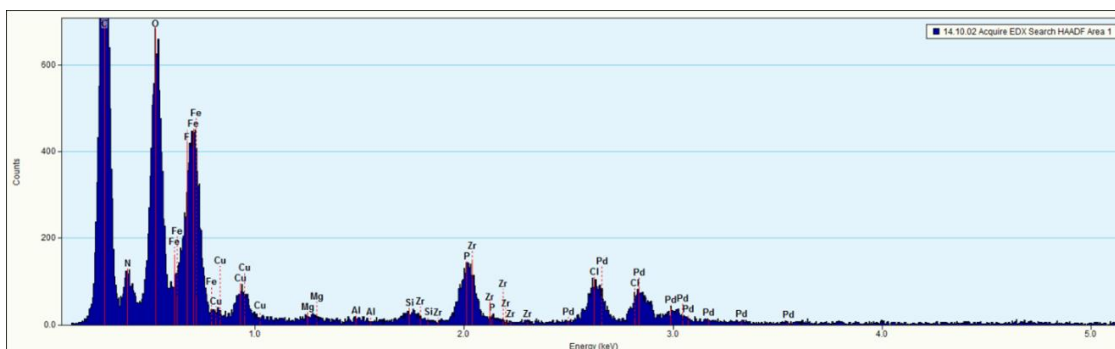
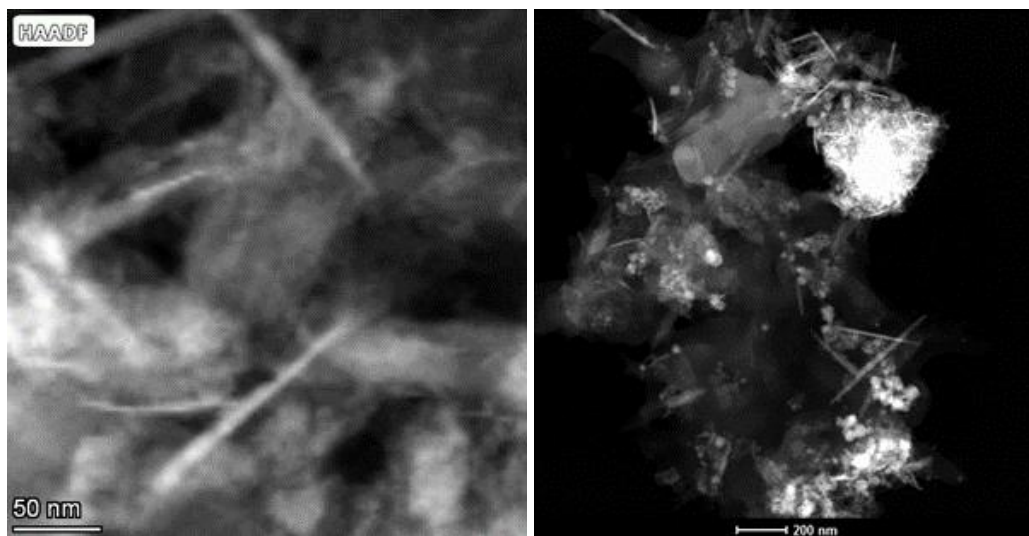


Figure S4. (A) Bright Field TEM image for nanoparticle in 2 wt % TPGS-750-M/H₂O solution on a 500 nm scale. (B) Bright Field TEM image for nanoparticle in 2 wt % TPGS-750-M/H₂O solution on a 200 nm scale.



Quantification Results

Correction method: None

Element	Weight %	Atomic %	Uncert. %	Detector Correction	k-Factor
C(K)	39.04	60.47	0.44	0.28	3.601
N(K)	4.03	5.35	0.14	0.28	3.466
O(K)	14.32	16.65	0.18	0.51	1.889
F(K)	5.64	5.52	0.14	0.63	1.573
Mg(K)	0.08	0.06	0.01	0.88	1.050
P(K)	2.68	1.61	0.07	0.90	1.067
S(K)	0.00	0.00	NaN	0.93	1.021
Cl(K)	1.64	0.86	0.04	0.95	1.063
Fe(K)	13.18	4.38	0.13	0.99	1.401
Cu(K)	13.92	4.07	0.15	0.99	1.663
Zr(K)	1.17	0.24	0.04	0.99	3.728
Pd(L)	4.25	0.74	0.07	0.95	2.596

Figure S5. (A) HADDF STEM image for nanoparticles in 2 wt % TPGS-750-M/H₂O solution on a 50 nm scale. (B) HADDF STEM image for nanoparticles in 2 wt % TPGS-750-M/H₂O solution on a 200 nm scale. (C) EDX analysis spectrum for nanoparticles in 2 wt % TPGS-750-M/H₂O solution. (D) EDX quantification results for nanoparticles in 2 wt % TPGS-750-M/H₂O solution.

Cryo-TEM image for NPs in 2 wt % TPGS-750-M/H₂O solution

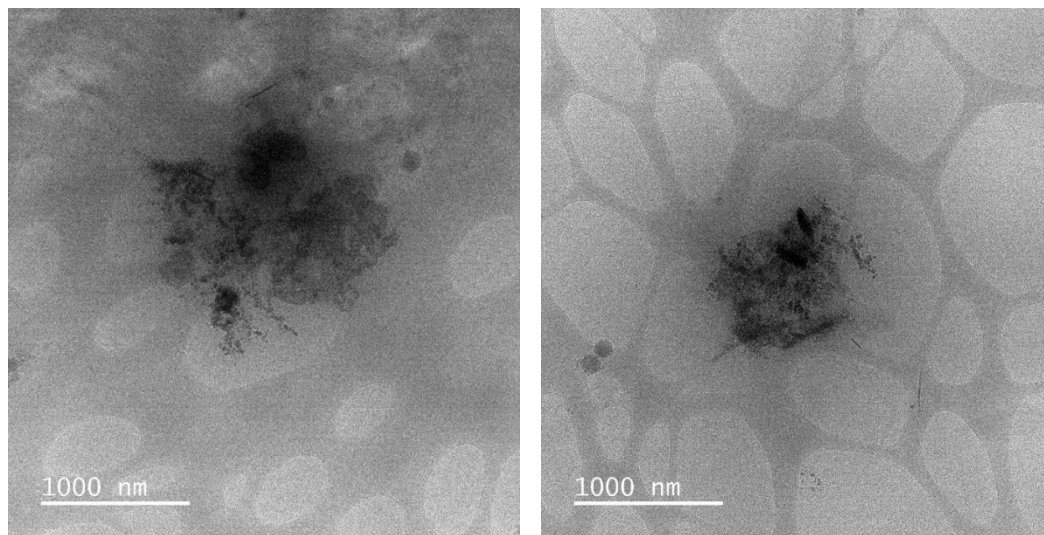


Figure S7. Cryo-TEM images for nanoparticle in 2 wt % TPGS-750-M/H₂O solution on a 1000 nm scale.

Dynamic Light Scattering (DLS) analysis for NPs in degassed water

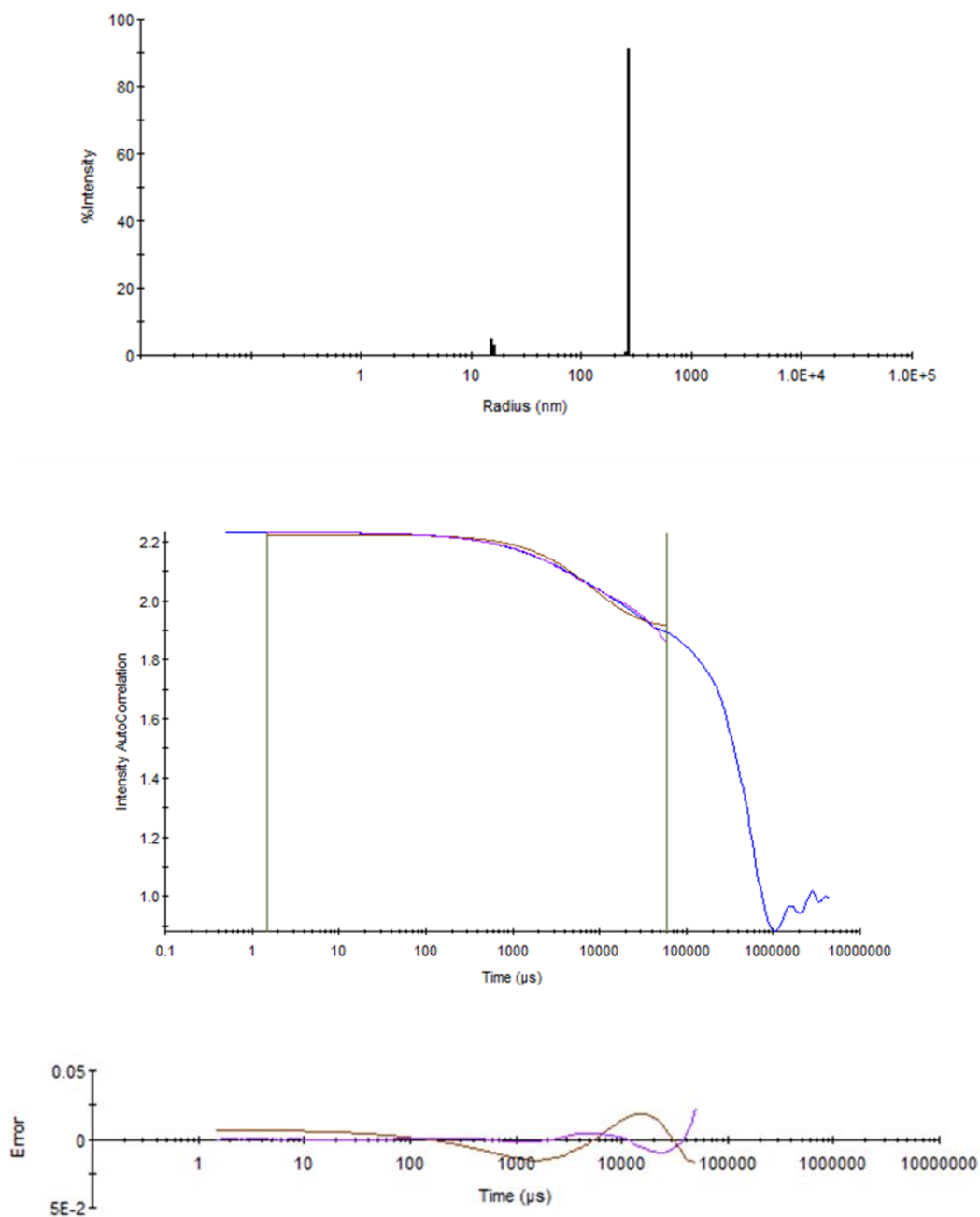
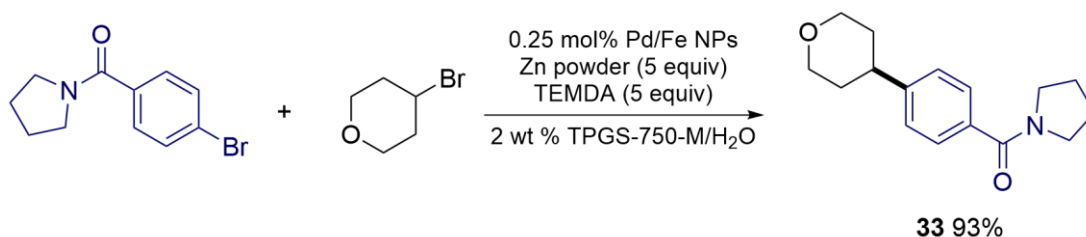


Figure S8. (A) DLS (dynamic light scattering) radius analysis for sample containing nanoparticles in 2 wt % TPGS-750-M/H₂O. (B) Intensity correlation for sample containing nanoparticles in 2 wt % TPGS-750-M/H₂O. (C) Error for sample containing nanoparticles in 2 wt % TPGS-750-M/H₂O.

Table S4 DLS analysis for sample containing nanoparticles in 2 wt % TPGS-750-M/H₂O

Peak	Radius (nm)	Mw-R (kDa)	% Intensity	% Mass	% Number
Peak 1 (True)	1.4	7.8	1	60	98.3
Peak 2 (True)	5	145.5	28.2	39.5	1.7
Peak 3 (True)	35.1	13937.5	20.7	0.1	0
Peak 4 (True)	162.8	503156.3	50.1	0.3	0

E Factor evaluation



To a flame dried 1-dram vial equipped with an oven dried stir bar inside a glove box was added optimized Fe/ppm NPs (15.5 mg, 0.25 mol % Pd). The vial was then sealed with a rubber septum. A 2 wt % TPGS/H₂O solution was added to the vial by syringe and the mixture was stirred vigorously at rt for 1 h. Then (4-bromophenyl)(pyrrolidin-1-yl)methanone (50.8 mg, 0.2 mmol) and zinc (65 mg, 1.0 mmol, 5 equiv) were added to the vial under an argon flow. The vial was then sealed with a rubber septum under an argon flow and stirred for 15 min. Then 4-bromotetrahydro-2H-pyran (99 mg, 0.6 mmol) and TMEDA (0.15 mL, 1.0 mmol, 5 equiv) were added to the vial via syringe. The vial was then stirred vigorously at 45 °C for 72 h. After 72 h, the septum was removed and the reaction mixture was then filtered through a short pipette blocked with cotton. The solid in the pipette was washed with 1 mL DI water. The liquid was concentrated in vacuo and purified

by flash chromatography over silica gel to give 48.3 mg (93%) pyrrolidin-1-yl(4-(tetrahydro-2H-pyran-4-yl)phenyl)methanone as a colorless oil.

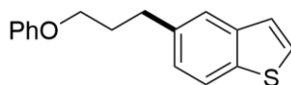
E factor calculation (this work):

$$\begin{aligned} \text{E factor} &= \frac{\text{mass of organic wastet}}{\text{mass of product}} \\ &= \frac{\text{mass of excess alkyl bromide} + \text{mass of TEMDA}}{\text{mass of product}} \\ &= \frac{66 \text{ mg} + 116.2 \text{ mg}}{48.3 \text{ mg}} \\ &= 3.77 \end{aligned}$$

E factor calculation (literature):

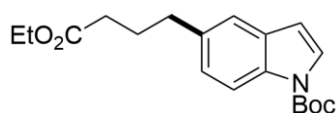
$$\begin{aligned} \text{E factor} &= \frac{\text{mass of organic wastet}}{\text{mass of product}} \\ &= \frac{\text{mass of IPAc} + \text{mass of excess alkyl bromide} + \text{mass of TTMSS} + \text{mass of collidine}}{\text{mass of product}} \\ &= \frac{2180 \text{ mg} + 20 \text{ mg} + 136.76 \text{ mg} + 363.5 \text{ mg}}{31 \text{ mg}} \\ &= 87 \end{aligned}$$

Residual metal as measured by ICP-MS



To a flame-dried 1-dram vial equipped with an oven dried stir bar inside a glove box was added optimized Fe/ppm NPs (15.5 mg, 0.25 mol % Pd). The vial was then sealed with a rubber septum inside of the glovebox. A 2 wt % TPGS-750-M/H₂O solution was added to the vial by syringe and the mixture was stirred vigorously at rt for 1 h. Then 5-

bromobenzo[b]thiophene (42.6 mg, 0.2 mmol) and zinc (52 mg, 0.8 mmol, 4 equiv) were added to the vial under argon flow. The vial was then sealed with a rubber septum under an argon flow and stirred for 15 min. Then (3-bromopropoxy)benzene (0.10 mL, 0.6 mmol) and TMEDA (0.15 mL, 1.0 mmol, 5 equiv) were added to the vial via syringe. The vial was then stirred vigorously at rt for 16 h. Then 1.0 mL MTBE was added and the mixture stirred gently for 2 min at rt. Stirring was then stopped and the organic layer was decanted via pipette after centrifugation. The same extraction procedure was repeated twice. The combined organic extracts were dried over anhydrous Na₂SO₄ and the solvent removed under reduced pressure and the crude material then purified by flash chromatography with pre-packed 100-gram KP-Sil Biotage[®] SNAP Cartridges on the Biotage[®] Isolera One autocolumn to obtain 5-(3-phenoxypropyl)benzo[b]thiophene (HYT-2-20-6) (51.1 mg, 95 %). The product was sealed in a 4 mL vial and sent to the UC Center for Environmental Implications of Nanotechnology at the University of California, Los Angeles, to get ICP-MS analysis.



To a flame dried 1-dram vial equipped with an oven dried stir bar inside of a glove box was added optimized Fe/ppm NPs (15.5 mg, 0.25 mol % Pd). The vial was then sealed with a rubber septum. A 2 wt % TPGS-750-M/H₂O solution was added to the vial by syringe and the mixture was stirred vigorously at rt for 1 h. Then *t*-butyl 5-bromo-1H-indole-1-carboxylate (59.2 mg, 0.2 mmol) and zinc (65 mg, 1.0 mmol, 5 equiv) were added to the vial under an argon flow. The vial was then sealed with a rubber septum under an argon flow and then stirred for 15 min. Then ethyl 4-bromobutanoate (0.11 mL, 0.8 mmol) and TMEDA

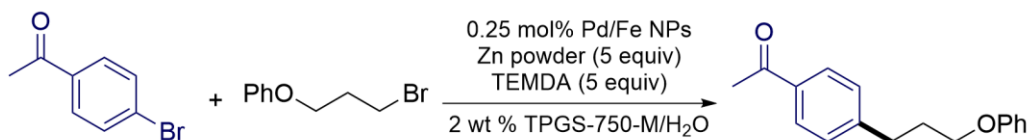
(0.15 mL, 1.0 mmol, 5 equiv) were added to the vial via syringe. The vial was then stirred vigorously at 45 °C for 16 h. Then 1.0 mL MTBE was added, and the mixture stirred gently for 2 min at rt. Stirring was then stopped and the organic layer was decanted via pipette after centrifugation. The same extraction procedure was repeated twice. The combined organic extracts were dried over anhydrous Na₂SO₄ and the solvent removed under reduced pressure and the crude material was purified by flash chromatography with pre-packed 100-gram KP-Sil Biotage[®] SNAP Cartridges on the Biotage[®] Isolera One autocolumn to obtain *t*-butyl 5-(4-ethoxy-4-oxobutyl)-1H-indole-1-carboxylate (HYT-2-50-2) (54.2 mg, 82%). The product was sealed in a 4 mL vial and sent to the UC Center for Environmental Implications of Nanotechnology at the University of California, Los Angeles, to get ICP-MS analyses.

		Magnesium		Zinc		Palladium	
		[μg/g]		[μg/g]		[μg/g]	
Sample #	Sample weight in analysis [mg]	Average*	std dev	Average*	std dev	Average*	std dev
HYT-2-20-6	2.61	30.014	0.418	0.000	0.000	n/a	n/a
HYT-2-50-2	11.20	79.592	0.878	0.000	0.000	0.037	0.005

**Each sample was done in triplicated measurements with background correction.
n/a represents below detection limit.*

Recycle study

Table S10. Recycle of NPs and reaction media



Entry ^a	Recharge (relative to aryl bromide)	Yield ^b
1st run	-	86
2nd run	4 eq zinc powder, 5 eq TEMDA, 5 % ligand	84
3rd run	1500 ppm Pd(OAc) ₂ , 4 eq zinc powder, 5 eq TEMDA, 5 % ligand	80

1st run:

To a flame dried 1-dram vial equipped with an oven dried stir bar inside of a glove box was added optimized Fe/ppm NPs (15.5 mg, 0.25 mol % Pd). The vial was then sealed with a rubber septum inside the glovebox. A 2 wt % TPGS-750-M/H₂O solution was added to the vial by syringe and the mixture was stirred vigorously at rt for 1 h. Then 1-(4-bromophenyl)ethan-1-one (40 mg, 0.2 mmol) and zinc (52 mg, 0.8 mmol, 4 equiv) were added to the vial under argon flow. The vial was then sealed with a rubber septum under an argon flow and stirred for 15 min. Then (3-bromopropoxy)benzene (0.1 mL, 0.6 mmol) and TMEDA (0.15 mL, 1.0 mmol, 5 equiv) were added to the vial via syringe. The vial was then stirred vigorously at rt for 8 h. Then 0.4 mL degassed MTBE was added and the mixture via syringe and stirred gently for 2 min at rt. Stirring was then stopped and the organic layer was decanted via syringe after centrifugation. The same extraction procedure was repeated twice. The combined organic extracts were dried over anhydrous Na₂SO₄ and the solvent removed

under reduced pressure and the crude material was purified by flash chromatography using EtOAc/hexanes: 95/5 to obtain 1-(4-(3-phenoxypropyl)phenyl)ethan-1-one. (43.7 mg, 86%).

2nd run:

To the same vial, 1-(4-bromophenyl)ethan-1-one (40 mg, 0.2 mmol), AmPhos (2.6 mg, 5 mol %) and zinc (52 mg, 0.8 mmol, 4 equiv) were added to the vial under an argon flow. The vial was then sealed with a rubber septum under an argon flow and stirred for 15 min. Then (3-bromopropoxy)benzene (0.13 mL, 0.8 mmol) and TMEDA (0.15 mL, 1.0 mmol, 5 equiv) were added to the vial via syringe. The vial was then stirred vigorously at rt for 8 h. Then 0.4 mL degassed MTBE was added via syringe and the mixture stirred gently for 2 min at rt. Stirring was then stopped and the organic layer was decanted via syringe after centrifugation. The same extraction procedure was repeated twice. The combined organic extracts were dried over anhydrous Na₂SO₄ and the solvent removed under reduced pressure and purified by flash chromatography over silica gel with EtOAc/hexanes: 95/5 to obtain 1-(4-(3-phenoxypropyl)phenyl)ethan-1-one. (42.5 mg, 84%).

3rd run:

To another flame dried 2-dram vial inside of an argon purged glove box was added Pd(OAc)₂ (1.3 mg) and the vial was sealed using a rubber septum and maintained under a steady pressure of argon. Degassed THF (8 mL) was then added through the septum and the vial was stirred at rt until the solids had dissolved to prepare a yellow catalyst stock solution. To the same vial from 1st recycle, AmPhos (2.6 mg, 5 mol %) and 0.4 mL stock solution (1500 ppm Pd) were added, the vial was sealed and stirred vigorously for 1 h. To the same

vial in 1st recycle, 1-(4-bromophenyl)ethan-1-one (40 mg, 0.2 mmol) and zinc (52 mg, 0.8 mmol, 4 equiv) were added to the vial under an argon flow. The vial was then sealed with a rubber septum under argon flow and stirred for 15 min. Then (3-bromopropoxy)benzene (0.13 mL, 0.8 mmol) and TMEDA (0.15 mL, 1.0 mmol, 5 equiv) were added to the vial via syringe. The vial was then stirred vigorously at rt for 8 h. Then 0.4 mL degassed MTBE was added via syringe and the mixture stirred gently for 2 min at rt. Stirring was then stopped and the organic layer was decanted via syringe after centrifugation. The same extraction procedure was repeated twice. The combined organic extracts were dried over anhydrous Na₂SO₄ and the solvent removed in vacuo. The crude material was purified by flash chromatography over silica gel with EtOAc/hexanes: 95/5 to obtain 1-(4-(3-phenoxypropyl)phenyl)ethan-1-one. (40.5 mg, 80%).

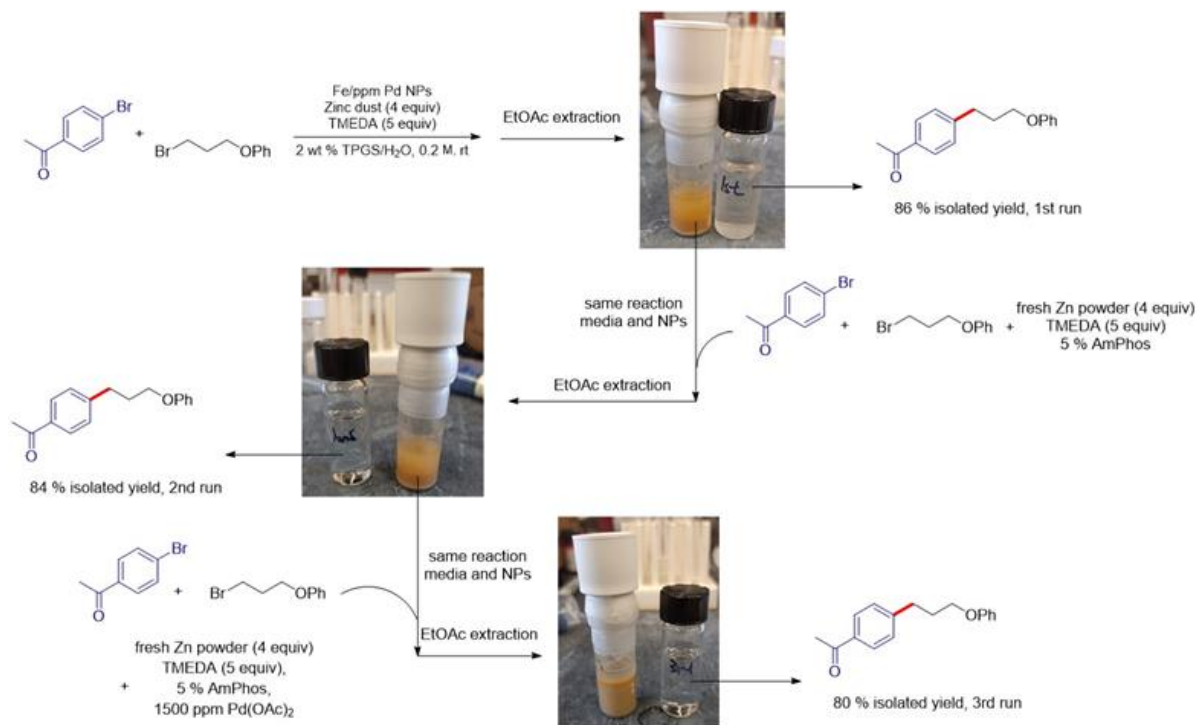
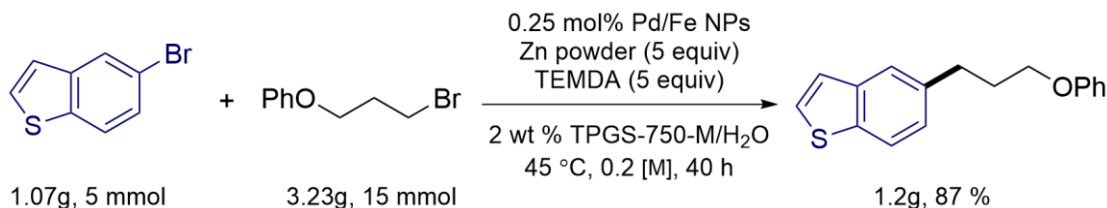


Figure S9. Illustration associated with recycling studies

Gram scale reaction



To an oven dried 50 mL round bottom flask with an oven dried stir bar inside of a glove box was added optimized Fe/ppm NPs (388 mg, 0.25 mol % Pd). The vial was then sealed with a rubber septum inside of the glovebox after which 25 mL 2 wt % TPGS-750-M/H₂O solution was added to the vial by syringe and the mixture was stirred vigorously at rt for 1 h. Then 5-bromobenzo[b]thiophene (1.07 g, 5.02 mmol) and zinc (1.63 g, 25 mmol, 5 equiv) were added to the vial under an argon flow. The vial was then sealed with a rubber septum under argon flow and stirred for 15 min. Then (3-bromopropoxy)benzene (3.23 g, 15 mmol) and TMEDA (3.75 mL, 25 mmol, 5 equiv) were added to the vial via syringe. The vial was then stirred vigorously at rt for 72 h. After complete consumption of starting material, the septum was removed and the reaction mixture was then filtered by a fritted filter with EtOAc (3 x 10 mL) to wash the solid. Then the organic layer was separated and the aqueous layer was extracted with EtOAc (2 x 20 mL). The combined organic layer was dried with anhydrous Na₂SO₄. After filtration, the combined organic extracts were concentrated under reduced pressure and purified by flash chromatography (hexane/EtOAc: 90/10) to obtain 5-(3-phenoxypropyl)benzo[b]thiophene (1.2 g, 87%) as a yellow oil.

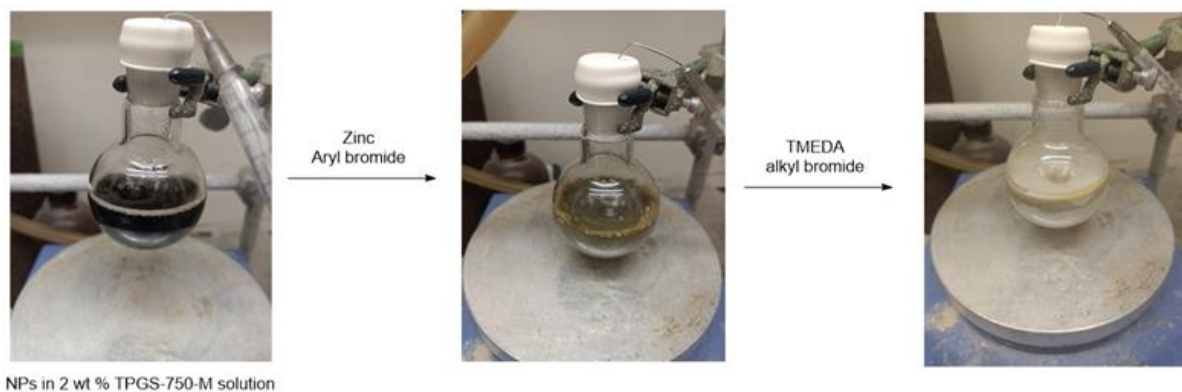
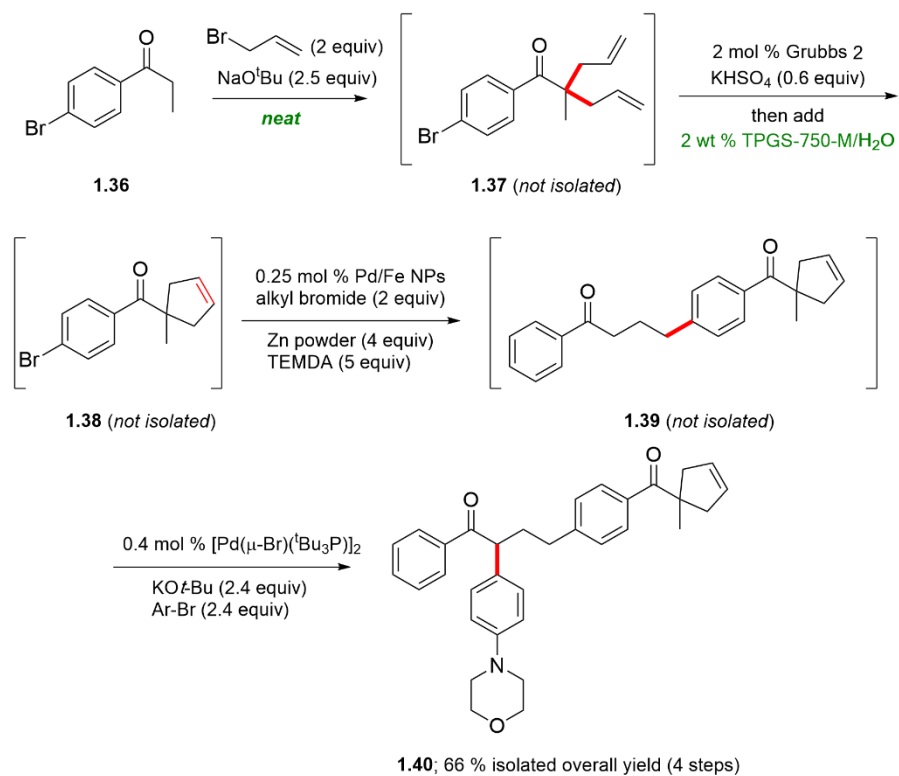


Figure S10. Illustration associated with gram scale reaction

1-Pot sequence of reactions



Step 1: To a flame dried 1-dram vial equipped with an oven dried stir bar was added 1-(4-bromophenyl)propan-1-one (106.5 mg, 0.5 mmol), after which the vial was transferred into a glove box to which was added NaO^tBu (120 mg, 1.25 mmol, 2.5 equiv) inside of an

argon purged glove box. The vial was sealed with a rubber septum and removed from the glove box. Then, allyl bromide (86 μL , 1.0 mmol, 2 equiv) was added to the vial via syringe and the vial were stirred vigorously under constant argon pressure at rt for 1 h. The progress of the reaction was monitored by TLC.

Step 2: After complete consumption of starting material, the septum was opened and KHSO_4 (40.8 mg, 0.3 mmol, 0.6 equiv) was added to the vial. The vial was transferred into glove box and the Grubbs catalyst 2nd generation catalyst was added (8.5 mg, 0.01 mmol, 2 mol %). The vial was sealed with a rubber septum and removed from the glove box. Then, 1 mL 2 wt % TPGS-750-M/ H_2O solution was added to the vial via syringe and the vial was stirred vigorously under constant argon pressure at 45 $^\circ\text{C}$ for overnight. The progress of the reaction was monitored by TLC.

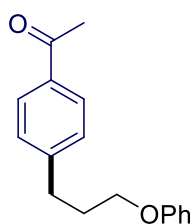
Step 3: To another flame dried 1-dram vial inside of an argon purged glove box was added Fe/ppm Pd NPs (40 mg, 0.25 mol % Pd) and the vial was sealed using a rubber septum and maintained under a steady pressure of argon. 1.5 mL 2 wt % TPGS-750-M/ H_2O solution was then added through the septum and the vial was stirred at rt for 1 h. Then, the suspension was added to the vial from step 2 via syringe, then zinc powder (130 mg, 2.0 mmol, 4 equiv) was added quickly under an argon flow. The vial was sealed with a rubber septum and stirred for 15 min at rt. Then 4-bromo-1-phenylbutan-1-one (227.1 mg, 1.0 mmol, 2 equiv) and TMEDA (0.38 mL, 2.5 mmol, 5 equiv) was added to the vial via syringe and the vial was stirred vigorously under constant argon pressure at 45 $^\circ\text{C}$ for 48 h. The progress of the reaction was monitored by TLC.

Step 4: To a flame dried 1-dram vial equipped with an oven dried stir bar was added 4-bromophenyl-morpholine (201.8 mg, 0.83 mmol, 1.0 equiv), the vial was then transferred

into a glove box where to the vial was added $[\text{Pd}(\mu\text{-Br})(t\text{-Bu})_3\text{P}]_2$ (3.3 mg, 0.004 mmol, 0.4 mol %) and KO^tBu (225 mg, 2 mmol, 2.4 equiv). The vial was then sealed using a rubber septum inside of the glovebox and then transferred to a manifold under argon pressure. The suspension from step 3 was transferred to the vial via syringe. The contents of the vial were then allowed to stir vigorously under constant argon pressure at 45 °C. The reaction was then monitored by thin-layer chromatography until completion. Then 1.0 mL EtOAc was added to the mixture after which it was stirred gently for 2 min at rt. Stirring was then stopped and the organic layer was decanted via a pipette after centrifugation. The same extraction procedure was repeated four times. The combined organic extracts were dried over anhydrous Na_2SO_4 and the solvent removed in vacuo, with the resulting crude material being purified by flash chromatography over silica gel with EtOAc/hexanes: 70/30 to afford 4-(4-(1-methylcyclopent-3-ene-1-carbonyl)phenyl)-2-(4-morpholinophenyl)-1-phenylbutan-1-one (163.2 mg, 66% overall) as a yellow oil.

Analytical data

1-(4-(3-Phenoxypropyl)phenyl)ethan-1-one (1.1)



1-(4-Bromophenyl)ethan-1-one (40 mg, 0.2 mmol), (3-bromopropoxy)benzene (129.1 mg, 0.6 mmol), zinc powder (52 mg, 0.8 mmol), TMEDA (116.2 mg, 1.0 mmol) and Fe/ppm Pd NPs (15.5 mg, 0.25 mol % Pd), in 1.0 mL 2 wt % TPGS-750-M/ H_2O were

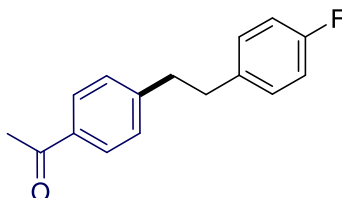
reacted at rt for 16 h yielding 43.5 mg (86%) of 1-(4-(3-phenoxypropyl)phenyl)ethan-1-one as a white solid (hexane/EtOAc: 90/10).

^1H NMR (500 MHz, chloroform-*d*) δ 7.89 (d, J = 8.2 Hz, 2H), 7.35 – 7.26 (m, 4H), 6.95 (t, J = 7.3 Hz, 1H), 6.91 – 6.86 (m, 2H), 3.97 (t, J = 6.2 Hz, 2H), 2.92 – 2.85 (m, 2H), 2.59 (s, 3H), 2.17 – 2.09 (m, 2H).

^{13}C NMR (126 MHz, chloroform-*d*) δ 197.96, 159.02, 147.54, 135.37, 129.61, 128.89, 128.75, 120.87, 114.64, 66.64, 32.38, 30.66, 26.71.

HRMS(ESI): Calcd. for $\text{C}_{17}\text{H}_{18}\text{O}_2\text{H}$ $[\text{M}+\text{H}]^+$ 255.1380. Found: 255.1378.

1-(4-(4-Fluorophenethyl)phenyl)ethan-1-one (1.2)



1-(4-Bromophenyl)ethan-1-one (40 mg, 0.2 mmol), 1-(2-bromoethyl)-4-fluorobenzene (121.8 mg, 0.6 mmol), zinc powder (52 mg, 0.8 mmol), TMEDA (116.2 mg, 1.0 mmol) and Fe/ppm Pd NPs (15.5 mg, 0.25 mol % Pd), in 1.0 mL 2 wt % TPGS-750-M/ H_2O were reacted at rt for 16 h yielding 46.9 mg (97%) of 1-(4-(4-fluorophenethyl)phenyl)ethan-1-one as a colorless oil (hexane/EtOAc: 90/10).

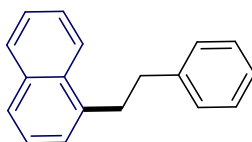
^1H NMR (400 MHz, chloroform-*d*) δ 7.87 (d, J = 7.7 Hz, 2H), 7.22 (d, J = 7.7 Hz, 2H), 7.12 – 7.04 (m, 2H), 6.95 (t, J = 8.4 Hz, 2H), 2.93 (m, 4H), 2.58 (s, 3H).

^{13}C NMR (101 MHz, chloroform-*d*) δ 197.97, 162.74, 160.32, 147.23, 136.78, 135.37, 129.95 (d, $J_{\text{C-F}} = 8$ Hz), 128.77 (d, $J_{\text{C-F}} = 21$ Hz), 115.28 (d, $J_{\text{C-F}} = 21$ Hz), 38.05, 36.69, 26.70.

^{19}F NMR (376 MHz, chloroform-*d*) δ -117.22.

HRMS(EI): Calcd. for $\text{C}_{16}\text{H}_{15}\text{FO}$ $[\text{M}]^+$ 242.1107. Found: 242.1110.

1-Phenethylnaphthalene (1.3)



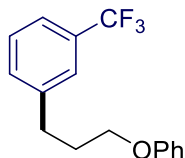
1-Bromonaphthalene (41.2 mg, 0.2 mmol), 1-phenyl-2-bromoethane (111 mg, 0.6 mmol), zinc powder (52 mg, 0.8 mmol), TMEDA (116.2 mg, 1.0 mmol) and Fe/ppm Pd NPs (15.5 mg, 0.25 mol % Pd), in 1.0 mL 2 wt % TPGS-750-M/ H_2O were reacted at rt for 16 h yielding 41.4 mg (89%) of 1-phenethylnaphthalene as a white solid (hexane/EtOAc : 95/5).

^1H NMR (400 MHz, chloroform-*d*) δ 8.14 (d, $J = 8.3$ Hz, 1H), 7.93 – 7.89 (m, 1H), 7.77 (d, $J = 8.2$ Hz, 1H), 7.60 – 7.50 (m, 2H), 7.45 – 7.39 (m, 1H), 7.36 – 7.31 (m, 3H), 7.30 – 7.27 (m, 3H), 3.42 (dd, $J = 9.7, 6.8$ Hz, 2H), 3.10 (dd, $J = 9.7, 6.8$ Hz, 2H).

^{13}C NMR (101 MHz, chloroform-*d*) δ 142.15, 137.94, 134.05, 131.92, 128.99, 128.57, 128.40, 126.91, 126.16, 126.15, 126.01, 125.70, 125.61, 123.78, 37.26, 35.27

HRMS(EI): Calcd. for $\text{C}_{18}\text{H}_{16}$ $[\text{M}]^+$ 232.1252. Found: 232.1253.

1-(3-Phenoxypropyl)-3-(trifluoromethyl)benzene (1.4)



1-Bromo-3-(trifluoromethyl)benzene (45 mg, 0.2 mmol), (3-bromopropoxy)benzene (129.1 mg, 0.6 mmol), zinc powder (52 mg, 0.8 mmol), TMEDA (116.2 mg, 1.0 mmol) and Fe/ppm Pd NPs (15.5 mg, 0.25 mol % Pd), in 1.0 mL 2 wt % TPGS-750-M/H₂O were reacted at rt for 16 h yielding 48.2 mg (86%) of 1-(3-phenoxypropyl)-3-(trifluoromethyl)benzene as a colorless oil (hexane/EtOAc : 95/5).

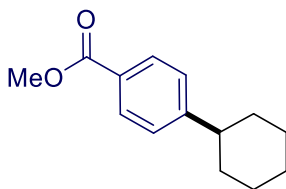
¹H NMR (500 MHz, chloroform-*d*) δ 7.41 – 7.34 (m, 2H), 7.31 (m, 2H), 7.23 – 7.17 (m, 2H), 6.86 (t, *J* = 7.3 Hz, 1H), 6.81 (d, *J* = 7.9 Hz, 2H), 3.88 (t, *J* = 6.1 Hz, 2H), 2.83 – 2.75 (m, 2H), 2.08 – 1.99 (m, 2H).

¹³C NMR (126 MHz, chloroform-*d*) δ 158.76, 142.37, 131.85, 130.62 (q, *J*_(C-F) = 32 Hz), 129.36, 128.70, 125.05 (q, *J*_(C-F) = 4 Hz), 124.13 (q, *J*_(C-F) = 272 Hz), 122.74 (q, *J*_(C-F) = 4 Hz), 120.63, 114.38, 66.41, 31.96, 30.58.

¹⁹F NMR (376 MHz, chloroform-*d*) δ -62.58.

HRMS: Calcd. for C₁₆H₁₅F₃O [M]⁺ 280.1075. Found: 280.1079.

Methyl 4-cyclohexylbenzoate (1.5)



Methyl 4-bromobenzoate (43 mg, 0.2 mmol), bromocyclohexane (130.4 mg, 0.6 mmol), zinc powder (52 mg, 0.8 mmol), TMEDA (116.2 mg, 1.0 mmol) and Fe/ppm Pd NPs (15.5

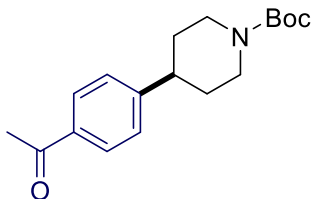
mg, 0.25 mol % Pd), in 1.0 mL 2 wt % TPGS-750-M/H₂O were reacted at rt for 16 h yielding 37.6 mg (86%) of methyl 4-cyclohexylbenzoate as a colorless oil (hexane/EtOAc : 90/10).

¹H NMR (400 MHz, chloroform-*d*) δ 7.99 – 7.92 (m, 2H), 7.28 (m, 2H), 3.90 (s, 3H), 2.56 (tt, *J* = 11.6, 3.6 Hz, 1H), 1.91 – 1.82 (m, 4H), 1.76 (m, 1H), 1.46 – 1.34 (m, 4H), 1.32 – 1.24 (m, 1H).

¹³C NMR (126 MHz, chloroform-*d*) δ 167.36, 153.62, 129.83, 127.88, 127.01, 52.09, 44.84, 34.29, 26.89, 26.19.

Spectral data matched those previously reported.^[1]

***t*-Butyl 4-(4-acetylphenyl)piperidine-1-carboxylate (1.6)**



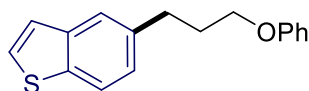
1-(4-Bromophenyl)ethan-1-one (40 mg, 0.2 mmol), *t*-butyl 4-bromopiperidine-1-carboxylate (211 mg, 0.8 mmol), zinc powder (52 mg, 0.8 mmol), TMEDA (116.2 mg, 1.0 mmol) and Fe/ppm Pd NPs (15.5 mg, 0.25 mol % Pd), in 1.0 mL 2 wt % TPGS-750-M/H₂O were reacted at rt for 16 h yielding 53.3 mg (88%) of *t*-butyl 4-(4-acetylphenyl)piperidine-1-carboxylate as a colorless oil (hexane/acetone: 80/20).

¹H NMR (400 MHz, chloroform-*d*) δ 7.91 (d, *J* = 8.3 Hz, 2H), 7.29 (d, *J* = 8.3 Hz, 2H), 4.26 (d, *J* = 13.0 Hz, 2H), 2.81 (td, *J* = 14.7, 13.2, 2.1 Hz, 2H), 2.71 (tt, *J* = 12.2, 3.6 Hz, 1H), 2.58 (s, 3H), 1.83 (d, *J* = 13.3 Hz, 2H), 1.70 – 1.61 (m, 2H), 1.48 (s, 9H)

^{13}C NMR (101 MHz, chloroform-*d*) δ 197.90, 154.95, 151.46, 135.68, 128.86, 127.17, 79.73, 44.39, 42.95, 33.00, 28.62, 26.72.

Spectral data matched those previously reported.^[1]

5-(3-Phenoxypropyl)benzo[b]thiophene (1.7)



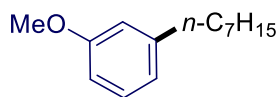
5-Bromobenzo[b]thiophene (42.6 mg, 0.2 mmol), (3-bromopropoxy)benzene (129.1 mg, 0.6 mmol), zinc powder (52 mg, 0.8 mmol), TMEDA (116.2 mg, 1.0 mmol) and Fe/ppm Pd NPs (15.5 mg, 0.25 mol % Pd), in 1.0 mL 2 wt % TPGS-750-M/H₂O were reacted at rt for 16 h yielding 50.8 mg (95%) of 5-(3-phenoxypropyl)benzo[b]thiophene as a white solid (hexane/EtOAc : 90/10).

^1H NMR (400 MHz, chloroform-*d*) δ 7.80 (d, J = 8.3 Hz, 1H), 7.67 (s, 1H), 7.42 (d, J = 5.4 Hz, 1H), 7.28 (t, J = 7.1 Hz, 3H), 7.22 (d, J = 8.2 Hz, 1H), 6.95 (d, J = 7.3 Hz, 1H), 6.91 (d, J = 8.0 Hz, 2H), 3.99 (t, J = 6.1 Hz, 2H), 2.94 (t, J = 7.5 Hz, 2H), 2.17 (p, J = 6.8 Hz, 2H).

^{13}C NMR (101 MHz, chloroform-*d*) δ 159.16, 140.12, 137.79, 137.58, 129.58, 126.68, 125.54, 123.76, 123.29, 122.48, 120.74, 114.69, 66.85, 32.23, 31.34.

HRMS(EI): Calcd. for C₁₇H₁₆OS [M]⁺ 268.0922. Found: 268.0926.

1-Heptyl-3-methoxybenzene (1.8)



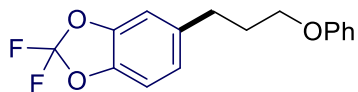
1-Bromo-3-methoxybenzene (37.4 mg, 0.2 mmol), 1-bromoheptane (107.4 mg, 0.6 mmol), zinc powder (52 mg, 0.8 mmol), TMEDA (116.2 mg, 1.0 mmol) and Fe/ppm Pd NPs (15.5 mg, 0.25 mol % Pd), in 1.0 mL 2 wt % TPGS-750-M/H₂O were reacted at rt for 16 h yielding 29.2 mg (71%) of 1-heptyl-3-methoxybenzene as a colorless oil (hexane/EtOAc : 95/5).

¹H NMR (400 MHz, chloroform-*d*) δ 7.19 (m, 1H), 6.77 (d, *J* = 7.7 Hz, 1H), 6.72 (m, 2H), 3.80 (s, 3H), 2.58 (t, *J* = 7.6 Hz, 2H), 1.65 – 1.55 (m, 4H), 1.36 – 1.29 (m, 6H), 0.88 (t, *J* = 6.9 Hz, 3H).

¹³C NMR (126 MHz, chloroform-*d*) δ 159.70, 144.80, 129.29, 121.01, 114.33, 110.93, 55.27, 36.19, 31.96, 31.56, 29.46, 29.33, 22.82, 14.25.

Spectral data matched those previously reported.^[2]

2,2-Difluoro-5-(3-phenoxypropyl)benzo[d][1,3]dioxole (1.9)



5-Bromo-2,2-difluorobenzo[d][1,3]dioxole (47.4 mg, 0.2 mmol), (3-bromopropoxy)benzene (129.1 mg, 0.6 mmol), zinc powder (52 mg, 0.8 mmol), TMEDA (116.2 mg, 1.0 mmol) and Fe/ppm Pd NPs (15.5 mg, 0.25 mol % Pd), in 1.0 mL 2 wt % TPGS-750-M/H₂O were reacted at rt for 16 h yielding 48.7 mg (83%) of 2,2-difluoro-5-(3-phenoxypropyl)benzo[d][1,3]dioxole as a colorless oil (hexane/EtOAc : 90/10).

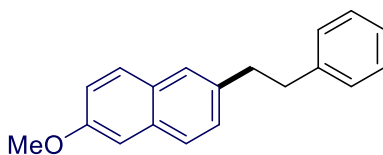
^1H NMR (400 MHz, chloroform-*d*) δ 7.29 (m, 2H), 6.98 – 6.92 (m, 3H), 6.92 – 6.87 (m, 3H), 3.96 (t, J = 6.1 Hz, 2H), 2.86 – 2.77 (m, 2H), 2.15 – 2.03 (m, 2H).

^{13}C NMR (126 MHz, chloroform-*d*) δ 159.00, 143.09 (d, $J_{\text{C-F}}$ = 230 Hz), 137.81, 133.80, 131.78, 129.62, 123.49, 120.89, 114.62, 109.50 (d, $J_{\text{C-F}}$ = 63 Hz), 66.46, 32.18, 32.08 (t, $J_{\text{C-F}}$ = 286 Hz), 31.17.

^{19}F NMR (376 MHz, chloroform-*d*) δ -50.10.

HRMS: Calcd. for $\text{C}_{16}\text{H}_{14}\text{F}_2\text{O}_3$ $[\text{M}]^+$ 292.0911. Found: 292.0917.

2-Methoxy-6-phenethylnaphthalene (1.10)



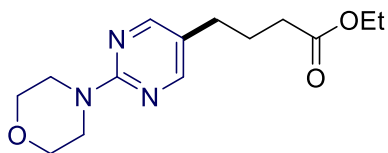
2-Bromo-6-methoxynaphthalene (47.4 mg, 0.2 mmol), 1-phenyl-2-bromoethane (111 mg, 0.6 mmol), zinc powder (52 mg, 0.8 mmol), TMEDA (116.2 mg, 1.0 mmol) and Fe/ppm Pd NPs (15.5 mg, 0.25 mol % Pd), in 1.0 mL 2 wt % TPGS-750-M/ H_2O were reacted at rt for 16 h yielding 39.5 mg (75%) of 2-methoxy-6-phenethylnaphthalene as a yellow solid (hexane/EtOAc : 95/5).

^1H NMR (400 MHz, chloroform-*d*) δ 7.67 (d, J = 8.2 Hz, 2H), 7.55 (s, 1H), 7.29 (t, J = 8.0 Hz, 3H), 7.22 (m, 3H), 7.13 (m, 2H), 3.92 (s, 3H), 3.09 – 3.03 (m, 2H), 3.03 – 2.97 (m, 2H).

^{13}C NMR (126 MHz, chloroform-*d*) δ 157.33, 141.98, 137.11, 133.17, 129.23, 129.09, 128.64, 128.49, 127.97, 126.86, 126.48, 126.06, 118.81, 105.78, 55.43, 38.11, 38.06.

HRMS(EI): Calcd. for C₁₉H₁₈O [M]⁺ 262.1358. Found: 262.1352.

Ethyl 4-(2-morpholinopyrimidin-5-yl)butanoate (1.11)



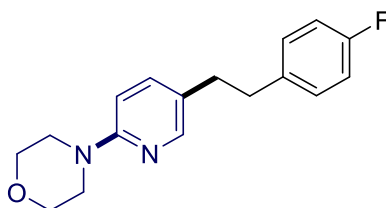
4-(5-Bromopyrimidin-2-yl)morpholine (48.8 mg, 0.2 mmol), ethyl 4-bromobutanoate (156 mg, 0.8 mmol), zinc powder (52 mg, 0.8 mmol), TMEDA (116.2 mg, 1.0 mmol) and Fe/ppm Pd NPs (15.5 mg, 0.25 mol % Pd), in 1.0 mL 2 wt % TPGS-750-M/H₂O were reacted at rt for 16 h yielding 51.2 mg (92%) of ethyl 4-(2-morpholinopyrimidin-5-yl)butanoate as a yellow oil (hexane/EtOAc : 75/25).

¹H NMR (500 MHz, chloroform-*d*) δ 8.18 (s, 2H), 4.13 (q, *J* = 7.1 Hz, 2H), 3.76 (s, 8H), 2.52 – 2.45 (t, *J* = 7.6 Hz, 2H), 2.32 (t, *J* = 7.4 Hz, 2H), 1.88 (quin, *J* = 7.4 Hz, 2H), 1.26 (t, *J* = 7.2 Hz, 3H).

¹³C NMR (126 MHz, chloroform-*d*) δ 186.08, 173.27, 157.69, 122.60, 66.98, 60.56, 44.58, 33.46, 28.90, 26.52, 14.39.

HRMS(ESI): Calcd. for C₁₄H₂₁N₃O₃H [M+H]⁺ 280.1656. Found: 280.1654.

4-(5-(4-Fluorophenethyl)pyridin-2-yl)morpholine (1.12)



4-(5-Bromopyridin-2-yl)morpholine (48.6 mg, 0.2 mmol), 1-(2-bromoethyl)-4-fluorobenzene (121.8 mg, 0.6 mmol), zinc powder (52 mg, 0.8 mmol), TMEDA (116.2 mg, 1.0 mmol) and Fe/ppm Pd NPs (15.5 mg, 0.25 mol % Pd), in 1.0 mL 2 wt % TPGS-750-M/H₂O were reacted at rt for 16 h yielding 52.8 mg (92%) of 4-(5-(4-fluorophenethyl)pyridin-2-yl)morpholine as a yellow oil (hexane/EtOAc : 80/20).

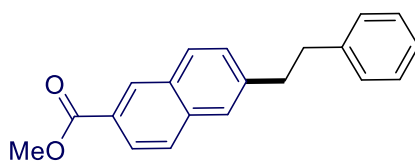
¹H NMR (500 MHz, chloroform-*d*) δ 7.99 (d, *J* = 2.0 Hz, 1H), 7.26 – 7.24 (m, 1H), 7.08 (dd, *J* = 8.4, 5.6 Hz, 2H), 6.95 (t, *J* = 8.7 Hz, 2H), 6.57 (d, *J* = 8.6 Hz, 1H), 3.84 – 3.80 (m, 4H), 3.48 – 3.43 (m, 4H), 2.87 – 2.75 (m, 4H).

¹³C NMR (126 MHz, chloroform-*d*) δ 162.46, 160.52, 138.10, 136.97, 130.55 (d, *J*_(C-F) = 8.8 Hz) 130.01 (d, *J*_(C-F) = 7.6 Hz), 126.57, 115.24 (d, *J*_(C-F) = 21.4 Hz), 106.92, 66.93, 46.10, 37.11, 34.19.

¹⁹F NMR (376 MHz, chloroform-*d*) δ -117.44.

HRMS(ESI): Calcd. for C₁₇H₁₉FN₂OH [M+H]⁺ 287.1555. Found: 287.1555.

Methyl 6-phenethyl-2-naphthoate (1.13)



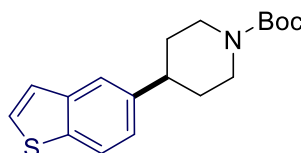
Methyl 6-bromo-2-naphthoate (54 mg, 0.2 mmol), 1-phenyl-2-bromoethane (111 mg, 0.6 mmol), zinc powder (52 mg, 0.8 mmol), TMEDA (116.2 mg, 1.0 mmol) and Fe/ppm Pd NPs (15.5 mg, 0.25 mol % Pd), in 1.0 mL 2 wt % TPGS-750-M/H₂O were reacted at rt for 16 h yielding 50.9 mg (88%) of methyl 6-phenethyl-2-naphthoate as a yellow solid (hexane/EtOAc : 95/5).

^1H NMR (500 MHz, chloroform-*d*) δ 8.58 (s, 1H), 8.04 (dd, $J = 8.6, 1.6$ Hz, 1H), 7.88 (d, $J = 8.4$ Hz, 1H), 7.80 (d, $J = 8.6$ Hz, 1H), 7.64 (s, 1H), 7.40 (dd, $J = 8.4, 1.5$ Hz, 1H), 7.29 (m, 2H), 7.21 (m, 3H), 3.98 (s, 3H), 3.12 (m, 2H), 3.03 (m, 2H).

^{13}C NMR (126 MHz, chloroform-*d*) δ 167.50, 142.24, 141.53, 135.90, 131.22, 130.98, 129.46, 128.61, 128.56, 128.35, 127.82, 126.90, 126.57, 126.21, 125.49, 52.33, 38.31, 37.74.

HRMS(ESI): Calcd. for $\text{C}_{20}\text{H}_{18}\text{O}_2$ $[\text{M}]^+$ 290.1307. Found: 290.1307.

***t*-Butyl 4-(benzo[*b*]thiophen-5-yl)piperidine-1-carboxylate (1.14)**



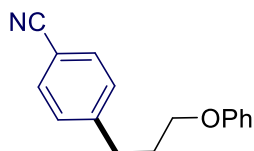
5-Bromobenzo[*b*]thiophene (42.6 mg, 0.2 mmol), *t*-butyl 4-bromopiperidine-1-carboxylate (211 mg, 0.8 mmol), zinc powder (52 mg, 0.8 mmol), TMEDA (116.2 mg, 1.0 mmol) and Fe/ppm Pd NPs (15.5 mg, 0.25 mol % Pd), in 1.0 mL 2 wt % TPGS-750-M/ H_2O were reacted at rt for 16 h yielding 56.4 mg (89%) of *t*-butyl 4-(benzo[*b*]thiophen-5-yl)piperidine-1-carboxylate as a yellow solid (hexane/acetone: 85/15).

^1H NMR (400 MHz, chloroform-*d*) δ 7.81 (d, $J = 8.3$ Hz, 1H), 7.65 (d, $J = 1.4$ Hz, 1H), 7.43 (d, $J = 5.4$ Hz, 1H), 7.29 (d, $J = 5.4$ Hz, 1H), 7.21 (dd, $J = 8.3, 1.6$ Hz, 1H), 4.27 (d, $J = 12.9$ Hz, 2H), 2.88 – 2.72 (m, 3H), 1.88 (d, $J = 13.4$ Hz, 2H), 1.69 (qd, $J = 12.7, 4.3$ Hz, 2H), 1.50 (s, 9H).

^{13}C NMR (101 MHz, chloroform-*d*) δ 155.03, 142.23, 140.10, 137.89, 126.85, 123.94, 123.85, 122.59, 121.42, 79.60, 44.61, 42.86, 33.68, 28.64.

Spectral data matched those previously reported.^[3]

4-(3-Phenoxypropyl) benzonitrile (1.15)



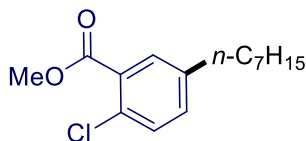
4-Bromobenzonitrile (36.4 mg, 0.2 mmol), (3-bromopropoxy)benzene (129.1 mg, 0.6 mmol), zinc powder (52 mg, 0.8 mmol), TMEDA (116.2 mg, 1.0 mmol) and Fe/ppm Pd NPs (15.5 mg, 0.25 mol % Pd), in 1.0 mL 2 wt % TPGS-750-M/H₂O were reacted at rt for 16 h yielding 36.9 mg (78%) of 4-(3-phenoxypropyl) benzonitrile as a yellow oil (hexane/EtOAc : 90/10).

¹H NMR (400 MHz, chloroform-*d*) δ 7.54 (d, $J = 8.3$ Hz, 2H), 7.28 (d, $J = 8.6$ Hz, 2H), 7.25 (d, $J = 1.2$ Hz, 1H), 7.22 (d, $J = 2.7$ Hz, 1H), 6.91 (t, $J = 7.4$ Hz, 1H), 6.87 – 6.82 (m, 2H), 3.92 (t, $J = 6.1$ Hz, 2H), 2.85 (t, $J = 8.0$ Hz, 2H), 2.11 – 2.03 (m, 2H).

¹³C NMR (101 MHz, chloroform-*d*) δ 158.90, 147.42, 132.40, 129.64, 129.48, 120.97, 119.18, 114.58, 110.04, 66.42, 32.56, 30.53.

HRMS(ED): Calcd. for C₁₆H₁₅NO [M]⁺ 237.1154. Found: 237.1158.

Methyl 2-chloro-5-heptylbenzoate (1.16)



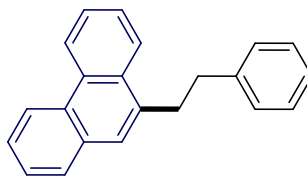
Methyl 5-bromo-2-chlorobenzoate (49.9 mg, 0.2 mmol), 1-bromoheptane (107 mg, 0.6 mmol), zinc powder (52 mg, 0.8 mmol), TMEDA (116.2 mg, 1.0 mmol) and Fe/ppm Pd NPs (15.5 mg, 0.25 mol % Pd), in 1.0 mL 2 wt % TPGS-750-M/H₂O were reacted at rt for 16 h yielding 48.2 mg (90%) of methyl 2-chloro-5-heptylbenzoate as a colorless oil (hexane/EtOAc : 97/3).

¹H NMR (400 MHz, chloroform-*d*) δ 7.86 (s, 1H), 7.40 – 7.30 (m, 2H), 3.91 (s, 3H), 2.65 (t, *J* = 7.7 Hz, 2H), 1.63 (m, 2H), 1.33 – 1.26 (m, 8H), 0.88 (t, *J* = 6.7 Hz, 3H).

¹³C NMR (126 MHz, chloroform-*d*) δ 167.50, 143.38, 133.22, 130.21, 129.64, 128.39, 127.06, 52.17, 35.89, 31.92, 31.53, 29.34, 29.28, 22.79, 14.22.

HRMS: Calcd. for C₁₅H₂₁ClO₂ [M]⁺ 268.1230. Found: 268.1234.

9-Phenethylphenanthrene (1.17)



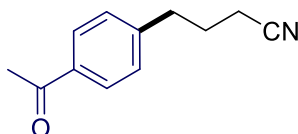
9-Bromophenanthrene (51.4 mg, 0.2 mmol), 1-phenyl-2-bromoethane (111 mg, 0.6 mmol), zinc powder (52 mg, 0.8 mmol), TMEDA (116.2 mg, 1.0 mmol) and Fe/ppm Pd NPs (15.5 mg, 0.25 mol % Pd), in 1.0 mL 2 wt % TPGS-750-M/H₂O were reacted at rt for 16 h yielding 39.7 mg (70%) of 9-phenethylphenanthrene as a white solid (hexane/EtOAc : 95/5).

¹H NMR (400 MHz, chloroform-*d*) δ 8.78 (d, *J* = 8.8 Hz, 1H), 8.69 (d, *J* = 7.9 Hz, 1H), 8.24 – 8.17 (m, 1H), 7.84 (d, *J* = 7.5 Hz, 1H), 7.73 – 7.68 (m, 2H), 7.68 – 7.59 (m, 3H), 7.40 – 7.31 (m, 4H), 7.30 – 7.26 (m, 1H), 3.49 – 3.41 (m, 2H), 3.21 – 3.12 (m, 2H).

^{13}C NMR (101 MHz, chloroform-*d*) δ 142.05, 135.91, 131.91, 131.16, 130.78, 129.74, 128.51, 128.48, 128.13, 126.66, 126.23, 126.10, 126.08, 124.27, 123.35, 122.49, 36.62, 35.48.

HRMS(ED): Calcd. for $\text{C}_{22}\text{H}_{18}$ $[\text{M}]^+$ 282.1408. Found: 282.1411.

4-(4-Acetylphenyl)butanenitrile (1.18)



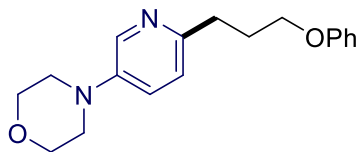
1-(4-Bromophenyl)ethan-1-one (40 mg, 0.2 mmol), 4-bromobutanenitrile (118.4 mg, 0.8 mmol), zinc powder (52 mg, 0.8 mmol), TMEDA (116.2 mg, 1.0 mmol) and Fe/ppm Pd NPs (15.5 mg, 0.25 mol % Pd), in 1.0 mL 2 wt % TPGS-750-M/ H_2O were reacted at 45 °C for 40 h yielding 29.7 mg (79%) of 4-(4-acetylphenyl)butanenitrile as a yellow oil (hexane/EtOAc : 90/10).

^1H NMR (500 MHz, chloroform-*d*) δ 7.91 (d, $J = 8.3$ Hz, 2H), 7.29 (d, $J = 8.4$ Hz, 2H), 2.85 (t, $J = 7.5$ Hz, 2H), 2.59 (s, 3H), 2.34 (t, $J = 7.0$ Hz, 2H), 2.01 (p, $J = 7.1$ Hz, 2H).

^{13}C NMR (126 MHz, chloroform-*d*) δ 197.80, 145.48, 135.87, 128.97, 128.83, 119.30, 34.48, 26.68, 16.63.

HRMS(ED): Calcd. for $\text{C}_{12}\text{H}_{13}\text{NO}$ $[\text{M}]^+$ 187.0997. Found: 187.0994.

4-(6-(3-Phenoxypropyl)pyridin-3-yl)morpholine (1.19)



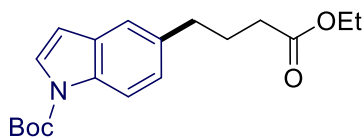
4-(6-Bromopyridin-3-yl)morpholine (48.6 mg, 0.2 mmol), (3-bromopropoxy)benzene (172.1 mg, 0.8 mmol), zinc powder (52 mg, 0.8 mmol), TMEDA (116.2 mg, 1.0 mmol) and Fe/ppm Pd NPs (15.5 mg, 0.25 mol % Pd), in 1.0 mL 2 wt % TPGS-750-M/H₂O were reacted at rt for 16 h yielding 47 mg (79%) of 4-(4-acetylphenyl)butanenitrile as a yellow oil (hexane/EtOAc : 90/10).

¹H NMR (600 MHz, chloroform-*d*) δ 8.23 (s, 1H), 7.27 (m, 2H), 7.16 – 7.11 (m, 1H), 7.08 (m, 1H), 6.93 (t, *J* = 7.3 Hz, 1H), 6.89 (d, *J* = 8.3 Hz, 2H), 3.99 (t, *J* = 6.2 Hz, 2H), 3.90 – 3.84 (m, 4H), 3.18 – 3.12 (m, 4H), 2.92 (t, *J* = 7.5 Hz, 2H), 2.20 (p, *J* = 6.6 Hz, 2H).

¹³C NMR (126 MHz, chloroform-*d*) δ 159.16, 152.50, 145.31, 137.69, 129.54, 123.57, 123.04, 120.68, 114.66, 67.07, 66.86, 49.18, 33.62, 29.49.

HRMS: Calcd. for C₁₈H₂₂N₂O₂ [M]⁺ 298.1681. Found: 298.1677.

***t*-Butyl 5-(4-ethoxy-4-oxobutyl)-1H-indole-1-carboxylate (1.20)**



t-Butyl 5-bromo-1H-indole-1-carboxylate (59.2 mg, 0.2 mmol), ethyl 4-bromobutanoate (156 mg, 0.8 mmol), zinc powder (52 mg, 0.8 mmol), TMEDA (116.2 mg, 1.0 mmol) and Fe/ppm Pd NPs (15.5 mg, 0.25 mol % Pd), in 1.0 mL 2 wt % TPGS-750-M/H₂O were

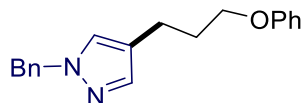
reacted at 45 °C for 40 h yielding 54.2 mg (82%) of *t*-butyl 5-(4-ethoxy-4-oxobutyl)-1H-indole-1-carboxylate as a yellow oil (hexane/EtOAc : 85/15).

¹H NMR (400 MHz, chloroform-*d*) δ 8.04 (d, *J* = 8.0 Hz, 1H), 7.57 (d, *J* = 3.5 Hz, 1H), 7.36 (s, 1H), 7.14 (dd, *J* = 8.5, 1.5 Hz, 1H), 6.51 (d, *J* = 3.6 Hz, 1H), 4.12 (q, *J* = 7.1 Hz, 2H), 2.74 (t, *J* = 7.5 Hz, 2H), 2.32 (t, *J* = 7.5 Hz, 2H), 1.99 (quin, *J* = 7.5 Hz, 2H), 1.67 (s, 9H), 1.25 (t, *J* = 7.1 Hz, 3H).

¹³C NMR (101 MHz, chloroform-*d*) δ 173.71, 149.91, 135.88, 133.83, 130.90, 126.15, 125.09, 120.55, 115.07, 107.21, 83.62, 60.34, 35.11, 33.74, 28.31, 27.12, 14.36.

HRMS(ESI): Calcd. for C₁₈H₂₂N₂O₂Na [M+Na]⁺ 354.1681. Found: 354.1672

1-Benzyl-4-(3-phenoxypropyl)-1H-pyrazole (1.21)



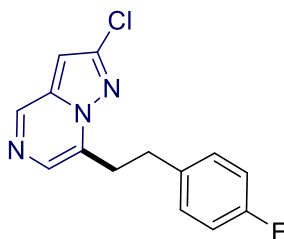
1-Benzyl-4-bromo-1H-pyrazole (47.4 mg, 0.2 mmol), (3-bromopropoxy)benzene (172.1 mg, 0.8 mmol), zinc powder (52 mg, 0.8 mmol), TMEDA (116.2 mg, 1.0 mmol) and Fe/ppm Pd NPs (15.5 mg, 0.25 mol % Pd), in 1.0 mL 2 wt % TPGS-750-M/H₂O were reacted at 45 °C for 40 h yielding 39.9 mg (68%) of 1-benzyl-4-(3-phenoxypropyl)-1H-pyrazole as a colorless oil (hexane/EtOAc : 85/15).

¹H NMR (500 MHz, chloroform-*d*) δ 7.41 (s, 1H), 7.33 (m, 4H), 7.28 (m, 1H), 7.21 (m, 3H), 6.98 – 6.91 (m, 1H), 6.88 (dd, *J* = 7.7, 2.1 Hz, 2H), 5.27 (s, 2H), 3.97 (m, 2H), 2.69 – 2.62 (m, 2H), 2.07 – 1.99 (m, 2H).

¹³C NMR (126 MHz, chloroform-*d*) δ 159.09, 138.75, 136.64, 129.59, 128.98, 128.22, 128.04, 127.89, 121.41, 120.78, 114.62, 66.83, 56.07, 30.49, 20.76.

HRMS(ESI): Calcd. for C₁₉H₂₀N₂O [M+H]⁺ 293.1654. Found: 293.1647.

2-Chloro-7-(4-fluorophenethyl)pyrazolo[1,5-a]pyrazine (1.22)



7-Bromo-2-chloropyrazolo[1,5-a]pyrazine (46.4 mg, 0.2 mmol), 1-(2-bromoethyl)-4-fluorobenzene (162.4 mg, 0.8 mmol), zinc powder (52 mg, 0.8 mmol), TMEDA (116.2 mg, 1.0 mmol) and Fe/ppm Pd NPs (15.5 mg, 0.25 mol % Pd), in 1.0 mL 2 wt % TPGS-750-M/H₂O were reacted at 45 °C for 40 h yielding 36.2 mg (66%) of 2-chloro-7-(4-fluorophenethyl)pyrazolo[1,5-a]pyrazine as a yellow oil (hexane/EtOAc : 60/40).

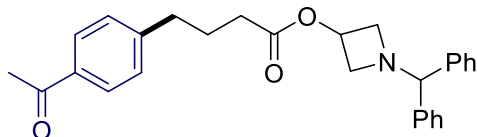
¹H NMR (400 MHz, chloroform-*d*) δ 7.91 (d, *J* = 1.1 Hz, 1H), 7.75 (d, *J* = 1.0 Hz, 1H), 7.16 (dd, *J* = 8.5, 5.4 Hz, 2H), 6.97 (t, *J* = 8.7 Hz, 2H), 6.77 (s, 1H), 3.36 – 3.28 (m, 2H), 3.20 – 3.10 (m, 2H).

¹³C NMR (126 MHz, chloroform-*d*) δ 162.69, 160.75, 147.03, 141.95, 138.28, 135.94 (d, *J*_(C-F) = 2.5 Hz), 133.56, 129.96 (d, *J*_(C-F) = 7.6 Hz), 117.44 (d, *J*_(C-F) = 26 Hz), 115.51 (d, *J*_(C-F) = 21 Hz), 33.57, 32.71.

¹⁹F NMR (376 MHz, chloroform-*d*) δ -116.67.

HRMS(ESI): Calcd. for C₁₄H₁₁ClFN₃H [M+H]⁺ 276.0704. Found: 276.0697.

1-Benzhydrylazetid-3-yl 4-(4-acetylphenyl)butanoate (1.23)



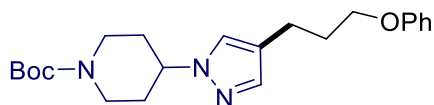
1-(4-Bromophenyl)ethan-1-one (40 mg, 0.2 mmol), 1-benzhydrylazetididin-3-yl 4-bromobutanoate (310.6 mg, 0.8 mmol), zinc powder (52 mg, 0.8 mmol), TMEDA (116.2 mg, 1.0 mmol) and Fe/ppm Pd NPs (15.5 mg, 0.25 mol % Pd), in 1.0 mL 2 wt % TPGS-750-M/H₂O were reacted at 45 °C for 40 h yielding 55.6 mg (65%) of 1-benzhydrylazetididin-3-yl 4-(4-acetylphenyl)butanoate as a white solid (hexane/EtOAc: 80/20).

¹H NMR (400 MHz, chloroform-*d*) δ 7.89 (d, *J* = 8.2 Hz, 2H), 7.43 – 7.35 (m, 4H), 7.31 – 7.27 (m, 4H), 7.25 – 7.23 (m, 2H), 7.23 – 7.17 (m, 2H), 5.14 – 5.01 (m, 1H), 4.37 (s, 1H), 3.59 (s, 2H), 3.00 (s, 2H), 2.70 (d, *J* = 7.4 Hz, 2H), 2.58 (s, 3H), 2.33 (t, *J* = 7.4 Hz, 2H), 1.96 (quin, *J* = 7.5 Hz, 2H).

¹³C NMR (101 MHz, chloroform-*d*) δ 197.94, 172.72, 147.19, 141.97, 135.46, 134.14, 131.70, 128.84, 128.76, 127.55, 78.36, 60.26, 55.69, 35.16, 33.37, 26.71, 26.10.

HRMS(ESI): Calcd. for C₂₈H₂₉NO₃H [M+H]⁺ 428.2226. Found: 428.2211.

***t*-Butyl 4-(4-(3-phenoxypropyl)-1H-pyrazol-1-yl)piperidine-1-carboxylate (1.24)**



t-Butyl 4-(4-bromo-1H-pyrazol-1-yl)piperidine-1-carboxylate (66 mg, 0.2 mmol), (3-bromopropoxy)-benzene (172.1 mg, 0.8 mmol), zinc powder (52 mg, 0.8 mmol), TMEDA (116.2 mg, 1.0 mmol) and Fe/ppm Pd NPs (15.5 mg, 0.25 mol % Pd), in 1.0 mL 2 wt % TPGS-750-M/H₂O were reacted at 45 °C for 40 h yielding 39.9 mg (52%) of *t*-butyl 4-(4-(3-

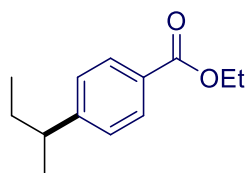
phenoxypropyl)-1H-pyrazol-1-yl)piperidine-1-carboxylate as a colorless oil (hexane/EtOAc : 75/25).

^1H NMR (400 MHz, chloroform-*d*) δ 7.36 (s, 1H), 7.29 (m, 2H), 7.21 (s, 1H), 6.92 (m, 3H), 4.20 (m, 3H), 3.97 (t, $J = 6.1$ Hz, 2H), 2.86 (t, $J = 11.7$ Hz, 2H), 2.66 (t, $J = 7.5$ Hz, 2H), 2.11 – 1.99 (m, 4H), 1.91 – 1.82 (m, 2H), 1.47 (s, 9H).

^{13}C NMR (126 MHz, chloroform-*d*) δ 159.12, 154.74, 138.56, 129.59, 125.12, 120.77, 120.55, 114.63, 79.99, 66.89, 59.24, 32.58, 30.56, 29.84, 28.56, 20.77.

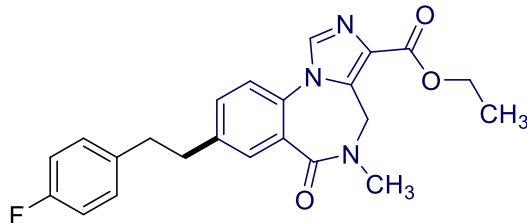
HRMS(ESI): Calcd. for $\text{C}_{22}\text{H}_{31}\text{N}_3\text{O}_3\text{H} [\text{M}+\text{H}]^+$ 386.2444. Found: 386.2436.

Ethyl 4-(*s*-butyl)benzoate (1.26)



Ethyl 4-bromobenzoate (45.8 mg, 0.2 mmol), 2-bromobutane (82.2 mg, 0.6 mmol), zinc powder (52 mg, 0.8 mmol), TMEDA (116.2 mg, 1.0 mmol) and Fe/ppm Pd NPs (15.5 mg, 0.25 mol % Pd), in 1.0 mL 2 wt % TPGS-750-M/ H_2O were reacted at rt for 16 h. The crude product was washed by column chromatography hexane/EtOAc: 95/5 to remove the 2-bromobutane and TMEDA. Then the mixture was analyzed by ^1H NMR using ethylene carbonate as internal standard.

Ethyl 8-(4-fluorophenethyl)-5-methyl-6-oxo-5,6-dihydro-4H-benzo[f]imidazo[1,5-a][1,4]diazepine-3-carboxylate (1.27)



Ethyl 8-bromo-5-methyl-6-oxo-5,6-dihydro-4H-benzo[f]imidazo[1,5-a][1,4]diazepine-3-carboxylate (72.8 mg, 0.2 mmol), 1-(2-bromoethyl)-4-fluorobenzene (162.4 mg, 0.8 mmol), zinc powder (52 mg, 0.8 mmol), TMEDA (116.2 mg, 1.0 mmol) and Fe/ppm Pd NPs (25 mg, 0.40 mol % Pd), in 1.0 mL 2 wt % TPGS-750-M/H₂O were reacted at 45 °C for 40 h yielding 54.5 mg (67%) of ethyl 8-(4-fluorophenethyl)-5-methyl-6-oxo-5,6-dihydro-4H-benzo[f]imidazo[1,5-a][1,4]diazepine-3-carboxylate as a white solid (hexane/EtOAc : 70/30).

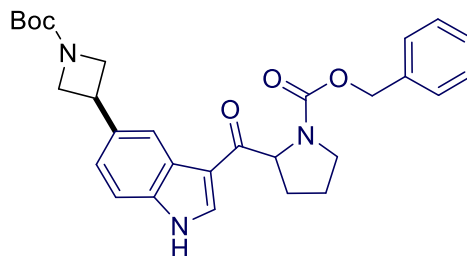
¹H NMR (400 MHz, chloroform-*d*) δ 7.90 (d, *J* = 1.8 Hz, 1H), 7.87 (s, 1H), 7.38 – 7.29 (m, 2H), 7.12 (dd, *J* = 8.5, 5.5 Hz, 2H), 6.97 (t, *J* = 8.7 Hz, 2H), 5.18 (br, s, 1H), 4.44 (br, m, 3H), 3.25 (s, 3H), 3.08 – 2.86 (m, 4H), 1.45 (t, *J* = 7.1 Hz, 3H).

¹³C NMR (126 MHz, chloroform-*d*) δ 166.73, 163.13, 162.59, 160.64, 142.49, 136.48 (d, *J*_(C-F) = 3.8 Hz), 135.70, 135.06, 133.00, 132.54, 130.26, 129.95 (d, *J*_(C-F) = 7.6 Hz), 129.17, 121.95, 115.43 (d, *J*_(C-F) = 21.4 Hz), 61.18, 42.56, 37.39, 36.59, 36.04, 14.54.

¹⁹F NMR (376 MHz, chloroform-*d*) δ -116.94.

HRMS(ESI): Calcd. for C₂₃H₂₂FN₃O₃H [M+H]⁺ 408.1723. Found: 408.1718.

Benzyl (*S*)-2-(5-(1-(*t*-butoxycarbonyl)azetidin-3-yl)-1H-indole-3-carbonyl)pyrrolidine-1-carboxylate (mixture of two rotamers, ratio = 3:7) (1.28)



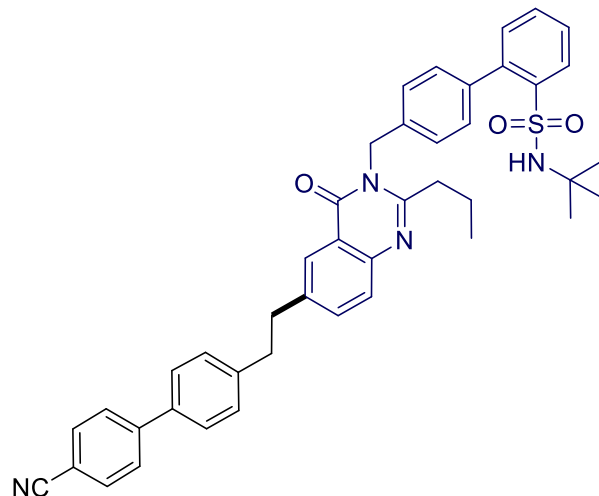
Benzyl (*S*)-2-(5-(1-(*t*-butoxycarbonyl)azetidin-3-yl)-1H-indole-3-carbonyl)pyrrolidine-1-carboxylate (85.5 mg, 0.2 mmol), *t*-butyl 3-bromoazetidine-1-carboxylate (188.9 mg, 0.8 mmol), zinc powder (52 mg, 0.8 mmol), TMEDA (116.2 mg, 1.0 mmol) and Fe/ppm Pd NPs (25 mg, 0.40 mol % Pd), in 1.0 mL 2 wt % TPGS-750-M/H₂O were reacted at 45 °C for 40 h yielding 58.3 mg (58%) of benzyl (*S*)-2-(5-(1-(*t*-butoxycarbonyl)azetidin-3-yl)-1H-indole-3-carbonyl)pyrrolidine-1-carboxylate as a white solid (hexane/EtOAc : 60/40).

¹H NMR (400 MHz, chloroform-*d*) δ 9.65 – 9.12 (m, 1H), 8.34 – 8.05 (m, 1H), 7.75 – 7.69 (m, 1H), 7.45 – 7.29 (m, 4H), 7.21 – 6.95 (m, 3H), 5.30 – 5.09 (m, 2H), 5.04 – 4.95 (m, 1H), 4.42 – 4.27 (m, 2H), 4.10 – 3.92 (m, 2H), 3.83 – 3.56 (m, 3H), 2.37 – 2.20 (m, 1H), 2.15 – 1.86 (m, 3H), 1.48 (s, 9H)..

¹³C NMR (126 MHz, chloroform-*d*) δ 194.74, 193.73, 156.56, 155.43, 154.76, 136.91, 136.65, 136.20, 135.42, 131.98, 131.38, 128.66, 128.17, 128.13, 127.93, 127.80, 127.64, 126.29, 125.92, 122.64, 122.53, 120.93, 120.19, 115.07, 114.95, 112.03, 79.70, 79.59, 67.30, 67.12, 62.65, 62.43, 57.09, 56.81, 47.61, 47.14, 33.94, 33.83, 32.04, 30.98, 28.61, 24.41, 23.84.

HRMS(ESI): Calcd. for C₂₉H₃₃N₃O₅Na [M+Na]⁺ 526.2318. Found: 526.2304.

***N*-(*t*-Butyl)-4'-((6-(2-(4'-cyano-[1,1'-biphenyl]-4-yl)ethyl)-4-oxo-2-propylquinazolin-3(4H)-yl)methyl)-[1,1'-biphenyl]-2-sulfonamide (1.29)**



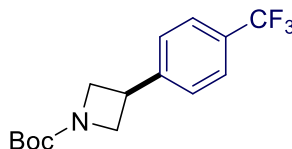
4'-((6-Bromo-4-oxo-2-propylquinazolin-3(4H)-yl)methyl)-N-(*t*-butyl)-[1,1'-biphenyl]-2-sulfonamide (113.7 mg, 0.2 mmol), 4'-(2-bromoethyl)-[1,1'-biphenyl]-4-carbonitrile (228.9 mg, 0.8 mmol), zinc powder (52 mg, 0.8 mmol), TMEDA (116.2 mg, 1.0 mmol) and Fe/ppm Pd NPs (25 mg, 0.40 mol % Pd), in 1.0 mL 2 wt % TPGS-750-M/H₂O were reacted at 45 °C for 40 h yielding 65.2 mg (47%) of *N*-(*t*-butyl)-4'-((6-(2-(4'-cyano-[1,1'-biphenyl]-4-yl)ethyl)-4-oxo-2-propylquinazolin-3(4H)-yl)methyl)-[1,1'-biphenyl]-2-sulfonamide as a white solid (hexane/acetone : 65/35).

¹H NMR (400 MHz, chloroform-*d*) δ 8.16 (d, *J* = 7.4 Hz, 2H), 7.74 – 7.59 (m, 7H), 7.58 – 7.47 (m, 7H), 7.30 (m, 3H), 5.47 (m, 2H), 3.51 (m, 1H), 3.08 (dddd, *J* = 16.6, 9.3, 5.6, 3.5 Hz, 4H), 2.77 – 2.72 (t, *J* = 8.2 Hz, 2H), 1.86 (m, 2H), 1.03 (t, *J* = 7.3 Hz, 3H), 0.98 (s, 9H).

¹³C NMR (126 MHz, chloroform-*d*) δ 162.72, 145.59, 142.20, 142.11, 139.38, 139.12, 137.12, 136.65, 135.45, 132.73, 132.41, 132.00, 130.55, 129.42, 128.44, 128.13, 127.73, 127.68, 127.60, 127.50, 127.42, 126.32, 126.17, 125.01, 120.34, 119.15, 110.81, 54.56, 46.38, 37.58, 37.48, 37.28, 29.90, 20.88, 14.07.

HRMS(ESI): Calcd. for C₄₃H₄₂N₄O₃SH [M+H]⁺ 695.3056. Found: 695.3041.

***t*-Butyl 3-(4-(trifluoromethyl)phenyl)azetidine-1-carboxylate (1.30)**



1-Bromo-4-(trifluoromethyl)benzene (45 mg, 0.2 mmol), *t*-butyl 3-bromoazetidine-1-carboxylate (141.7 mg, 0.6 mmol), zinc powder (52 mg, 0.8 mmol), TMEDA (116.2 mg, 1.0 mmol) and Fe/ppm Pd NPs (15.5 mg, 0.25 % Pd), in 1.0 mL 2 wt % TPGS-750-M/H₂O were reacted at rt for 16 h yielding 49.2 mg (82%) of *t*-butyl 3-(4-(trifluoromethyl)phenyl)azetidine-1-carboxylate as a yellow oil (hexane/EtOAc: 85/15).

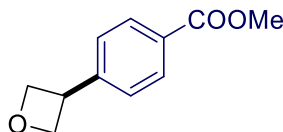
¹H NMR (400 MHz, chloroform-*d*) δ 7.61 (d, *J* = 8.1 Hz, 2H), 7.43 (d, *J* = 8.1 Hz, 2H), 4.36 (t, *J* = 8.7 Hz, 2H), 3.97 (dd, *J* = 8.5, 6.0 Hz, 2H), 3.78 (ddd, *J* = 14.5, 8.6, 6.0 Hz, 1H), 1.47 (s, 9H).

¹³C NMR (126 MHz, chloroform-*d*) δ 156.48, 146.45, 129.49 (q, *J*_(C-F) = 33 Hz), 127.31, 125.85 (q, *J*_(C-F) = 3.8 Hz), 123.16, 79.95, 33.46, 29.85, 28.55.

¹⁹F NMR (376 MHz, chloroform-*d*) δ -62.50.

Spectral data matched those previously reported.^[4]

Methyl 4-(oxetan-3-yl)benzoate (1.31)



Methyl 4-bromobenzoate (43 mg, 0.2 mmol), 3-bromooxetane (82.2 mg, 0.6 mmol), zinc powder (52 mg, 0.8 mmol), TMEDA (116.2 mg, 1.0 mmol) and Fe/ppm Pd NPs (15.5 mg,

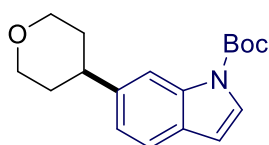
0.25 % Pd), in 1.0 mL 2 wt % TPGS-750-M/H₂O were reacted at rt for 16 h yielding 33.1 mg (86%) of methyl 4-(oxetan-3-yl)benzoate as a colorless oil (hexane/EtOAc : 90/10).

¹H NMR (400 MHz, chloroform-*d*) δ 8.04 (d, *J* = 8.3 Hz, 2H), 7.46 (d, *J* = 8.2 Hz, 2H), 5.10 (dd, *J* = 8.3, 6.1 Hz, 2H), 4.77 (t, *J* = 6.3 Hz, 2H), 4.33 – 4.22 (m, 1H), 3.92 (s, 3H).

¹³C NMR (101 MHz, chloroform-*d*) δ 166.97, 146.89, 130.25, 129.11, 126.96, 78.54, 52.26, 40.39.

Spectral data matched those previously reported.^[4]

***t*-Butyl 6-(tetrahydro-2H-pyran-4-yl)-1H-indole-1-carboxylate (1.32)**



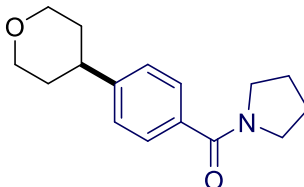
t-Butyl 6-bromo-1H-indole-1-carboxylate (59.2 mg, 0.2 mmol), 4-bromotetrahydro-2H-pyran (99 mg, 0.6 mmol), zinc powder (52 mg, 0.8 mmol), TMEDA (116.2 mg, 1.0 mmol) and Fe/ppm Pd NPs (15.5 mg, 0.25 % Pd), in 1.0 mL 2 wt % TPGS-750-M/H₂O were reacted at rt for 16 h yielding 54.6 mg (91%) of *t*-butyl 6-(tetrahydro-2H-pyran-4-yl)-1H-indole-1-carboxylate as a yellow powder (hexane/EtOAc : 85/15).

¹H NMR (400 MHz, chloroform-*d*) δ 8.08 (s, 1H), 7.54 (d, *J* = 3.6 Hz, 1H), 7.50 (d, *J* = 8.1 Hz, 1H), 7.12 (dd, *J* = 8.1, 1.2 Hz, 1H), 6.53 (d, *J* = 3.7 Hz, 1H), 4.10 (dd, *J* = 11.0, 3.7 Hz, 2H), 3.56 (td, *J* = 11.6, 2.4 Hz, 2H), 2.89 (tt, *J* = 11.6, 4.2 Hz, 1H), 1.93 – 1.79 (m, 4H), 1.68 (s, 9H).

¹³C NMR (101 MHz, chloroform-*d*) δ 149.96, 142.56, 129.13, 125.86, 121.99, 120.93, 113.39, 107.21, 83.67, 77.36, 68.67, 42.24, 34.60, 28.37.

Spectral data matched those previously reported.^[5]

Pyrrolidin-1-yl(4-(tetrahydro-2H-pyran-4-yl)phenyl)methanone (1.33)



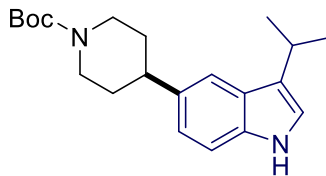
(4-Bromophenyl)(pyrrolidin-1-yl)methanone (50.8, 0.2 mmol), 4-bromotetrahydro-2H-pyran (99 mg, 0.6 mmol), zinc powder (52 mg, 0.8 mmol), TMEDA (116.2 mg, 1.0 mmol) and Fe/ppm Pd NPs (15.5 mg, 0.25 % Pd), in 1.0 mL 2 wt % TPGS-750-M/H₂O were reacted at rt for 16 h yielding 48.3 mg (93 %) of pyrrolidin-1-yl(4-(tetrahydro-2H-pyran-4-yl)phenyl)methanone as a colorless oil (hexane/EtOAc : 80/20).

¹H NMR (400 MHz, chloroform-*d*) δ 7.51 (d, J = 8.1 Hz, 2H), 7.31 – 7.24 (m, 2H), 4.11 (dd, J = 11.4, 2.7 Hz, 2H), 3.67 (t, J = 6.9 Hz, 2H), 3.56 (td, J = 11.4, 2.6 Hz, 2H), 3.48 (t, J = 6.5 Hz, 2H), 2.81 (ddd, J = 15.7, 11.2, 4.4 Hz, 1H), 1.99 (quin, J = 6.6 Hz, 2H), 1.90 (m, 2H), 1.86 – 1.76 (m, 4H).

¹³C NMR (126 MHz, chloroform-*d*) δ 169.76, 147.78, 135.41, 127.59, 126.73, 68.43, 49.78, 46.32, 41.60, 33.88, 26.56, 24.60.

Spectral data matched those previously reported.^[5]

***t*-Butyl 4-(3-isopropyl-1H-indol-6-yl)piperidine-1-carboxylate (1.34)**



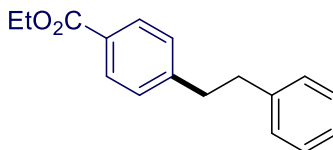
6-Bromo-3-isopropyl-1H-indole (47.6 mg, 0.2 mmol), *t*-butyl 4-bromopiperidine-1-carboxylate (158.3 mg, 0.6 mmol), zinc powder (52 mg, 0.8 mmol), TMEDA (116.2 mg, 1.0 mmol) and Fe/ppm Pd NPs (15.5 mg, 0.25 % Pd), in 1.0 mL 2 wt % TPGS-750-M/H₂O were reacted at rt for 16 h yielding 55.2 mg (81%) of *t*-butyl 4-(3-isopropyl-1H-indol-6-yl)piperidine-1-carboxylate as a yellow oil (hexane/EtOAc : 75/25).

¹H NMR (600 MHz, chloroform-*d*) δ 8.06 (s, 1H), 7.77 (d, $J = 1.6$ Hz, 1H), 7.27 – 7.24 (m, 1H), 7.21 (d, $J = 8.6$ Hz, 1H), 6.96 (d, $J = 2.1$ Hz, 1H), 4.34 (tt, $J = 7.6, 3.7$ Hz, 1H), 3.72 – 3.66 (m, 2H), 3.32 (ddd, $J = 13.5, 7.7, 3.6$ Hz, 2H), 3.15 (hept, $J = 6.8$ Hz, 1H), 2.11 – 2.05 (m, 2H), 1.93 (m, 2H), 1.47 (s, 9H), 1.35 (d, $J = 6.9$ Hz, 6H).

¹³C NMR (126 MHz, chloroform-*d*) δ 154.80, 135.28, 128.68, 124.68, 123.83, 122.06, 120.66, 112.65, 112.37, 80.00, 49.64, 35.71, 28.54, 25.46, 24.81, 23.39.

Spectral data matched those previously reported.^[6]

Ethyl 4-phenethylbenzoate (1.35)



Ethyl 4-bromobenzoate (45.8 mg, 0.2 mmol), (2-bromoethyl)benzene (109.8 mg, 0.6 mmol), zinc powder (52 mg, 0.8 mmol), TMEDA (116.2 mg, 1.0 mmol) and Fe/ppm Pd NPs

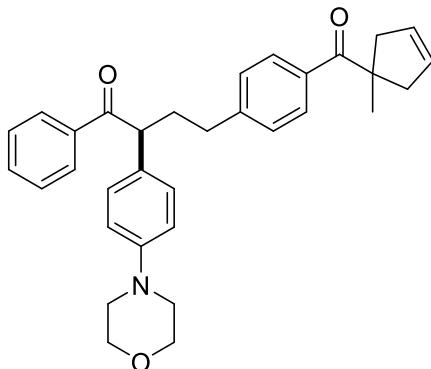
(15.5 mg, 0.25 % Pd), in 1.0 mL 2 wt % TPGS-750-M/H₂O were reacted at rt for 16 h yielding 50.4 mg (99%) of ethyl 4-phenethylbenzoate as a yellow oil (hexane/EtOAc : 95/5).

¹H NMR (400 MHz, chloroform-*d*) δ 8.00 – 7.92 (m, 2H), 7.31 – 7.26 (m, 2H), 7.25 – 7.13 (m, 5H), 4.37 (q, *J* = 7.1 Hz, 2H), 3.04 – 2.88 (m, 4H), 1.39 (t, *J* = 7.1 Hz, 3H).

¹³C NMR (126 MHz, chloroform-*d*) δ 166.81, 147.18, 141.30, 129.78, 128.63, 128.58, 128.52, 128.41, 126.21, 60.94, 38.01, 37.62, 14.49.

Spectral data matched those previously reported.^[7]

4-(4-(1-Methylcyclopent-3-ene-1-carbonyl)phenyl)-2-(4-morpholinophenyl)-1-phenylbutan-1-one (1.40)



¹H NMR (600 MHz, chloroform-*d*) δ 7.90 (d, *J* = 8.4 Hz, 2H), 7.77 (d, *J* = 8.2 Hz, 2H), 7.47 (t, *J* = 7.4 Hz, 1H), 7.36 (t, *J* = 7.8 Hz, 2H), 7.18 (d, *J* = 7.9 Hz, 4H), 6.83 (d, *J* = 8.4 Hz, 2H), 5.74 (s, 2H), 4.45 (t, *J* = 7.2 Hz, 1H), 3.86 – 3.78 (m, 4H), 3.17 – 3.10 (m, 6H), 2.68 – 2.58 (m, 2H), 2.54 – 2.45 (m, 1H), 2.37 (d, *J* = 14.1 Hz, 2H), 2.14 (m, 1H), 1.39 (s, 3H).

^{13}C NMR (126 MHz, chloroform-*d*) δ 204.91, 199.77, 150.32, 146.71, 136.90, 133.51, 132.95, 130.32, 129.24, 129.21, 128.78, 128.61, 128.50, 116.09, 66.99, 52.81, 51.90, 49.19, 46.37, 34.94, 33.62, 28.05.

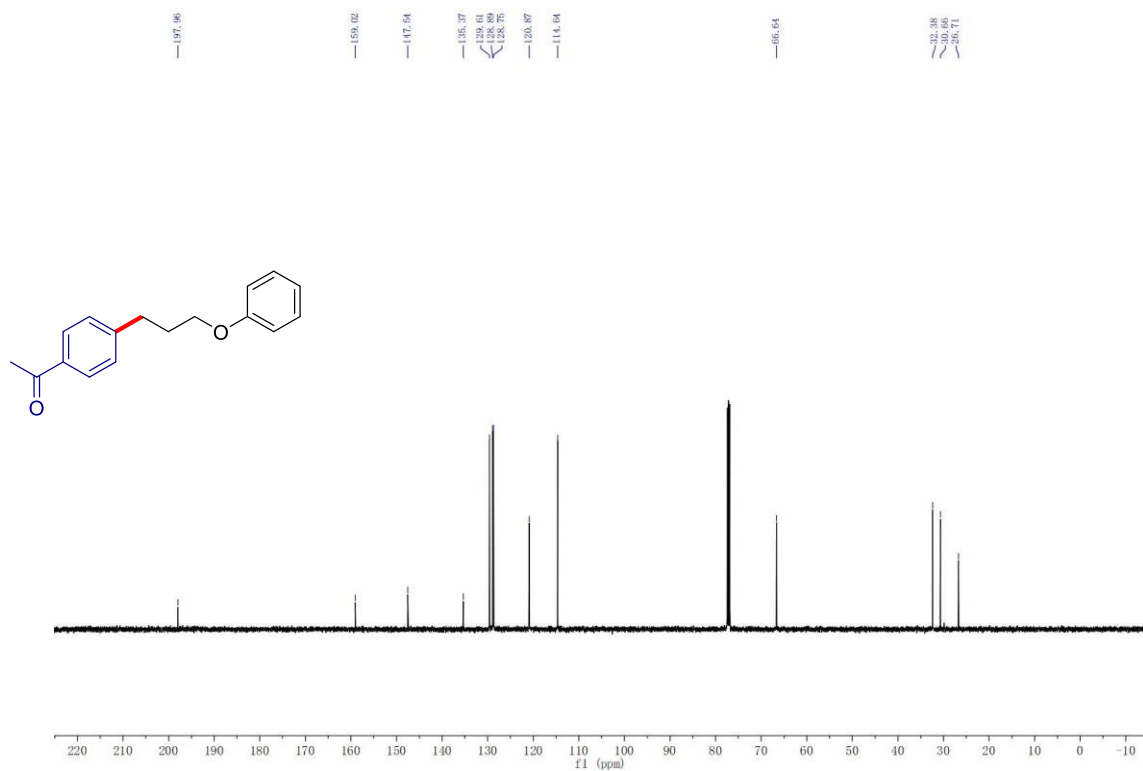
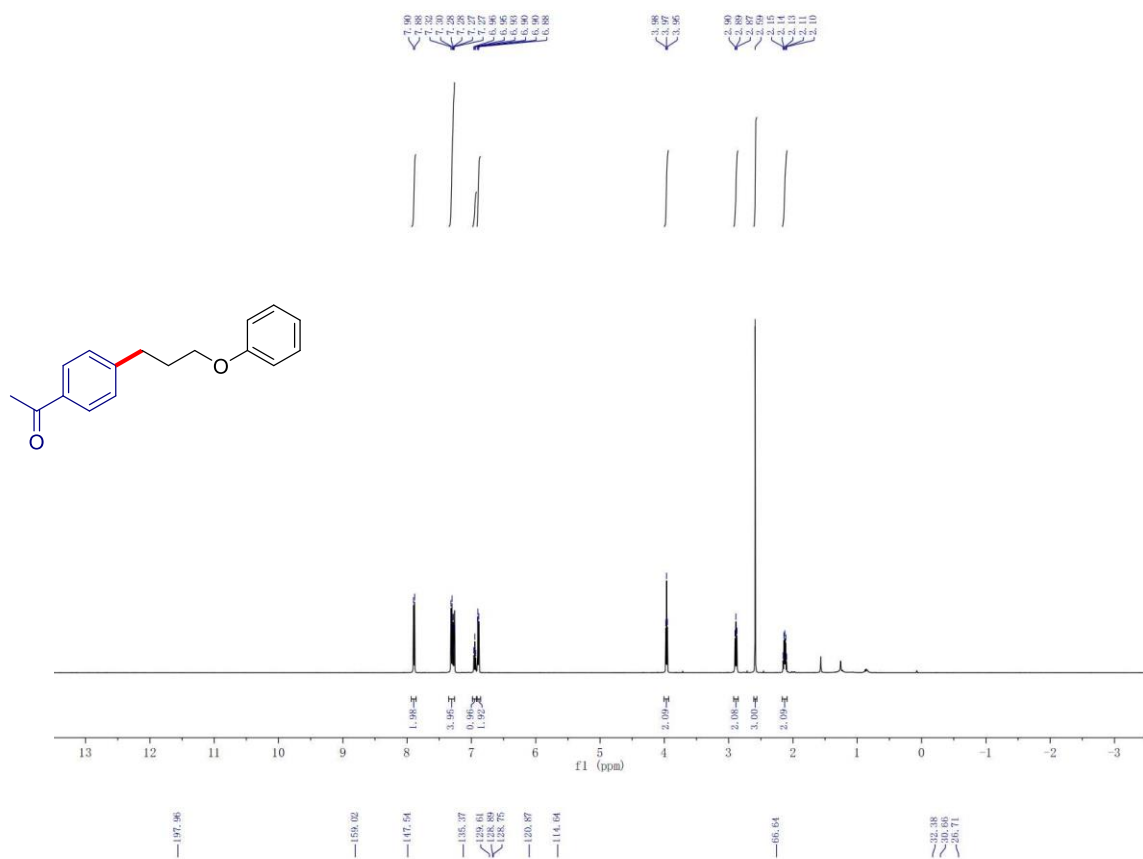
HRMS(ESI): Calcd. for $\text{C}_{33}\text{H}_{35}\text{NO}_3\text{H} [\text{M}+\text{H}]^+$ 494.2695. Found: 494.2678.

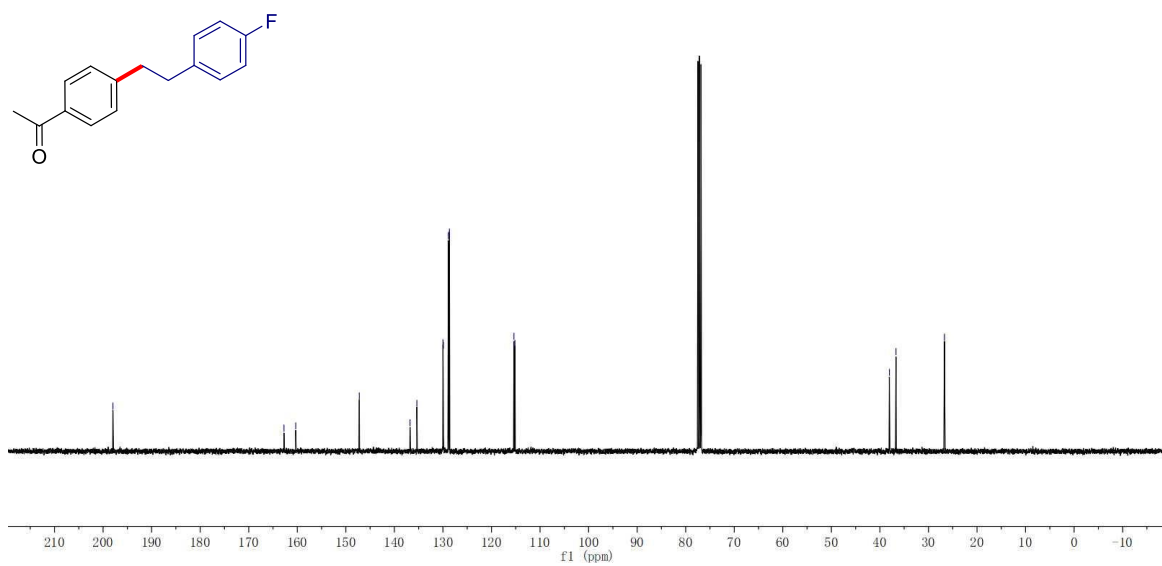
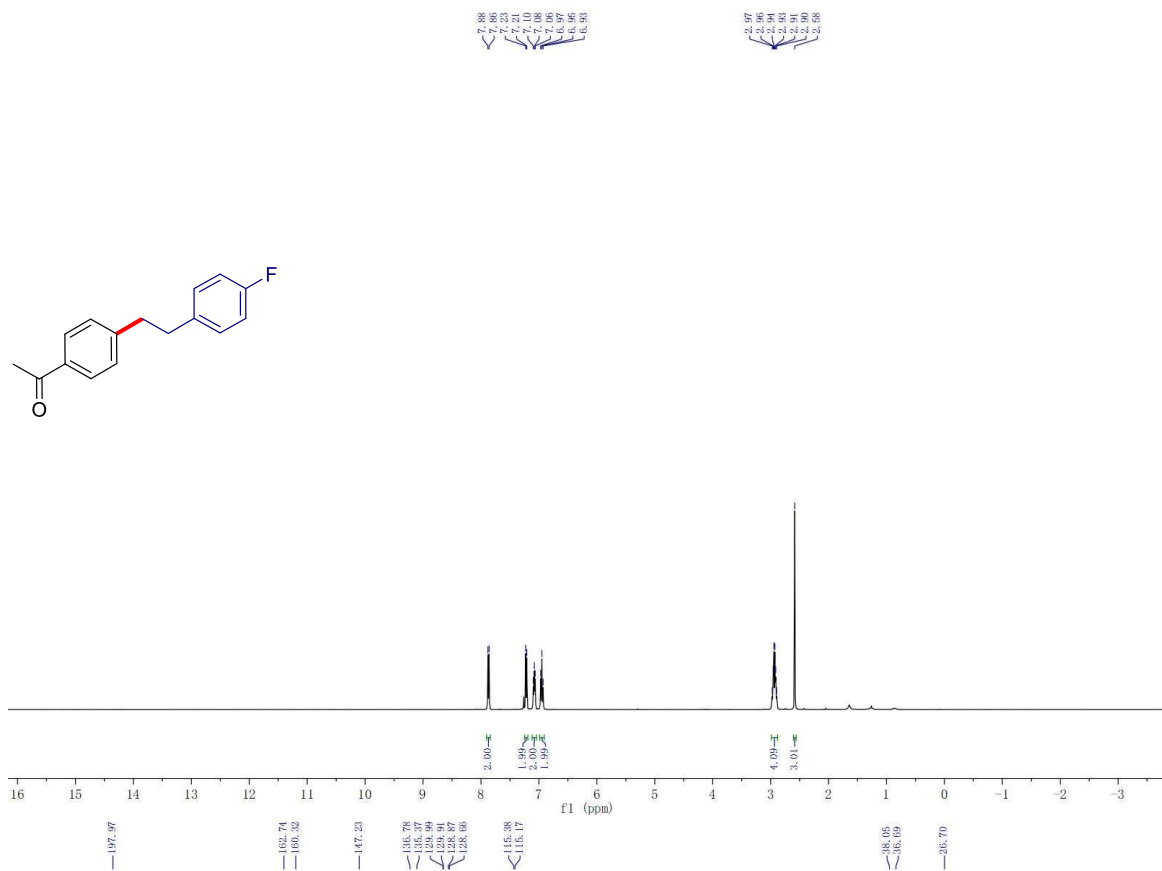
References

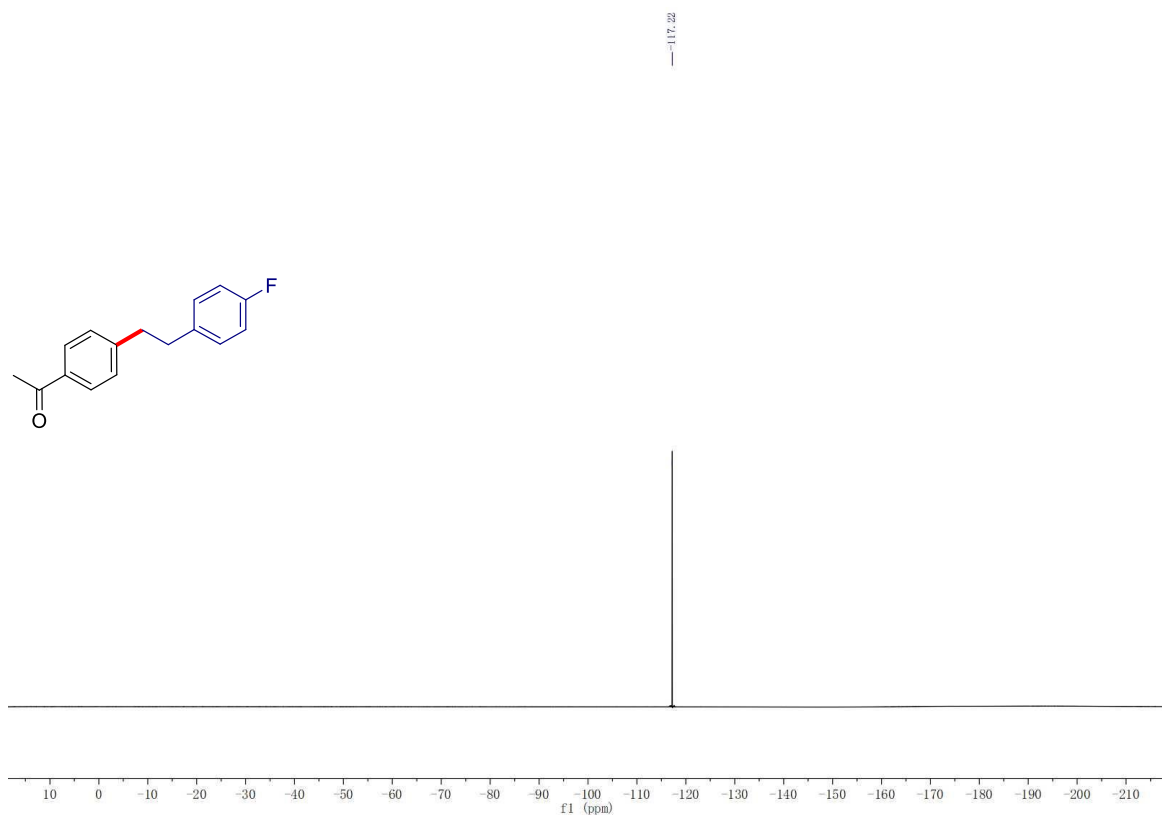
1. Yang, T.; Wei, Y.; Koh, M. J., Photoinduced Nickel-Catalyzed Deaminative Cross-Electrophile Coupling for $\text{C}(\text{sp}^2)\text{--C}(\text{sp}^3)$ and $\text{C}(\text{sp}^3)\text{--C}(\text{sp}^3)$ Bond Formation. *ACS Catal.* **2021**, *11*, 6519-6525.
2. Krasovskiy, A.; Duplais, C.; Lipshutz, B. H., Zn-Mediated, Pd-Catalyzed Cross-Couplings in Water at Room Temperature Without Prior Formation of Organozinc Reagents. *J. Am. Chem. Soc.* **2009**, *131*, 15592-15593.
3. Ye, N.; Wu, B.; Zhao, K.; Ge, X.; Zheng, Y.; Shen, X.; Shi, L.; Cortes-Clerget, M.; Regnier, M. L.; Parmentier, M.; Gallou, F., Micelle enabled $\text{C}(\text{sp}^2)\text{--C}(\text{sp}^3)$ cross-electrophile coupling in water via synergistic nickel and copper catalysis. *Chem. Comm.* **2021**, *57*, 7629-7632.
4. Borlinghaus, N.; Schönfeld, B.; Heitz, S.; Klee, J.; Vukelić, S.; Braje, W. M.; Jolit, A., Enabling Metallophotoredox Catalysis in Parallel Solution-Phase Synthesis Using Disintegrating Reagent Tablets. *J. Org. Chem.* **2021**, *86*, 16535-16547.
5. Delgado, P.; Glass, R. J.; Geraci, G.; Duvadie, R.; Majumdar, D.; Robinson, R. I.; Elmaarouf, I.; Mikus, M.; Tan, K. L., Use of Green Solvents in Metallaphotoredox Cross-Electrophile Coupling Reactions Utilizing a Lipophilic Modified Dual Ir/Ni Catalyst System. *J. Org. Chem.* **2021**, *86*, 17428-17436.
6. Beutner, G. L.; Simmons, E. M.; Ayers, S.; Bemis, C. Y.; Goldfogel, M. J.; Joe, C. L.; Marshall, J.; Wisniewski, S. R., A Process Chemistry Benchmark for $\text{sp}^2\text{--sp}^3$ Cross Couplings. *J. Org. Chem.* **2021**, *86*, 10380-10396.

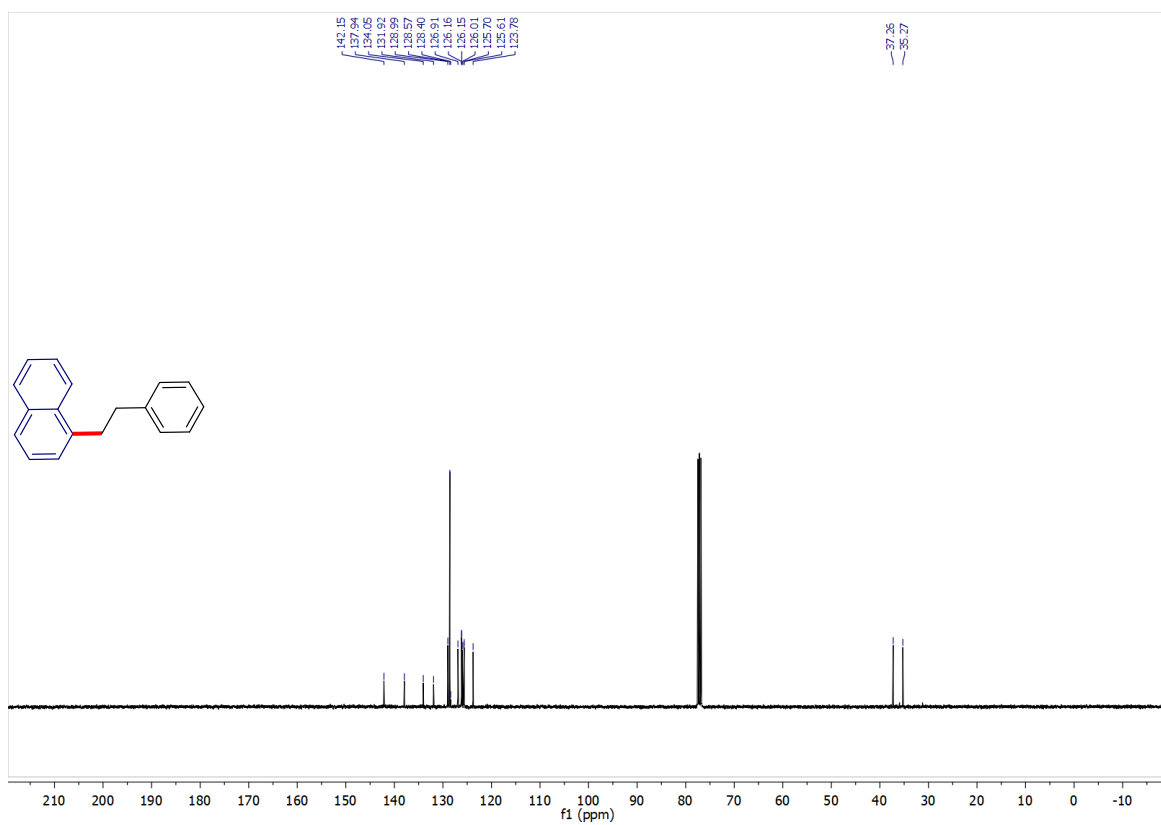
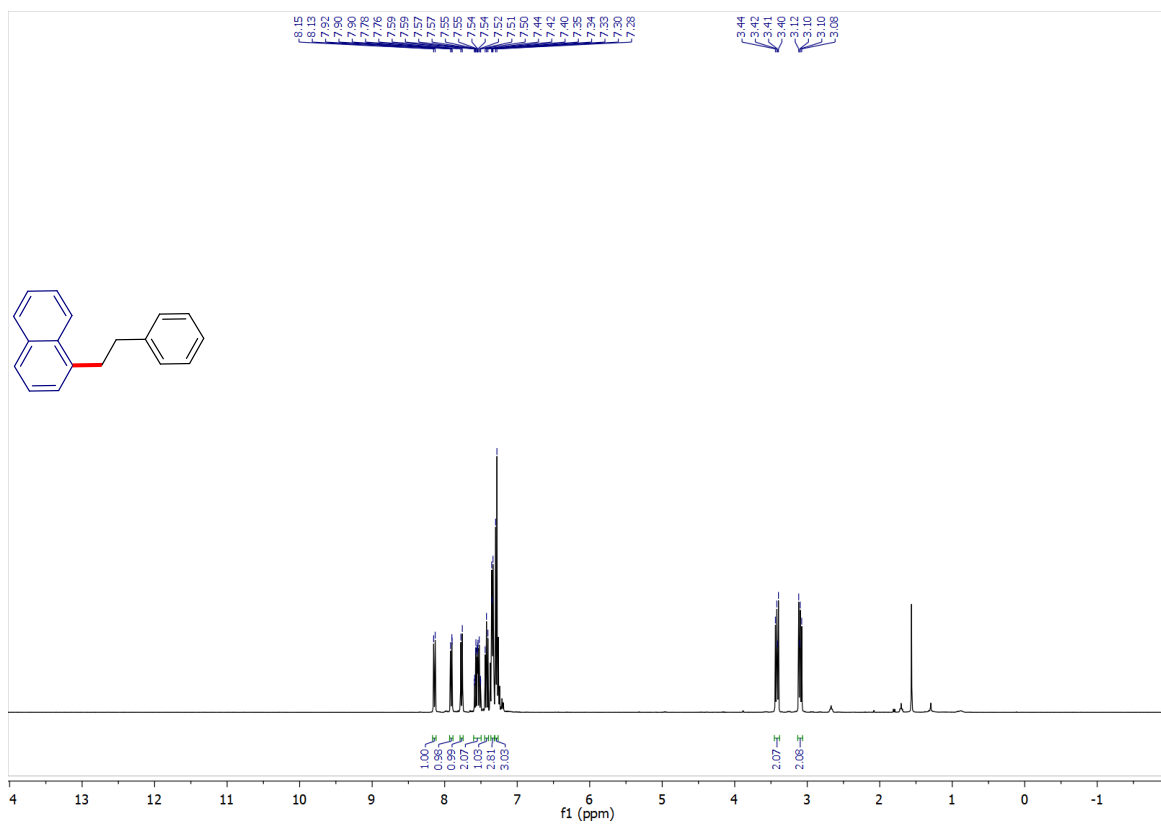
7. Shen, Z.-L.; Goh, K. K. K.; Yang, Y.-S.; Lai, Y.-C.; Wong, C. H. A.; Cheong, H.-L.; Loh, T.-P., Direct Synthesis of Water-Tolerant Alkyl Indium Reagents and Their Application in Palladium-Catalyzed Couplings with Aryl Halides. *Angew. Chem. Int. Ed.* **2011**, *50*, 511-514.

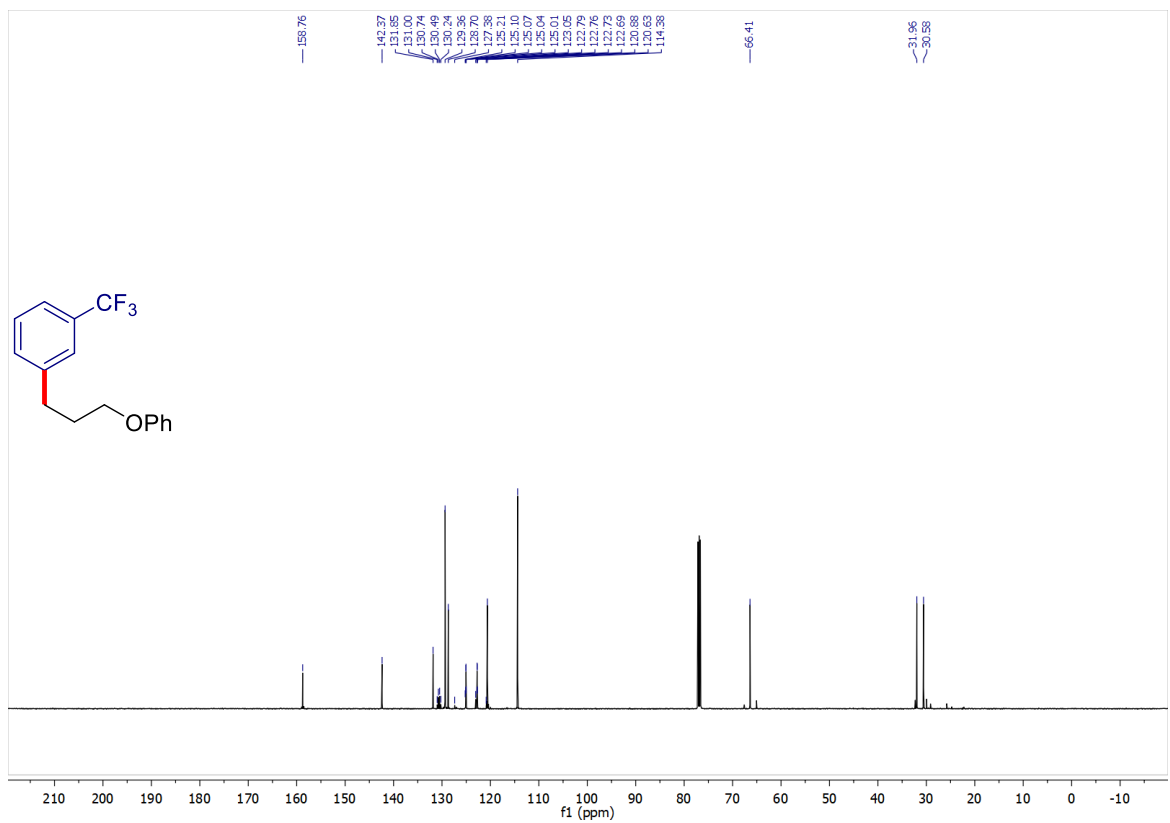
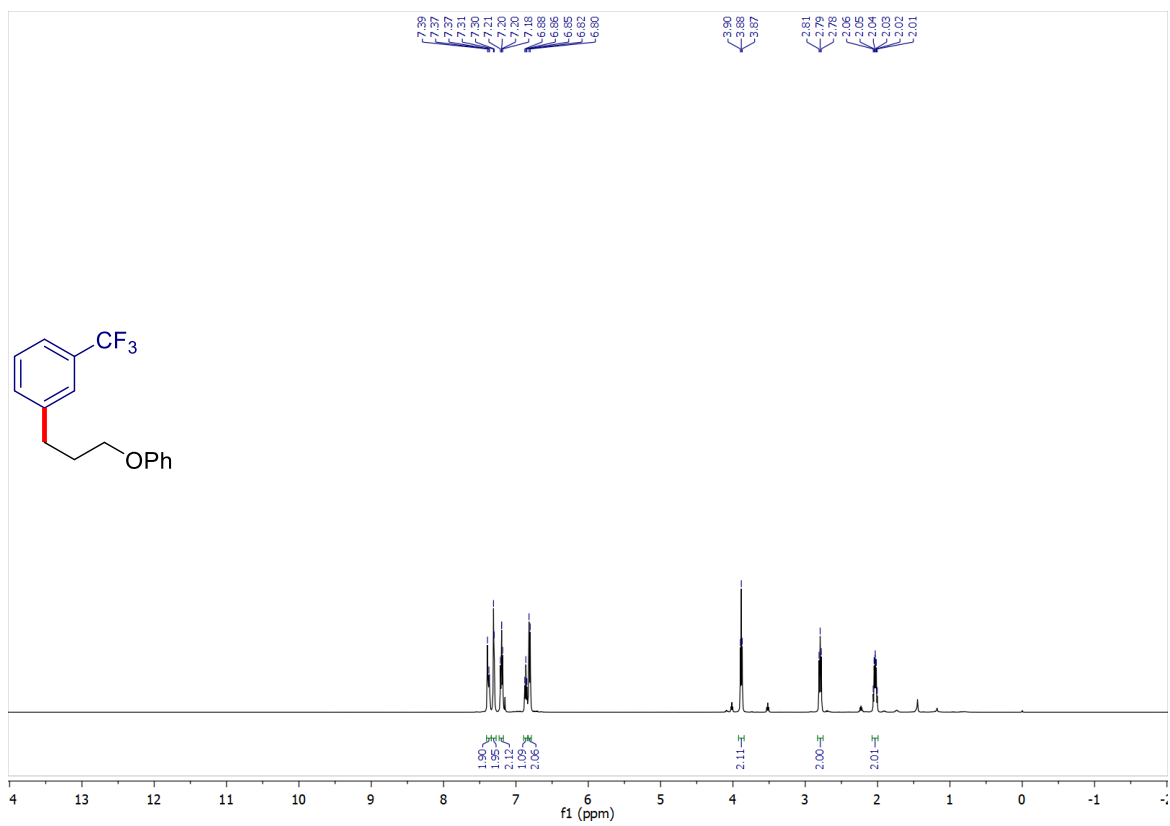
NMR spectra

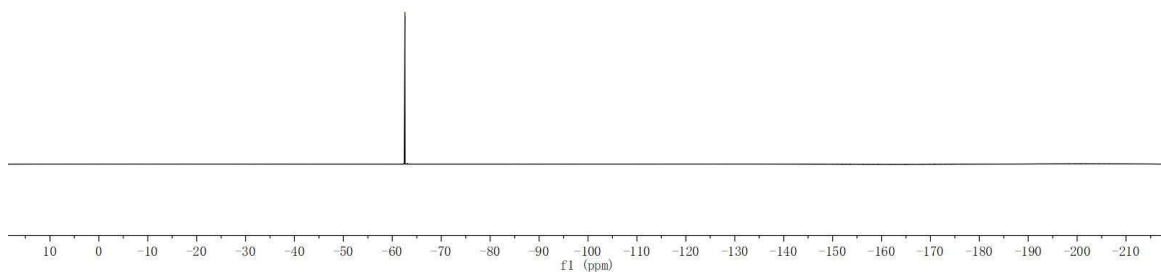
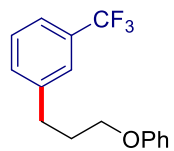




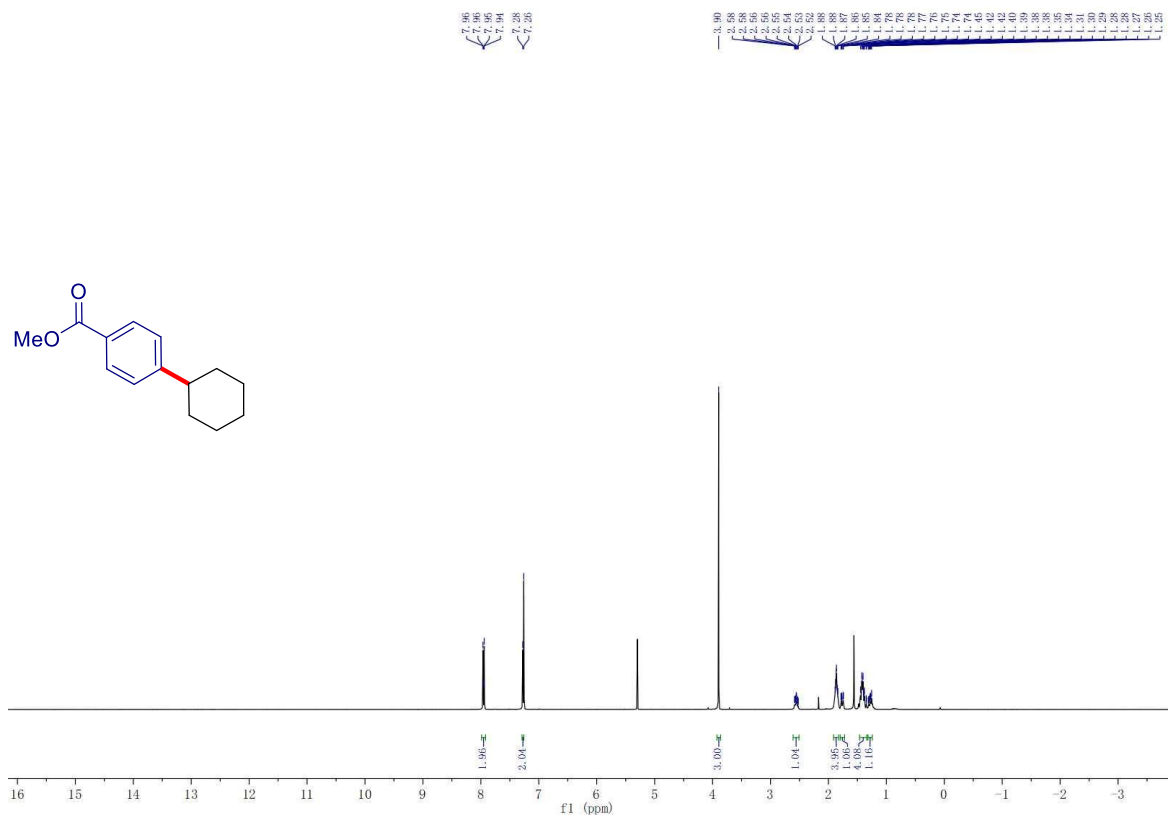
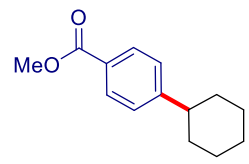


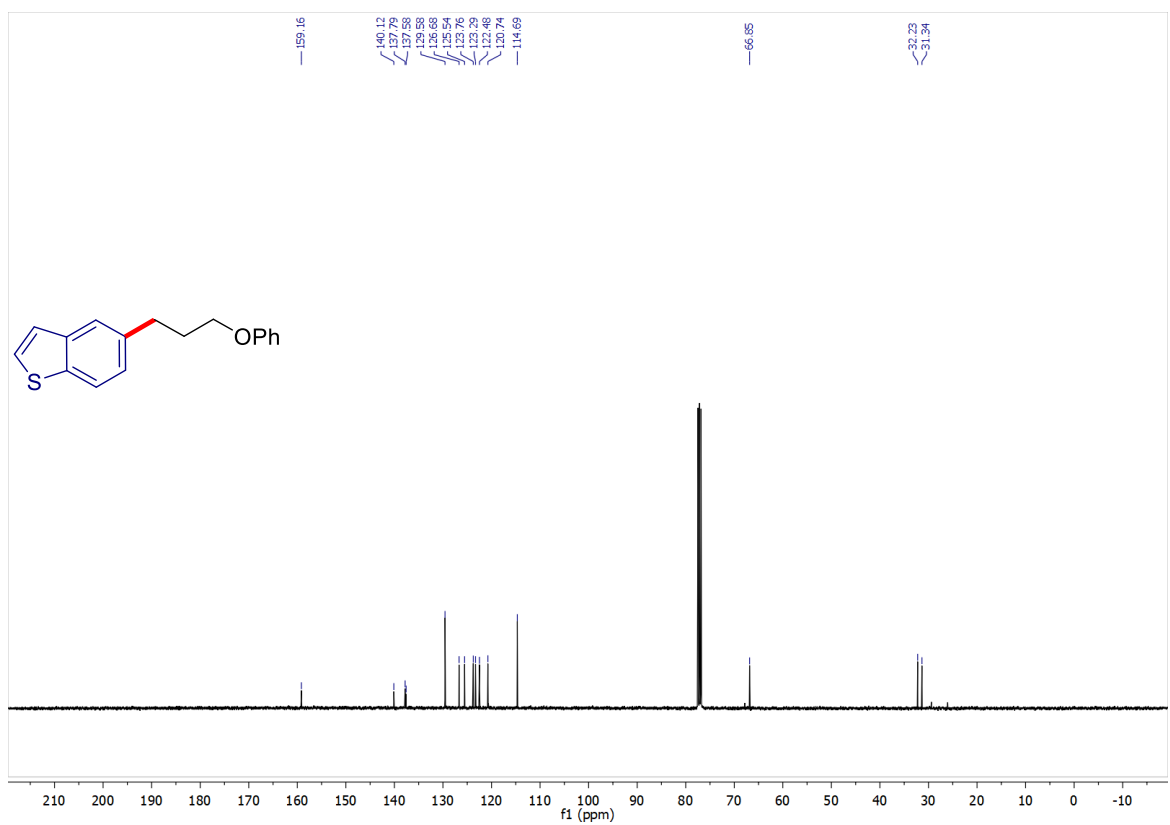
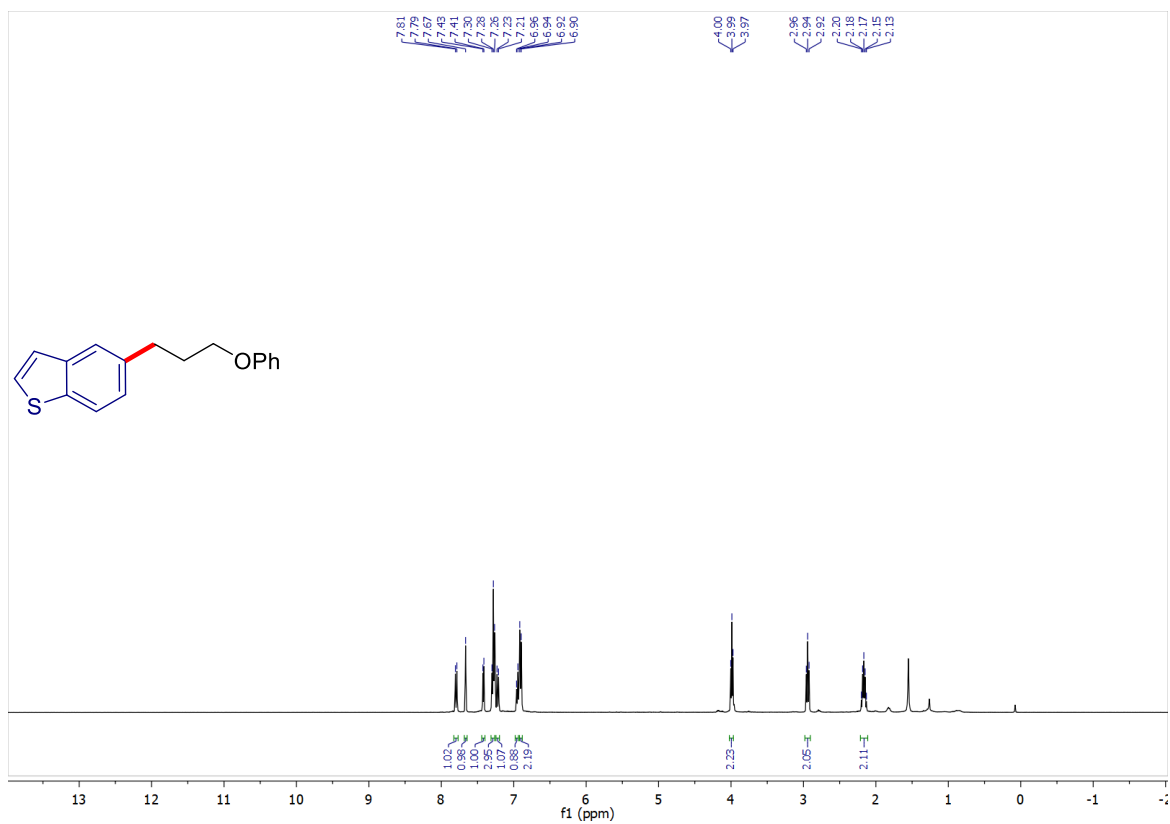


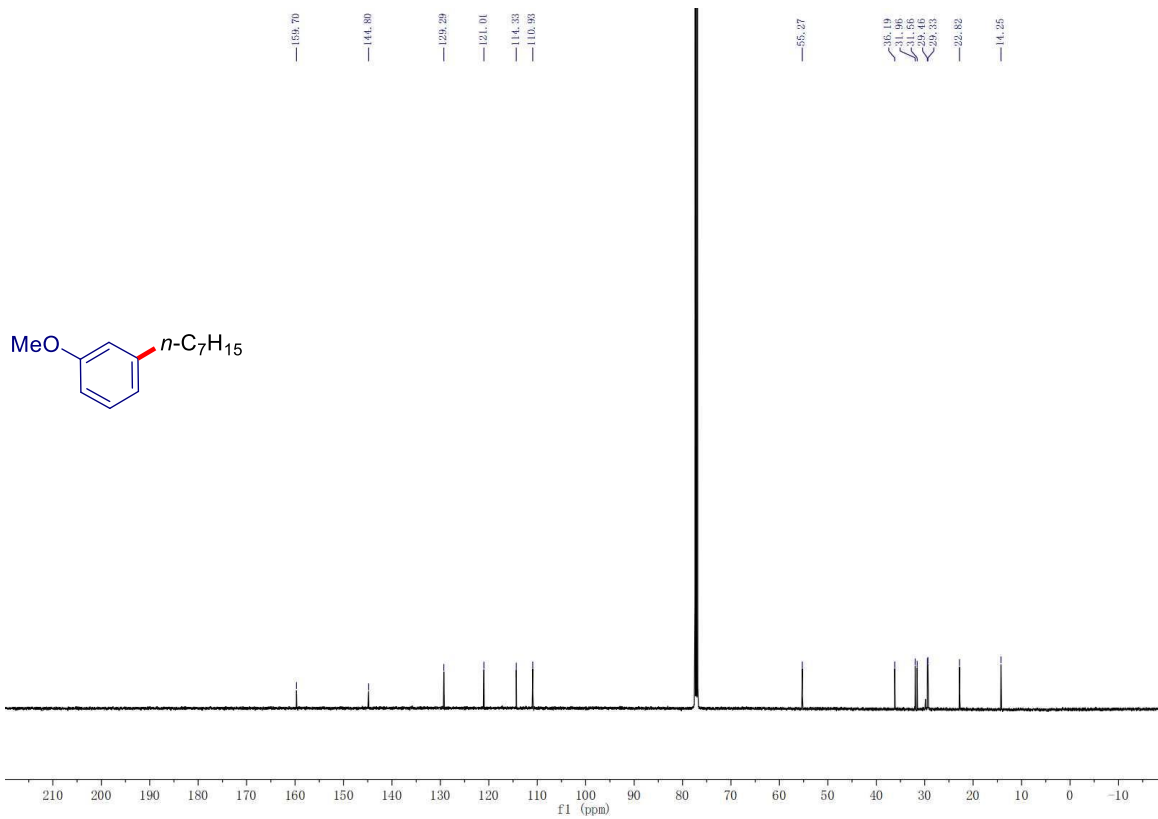
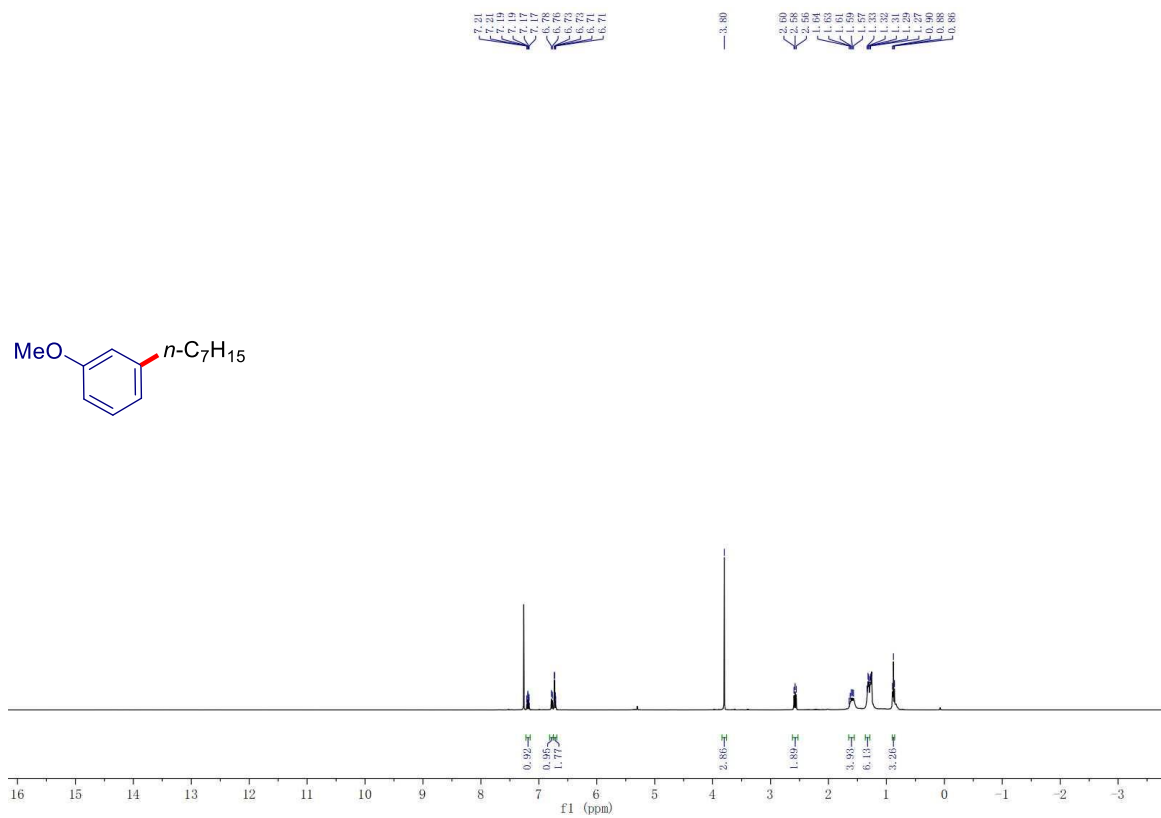


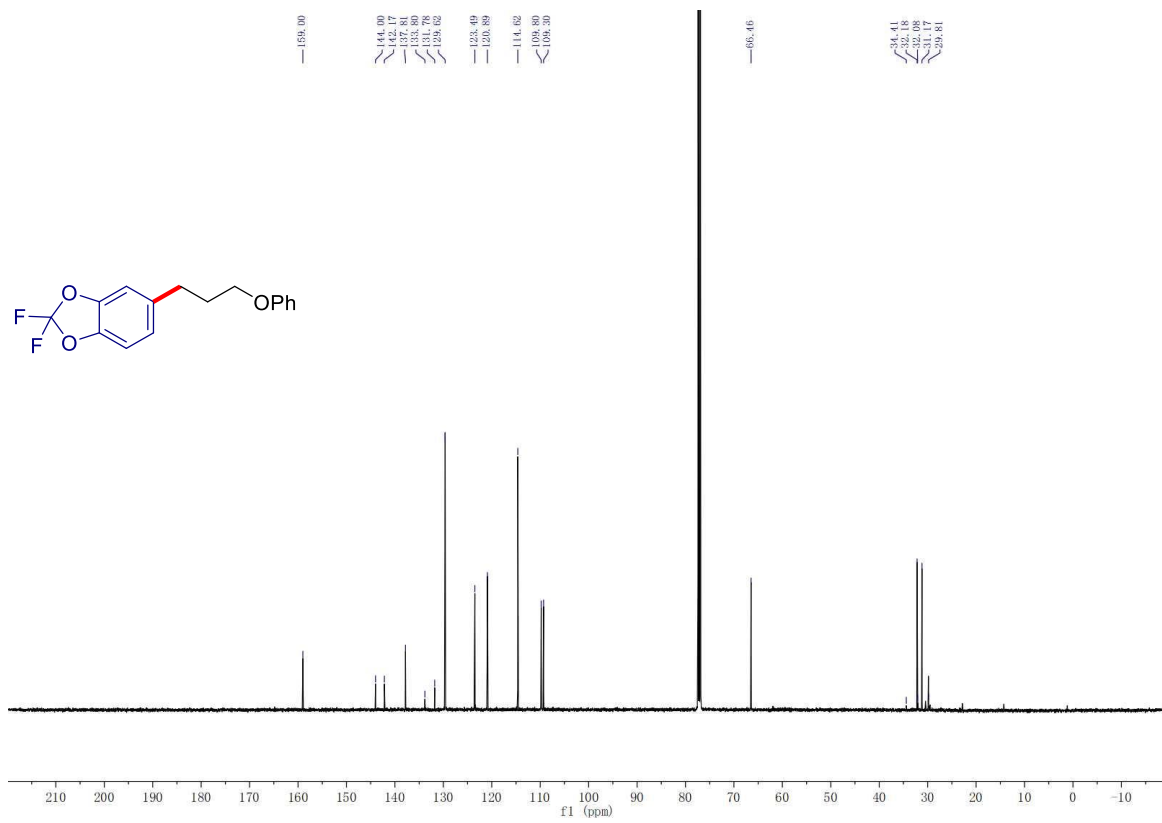
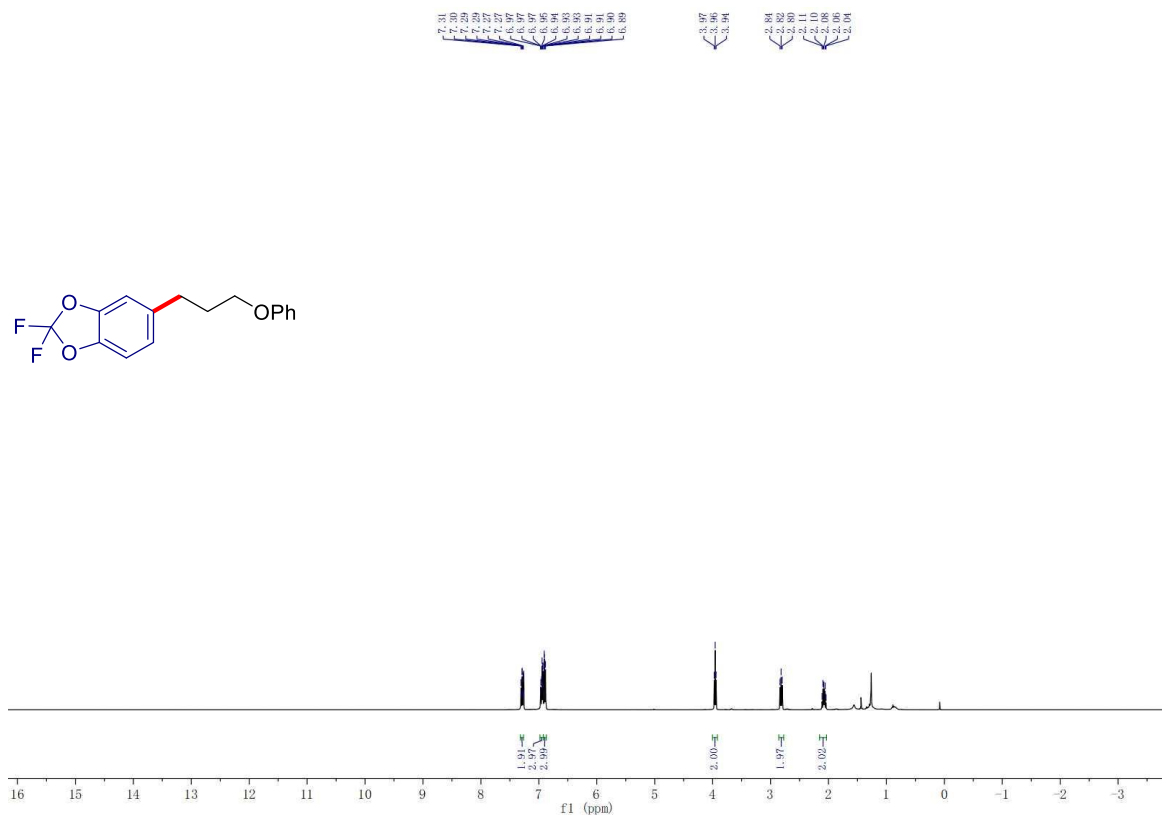
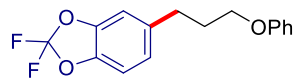


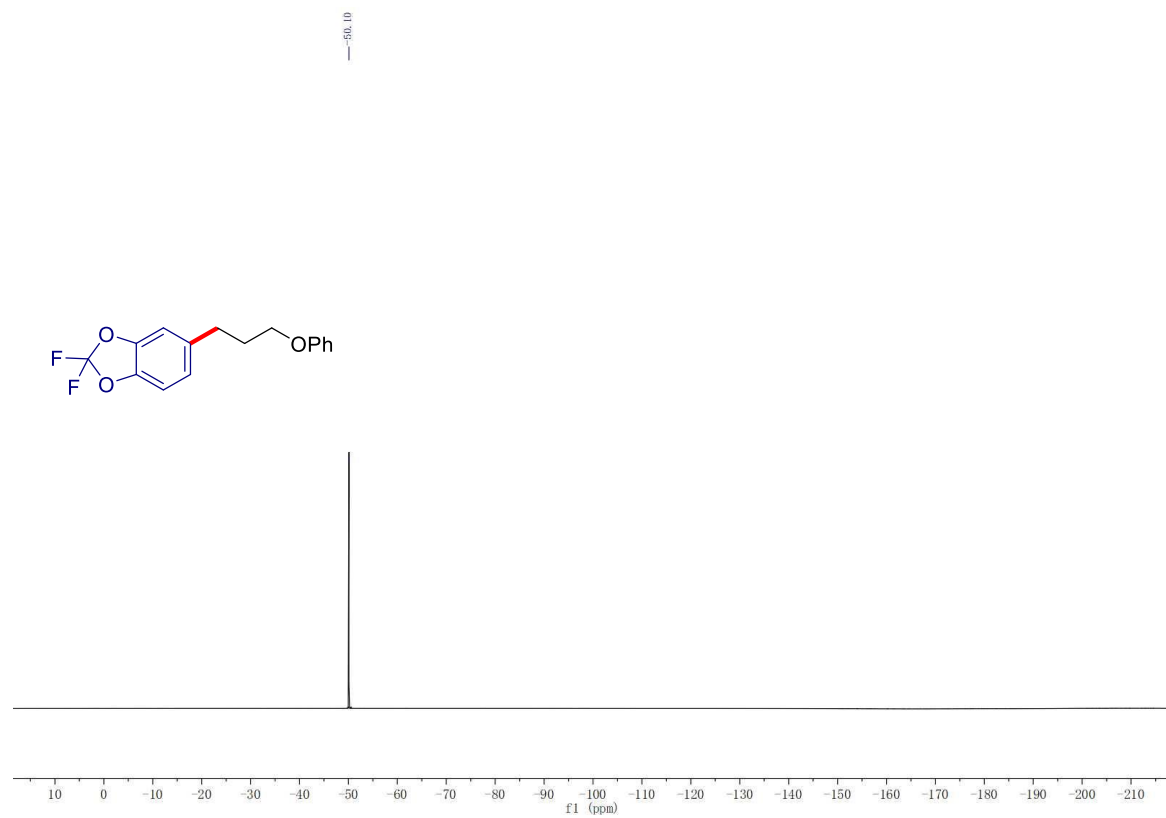
— 62.86

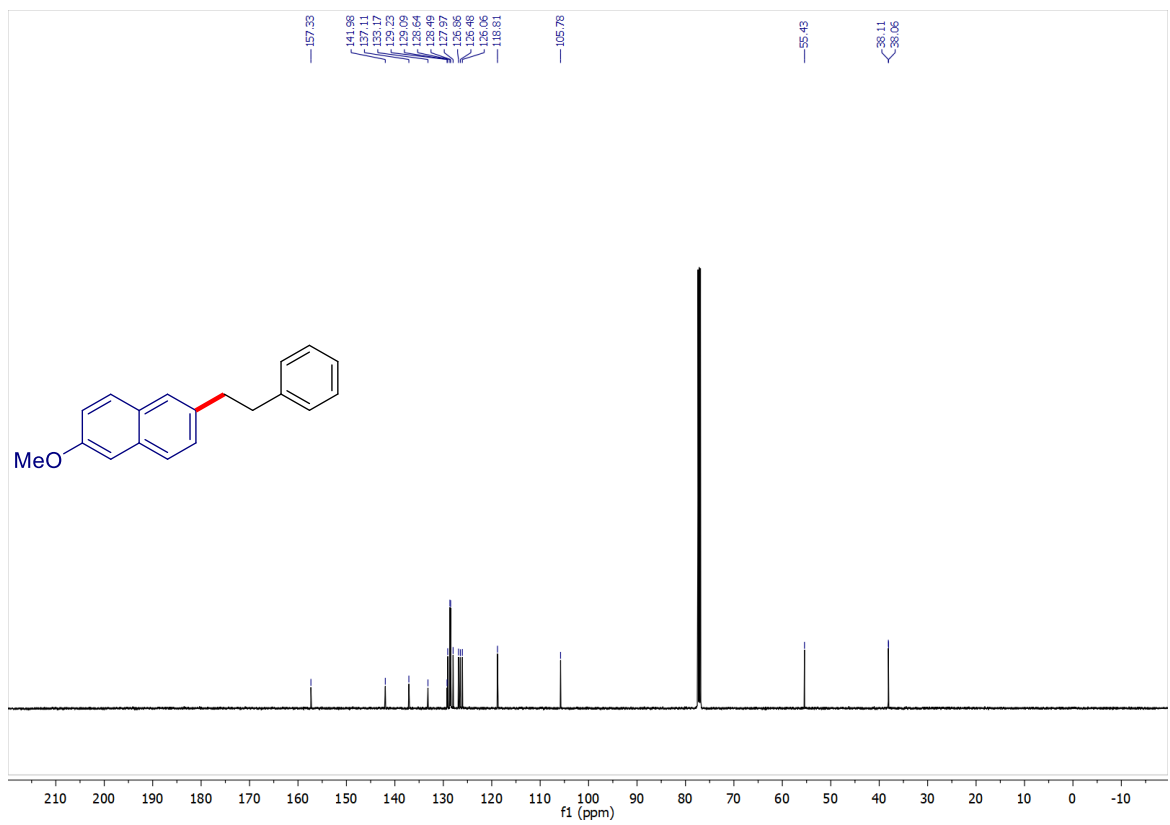
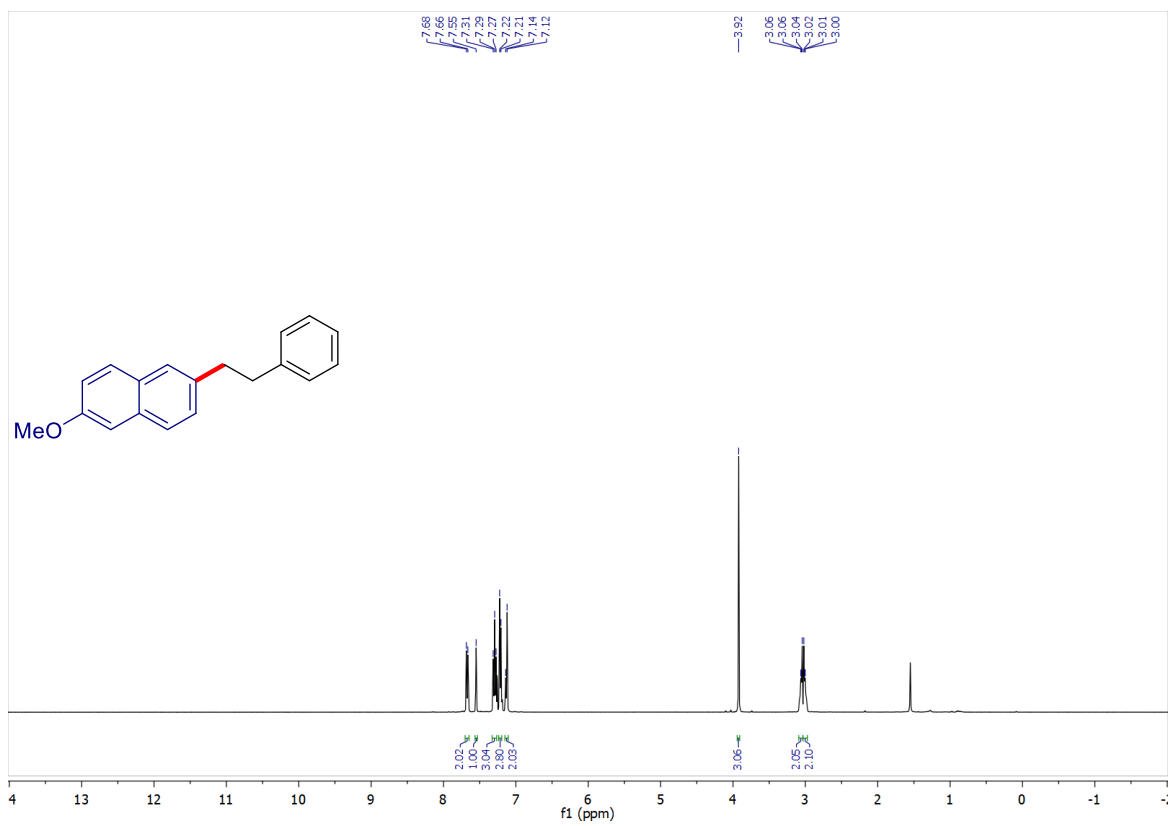


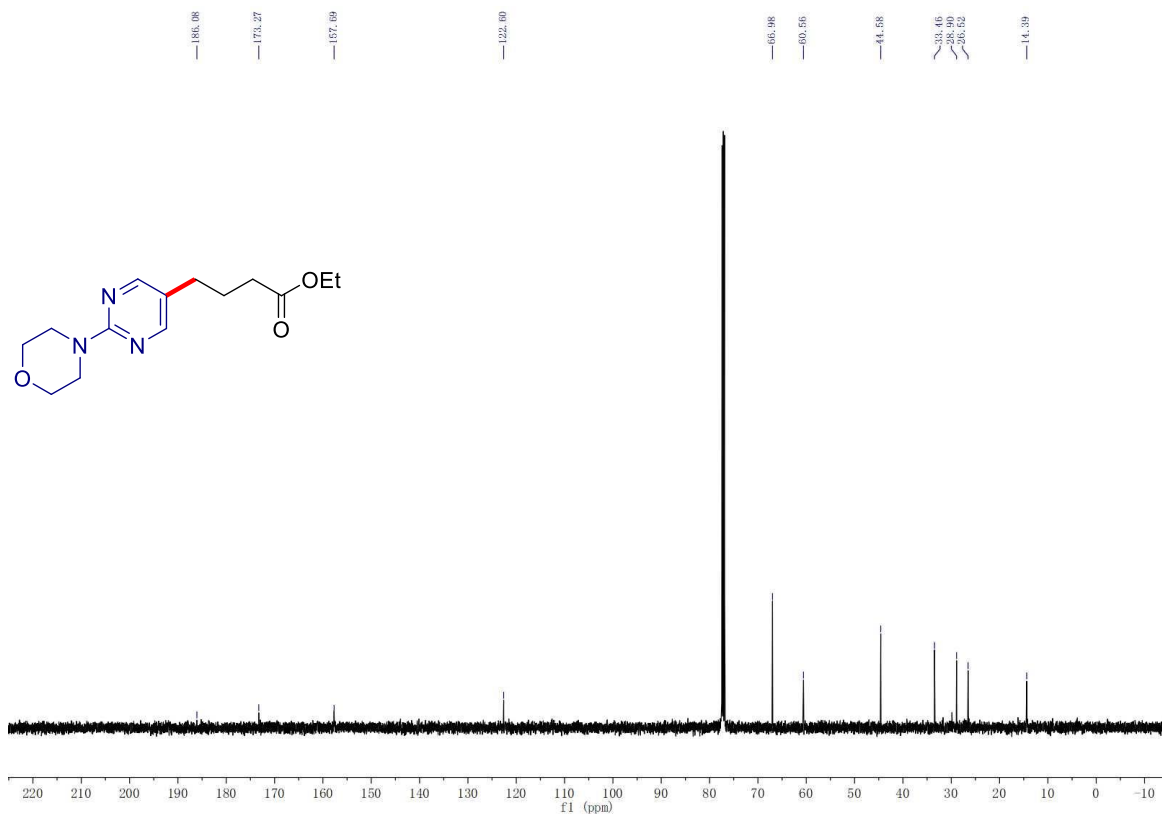
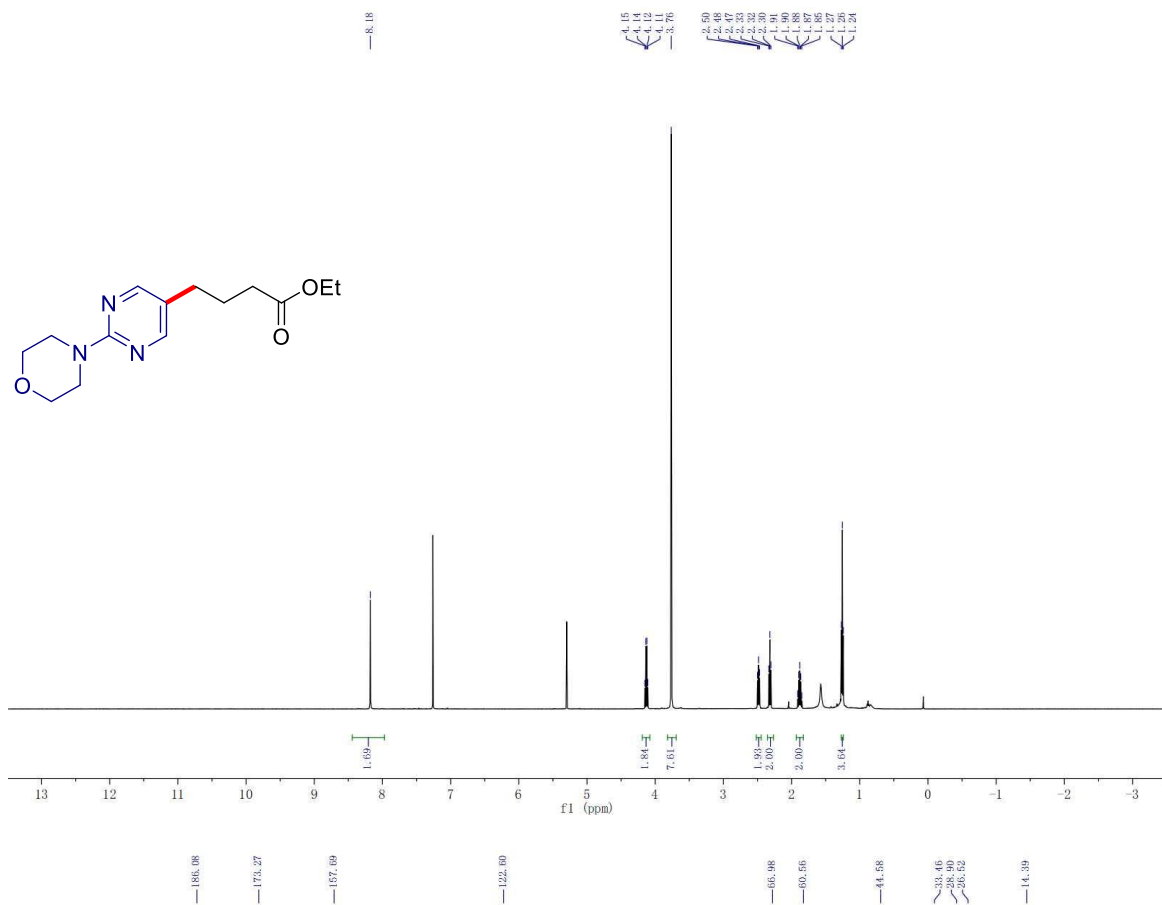




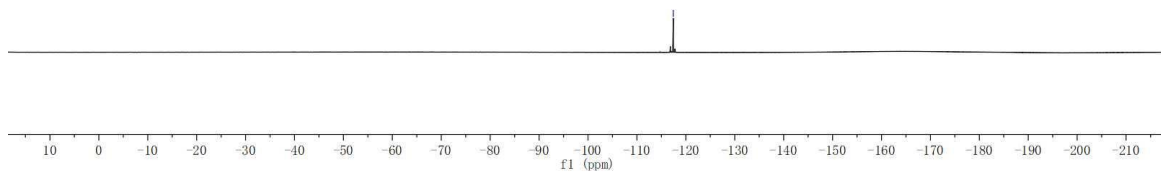
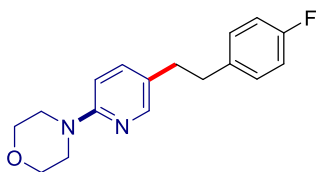


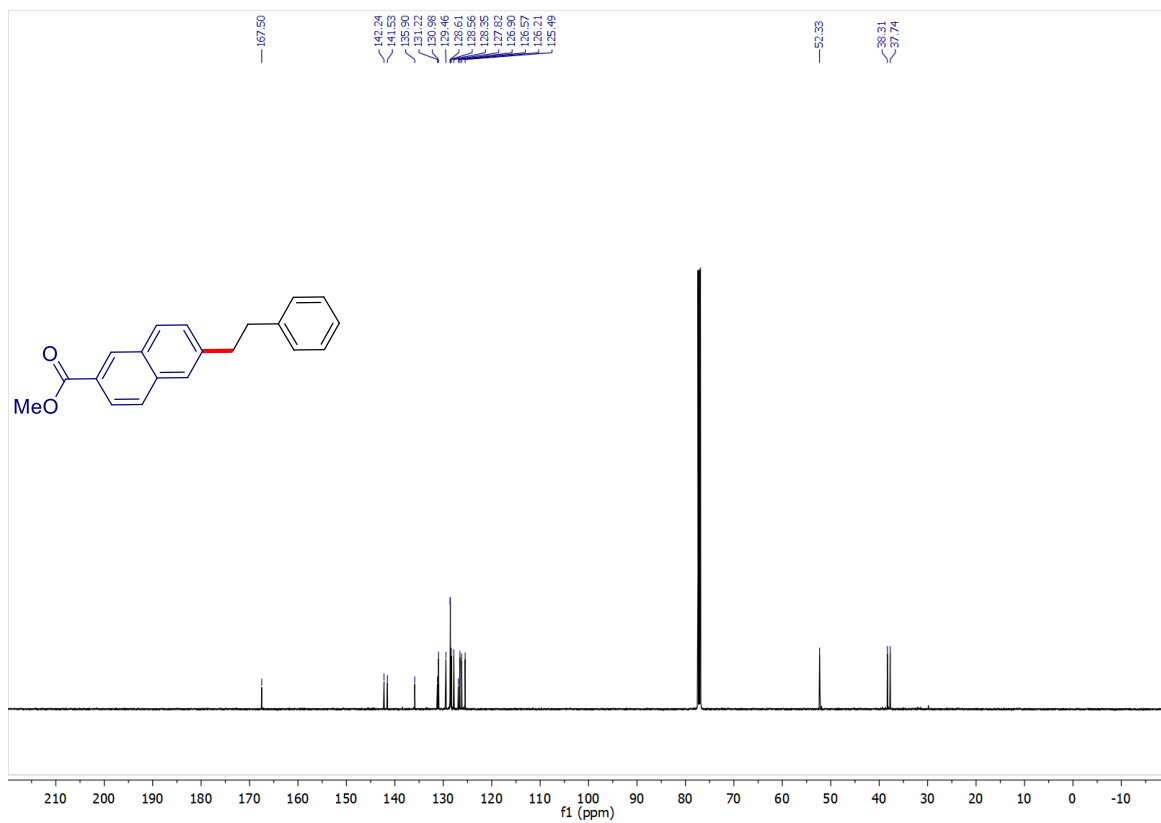
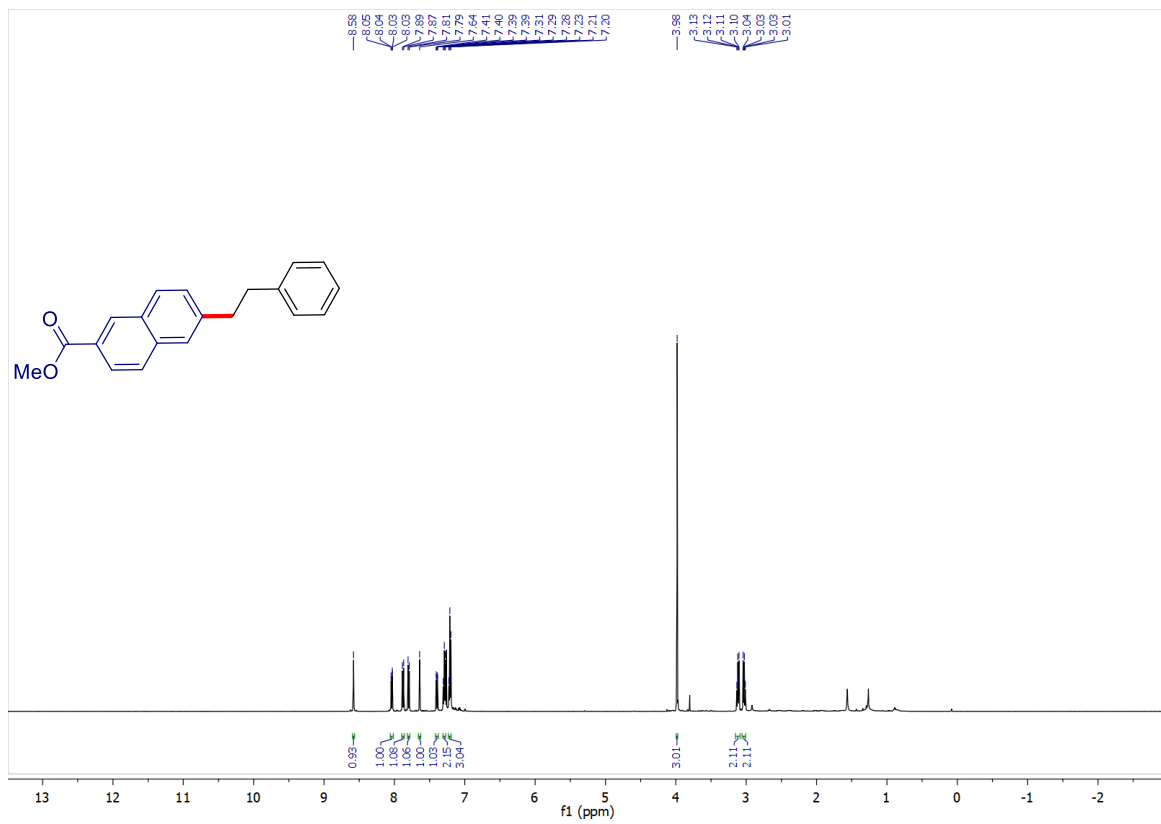


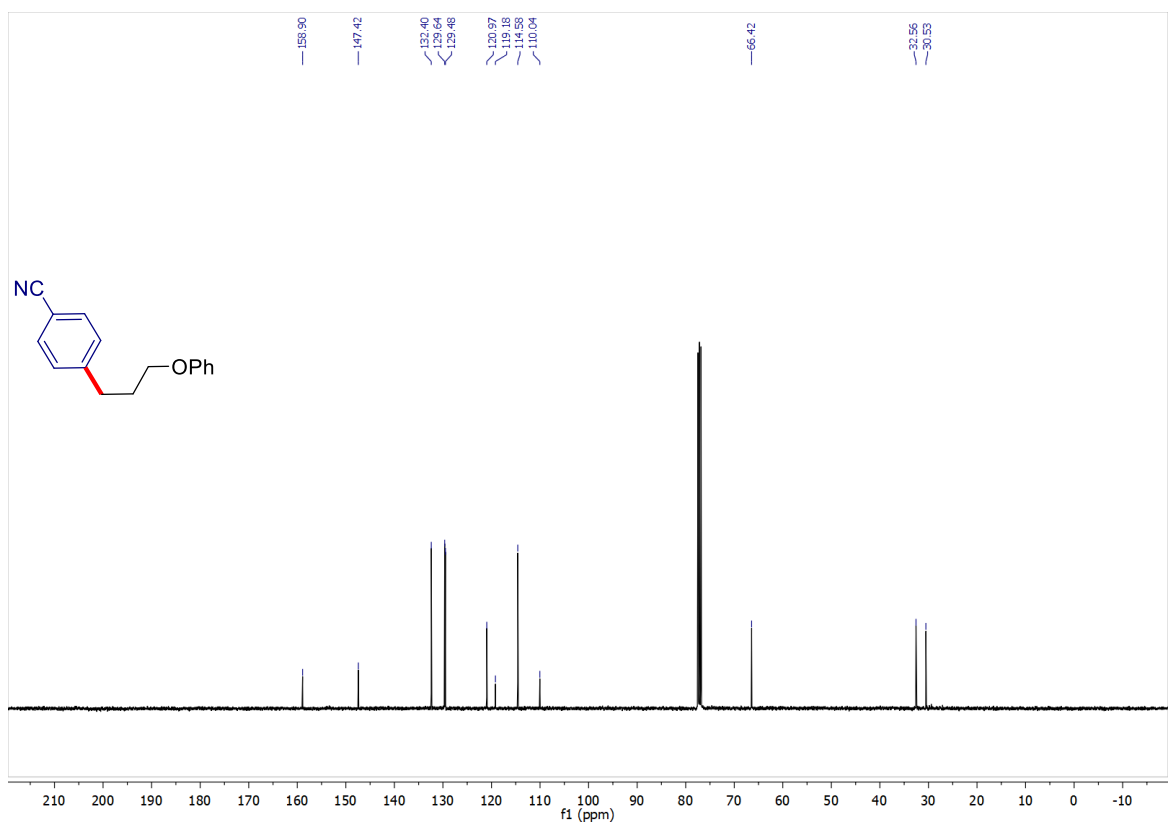
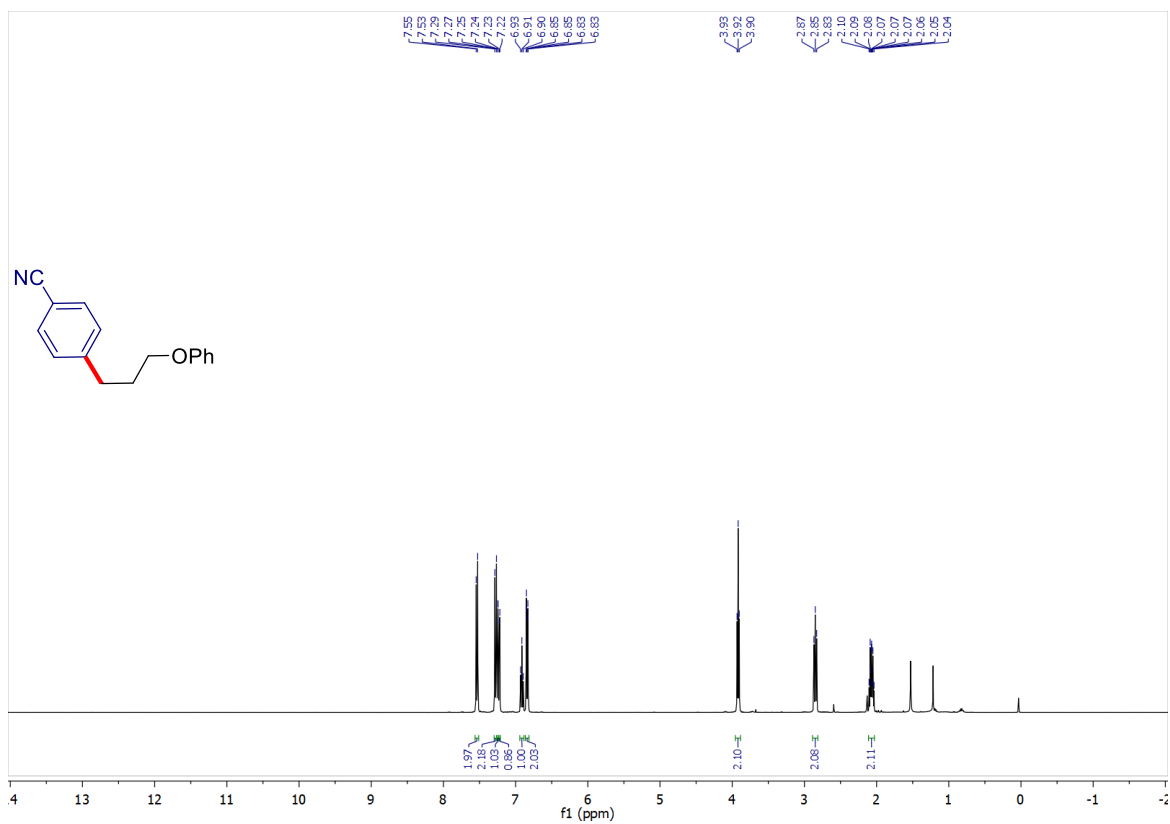


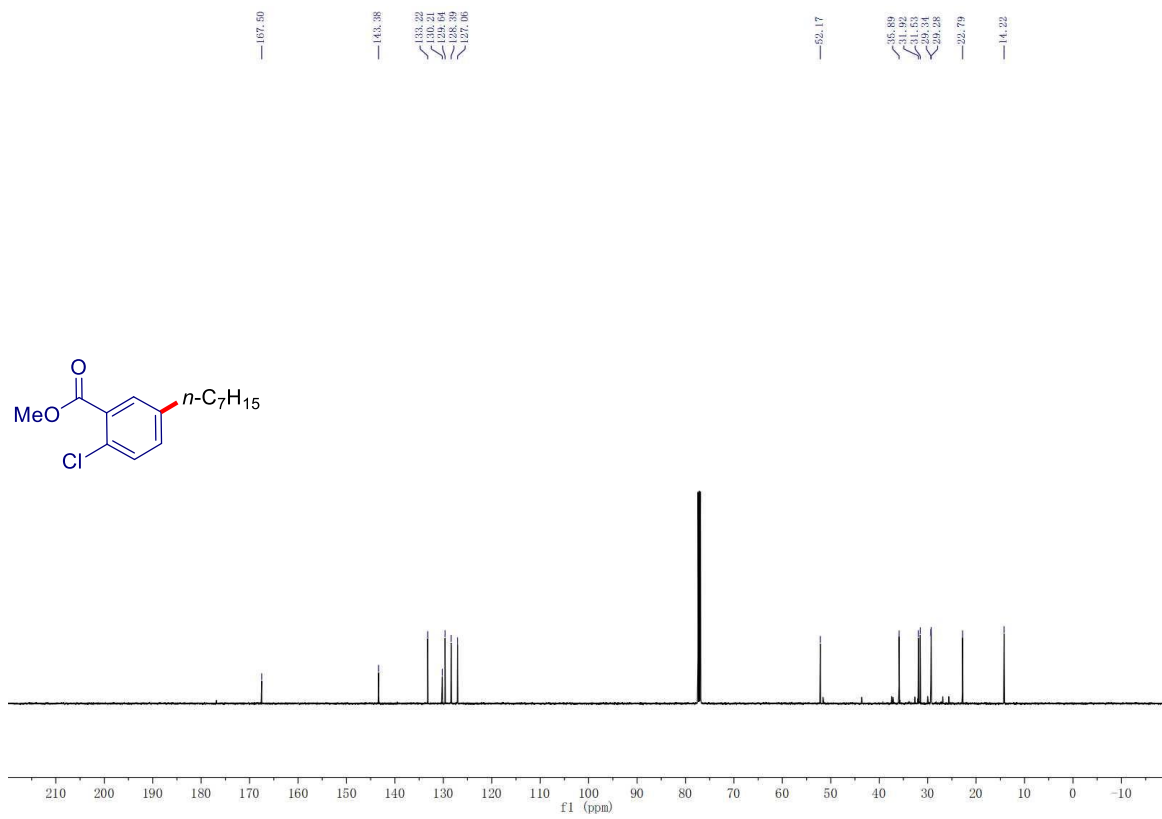
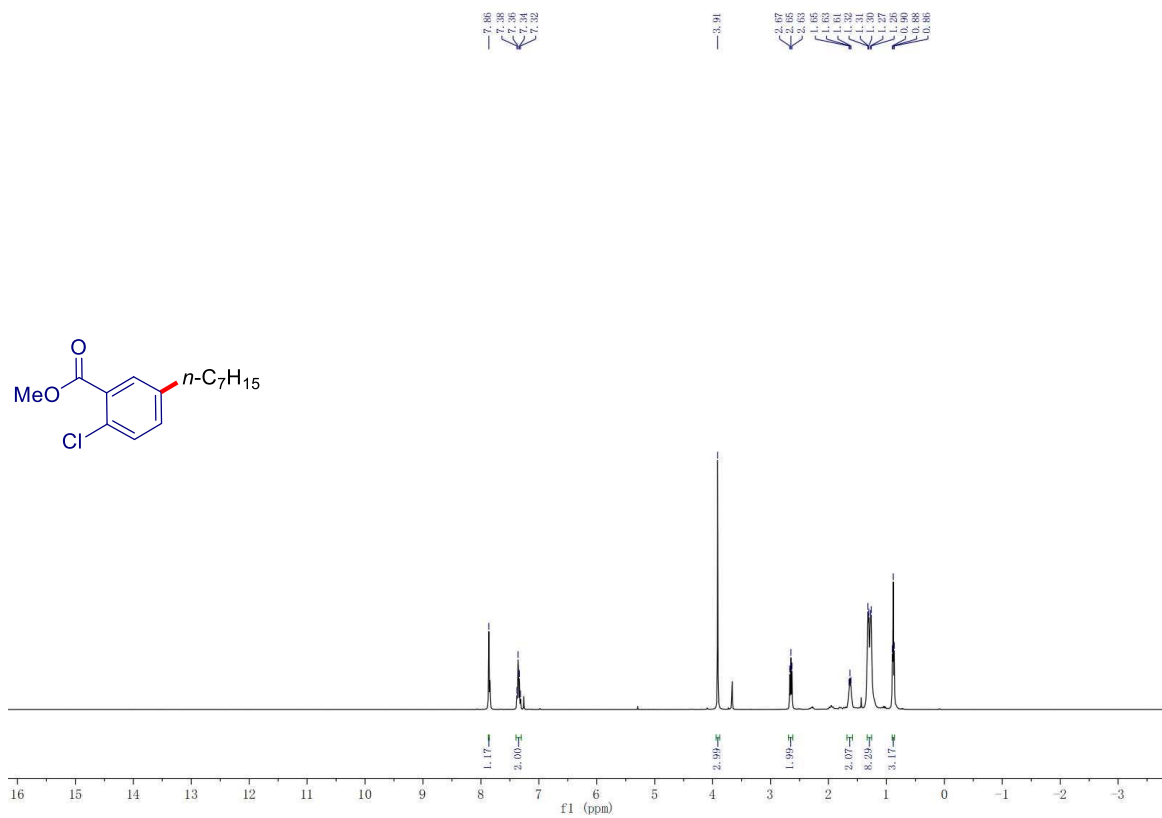


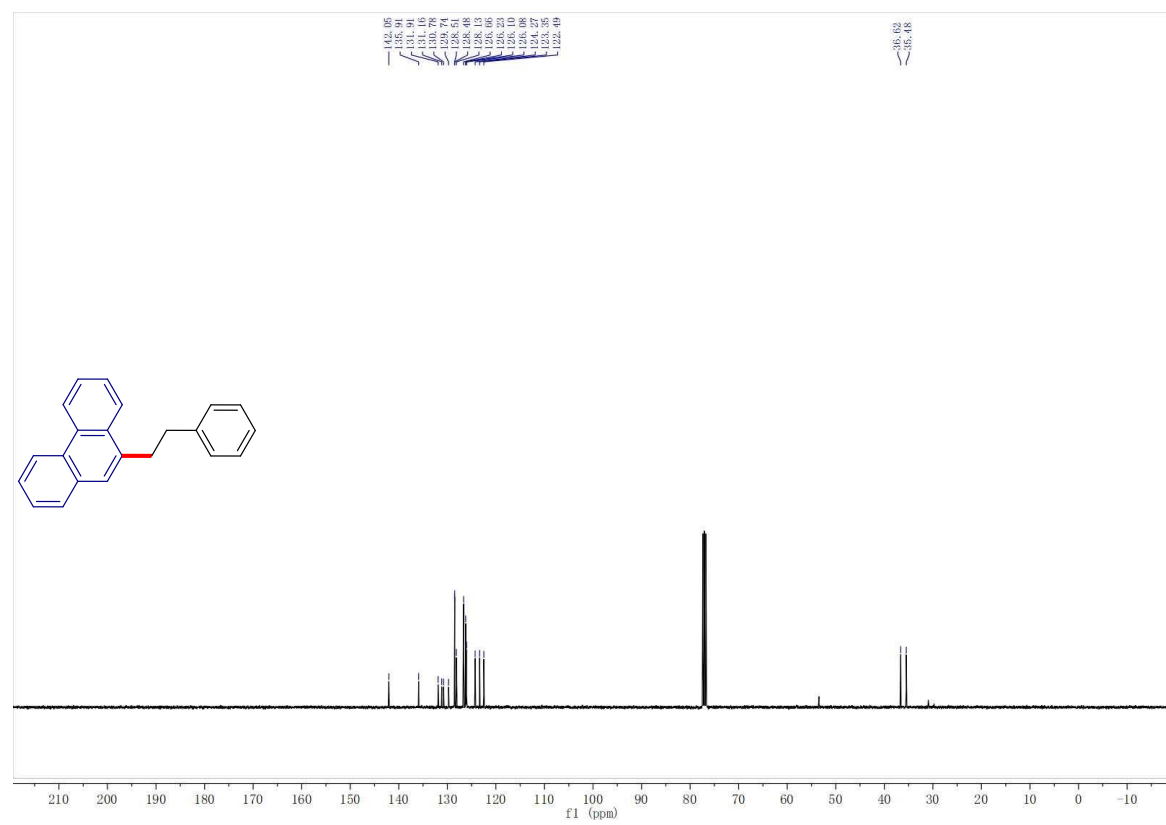
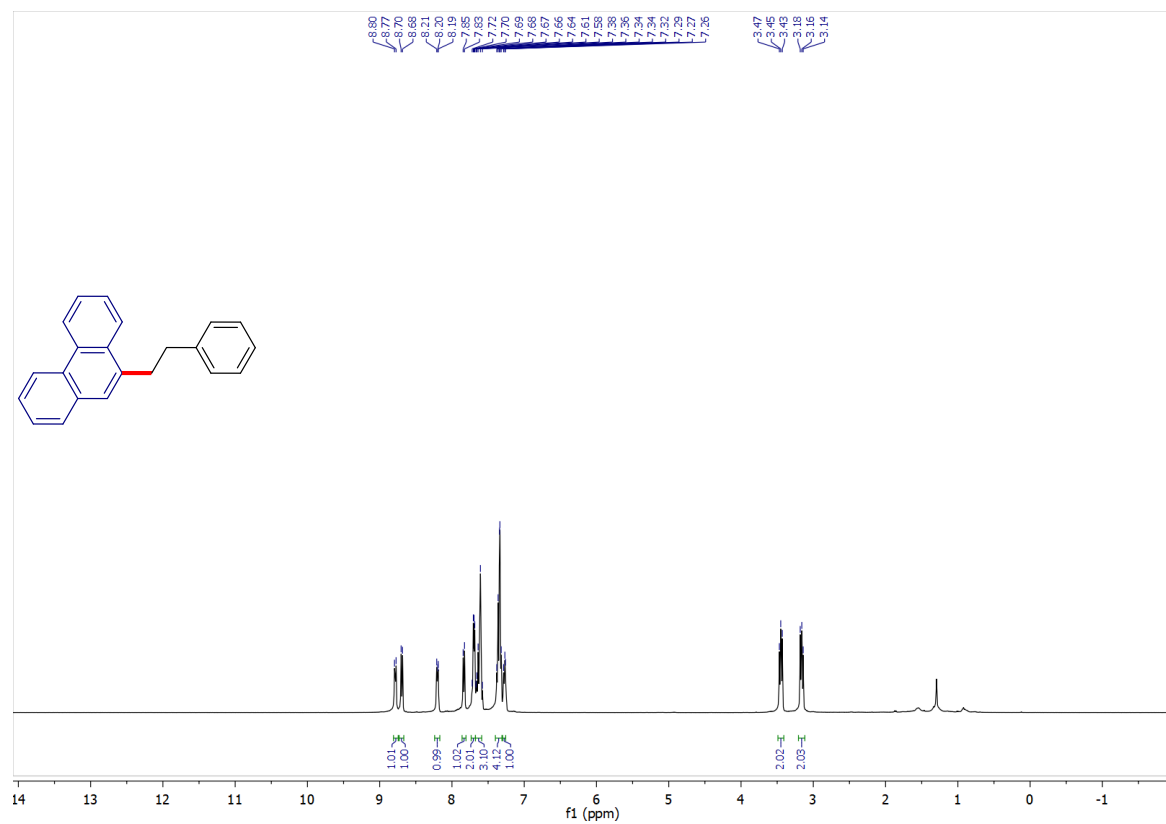
—117.34

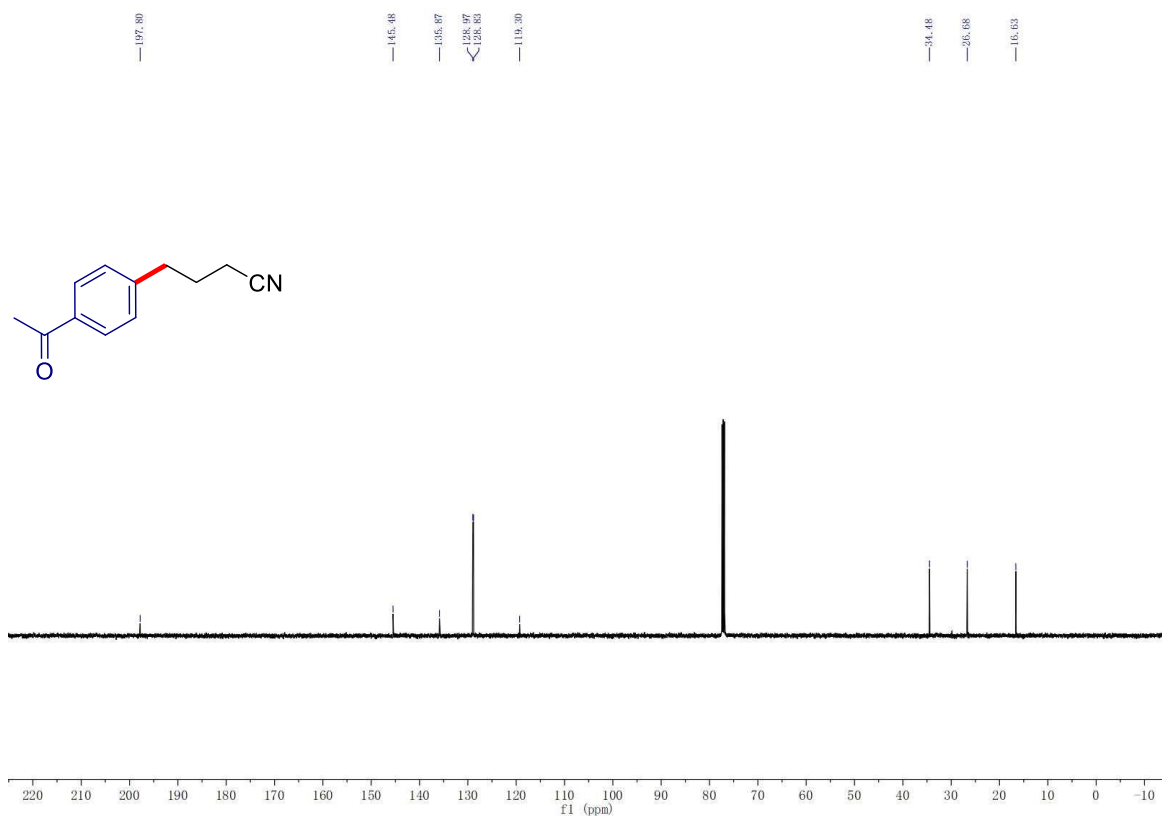
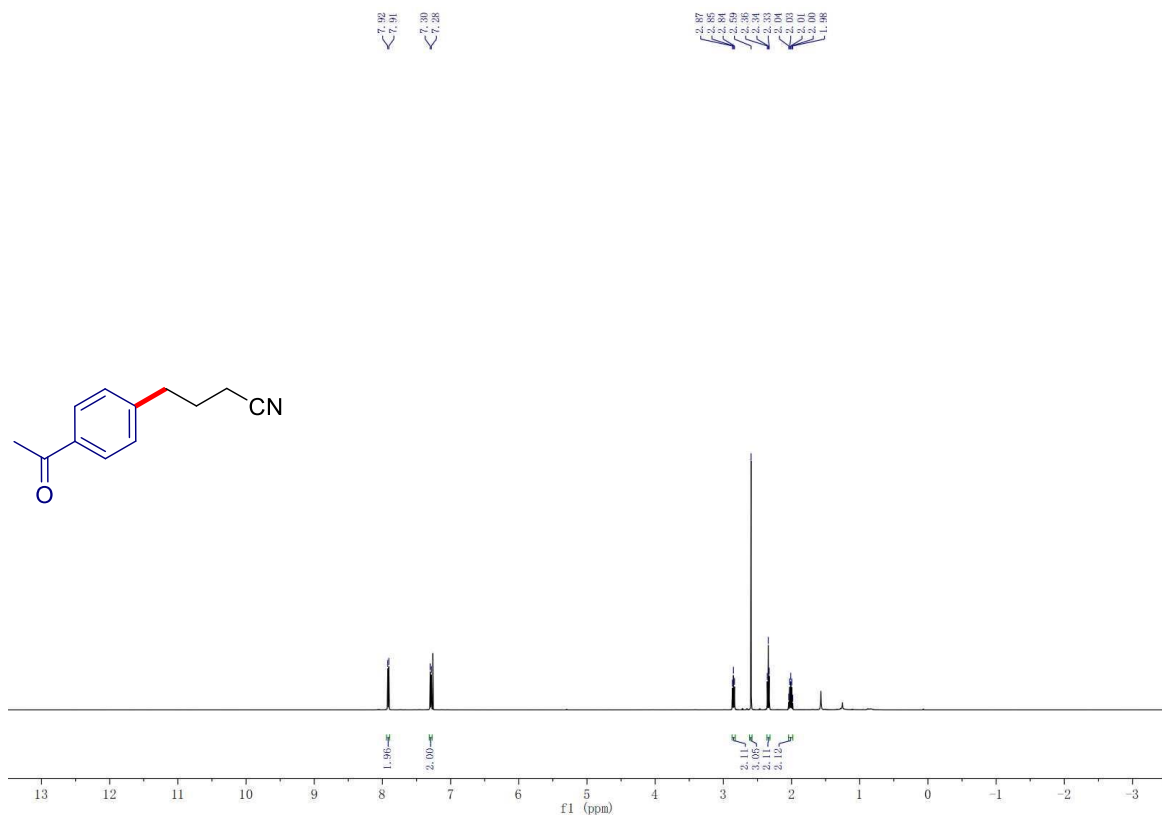


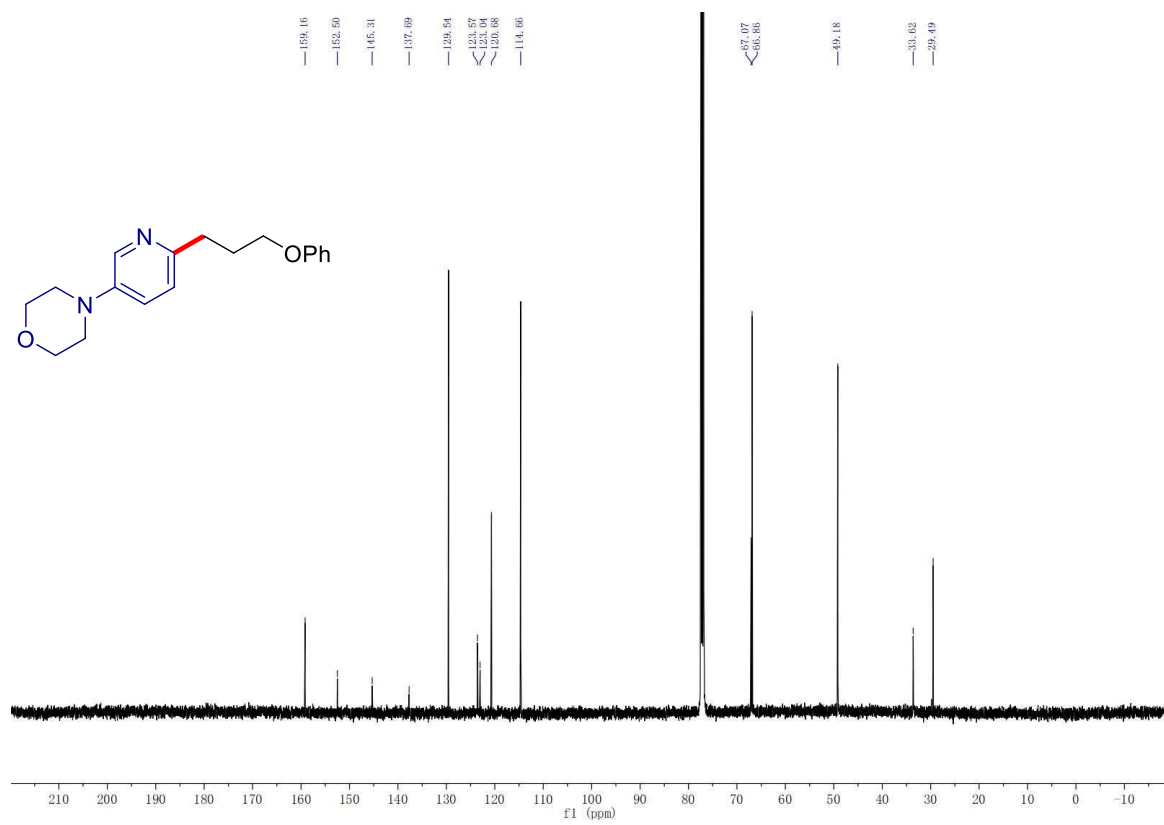
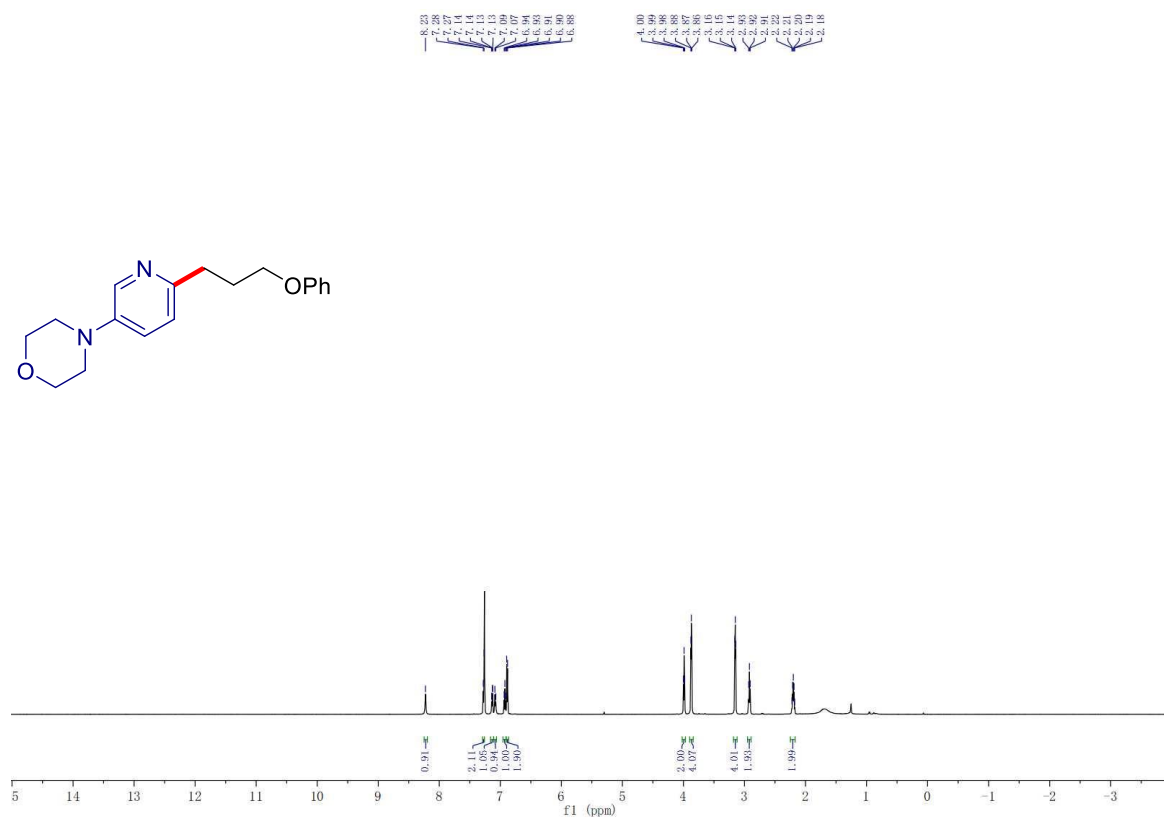
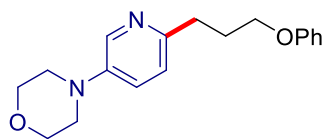


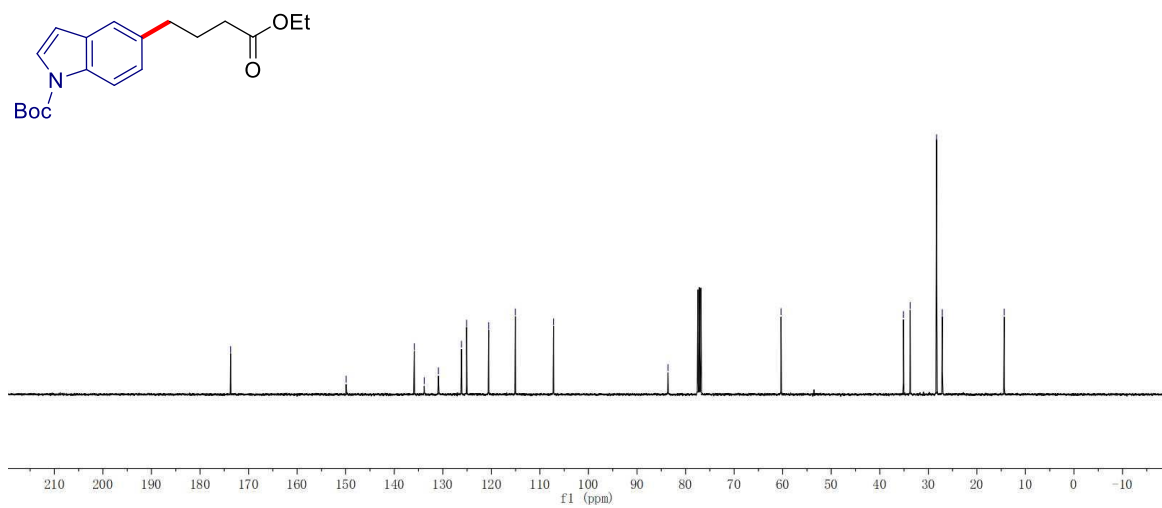
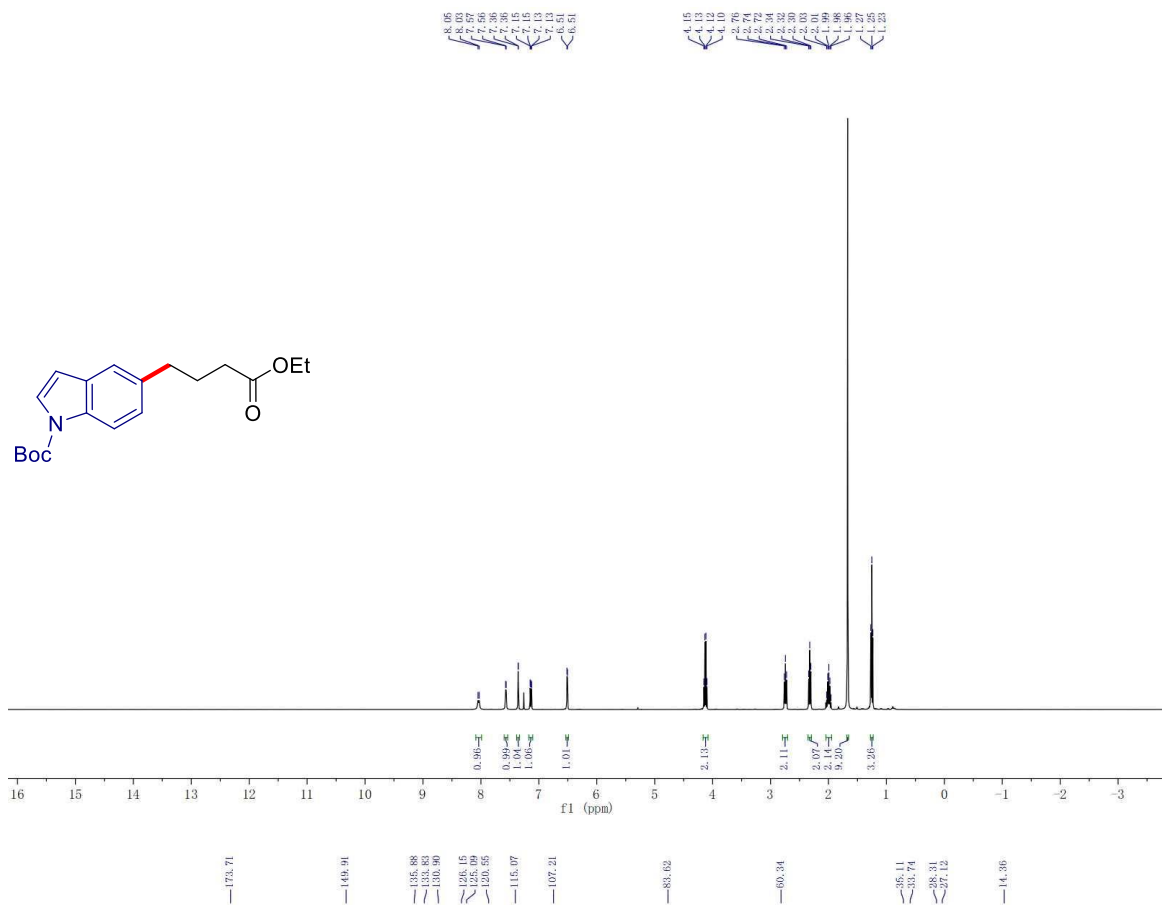


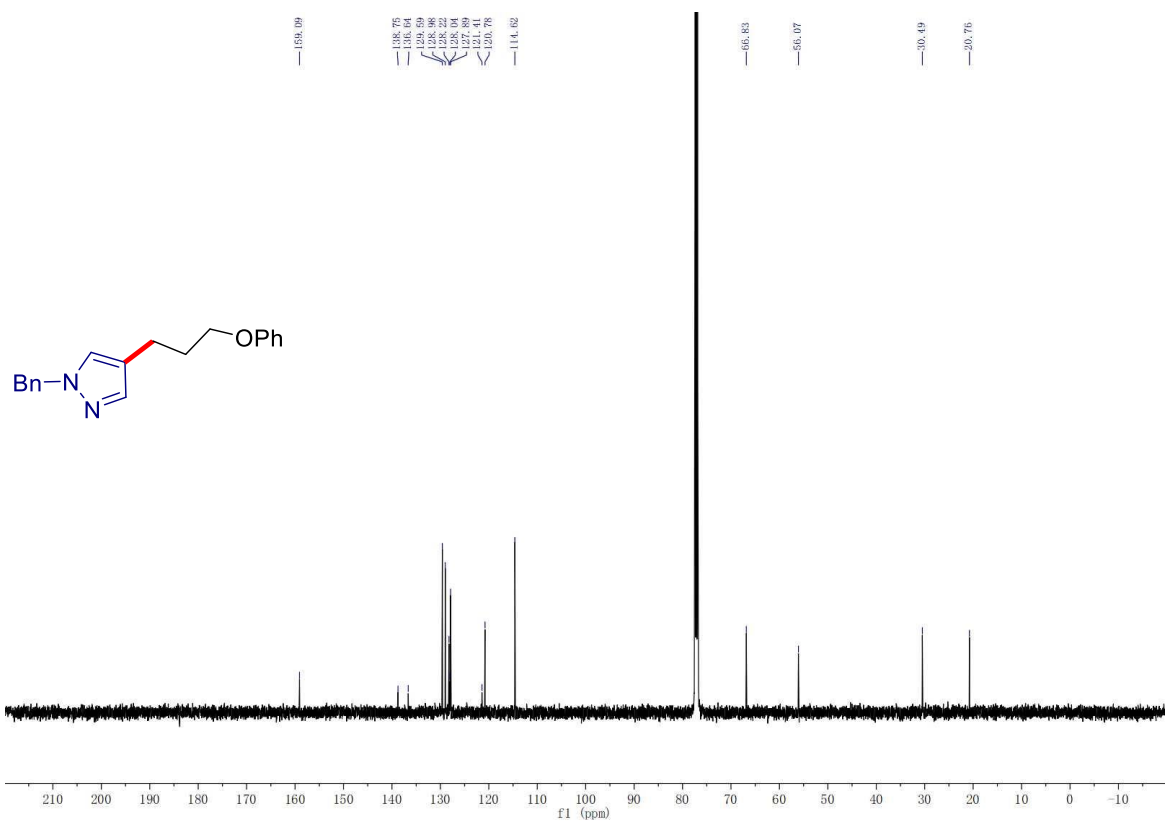
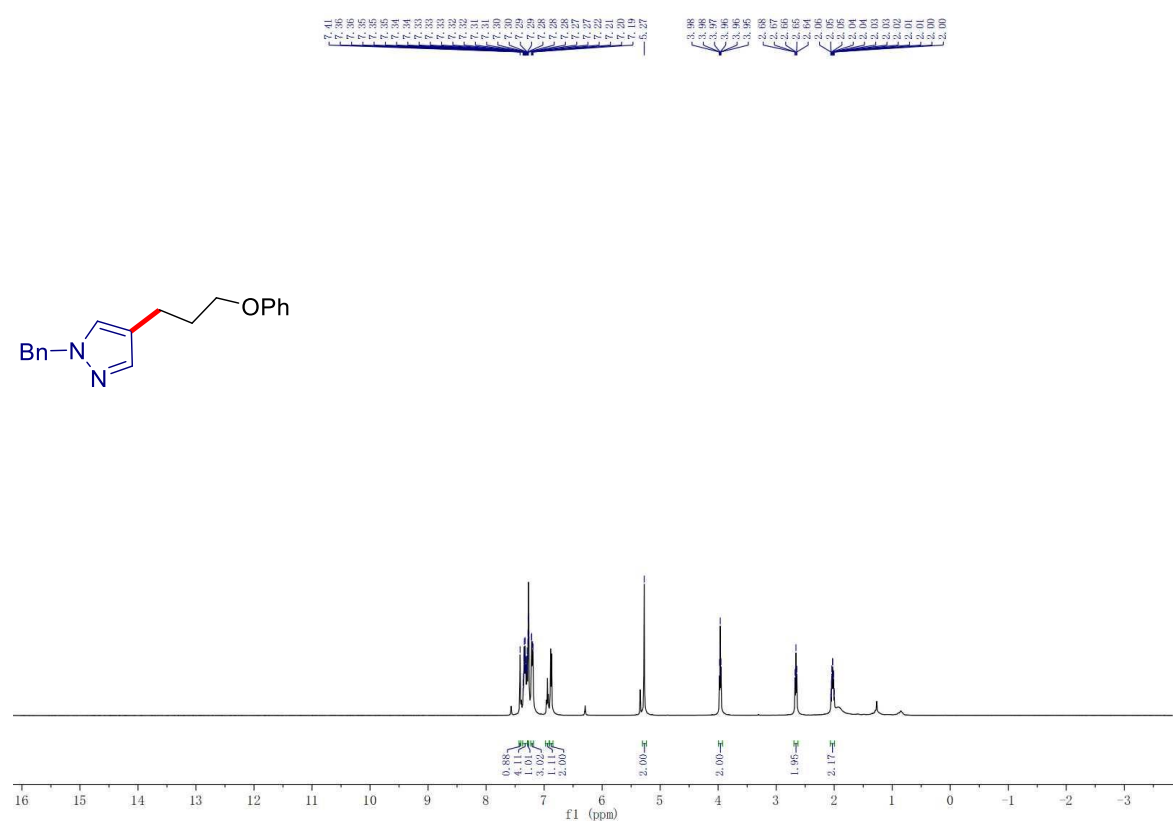
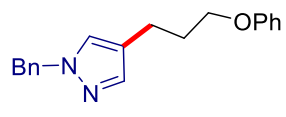


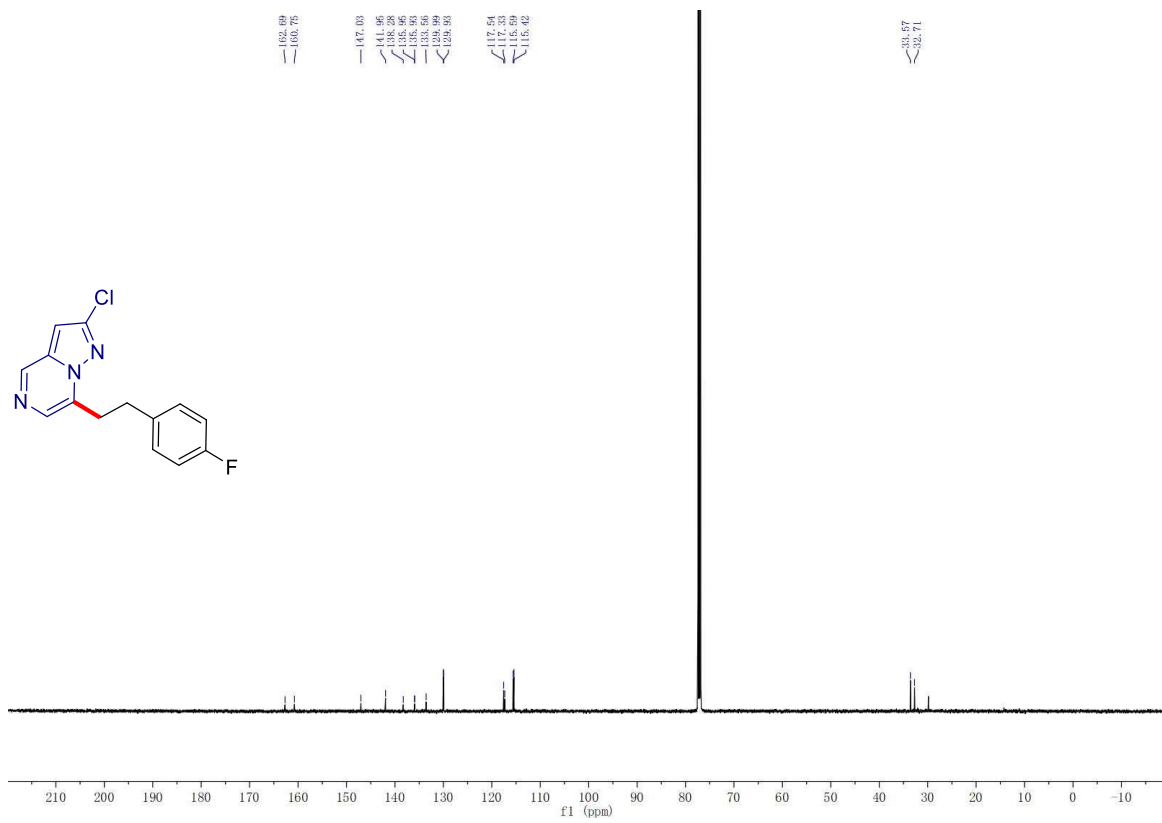
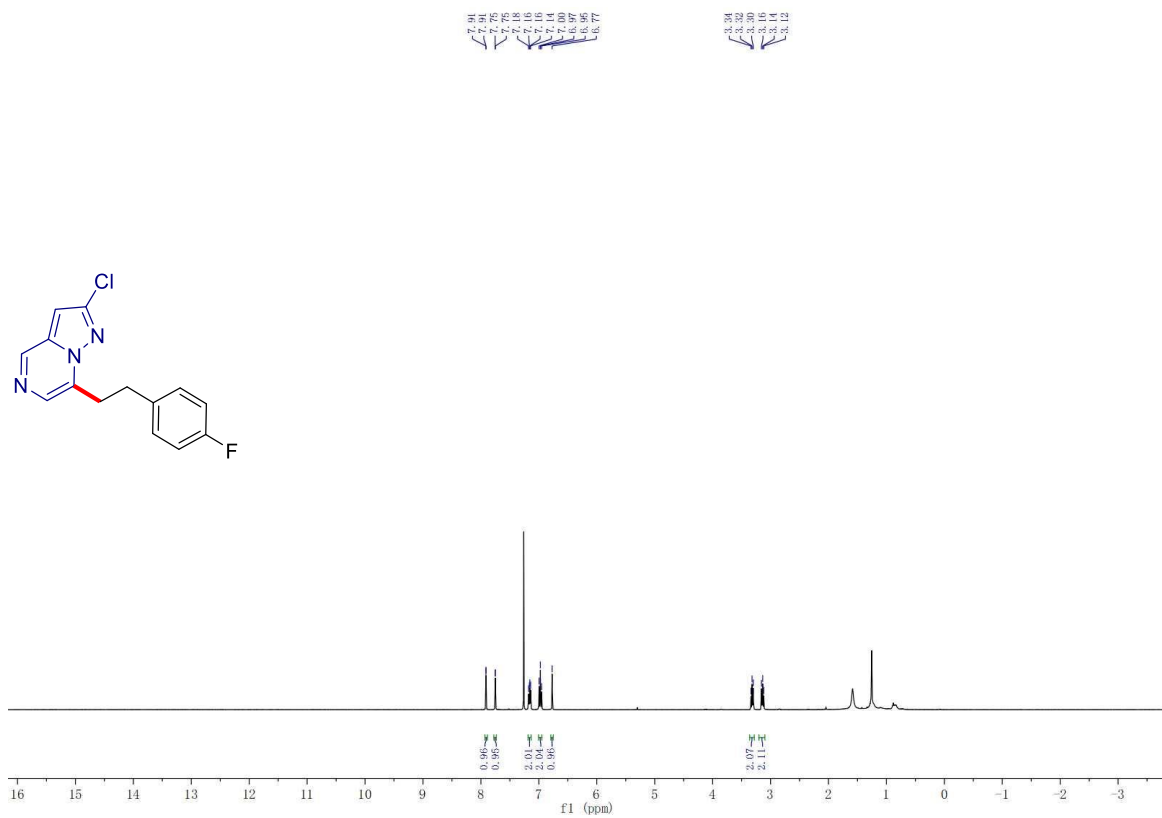


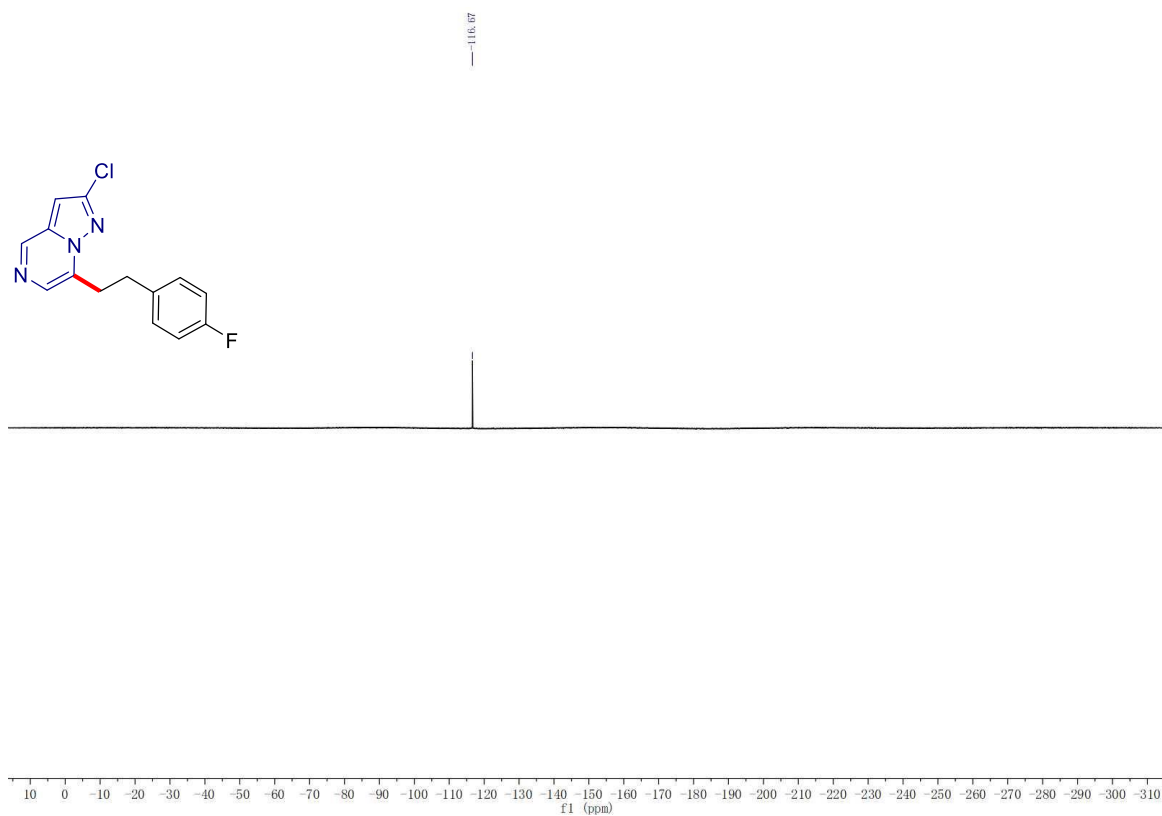


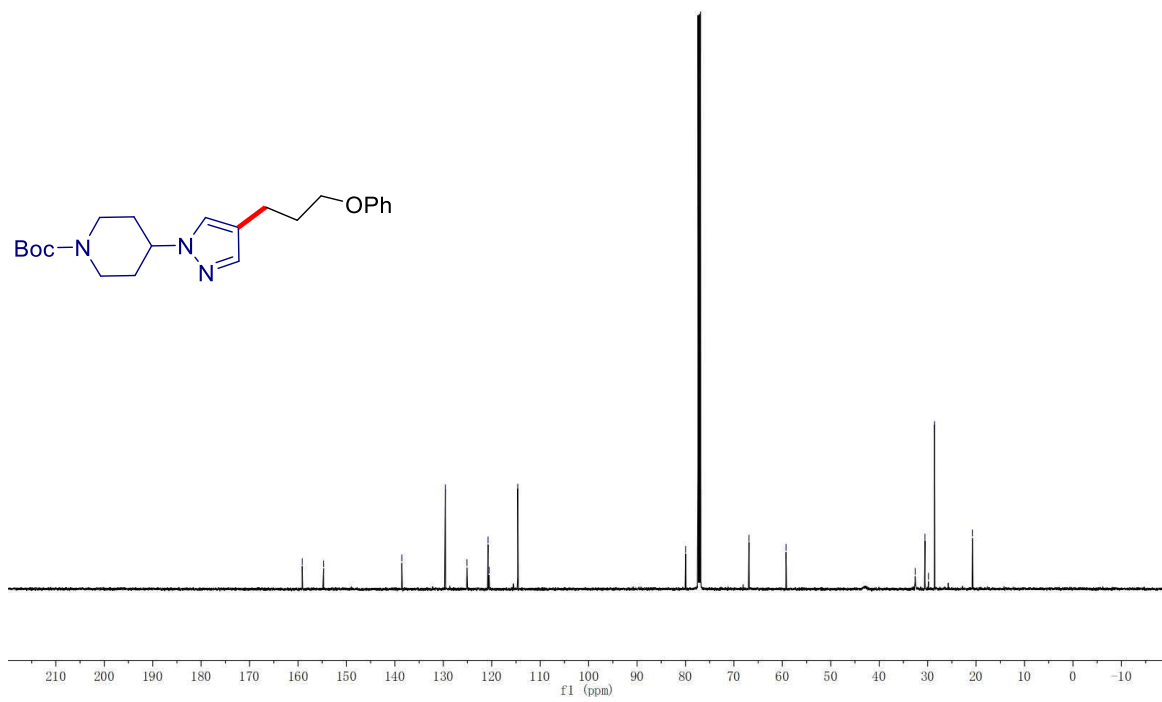
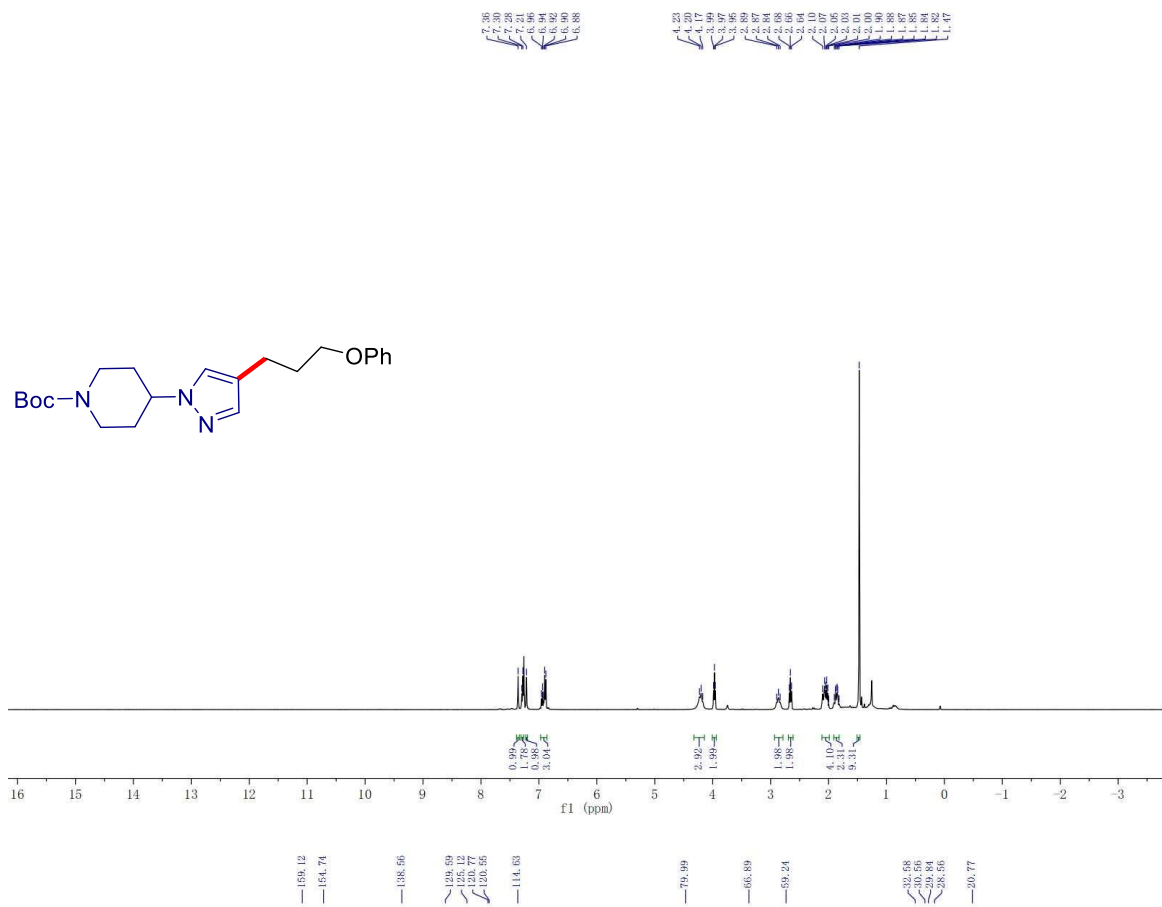


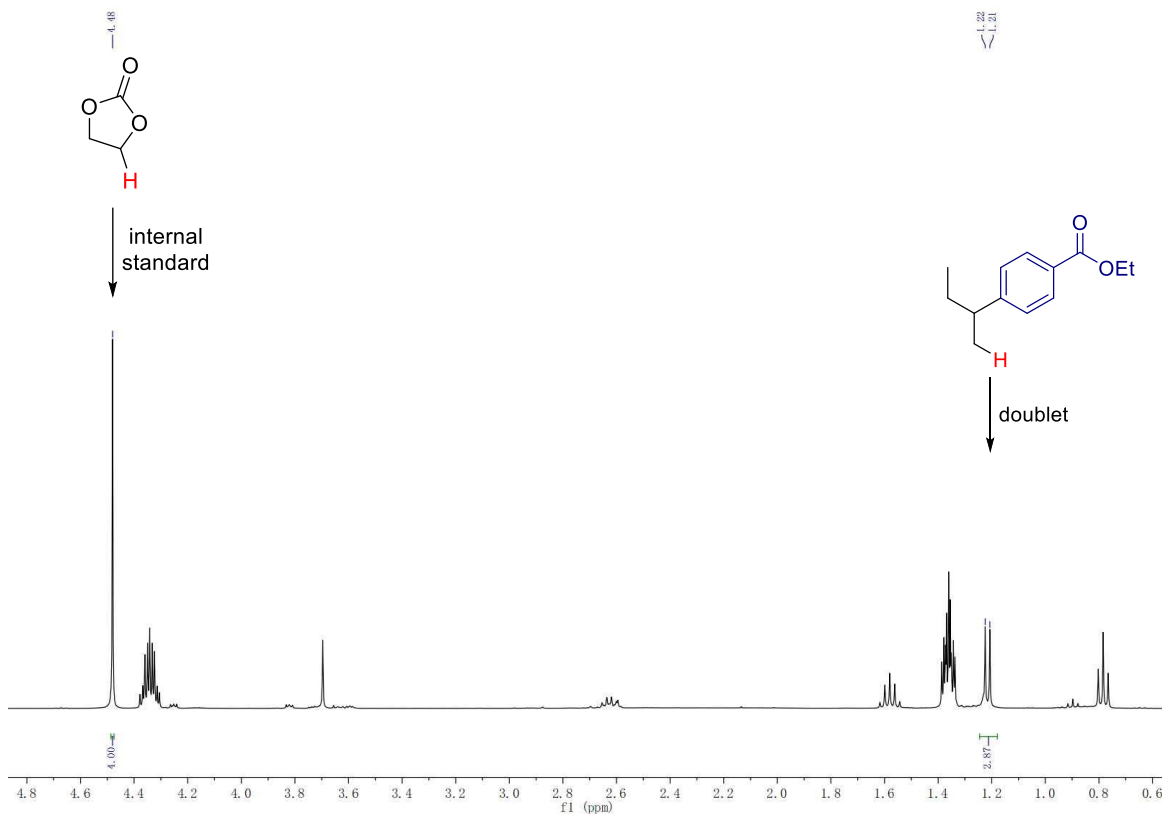
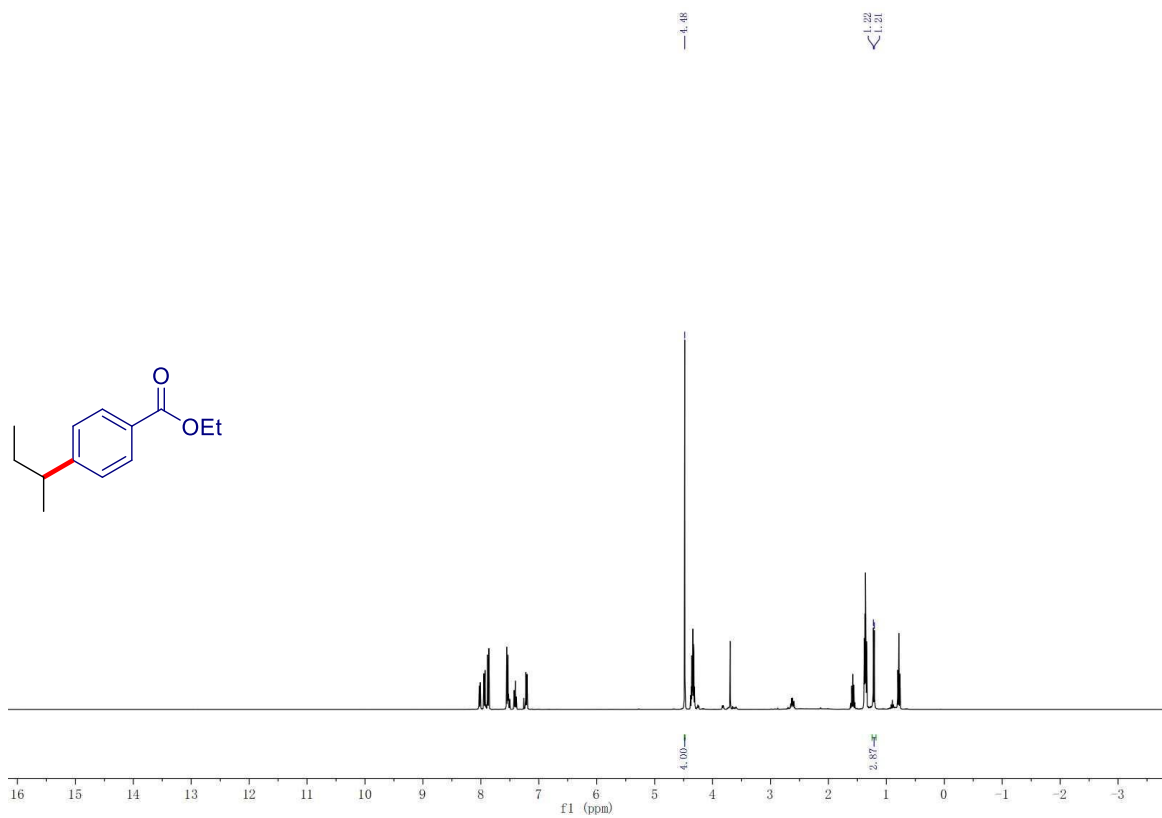


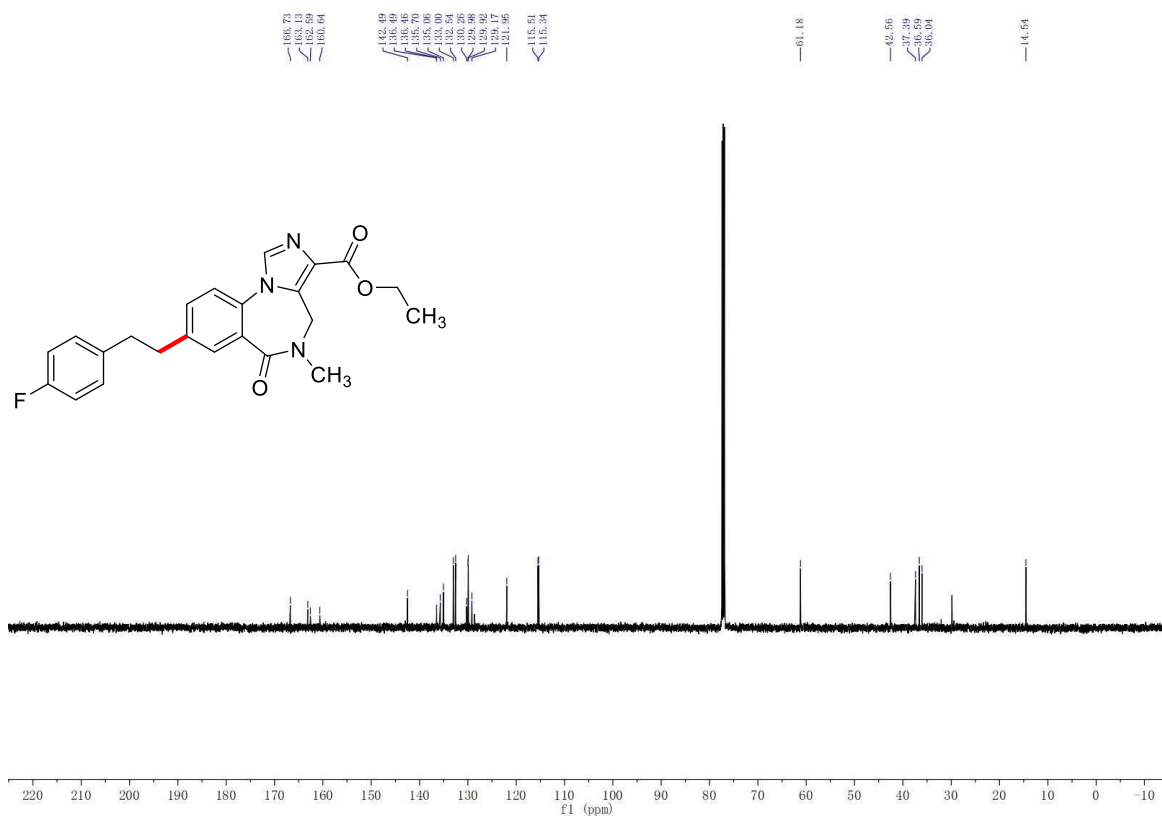
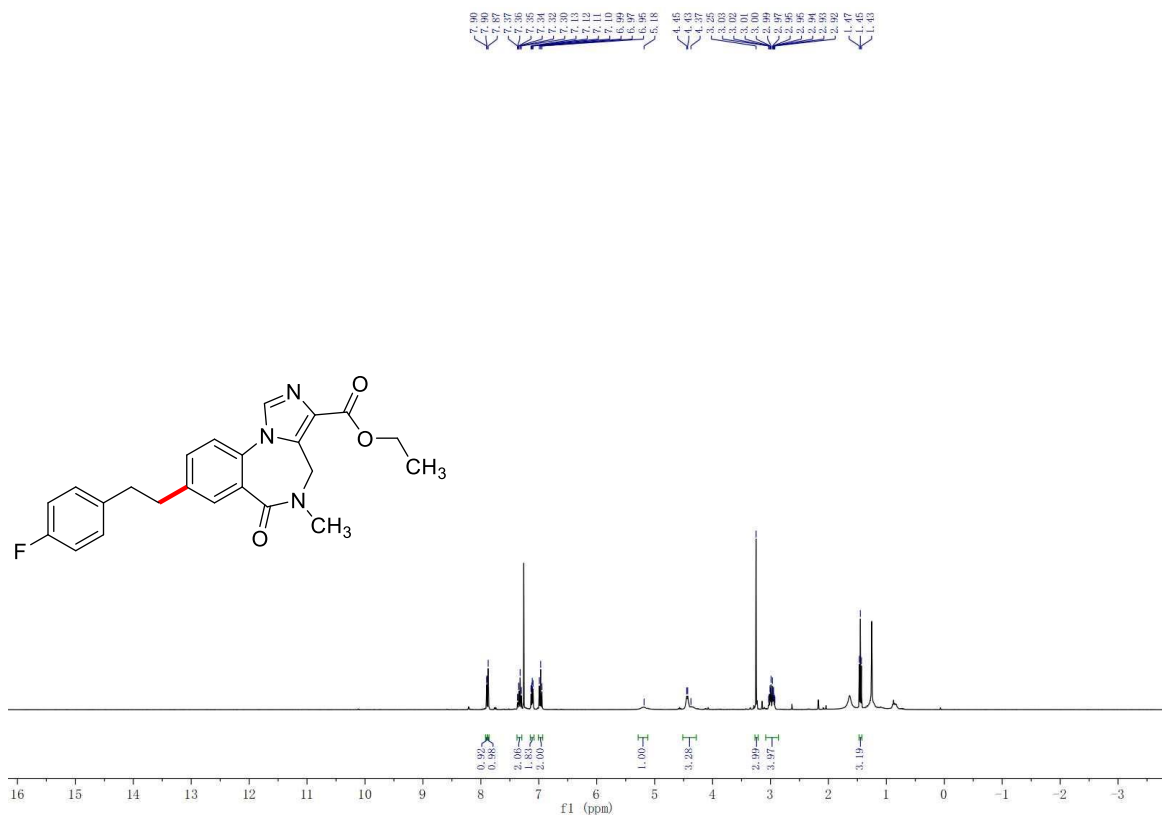


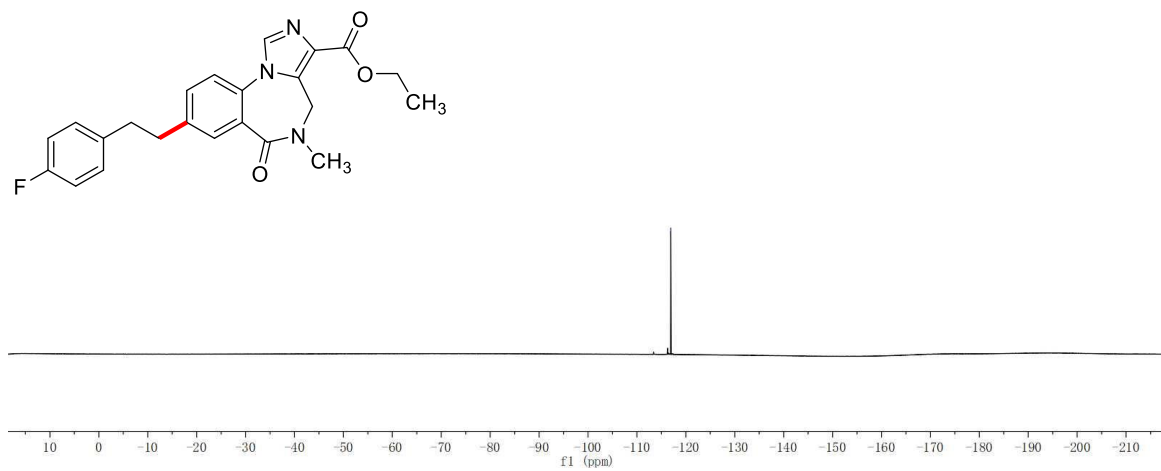


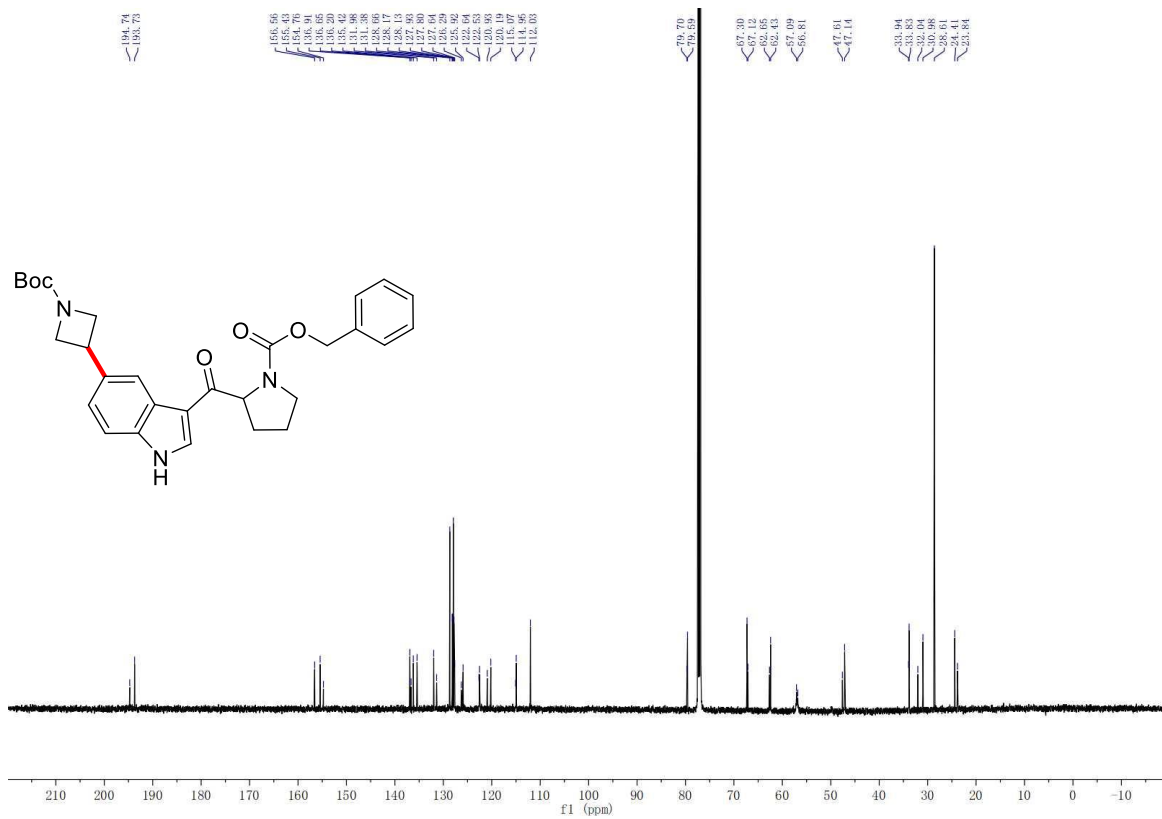
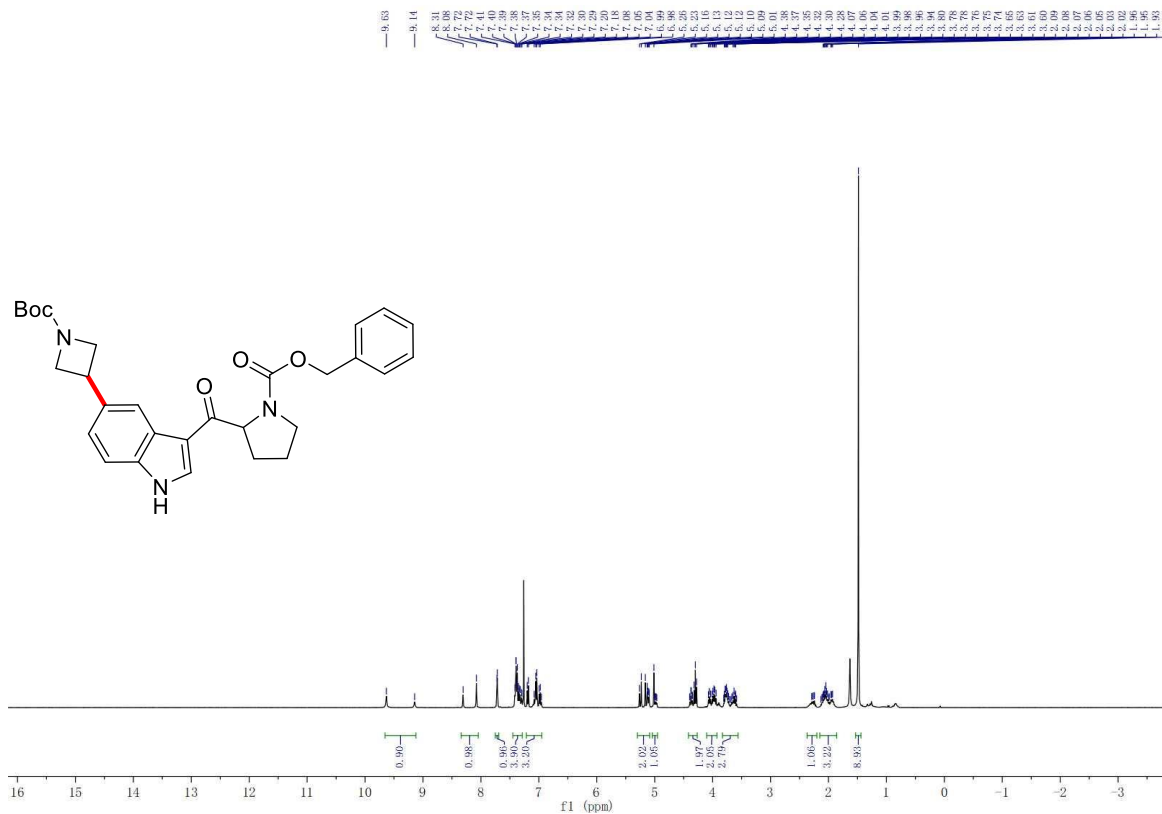












2. Simplified Preparation of ppm Pd-Containing Nanoparticles as Heterogeneous Catalysts for Chemistry in Water

Reproduced with permission from
Hu, Y.; Li, X.; Jin, G.; Lipshutz, B. H. Simplified Preparation of ppm Pd-Containing Nanoparticles as Catalysts for Chemistry in Water. *ACS. Catal.*, **2023**, *13*, 3179-3186
Copyright 2023 ACS Publication

2.1 Background Introduction

Cross coupling reactions, which typically rely on transitional metals to catalyze couplings between a sp^2 -hybridized halide and an organometallic reagent are widely used in both industry and academia.^{1,2,3} Traditional cross coupling reactions are differentiated by the organometallic reagent used. As shown in Figure 1, the use of organoboron, organozinc, organomagnesium (Grignard reagent), organotin, organolithium, organosilane, alkyne, alkene, and amine correspond, respectively, to the Suzuki-Miyaura, Negishi, Kumada, Stille, Murahashi, Hiyama, Sonogashira, Mizoroki-Heck, and Buchwald-Hartwig amination reactions. There are also some other cross couplings using thioesters to make ketones, such as reactions between thioesters and organozinc halides for Fukuyama reactions, or thioester and boronic acids for Liebeskind–Srogl reactions.

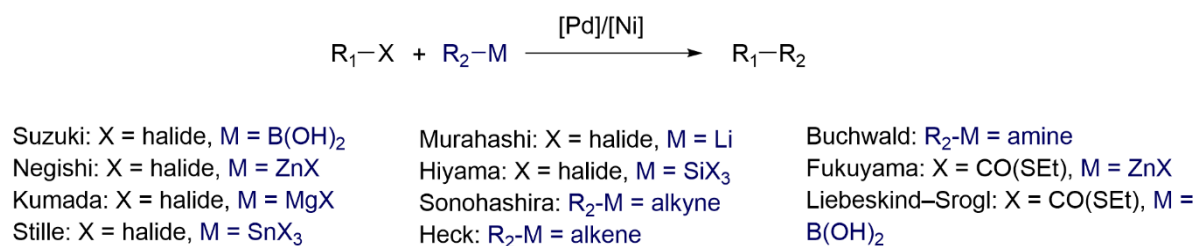


Figure 1. Different cross coupling reactions with their coupling partners

Those cross-coupling reactions hold great importance, as they enable the efficient formation of C-C, C-N, and C-O bonds, which are typically challenging using traditional methods. For instance, in material science, these reactions facilitate the selective and effective synthesis of innovative materials, including electron-conductive organic polymers⁴ and liquid crystals.⁵ Likewise, in the pharmaceutical industry, cross-coupling reactions have

not only simplified the synthesis of highly functionalized drug molecules but have also inspired the structural design of potential drug candidates.^{6,7}

Various transition metals, including Pd,⁸ Ni,⁹ Fe,¹⁰ Co,¹¹ Cu,¹² and Cr,¹³ have been utilized in cross-coupling reactions. While several of these metals are earth abundant and have successfully catalyzed cross-coupling reactions, palladium remains the most favored due to its excellent reproducibility and reactivity.^{14,15} It is worth noting that the 2010 Nobel Prize in Chemistry was awarded to Suzuki, Heck, and Negishi for the development of palladium-catalyzed cross-coupling reactions.

Organoboron compounds have been utilized in organic chemistry in 1970s, initially serving primarily for substitution reactions or in synthesizing dienes. Interestingly, in 1975, the Heck group observed that boronic acids can act as effective partners in cross-coupling reactions when used with stoichiometric quantities of palladium. This observation was further advanced in 1979 when the Suzuki group first demonstrated the use of a catalytic amount of palladium to catalyze the cross-coupling reaction between organoboron and alkenyl bromide, as shown in Scheme 1(1).¹⁶ Although initially limited to dienes as substrates, this method opened new avenues in the field of palladium-catalyzed cross-coupling reactions.

Over the past 40 years, a wide array of catalytic conditions has been investigated to optimize cross-coupling reactions, bringing the Suzuki reaction to one of the most frequently used reactions in synthetic chemistry. Among these developments, in 2005, the Buchwald group introduced a novel ligand, 'SPhos', specifically for the cross-coupling reaction.¹⁷ This innovation allows for the reaction to proceed with lower palladium loading or under milder conditions. Utilizing this approach, a diverse range of functionalized biaryls, heterobiaryls,

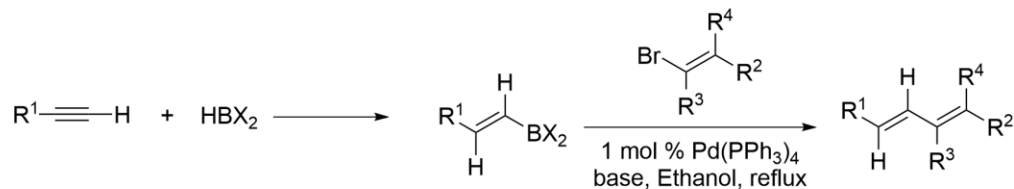
and alkenes have been successfully synthesized. Furthermore, SPhos and similar dialkylbiaryl phosphine ligands can be synthesized through a streamlined two-step, one-pot process, greatly enhancing their commercial availability and practicality.

While palladium has demonstrated exceptional reactivity in catalyzing cross-coupling reactions, extensive research has focused on substituting palladium with more abundant and cost-effective first-row transition metals. In 2012, the Hartwig group reported the successful use of a readily synthesized nickel catalyst for the Suzuki reaction.¹⁸ This catalyst, a nickel(II) complex [(dppf)Ni(cinnamyl)Cl], is prepared through the oxidative addition of cinnamyl chloride to [(dppf)Ni(cod)]. It efficiently catalyzes the coupling of five-membered heteroaryl boronic acids with various nitrogen- and sulfur-containing heteroaryl halides. The resulting hetero-biaryl products were obtained in good to excellent yields, using a mere 0.5 mol% loading of the nickel catalyst.

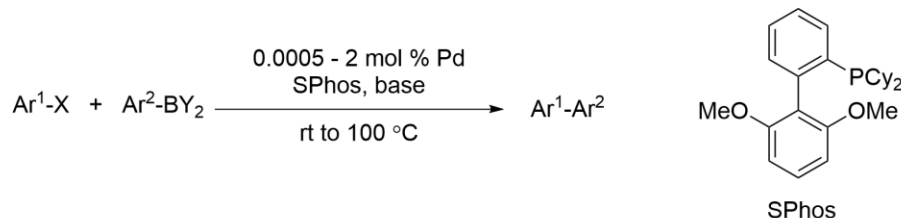
Despite being one of the most utilized organic reactions in the synthesis of small molecules, a universally applicable set of conditions for the Suzuki reaction had remained elusive. This is mainly because the late-stage optimization was typically conducted towards one or two specific targets. In a significant breakthrough in 2022, the Burke group employed a combination of machine learning and automated experimentation to establish general conditions applicable to a broad range of Suzuki cross-coupling partners.¹⁹ They conducted a comprehensive screening involving 11 different substrates under 48 distinct conditions. Leveraging machine learning algorithms, they were able to identify three sets of conditions that are general for the Suzuki reaction. These conditions either outperformed or matched the yields of benchmark methodologies, representing a major step forward in streamlining and standardizing this pivotal reaction in organic chemistry.

Scheme 1. Representative work for Suzuki reaction

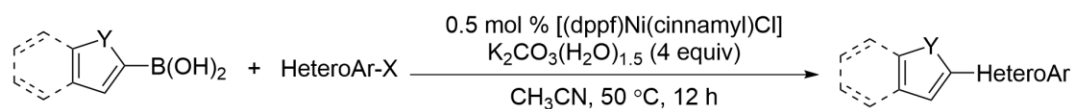
1) Suzuki group's first report on Pd catalyzed Suzuki reaction



2) Buchwald group's work on Pd/SPhos catalyzed Suzuki reaction



3) Hartwig group's work on Ni catalyzed Suzuki reaction



4) Burke group's work on machine learning identified general condition for Suzuki reaction



Alkynes have played a pivotal role since the inception of metal-catalyzed cross-coupling reactions. The historical moment began in 1869 with Glaser's groundbreaking report on the homocoupling of metallic acetylides, a process catalyzed by copper. Subsequently, in 1963, Chodkiewicz advanced the field by reporting the C(sp)-C(sp²) coupling, which involved the reaction of aryl or vinyl halides with alkynes derived as copper salts. A significant development occurred in 1975 with the concurrent disclosure of palladium-catalyzed coupling of acetylenes with aryl or vinyl halides by three independent groups: Sonogashira,

Cassar, and Heck. Among these, the coupling conditions introduced by Sonogashira, which incorporated copper co-catalysis, were notable for their exceptionally mild reaction conditions.²⁰ This contrasted sharply with the more rigorous conditions required in the non-co-catalyzed processes reported by Cassar and Heck. This development marked a significant milestone in the advancement of cross-coupling methodologies.

In 2000, a significant advancement in the field of Sonogashira reactions was made by the Fu and Buchwald groups, who jointly reported a highly versatile catalyst system.²¹ The system, consisting of Pd(PhCN)₂Cl₂ combined with P(*t*Bu)₃, proved to be an efficient catalyst for Sonogashira reactions for aryl bromides, enabling a broad spectrum of couplings to be conducted at room temperature. This represented a substantial improvement over previously reported catalyst systems, as it operated under much milder conditions. This study not only enhanced the versatility of the Sonogashira reaction but also underscored the effectiveness of bulky, electron-rich phosphines in facilitating palladium-catalyzed coupling reactions, contributing significantly to the field of organic synthesis.

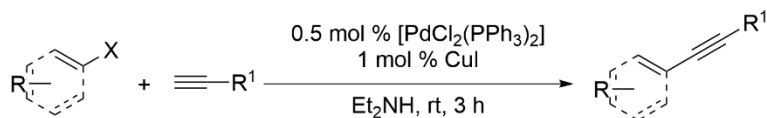
In 2015, the Lipshutz group made a notable contribution to the field of Suzuki reactions by introducing a novel ligand, 'HandaPhos'. This innovation enabled the catalysis of Suzuki reactions in water, remarkably requiring only 0.1 mol % of palladium. Building on this breakthrough, in 2018, the same group further demonstrated the versatility of HandaPhos by applying it as a ligand in the Sonogashira reaction, again in an aqueous environment and with the same low palladium loading of just 0.1 mol %.²² Significantly, the Sonogashira reaction they reported was conducted in the absence of copper, a departure from traditional methodologies. This development not only represented a more sustainable and

environmentally friendly approach but also marked a significant advance in the efficiency and practicality of conducting these important cross-coupling reactions.

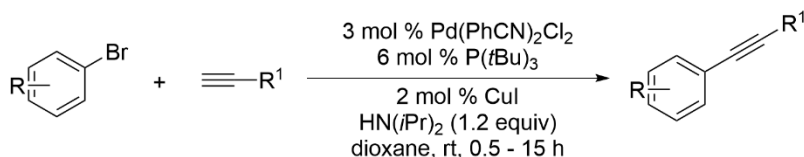
In 2019, the Liu group introduced a general asymmetric copper-catalyzed Sonogashira C(sp³)-C(sp) coupling.²³ This approach marked a significant leap in the field of enantioconvergent cross-coupling reactions. By employing a copper catalyst in conjunction with a cinchona-based chiral P,N-ligand, the group established a robust and versatile strategy for the construction of chiral C-C bonds, utilizing a radical intermediate. A notable aspect of this methodology was the successful direct incorporation of acetylene gas, highlighting its substantial potential for industrial applications. This innovative technique not only paves the way for new methods in enantioconvergent C-C bond formation but also sets a precedent for the exploration of novel catalyst systems. These systems were further applied to managing challenging asymmetric radical transformations by the same group, thus broadening the scope of possibilities in synthetic organic chemistry and catalysis.

Scheme 2. Representative work for Sonogashira reaction

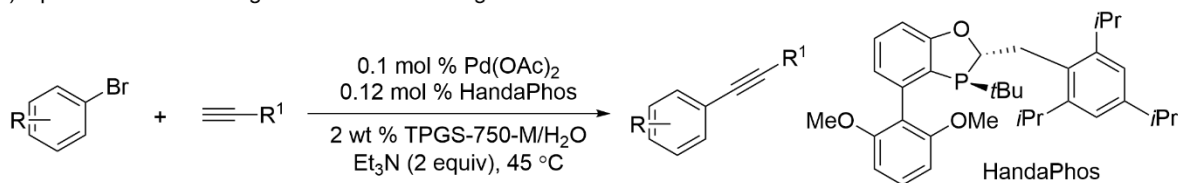
1) The Pd-Cu catalyzed first Sonogashira reaction reported



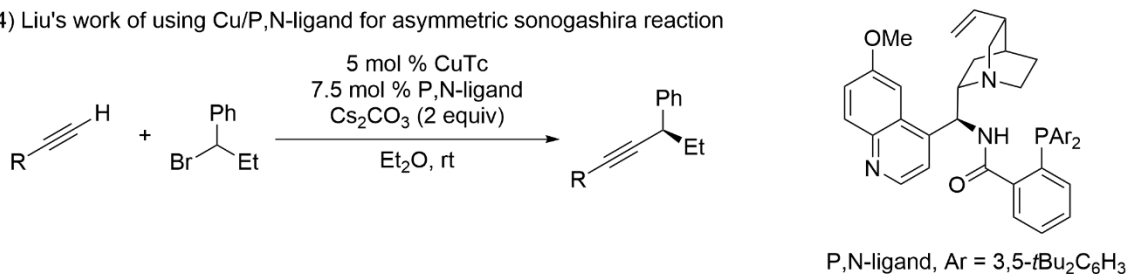
2) Fu and Buchwald's work of the versatile catalyst for sonogashira reaction



3) Lipshutz's work of using HandaPhos for sonogashira reaction



4) Liu's work of using Cu/P,N-ligand for asymmetric sonogashira reaction



The Heck reaction stands out among classic cross-coupling reactions due to its unique requirement: unlike others, it does not require an organometallic compound. The reaction traces back to Richard Heck's inspiration from Pat Henry's research on the Wacker process mechanism. Motivated by these findings, Heck initially tested the reaction of organomercurial compounds and alkenes in the presence of catalytic amounts of Li₂[PdCl₄].

This exploration culminated in 1968 with the publication of seven single-author back-to-back communications, a significant academic feat.

However, due to the high toxicity of organomercury reagents, there was a pressing need for safer alternatives. Addressing this concern, in 1972, Heck reported a method using just 1 mol % Pd(OAc)₂ to catalyze the C-C bond formation between aryl iodide and alkene.²⁴ This method was further refined by various researchers and is now commonly known as the Mizoroki-Heck reaction. The elegance of the Heck reaction lies not only in its avoidance of organometallic reagents but also in its profound impact on the field of cross-coupling chemistry. The research into and application of its mechanism laid a foundational stone for the development of cross-coupling reactions, illustrating a remarkable blend of innovative chemistry and practical application.

Regioselectivity and stereoselectivity have been central themes in the exploration and development of the Heck reaction since its discovery. The selectivity of this reaction is influenced by a multitude of factors, including the choice of ligand, electronic and steric effects, temperature, and the use of additives. A particularly noteworthy aspect is the role of halogen scavengers, such as silver (Ag) and titanium (Ti), which can potentially change the reaction mechanism towards a cationic pathway, thereby altering regioselectivity. A seminal example of this phenomenon was reported by the Hallberg group in 1985.²⁵ They discovered that the addition of silver nitrate to the Heck reaction involving a terminal alkene could shift the β -elimination regioselectivity from the vinyl product to allylic product. While this specific condition may not be universally applicable due to the influence of other factors on selectivity, the Hallberg group's work presented a promising approach to addressing the longstanding challenge of controlling selectivity in the Heck reaction.

Traditionally, the Heck reaction has required high temperatures, often around 100°C. However, in a significant development in 2001, the Fu group introduced a versatile catalyst that enabled Heck reactions of aryl chlorides and bromides under much milder conditions.²⁶ This advancement was an improvement on the previously reported Pd/P(*t*Bu)₃-based catalyst. The key to this enhancement was the use of Cy₂NMe instead of Cs₂CO₃ as the base. This modification allowed for the effective execution of Heck reactions involving a broad spectrum of aryl chlorides and bromides under exceptionally mild conditions. This catalyst system has since been recognized as one of the most universally applicable methods for conducting Heck couplings. Its ability to operate under milder conditions than traditionally required not only broadens the range of potential substrates but also represents a more environmentally friendly and energy-efficient approach to these types of chemical reactions.

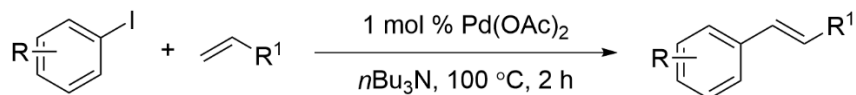
As the understanding of the Heck reaction's mechanisms deepens, there has been increasing development in research focused on selective β -elimination and alkene redistribution. Critical factors influencing these aspects include the choice of ligand (such as P,N-ligands or P,P-ligands), the selection of reactants (like aryl iodides or diaryliodonium salts), and the reaction pathway (involving Pd(II) or Pd(IV)). These variables can significantly determine the positioning of the alkene in the final product.

A particularly interesting example of this nuanced control was presented by the Mo group in 2022.²⁷ They demonstrated that, using the same palladacycle, the Heck reaction could yield two entirely different products simply by altering the reactant. This finding is significant as it underscores the multifaceted nature of the Heck reaction and the intricate interplay of various factors that govern its selectivity. While numerous factors can influence the outcome, the Mo group's work provides fresh insight into the Heck reaction, offering

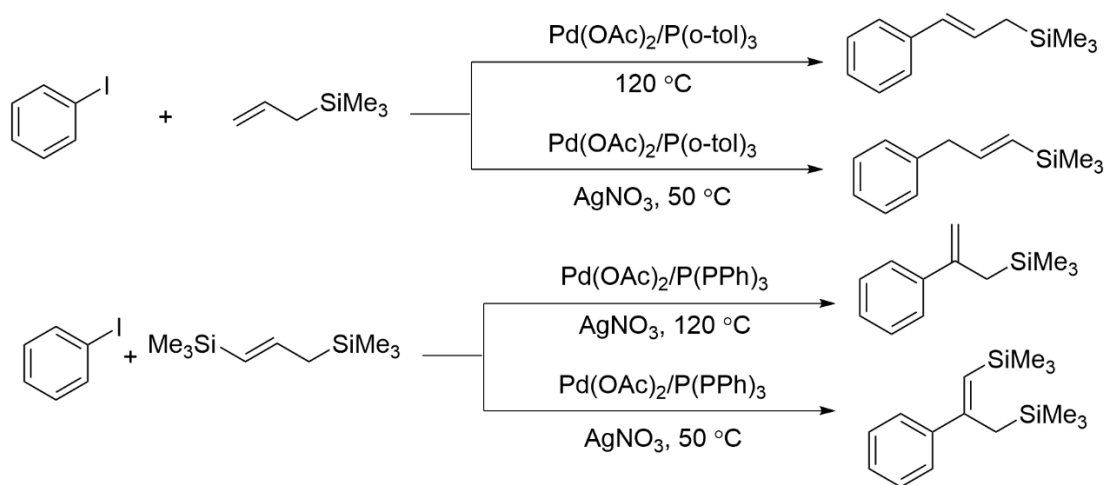
new possibilities for its application and a deeper understanding of its underlying mechanisms.

Scheme 3. Representative work for Mizoroki-Heck reaction

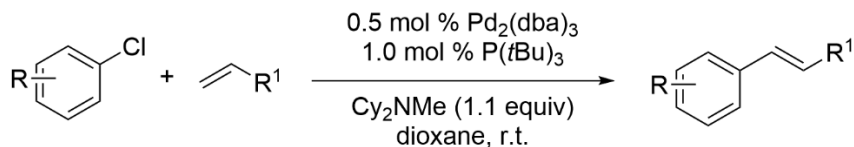
1) Reaction reported by Heck in 1972



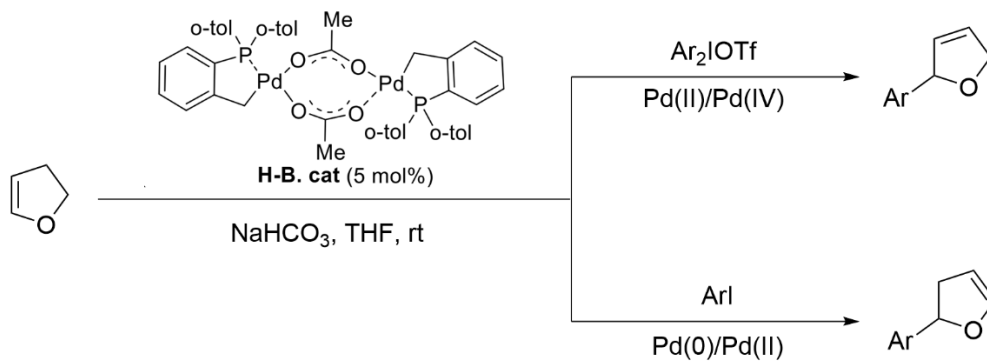
2) Hallberg's work on silver nitrate effect on the Heck reaction



3) Fu's work on general mild condition for the Heck reaction



4) Mo's work on selective the Heck reaction



In 1976, Negishi's work introduced the cross-coupling of organoaluminum reagents using nickel catalysts. However, this method encountered a notable loss of stereospecificity in synthesizing conjugated dienes with organoaluminum reagents. This limitation was overcome by replacing nickel catalysts with palladium complexes, enhancing the reaction's fidelity. Negishi later expanded this methodology by incorporating zinc reagents in cross-coupling processes.²⁸ Most importantly, these findings demonstrated that traditional magnesium and lithium reagents could be substituted with other metals, such as organoaluminum intermediates and zinc, effectively participating in the crucial transmetalation step. This insight drives further innovations in the field of cross coupling.

In 2001, Fu group pioneered the first comprehensive palladium-catalyzed Negishi cross-coupling of aryl and vinyl chlorides, utilizing the commercially accessible and air-stable catalyst $\text{Pd}(\text{P}(t\text{Bu})_3)_2$.²⁹ This methodology is distinguished by several notable features: the use of an easily obtainable catalyst, $\text{Pd}(\text{P}(t\text{Bu})_3)_2$; compatibility with nitro functional groups; the ability to synthesize highly sterically hindered biaryls; effective coupling of sterically demanding vinyl chlorides with arylzinc reagents; applicability to alkylzincs, including the more challenging secondary alkylzincs; and a high turnover number, showcasing its efficiency and versatility in the realm of cross-coupling reactions.

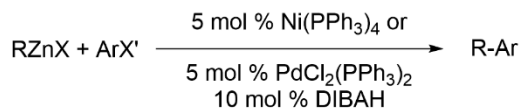
In 2009, the Buchwald group made a significant advancement in Negishi coupling, introducing 'CPhos' as a ligand for coupling secondary alkylzinc halides with aryl bromides and chlorides.³⁰ This methodology demonstrated exceptional efficacy in coupling a broad range of aryl bromides and activated chlorides with secondary alkyl zinc reagents, notably suppressing the undesirable β -hydride elimination pathway by using the novel CPhos. The process's wide substrate scope and remarkable selectivity make it a versatile and powerful

tool for creating C(sp³)-C(sp²) bonds, which is considered as challenge at that time. Additionally, the Buchwald group provided insightful evidence that the superior selectivity for branched over linear products, observed with secondary alkyl zincs using CPhos, is attributed to the relatively slow rates of β -hydride elimination-reinsertion as compared to reductive elimination, offering deeper understanding into the reaction mechanism.

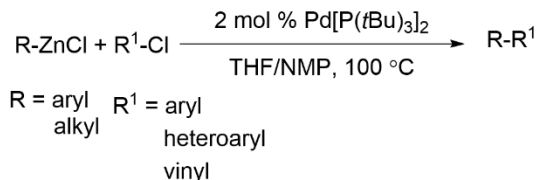
In 2006, the Organ group reported a versatile and user-friendly Pd-NHC precatalyst, PEPPSI-IPr, highlighting its role as a universal cross-coupling catalyst.³¹ This innovation marked the first time a Negishi protocol was capable of consistently achieving cross-coupling across a full range of alkyl and aryl partners on either side. The introduction of PEPPSI-IPr, an easily synthesized, air-stable, and highly active catalyst, significantly broadened the scope, reliability, and user-friendliness of the Negishi reaction. Furthermore, this method's practicality was enhanced by the fact that all reactions could be conducted using standard laboratory techniques, without the need for a glove box, as the precatalyst was stable and could be handled in air.

Scheme 4. Representative work for Negishi reaction

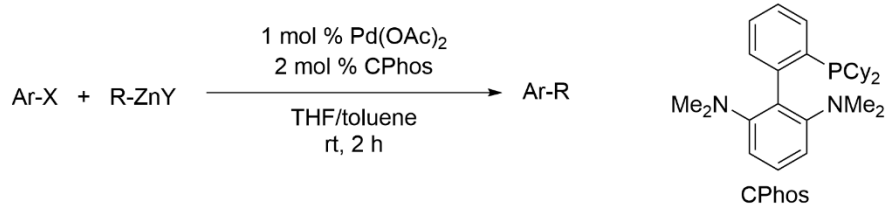
1) Eiichi Negishi's report in 1976



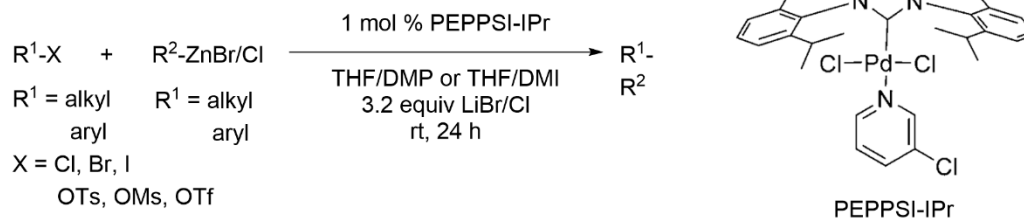
2) First general condition for Negishi reaction



3) Buchwald's CPhos for Negishi reaction of secondary alkylzinc halides and aryl halides



4) Organ's work of PEPPSI-IPr catalyzed Negishi reaction



Recent studies in our group have demonstrated the reactivity of Fe/ppm Pd nanoparticles (NPs) in cross-coupling reactions, under mild conditions in aqueous micellar solution. Tracing back to 2015, the initial NPs were synthesized by reducing FeCl₃ in the presence of SPhos and Pd(OAc)₂ in THF using MeMgCl.³² The resulting grey, powdery nanoparticles were observed to effectively catalyze the Suzuki-Miyaura reaction, requiring only 320 ppm of Pd, when used in the presence of an aqueous solution of "designer" surfactant TPGS-750-

M.³³ By altering the ligand and the amount of palladium involved, these nanoparticles can be engineered to catalyze each of these three couplings, all at ppm palladium levels (Figure 2).^{34,35,36} Interestingly, these spherical nanoparticles undergo a morphological change, transitioning into far larger needle-like nanorods in an aqueous environment. They then synergize with the ligand and palladium in solution, functioning as an effective catalytic system.

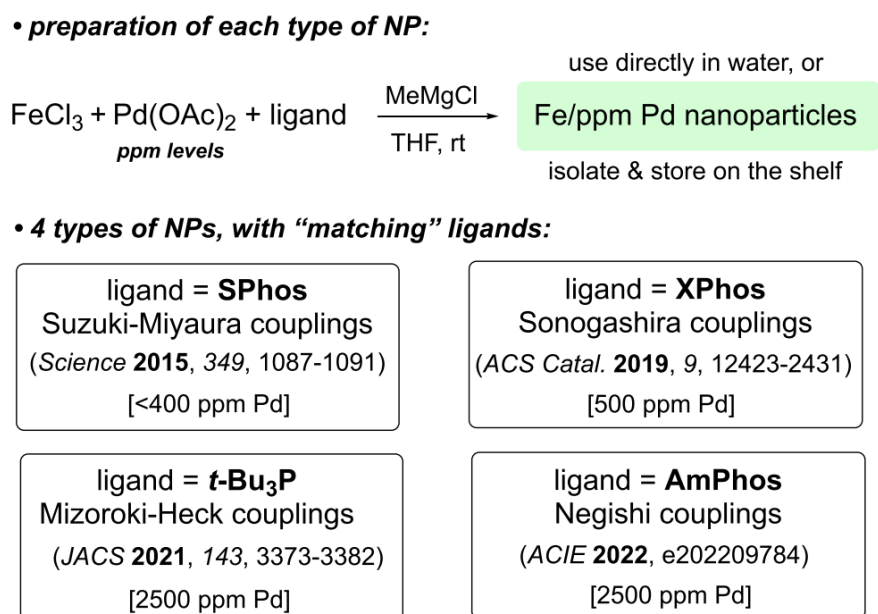


Figure 2. Different nanoparticles for cross coupling reactions in water

While catalysis with nanoparticles in aqueous micellar solutions has demonstrated remarkable reactivity and environmental sustainability, certain challenges still limit its commercialization and broader industrial application. The phosphine within the nanoparticles is sensitive to oxygen, particularly undergoing autoxidation. This could lead to inconsistencies between batches during commercial production, causing storage issues for both suppliers and industries. Additionally, once formulated, these nanoparticles are

designed for a specific reaction due to the inclusion of a particular ligand and palladium, thereby limiting their versatility. To deal with those challenges, we have developed a simplified way to synthesize Fe nanoparticles alone, which not only eliminates the issue of air sensitivity but also demonstrated versatility, as the same nanoparticles were applicable across all four reaction types (*vide infra*).

2.2 Results and discussion

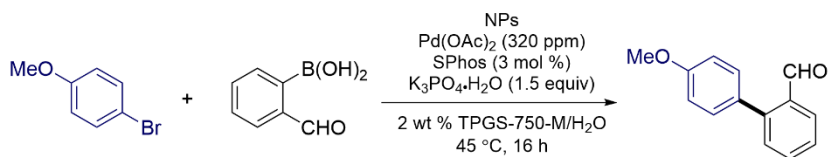
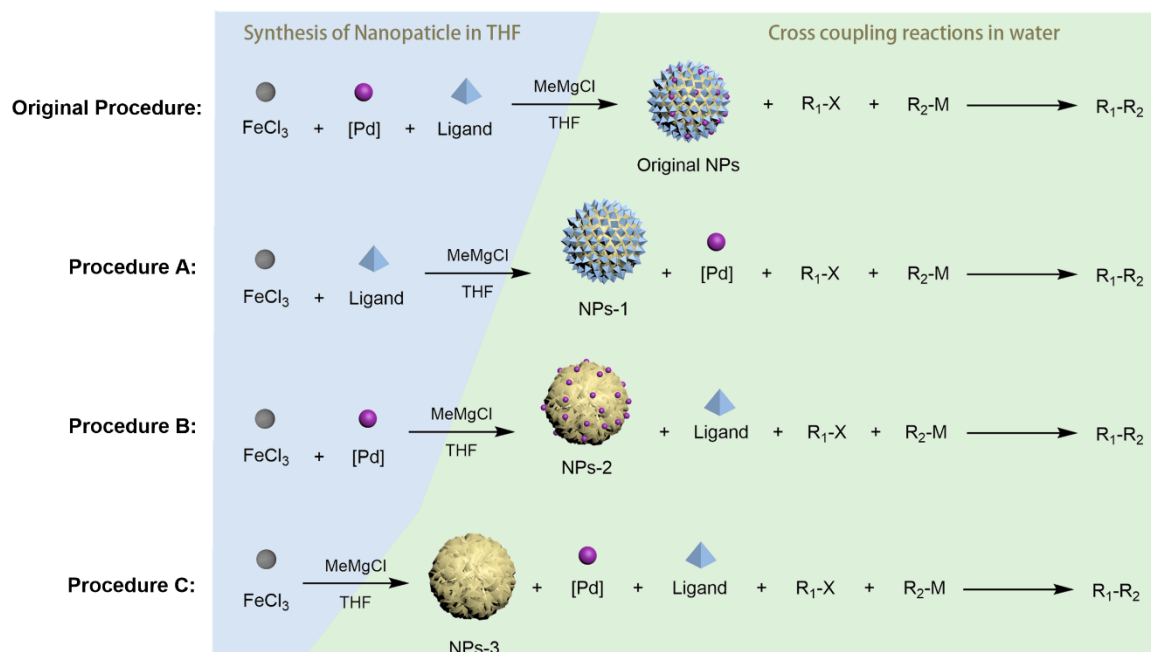
Optimization of reaction conditions and use in synthesis

A cross-coupling reaction catalyzed by nanoparticles (NPs) typically requires reagents such as iron chloride, palladium, a ligand, the cross-coupling partner, a base, and an aqueous reaction medium. The initial catalyst components, including iron trichloride, palladium, and the ligand, can be introduced into the reaction via two different methods: 1) they can be first reduced as part of the nanoparticles and subsequently added to the reaction vessel, or 2) they can be directly introduced into the reaction vessel. Considering the Suzuki-Miyaura reaction as an example, the traditional approach involves reducing the palladium, ligand, and iron trichloride to form an the initial, small (ca. 5 nm) NPs. These NPs were then added to a 2 wt % TPGS-750-M aqueous solution, accompanied by the cross-coupling partner and base (Table 1, original procedure). By taking the palladium or ligand out from the original preparation of the NPs and then directly introducing these NPs into the reaction vessel, various methods to synthesize nanoparticles with different compositions, along with different reaction conditions, have been tested (Table 1, procedure A, B, C).

As shown in Table 1, using 4-bromoanisole and (2-formylphenyl)boronic acid as cross-coupling partners for a model Suzuki-Miyaura reaction, the nanoparticles synthesized via the original procedure resulted in an 86% yield. Meanwhile, Procedure A and Procedure B, which involved the direct addition of palladium or the ligand to the reaction vial, yielded 11% and 42%, respectively. These decreased yields might be due to the separation of palladium and the ligand. Then, Procedure C, which added both the palladium and ligand directly into

the reaction vial, achieved a 71% isolated yield, marking the highest yield among the three tested procedures.

Table 1. Optimization of different procedures



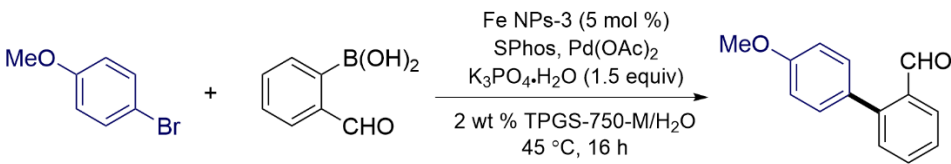
Entry ^a	Procedure used	Yield ^b
1	Original procedure	86
2	Procedure A	11
3	Procedure B	42
4	Procedure C	71

^a Conditions: 4-bromoanisole (0.2 mmol), (2-formylphenyl)boronic acid (0.3 mmol), $K_3PO_4 \cdot H_2O$ (0.3 mmol), $FeCl_3$ (5 mol %), $Pd(OAc)_2$ (320 ppm), SPhos (3 mol %), 2 wt % TPGS-750-M/ H_2O (0.4 mL), 45 °C, 16 h

^b Isolated yield

We subsequently optimized the loading of palladium and the ligand required for the reaction. As shown in Table 2, an optimal 5% SPhos concentration increased the yield to 87%. Further, by supplementing with 180 ppm of Pd(OAc)₂, a combination of 500 ppm of Pd(OAc)₂ and 5% SPhos yielded the best result, producing a 99% isolated product.

Table 2. Optimization of the palladium and ligand loading.



Entry ^a	Pd	Ligand	Yield
1	320 ppm Pd(OAc) ₂	3 % SPhos	71 ^b
2	320 ppm Pd(OAc) ₂	5 % SPhos	87 ^c
3	320 ppm Pd(OAc) ₂	7 % SPhos	82 ^c
4	320 ppm Pd(OAc) ₂	10 % SPhos	88 ^c
5	500 ppm Pd(OAc) ₂	5 % SPhos	99 ^b

^a Conditions: 4-bromoanisole (0.2 mmol), (2-formylphenyl)boronic acid (0.3 mmol), K₃PO₄·H₂O (0.3 mmol), Fe NPs-3 (8 mg, containing 5 mol % FeCl₃), Pd(OAc)₂, SPhos, 2 wt % TPGS-750-M/H₂O (0.4 mL), 45 °C, 16 h

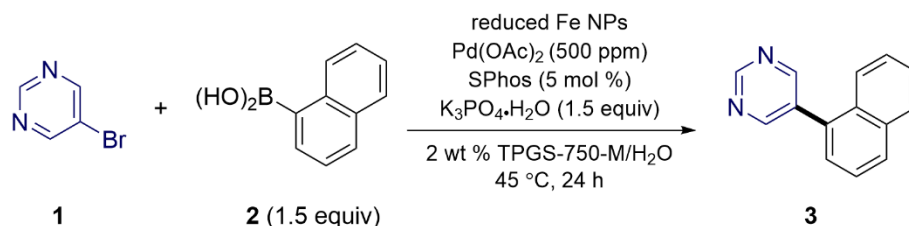
^b Isolated yield

^c Yield by ¹H NMR, ethylene carbonate as internal standard

A control experiment was subsequently carried out wherein either the palladium, ligand, or Fe NPs was removed from the reaction mixture in order to evaluate the importance of each component. As illustrated in Table 3, in the absence of any one of these components the reaction yielded less than 5% coupled product, as observed by ¹H NMR. This result clearly indicates that the successful reaction necessitates the presence of the ligand, the Fe

NPs, and the palladium, together constituting the reactive catalytic system. While the catalytic species could potentially be *in situ*-formed nanoparticles and/or a biphasic catalyst involving solid NPs and ligands in solution, the exact nature of the catalyst needs further investigation.

Table 3. Control experiment of Suzuki-Miyaura reaction



Entry ^a	Variation from above	Yield
1	none	98 ^b
2	without Fe NPs	<5% ^c
3	without Pd(OAc) ₂	<5% ^c
4	without SPhos	<5% ^c

^a 5-Bromopyrimidine (0.2 mmol), naphthalen-1-ylboronic acid (0.3 mmol), Fe NPs-3 (8 mg, 5% Fe NPs), Pd(OAc)₂ (500 ppm), SPhos (5 mol %), K₃PO₄·H₂O (0.3 mmol), 2 wt % TPGS-750-M/H₂O (0.4 mL), 45 °C, 24 h;

^b Isolated yield;

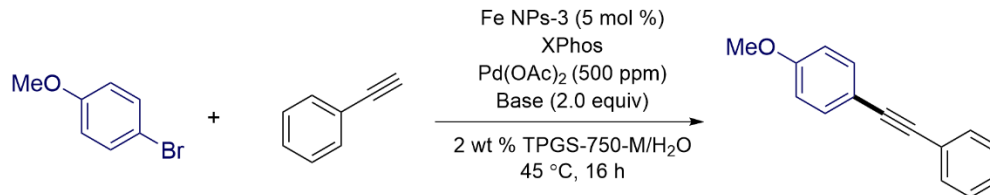
^c Yield by ¹H NMR, ethylene carbonate as internal standard.

The key to optimizing yield in various cross-coupling reactions is largely determined by the choice of the corresponding ligand (Figure 2). For instance, XPhos exhibits specific reactivity for the Sonogashira reaction in water. In this work, by adding the ligand directly into the pot, we gain flexibility as to which ligand to use based on the specific reaction conducted. This offers the versatility to run various cross-coupling reactions, and other

transition metal-catalyzed reactions, using the same Fe nanoparticles, all while requiring only ppm levels of metal.

To validate our hypothesis, we changed the ligand from SPhos to XPhos and executed a Sonogashira reaction in aqueous micellar solution, using 4-bromoanisole and ethynylbenzene as cross-coupling partners. As shown in Table 4 (entry 1), our preliminary trial with K_3PO_4 as base and 1.5 equivalents of alkyne yielded 62% product. While diisopropylethylamine (DIPEA) emerged as the most effective base, it only improved the yield by 12%. Analysis of by-products via 1H NMR revealed the consumption of some aromatic bromide via homocoupling. Consequently, we increased the amount of alkyne to two equivalents, leading to an improved yield of 83%. Interestingly, the ligand loading significantly affected the reaction. In the case shown in entry 6, using just 3 mol % of XPhos, an impressive 98% of the product was isolated. On the contrary, a higher loading (10 mol %) of XPhos decreased the yield to 70%. This decline is possibly due to the coordination of excess bulky XPhos to palladium, thereby blocking the further oxidative addition from the aromatic bromide. Lastly, even though utilizing 1 mol % of XPhos yielded a competitive 96% (as seen in entry 7), further investigation indicated that 3 mol % of XPhos is optimal for preparing more complex molecules.

Table 4. Optimization of the conditions for Sonogashira reactions



Entry ^a	Base	Equiv. of alkyne	Amount of XPhos	Yield ^b
1	K ₃ PO ₄	1.5 equiv.	5 mol %	62
2	Et ₃ N	1.5 equiv.	5 mol %	66
3	DIPEA	1.5 equiv.	5 mol %	74
4	DIPEA	2.0 equiv.	5 mol %	83
5	DIPEA	2.0 equiv.	10 mol %	70
6	DIPEA	2.0 equiv.	3 mol %	99(98)
7	DIPEA	2.0 equiv.	1 mol %	96

^a Conditions: 4-bromoanisole (0.2 mmol), ethynylbenzene, base (0.4 mmol), Fe NPs-3 (8 mg, containing 5 mol % FeCl₃), Pd(OAc)₂ (500 ppm), XPhos, 2 wt % TPGS-750-M/H₂O (0.4 mL), 45 °C, 16 h

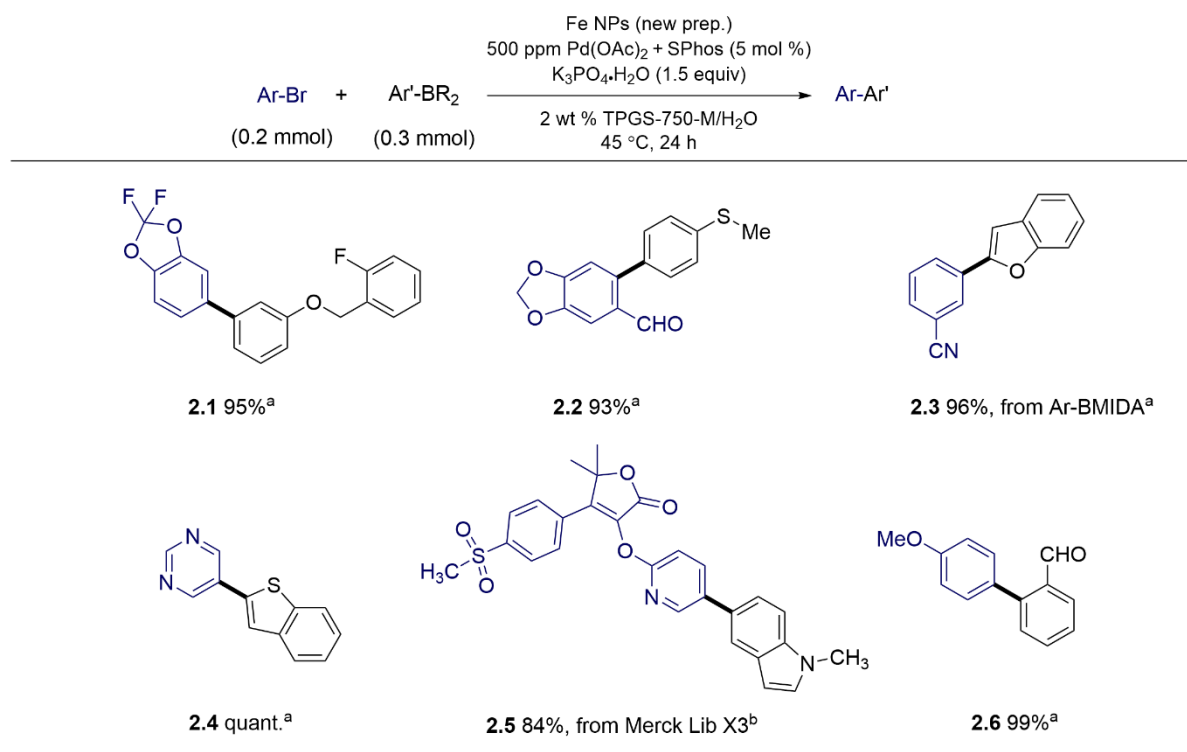
^b Yield determined by HPLC, 1-fluoro-4-(trifluoromethyl)benzene as internal standard, isolated yield in parentheses

Substrate scope

After optimization of the conditions for Suzuki-Miyaura, Sonogashira, Mizoroki-Heck, and Negishi reactions in water, we extended the application of the Fe nanoparticles to a broader library of molecules to assess their generality as catalysts. To emphasize the reactivity and functional group tolerance of this methodology, our substrate Table mainly featured complex or heterocycle-containing molecules (Table 5).

Table 5. Representative cases of coupling reactions using the new preparation of NPs.

Suzuki-Miyaura:

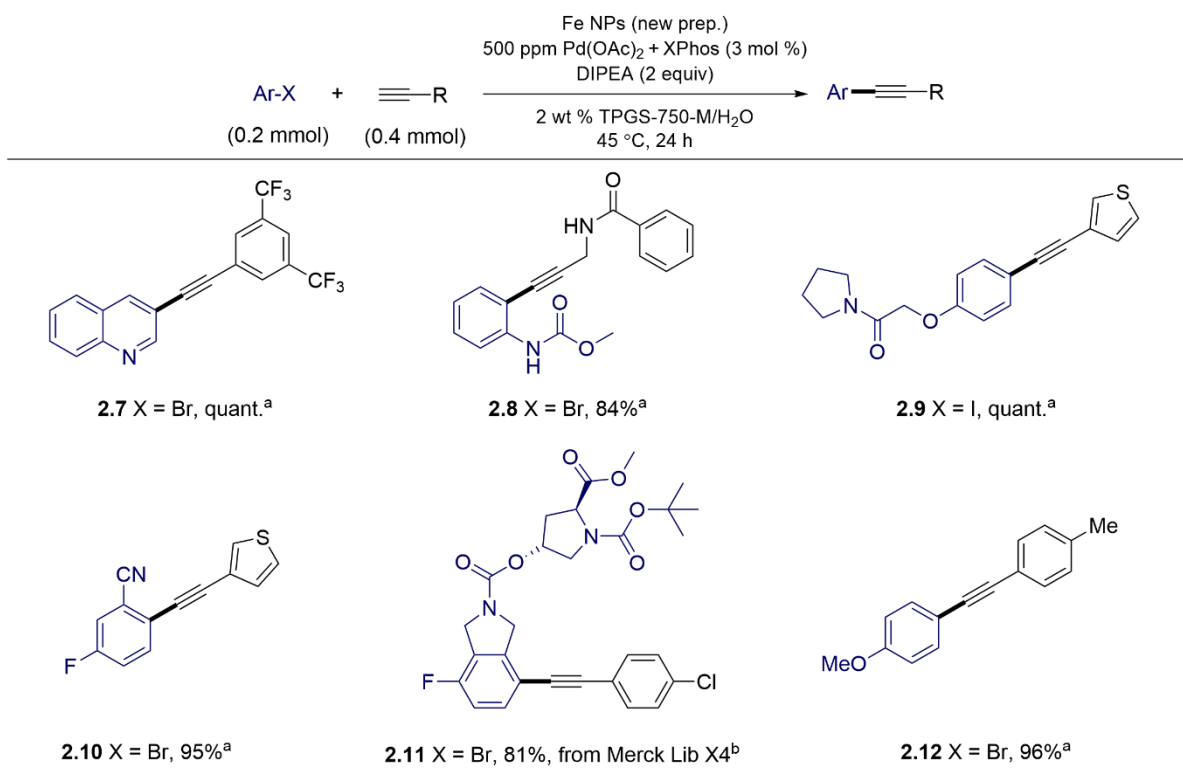


^a Aryl bromide (0.2 mmol), Ar'-BR₂ (0.3 mmol), Fe NPs (8 mg, 5% Fe NPs), Pd(OAc)₂ (500 ppm) in pot, SPhos (5 mol %), K₃PO₄·H₂O (0.3 mmol), 2 wt % TPGS-750-M/H₂O (0.4 mL), 45 °C, 24 h;

^b 55 °C, 48 h, 750 ppm Pd(OAc)₂

Table 5, continued

Sonogashira:

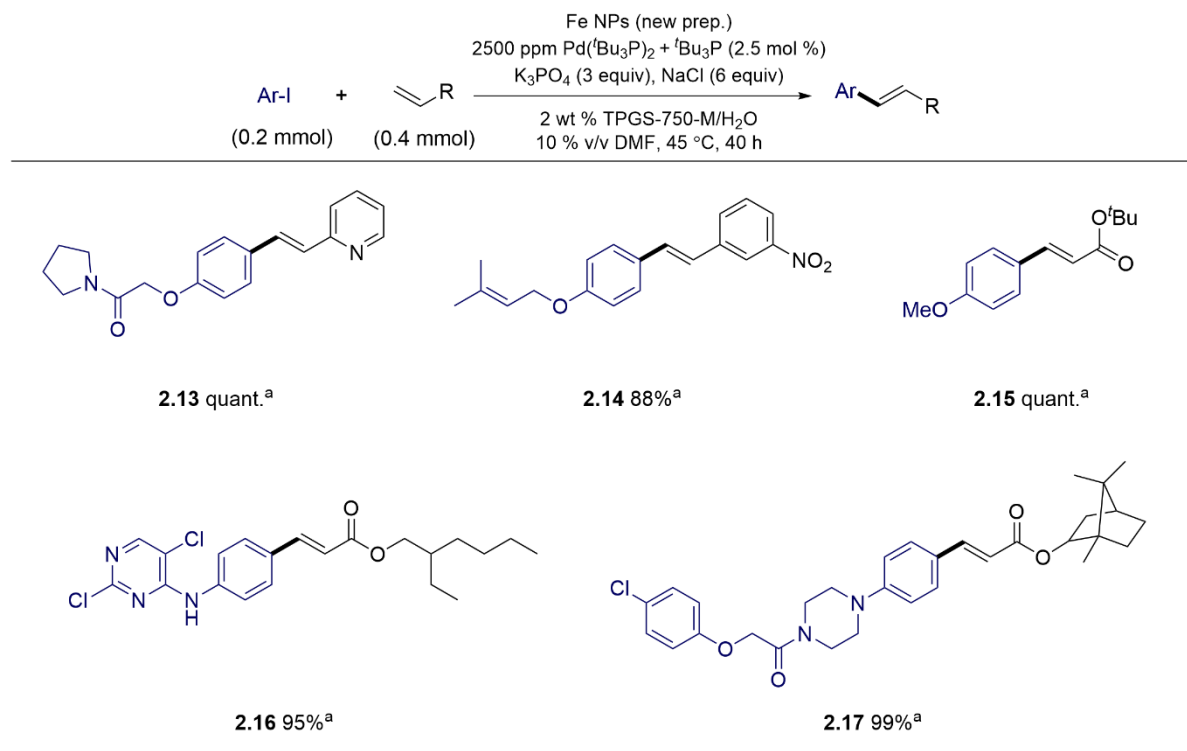


^a Aryl halide (0.2 mmol), alkyne (0.4 mmol), Fe NPs (8 mg, 5% Fe NPs), 500 ppm Pd(OAc)₂ in pot, XPhos (3 mol %), DIPEA (0.4 mmol), 2 wt % TPGS-750-M/H₂O (0.4 mL), 45 °C, 24 h;

^b 55 °C, 48 h, 750 ppm Pd(OAc)₂.

Table 5, continued

Mizoroki-Heck:



^a Aryl iodide (0.2 mmol), alkene (0.4 mmol), NPs (2.8 mg, 1.8% Fe NPs), 2500 ppm Pd(*t*Bu₃P)₂ in pot, *t*Bu₃P (2.5 mol %), K₃PO₄ (0.6 mmol), NaCl (1.2 mmol), 2 wt % TPGS-750-M/H₂O (0.4 mL), DMF (0.04 mL), 45 °C, 40 h.

This methodology demonstrates excellent reactivity and a broad tolerance for functional groups. For the Suzuki-Miyaura reaction, it effectively leads to products containing fluoride (**2.1**), an ether (**2.1**), aldehyde (**2.2,2.6**), a thioether (**2.2**), and nitrile (**2.3**), all giving over 90% yield. Moreover, this method has been successfully applied to various heterocycles, such as benzo[*d*][1,3]dioxole (**2.1,2.2**), benzofuran (**2.3**), pyrimidine (**2.4**), and benzothiophene (**2.4**), all of which afforded excellent yields. Notably, compound **2.5**, synthesized using an aryl halide from the Merck Informer Library³⁷ and coupled with *N*-methylindole, achieved an impressive 84% isolated yield. Even though the conditions required slightly higher temperature and an additional 250 ppm of palladium, the result was still considered good, especially given the compound's complexity and its significance to the pharmaceutical industry. Furthermore, compound **2.6**, the BMIDA derivative, yielded the desired product in an impressive 96%. This high yield, obtained from a BMIDA compound traditionally considered more stable and less reactive,³⁸ demonstrated the excellent reactivity of this catalyst system.

For Sonogashira reactions, this method exhibited excellent compatibility with a range of functional groups, delivering outstanding yields for products containing trifluoromethyl (**7**), amides (**2.8,2.9**), carbamates (**2.8**), ethers (**2.9**), nitriles (**2.10**), and fluorides (**2.10**). Additionally, another aryl halide from the Merck Informer Library was effectively coupled with 4-chloroethynylbenzene, achieving an 81% yield of product **2.11**. The Mizoroki-Heck reaction also showcased this methodology's versatility, with amides (**2.13, 2.17**), ether-containing products (**2.13,2.14**), internal alkenes (**2.14**), esters (**2.15, 2.16, 2.17**), amines (**2.16**), and chlorides (**2.16, 2.17**) all being well-accommodated, indicative of robust functional group tolerance. For Negishi reactions, the method proved equally efficient,

tolerating nitriles (**2.18**), amides (**2.19**), compounds with trifluoromethyl groups (**2.19**), fluorides (**2.20**), esters (**2.21**), and ether-containing products (**2.22**).

Perhaps more noteworthy, heterocycles have been successfully utilized in these reactions, yielding products with a diverse array of structures. Compounds containing quinoline (**2.7**), thiophene (**2.9**, **2.10**), pyrrolidine (**2.9**, **2.11**, **2.13**), pyridine (**2.13**), pyrimidine (**2.16**, **2.20**), piperazine (**2.17**), benzothiophene (**2.18**, **2.23**), oxetane (**2.19**), morpholine (**2.20**), indole (**2.21**), and tetrahydro-2H-pyran (**2.23**) were synthesized with remarkable efficiency, further exemplifying the methodology's broad functional group compatibility and its potential for generating high yields of structurally complex heterocycles.

Characterization of the nanoparticles

STEM imaging was utilized to characterize the structure and composition of the nanoparticles (NPs). Figure 3A illustrates that the NPs derived from only FeCl₃, upon exposure to an aqueous environment, exhibit the identical 100 nm needle-like morphology in TPGS-750-M aqueous solution as seen when synthesized via the original protocol. This observation serves as a control, indicating that the pivotal factor leading to the eventual morphological transformation in water is the initial reduction of FeCl₃ by MeMgCl.

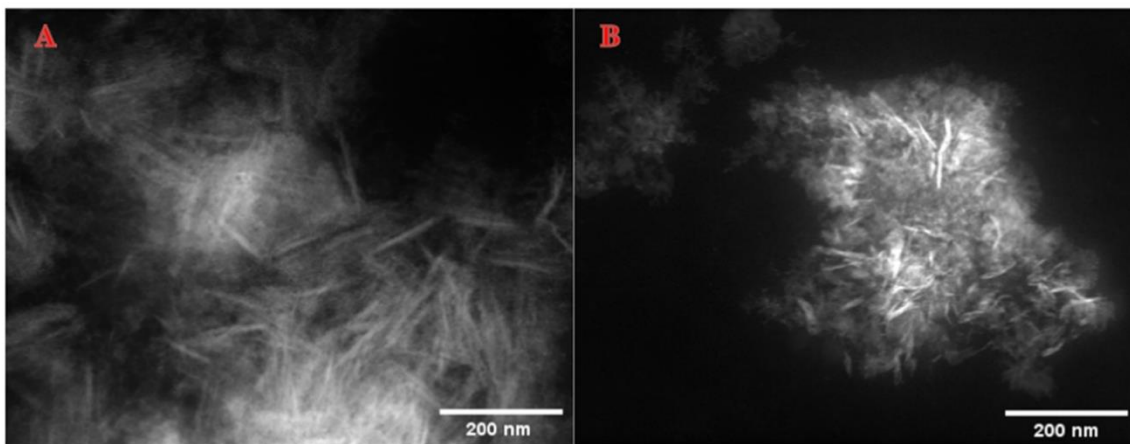
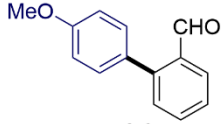
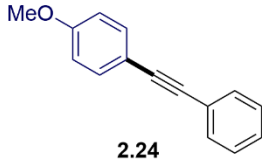
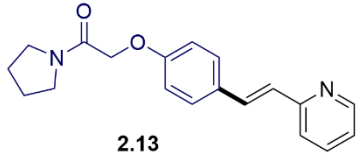
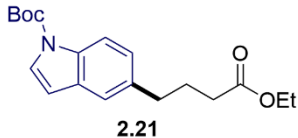


Figure 3, STEM image for the NPs formed via the new route vs those following the original recipe. (A) High-angle annular dark field-scanning transmission electron microscopy (HAADF-STEM) image of Fe NPs with Pd(OAc)₂ and SPhos in 2 wt % TPGS-750-M/H₂O following the new approach. (B) Fe/ppm Pd nanocatalyst with SPhos in 2 wt % TPGS-750-M/H₂O following the original procedure.

Direct comparison between new and original procedure

To evaluate the reactivity of the simplified method in comparison with the original procedure, four distinct products, each representing a different reaction, were selected for testing. Table 6 demonstrates that the yields for all four reactions using the new method were either higher or comparable to those obtained with the original protocol. The enhanced performance is attributed to the 'freshness' of the *in situ* generated NPs, which ensure the immediate availability of palladium on the NPs' surface for the upcoming reaction. Additionally, the minimized oxidation of the phosphine ligand also contributes significantly to this improvement, given its critical role in each of the coupling reactions.

Table 6. Comparisons between premade and *in situ*-prepared NPs as catalysts for coupling reactions

reaction type	product	original recipe	<i>new approach</i>
		Yield (%) pre-made NPs	Yield (%) <i>in-situ</i> made NPs
Suzuki-Miyaura ^a	 2.6	86	99
Sonogashira ^b	 2.24	92	95
Mizoroki-Heck ^c	 2.13	89	quant.
Negishi ^d	 2.21	82	86

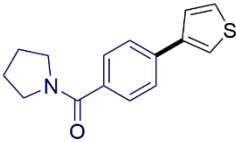
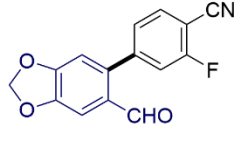
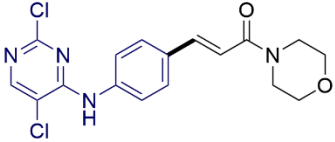
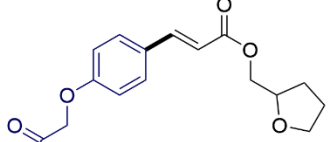
a, using 500 ppm Pd catalyst; see Table 5; b, using 2500 ppm Pd catalyst; see Table 5.

Application of air-stable ferrocene-based ligand in NPs catalysis

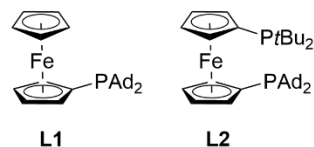
Another significant advantage of this novel approach to ppm Pd NPs catalysis lies in the ability to change ligands without the necessity of synthesizing new nanoparticles. This flexibility is particularly advantageous when dealing with ligands that may exhibit limitations, such as sensitivity to air³⁹ or when they offer poor reactivity when used with certain substrates. As shown in Table 7, the adaptability in this new catalytic system allows for the exchange of ligands, enabling the assessment of alternative, air-stable ferrocene-

based ligands that have been recently reported by Colacot *et al.*,⁴⁰ and which are currently commercially available from Sigma-Aldrich.⁴¹ These ligands avoid the limitations mentioned previously (*vide supra*). Specifically, the employment of ligand **L1**, instead of SPhos, markedly improved the results for the two tested Suzuki–Miyaura reactions, leading to biaryls **2.25** and **2.26**. Similarly, substituting ligand **L2** for Fu’s ligand removed the air-sensitivity challenges associated with *t*-Bu₃P and significantly enhanced the reactivity of the NP catalyst, resulting in better isolated yields of the unsaturated amide **2.27** and arylate **2.28**.

Table 7. Comparisons between ligands used in Suzuki–Miyaura and the Heck couplings

reaction type	product	Yield (%) with SPhos or <i>t</i> Bu ₃ P	Yield (%) with ferrocene-based ligand
Suzuki-Miyaura	 2.25	72 ^a	95 ^b
	 2.26	27 ^a	51 ^b
Mizoroki-Heck	 2.27	70 ^c	89 ^d
	 2.28	76 ^c	92 ^d

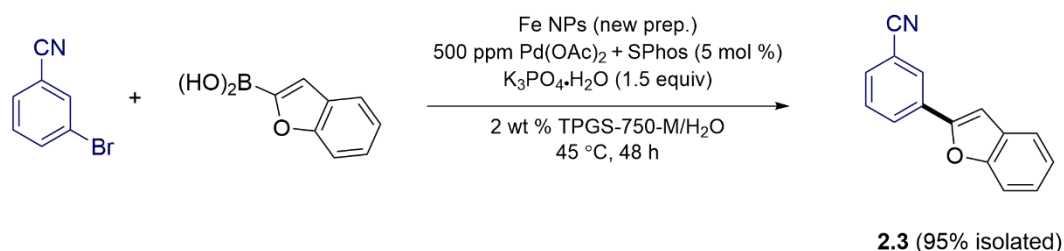
^a using SPhos as ligand; ^b using L1 as ligand;
^c using *t*Bu₃P as ligand; ^d using L2 as ligand;



E Factor evaluation

The NP-catalyzed Suzuki-Miyaura coupling between 3-bromobenzonitrile and benzofuran-2-ylboronic acid was carried out to determine the E Factor⁴² for this reaction (Scheme 5). While achieving a 95% yield of the desired product **2.3**, the E Factor without water was determined to be a remarkably low 0.39, primarily because of the recyclability of the solvent and the obviation of any extraction process, due to product precipitation. The E Factor with water, in the case of the water is not recycled, was calculated to be 10, which still remains comparatively low relative to reactions conducted in organic solvents.

Scheme 5. E Factor evaluation



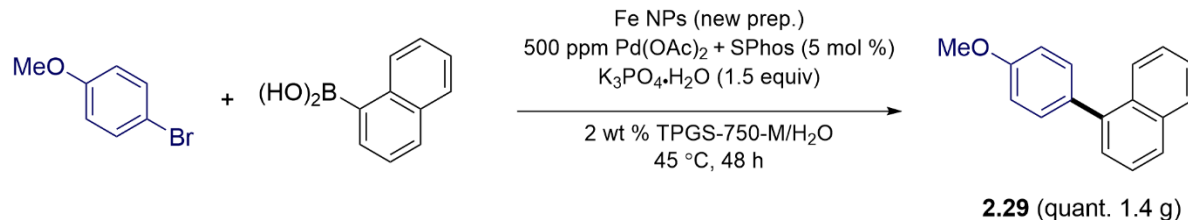
$$\text{E factor (without water)} = \frac{\text{Mass of organic waste}}{\text{Mass of product}} = 0.39$$

$$\text{E factor (with water)} = \frac{\text{Mass of organic waste} + \text{mass of water}}{\text{Mass of product}} = 10$$

Gram-scale reaction

A gram-scale Suzuki-Miyaura reaction between 4-bromoanisole and naphthalen-1-ylboronic acid was carried out, as shown in Scheme 6. This reaction successfully yielded 1.4 grams of the target product **2.29**, achieved in quantitative yield. This outcome represents the potential for upscaling production using this methodology.

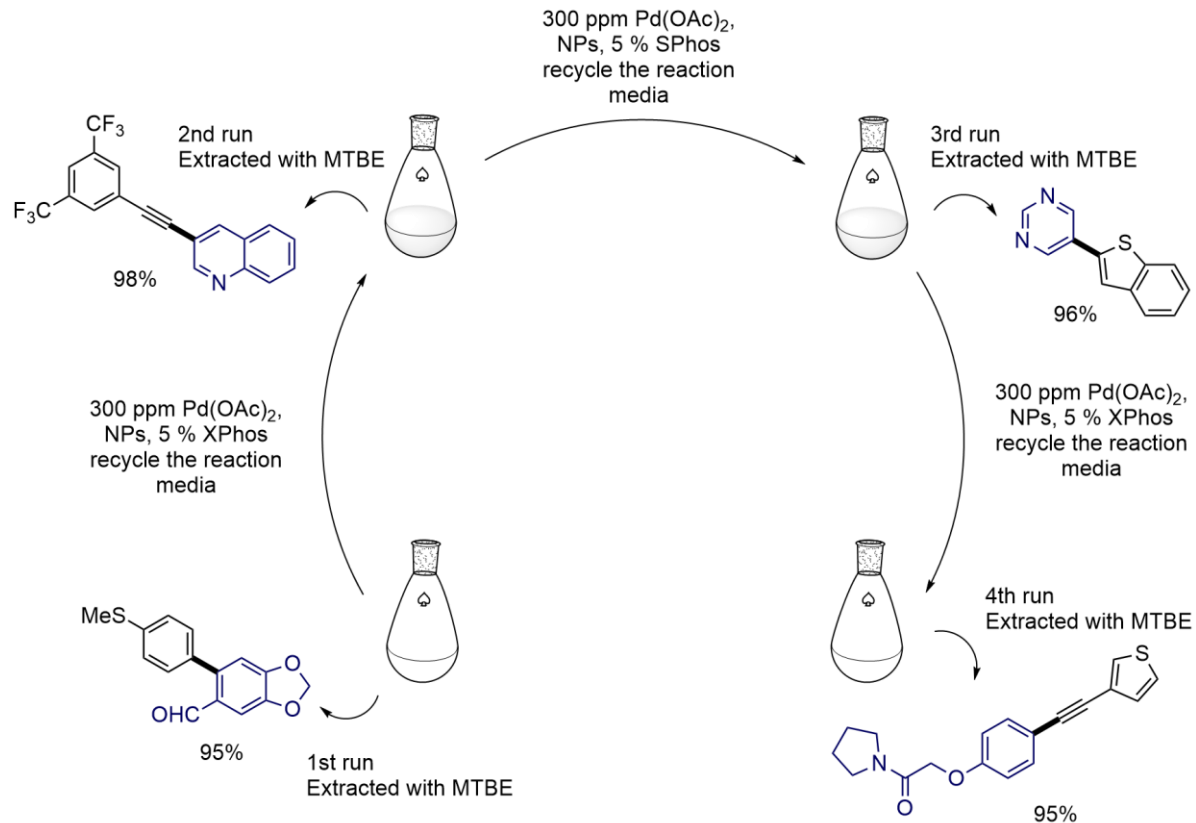
Scheme 6. Representative gram-scale coupling



Recycle study

A series of experiments was performed to evaluate the recyclability of the aqueous micellar solution. As illustrated in Scheme 7, an initial Suzuki-Miyaura coupling using a 2 wt % TPGS-750-M aqueous solution as the reaction medium was conducted. Upon completion of the reaction, a minimal volume of methyl *t*-butyl ether (MTBE) was added to extract the product. Subsequent purification yielded a 95% of the desired product. The reaction medium was then reused by introducing fresh catalyst and new substrates for a Sonogashira reaction. This subsequent reaction proceeded with high reactivity, delivering 98% of the desired product. After another Suzuki-Miyaura coupling and Sonogashira reaction, the reaction medium, therefore, was effectively recycled three times, accommodating four distinct sets of coupling partners with no loss of reactivity. The consistent high performance across multiple recycles highlights the sustainability and efficiency of this method.⁴³

Scheme 7. Recycle study

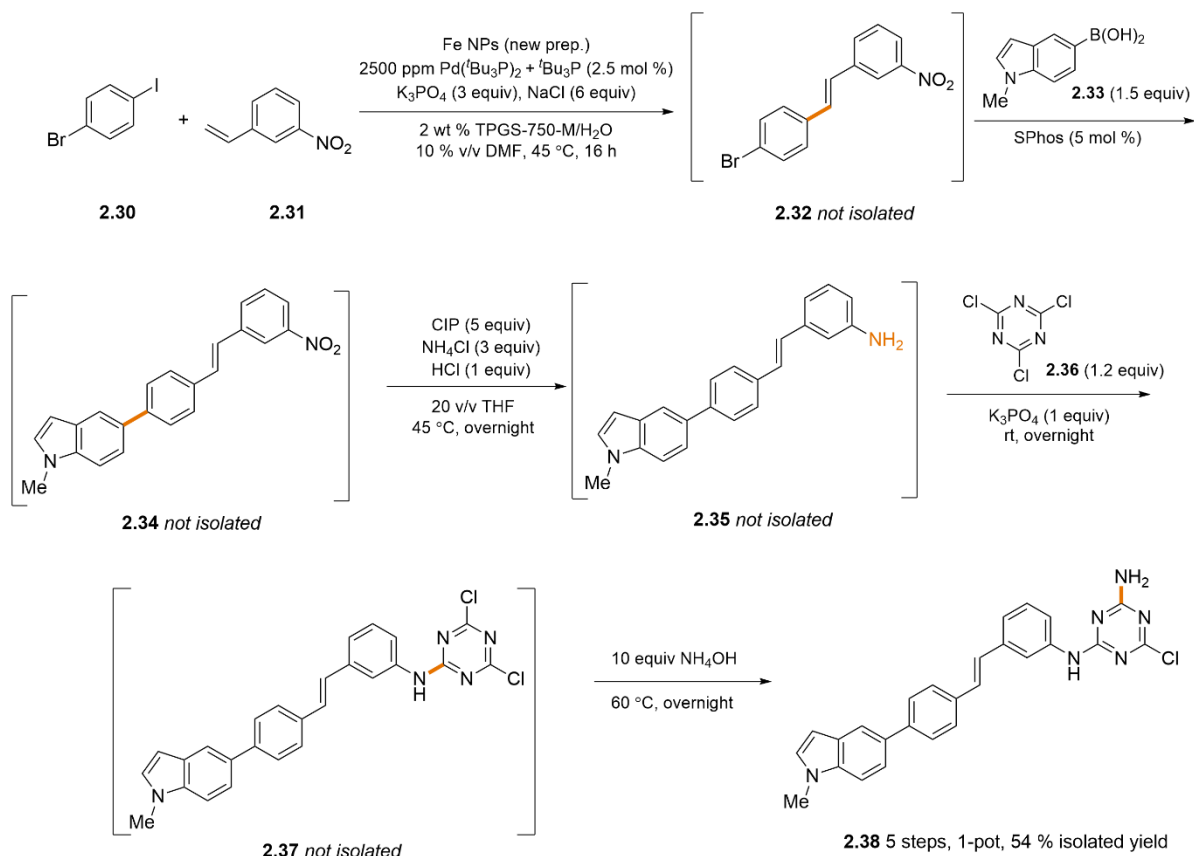


One-pot reaction sequence

The toolbox for reactions in water, including both bio-catalytic and chemo-catalytic processes, has seen significant expansion.^{44,45} Notably, the surfactant TPGS-750-M has shown potential benefits for both enzymatic catalysis and traditional organic synthetic reactions. Illustrated in Scheme 8 is a one-pot tandem sequence of reactions employing a micellar aqueous solution as the solvent system. Beginning with dihalide **2.30** and styrene **2.31**, a catalytic system composed of 2500 ppm Pd(*t*-Bu₃)₂, Fe NPs, and *t*-Bu₃P were introduced, selectively catalyzing the Mizoroki-Heck reaction at the iodide position.³⁵ Subsequent addition of boronic acid **2.33** and 5 mol % of a ligand allowed the palladium to

re-equilibrate and facilitate a subsequent Suzuki-Miyaura coupling, in one pot. Remarkably, both the Fe NPs and the palladium were recycled in these steps. Thus, with proper design of the reaction sequence, the palladium needed already at the ppm level in water can be used further to great advantage, leading to “metal economy.” Without isolation, the nitro group in compound **2.34** was reduced to the corresponding amine **2.35** using carbonyl iron powder (CIP).⁴⁶ Subsequently, a S_NAr reaction with triazine **2.36** introduced the heterocyclic triazine structure in compound **2.37**.⁴⁷ Finally, with no purification needed, the addition of ammonium hydroxide enabled the ultimate substitution reaction (*i.e.*, S_NAr), leading to product **2.38**. Final purification led to an overall yield of 54% for the entire five-step sequence.

Scheme 8. Sequential reactions, including two ppm Pd NP-catalyzed couplings, in water

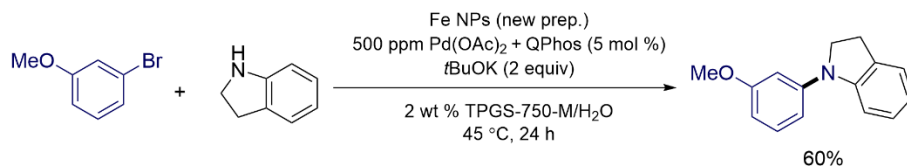


Other reactions tested

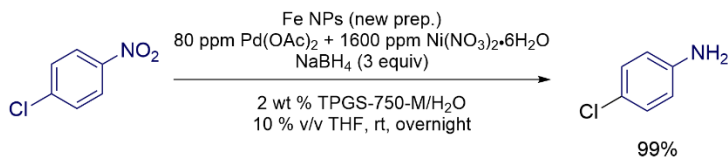
Other than the traditional C-C bond-forming cross-coupling reactions previously described, several other reactions catalyzed by transition metal catalysis have been explored. As shown in Scheme 9A, the substitution of the ligand with QPhos enabled the Fe NPs and Pd to effectively catalyze amination in aqueous media, requiring only 500 ppm of Pd. Furthermore, Scheme 9B illustrates that using dual metal catalysis, employing both 80 ppm Pd and 1600 ppm Ni, a nitro-containing precursor was efficiently converted to the corresponding amine. While the products in these reactions are relatively simple, they nevertheless provide a valuable foundation for future investigation.

Scheme 9. Other reactions tested with Fe NPs

(A) ppm Pd catalyzed amination



(B) ppm Pd/Ni catalyzed nitro reduction



Conclusion

In conclusion, this work has led to the introduction of a novel and streamlined methodology for the synthesis of iron nanoparticles (Fe NPs) and their applications to various cross-coupling reactions in aqueous media, utilizing ppm levels of Pd. This innovative approach not only simplifies the production of these sensitive nanoparticles but also establishes a standardized protocol that enhances reproducibility. Additionally, the newly developed Fe NPs removed the associated ligands and Pd, which are known to undergo autooxidation, thereby not only improving storability of the nanoparticles but also avoiding their variations in reactivity due to inconsistencies between batches. Significantly, the one-pot sequence demonstrated that the same Fe NPs and Pd can be employed in two different sequential cross-coupling reactions *via* re-equilibration of the ligand, which further highlights "metal economy". The success of this work provides the possibility to advance more transition metal catalyzed reactions, such as amination, nitro reduction, photocatalysis, C-H activation, etc. with less catalyst loading, greener reaction media, and milder conditions.

References

1. Campeau, L.-C.; Hazari, N., Cross-Coupling and Related Reactions: Connecting Past Success to the Development of New Reactions for the Future. *Organometallics* **2019**, *38*, 3-35.
2. Hazari, N.; Melvin, P. R.; Beromi, M. M., Well-defined nickel and palladium precatalysts for cross-coupling. *Nat. Rev. Chem.* **2017**, *1*, 0025.
3. Jana, R.; Pathak, T. P.; Sigman, M. S., Advances in Transition Metal (Pd,Ni,Fe)-Catalyzed Cross-Coupling Reactions Using Alkyl-organometallics as Reaction Partners. *Chem. Rev.* **2011**, *111*, 1417-1492.
4. Xu, S.; Kim, E.; Wei, A.; Negishi, E., Pd- and Ni-catalyzed cross-coupling reactions in the synthesis of organoelectronic materials. *Sci. Technol. Adv. Mater.* **2014**, *15*, 044201.
5. Xie, W.; Xiao, D.; Wen, Y.; Li, J.; Wang, L.; Guo, M., Efficient synthesis of fluoro-containing liquid crystal materials via Pd-catalysed room temperature aerobic Suzuki reactions in aqueous media. *Liquid Crystals* **2015**, *42*, 65-69.
6. Buskes, M. J.; Blanco, M.-J., Impact of Cross-Coupling Reactions in Drug Discovery and Development. *Molecules*, **2020**, *25*, 3493.
7. Rayadurgam, J.; Sana, S.; Sasikumar, M.; Gu, Q., Palladium catalyzed C–C and C–N bond forming reactions: an update on the synthesis of pharmaceuticals from 2015–2020. *Org. Chem. Front.* **2021**, *8*, 384-414.
8. Johansson Seechurn, C. C. C.; Kitching, M. O.; Colacot, T. J.; Snieckus, V., Palladium-Catalyzed Cross-Coupling: A Historical Contextual Perspective to the 2010 Nobel Prize. *Angew. Chem., Int. Ed.* **2012**, *51*, 5062-5085.
9. Tasker, S. Z.; Standley, E. A.; Jamison, T. F., Recent advances in homogeneous nickel catalysis. *Nature* **2014**, *509*, 299-309.
10. Mako, T. L.; Byers, J. A., Recent advances in iron-catalysed cross coupling reactions and their mechanistic underpinning. *Inorg. Chem. Front.* **2016**, *3*, 766-790.

11. Cahiez, G.; Moyeux, A., Cobalt-Catalyzed Cross-Coupling Reactions. *Chem. Rev.* **2010**, *110*, 1435-1462.
12. Thapa, S.; Shrestha, B.; Gurung, S. K.; Giri, R., Copper-catalysed cross-coupling: an untapped potential. *Org. Biomol. Chem.* **2015**, *13*, 4816-4827.
13. Li, J.; Knochel, P., Chromium-Catalyzed Cross-Couplings and Related Reactions. *Synthesis* **2019**, *51*, 2100-2106.
14. Cooper, A. K.; Burton, P. M.; Nelson, D. J., Nickel versus Palladium in Cross-Coupling Catalysis: On the Role of Substrate Coordination to Zerovalent Metal Complexes. *Synthesis* **2020**, *52*, 565-573.
15. Rimmel, A., Why Chemists Can't Quit Palladium. *Nature*, **2022**, *606*, 448-451.
16. Miyaura, N.; Yamada, K.; Suzuki, A., A new stereospecific cross-coupling by the palladium-catalyzed reaction of 1-alkenylboranes with 1-alkenyl or 1-alkynyl halides. *Tetrahedron Lett.* **1979**, *20*, 3437-3440.
17. Barder, T. E.; Walker, S. D.; Martinelli, J. R.; Buchwald, S. L., Catalysts for Suzuki–Miyaura Coupling Processes: Scope and Studies of the Effect of Ligand Structure. *J. Am. Chem. Soc.* **2005**, *127*, 4685-4696.
18. Ge, S.; Hartwig, J. F., Highly Reactive, Single-Component Nickel Catalyst Precursor for Suzuki–Miyaura Cross-Coupling of Heteroaryl Boronic Acids with Heteroaryl Halides. *Angew. Chem., Int. Ed.* **2012**, *51*, 12837-12841.
19. Angello, N. H.; Rathore, V.; Beker, W.; Wołos, A.; Jira, E. R.; Roszak, R.; Wu, T. C.; Schroeder, C. M.; Aspuru-Guzik, A.; Grzybowski, B. A.; Burke, M. D., Closed-loop optimization of general reaction conditions for heteroaryl Suzuki–Miyaura coupling. *Science* **2022**, *378*, 399-405.
20. Sonogashira, K.; Tohda, Y.; Hagihara, N., A convenient synthesis of acetylenes: catalytic substitutions of acetylenic hydrogen with bromoalkenes, iodoarenes and bromopyridines. *Tetrahedron Lett.* **1975**, *16*, 4467-4470.

21. Hundertmark, T.; Littke, A. F.; Buchwald, S. L.; Fu, G. C., Pd(PhCN)₂Cl₂/P(t-Bu)₃: A Versatile Catalyst for Sonogashira Reactions of Aryl Bromides at Room Temperature. *Org. Lett.* **2000**, *2*, 1729-1731.
22. Handa, S.; Smith, J. D.; Zhang, Y.; Takale, B. S.; Gallou, F.; Lipshutz, B. H., Sustainable HandaPhos-ppm Palladium Technology for Copper-Free Sonogashira Couplings in Water under Mild Conditions. *Org. Lett.* **2018**, *20*, 542-545.
23. Dong, X.-Y.; Zhang, Y.-F.; Ma, C.-L.; Gu, Q.-S.; Wang, F.-L.; Li, Z.-L.; Jiang, S.-P.; Liu, X.-Y., A general asymmetric copper-catalysed Sonogashira C(sp³)–C(sp) coupling. *Nat. Chem.* **2019**, *11*, 1158-1166
24. Heck, R. F.; Nolley, J. P., Jr., Palladium-catalyzed vinylic hydrogen substitution reactions with aryl, benzyl, and styryl halides. *J. Org. Chem.* **1972**, *37*, 2320-2322.
25. Karabelas, K.; Westerlund, C.; Hallberg, A., The effect of added silver nitrate on the palladium-catalyzed arylation of allyltrimethylsilanes. *J. Org. Chem.* **1985**, *50*, 3896-3900.
26. Littke, A. F.; Fu, G. C., A Versatile Catalyst for Heck Reactions of Aryl Chlorides and Aryl Bromides under Mild Conditions. *J. Am. Chem. Soc.* **2001**, *123*, 6989-7000.
27. Lei, L.; Zou, P.-S.; Wang, Z.-X.; Liang, C.; Hou, C.; Mo, D.-L., Palladacycle-Catalyzed Regioselective Heck Reaction Using Diaryliodonium Triflates and Aryl Iodides. *Org. Lett.* **2022**, *24*, 663-667.
28. Negishi, E.; King, A. O.; Okukado, N., Selective carbon-carbon bond formation via transition metal catalysis. 3. A highly selective synthesis of unsymmetrical biaryls and diarylmethanes by the nickel- or palladium-catalyzed reaction of aryl- and benzylzinc derivatives with aryl halides. *J. Org. Chem.* **1977**, *42*, 1821-1823.
29. Dai, C.; Fu, G. C., The First General Method for Palladium-Catalyzed Negishi Cross-Coupling of Aryl and Vinyl Chlorides: Use of Commercially Available Pd(P(t-Bu)₃)₂ as a Catalyst. *J. Am. Chem. Soc.* **2001**, *123*, 2719-2724.

30. Han, C.; Buchwald, S. L., Negishi Coupling of Secondary Alkylzinc Halides with Aryl Bromides and Chlorides. *J. Am. Chem. Soc.* **2009**, *131*, 7532-7533.
31. Organ, M. G.; Avola, S.; Dubovyk, I.; Hadei, N.; Kantchev, E. A. B.; O'Brien, C. J.; Valente, C., A User-Friendly, All-Purpose Pd–NHC (NHC=N-Heterocyclic Carbene) Precatalyst for the Negishi Reaction: A Step Towards a Universal Cross-Coupling Catalyst. *Chem. Eur. J.* **2006**, *12*, 4749-4755.
32. Handa, S.; Wang, Y.; Gallou, F.; Lipshutz, B. H., Sustainable Fe–ppm Pd nanoparticle catalysis of Suzuki–Miyaura cross-couplings in water. *Science* **2015**, *349*, 1087-1091.
33. Lipshutz, B. H.; Ghorai, S.; Abela, A. R.; Moser, R.; Nishikata, T.; Duplais, C.; Krasovskiy, A.; Gaston, R. D.; Gadwood, R. C., TPGS-750-M: A Second-Generation Amphiphile for Metal-Catalyzed Cross-Couplings in Water at Room Temperature. *J. Org. Chem.* **2011**, *76*, 4379-4391.
34. Handa, S.; Jin, B.; Bora, P. P.; Wang, Y.; Zhang, X.; Gallou, F.; Reilly, J.; Lipshutz, B. H., Sonogashira Couplings Catalyzed by Fe Nanoparticles Containing ppm Levels of Reusable Pd, under Mild Aqueous Micellar Conditions. *ACS Catal.* **2019**, *9*, 2423-2431.
35. Pang, H.; Hu, Y.; Yu, J.; Gallou, F.; Lipshutz, B. H., Water-Sculpting of a Heterogeneous Nanoparticle Precatalyst for Mizoroki–Heck Couplings under Aqueous Micellar Catalysis Conditions. *J. Am. Chem. Soc.* **2021**, *143*, 3373-3382.
36. Hu, Y.; Wong, M. J.; Lipshutz, B. H., ppm Pd-Containing Nanoparticles as Catalysts for Negishi Couplings ... in Water. *Angew. Chem., Int. Ed.* **2022**, *61*, e202209784.
37. Kutchukian, P. S.; Dropinski, J. F.; Dykstra, K. D.; Li, B.; DiRocco, D. A.; Streckfuss, E. C.; Campeau, L.-C.; Cernak, T.; Vachal, P.; Davies, I. W.; Krska, S. W.; Dreher, S. D., Chemistry informer libraries: a chemoinformatics enabled approach to evaluate and advance synthetic methods. *Chem. Sci.* **2016**, *7*, 2604-2613.

38. Knapp, D. M.; Gillis, E. P.; Burke, M. D., A General Solution for Unstable Boronic Acids: Slow-Release Cross-Coupling from Air-Stable MIDA Boronates. *J. Am. Chem. Soc.* **2009**, *131*, 6961-6963.
39. Netherton, M. R.; Fu, G. C., Air-Stable Trialkylphosphonium Salts: Simple, Practical, and Versatile Replacements for Air-Sensitive Trialkylphosphines. Applications in Stoichiometric and Catalytic Processes. *Org. Lett.* **2001**, *3*, 4295-4298.
40. Xu, G.; Gao, P.; Colacot, T. J., Tunable Unsymmetrical Ferrocene Ligands Bearing a Bulky Di-1-adamantylphosphino Motif for Many Kinds of Csp²-Csp³ Couplings. *ACS Catal.* **2022**, *12*, 5123-5135.
41. MPhos Ligands & Catalysts – Introduction, Advantages, and Applications [MPhos Ligands & Catalysts – Introduction, Advantages, and Applications \(sigmaaldrich.com\)](#). (Accessed Nov. 27, 2023)
42. Sheldon, R. A., The E factor 25 years on: the rise of green chemistry and sustainability. *Green Chem.* **2017**, *19*, 18-43.
43. Sheldon, R. A.; Bode, M. L.; Akakios, S. G., Metrics of green chemistry: Waste minimization. *Curr. Opin. Green. Sustain. Chem.* **2022**, *33*, 100569.
44. Gröger, H.; Gallou, F.; Lipshutz, B. H., Where Chemocatalysis Meets Biocatalysis: In Water. *Chem. Rev.* **2023**, *123*, 5262-5296.
45. Lipshutz, B. H., Nanomicelle-enabled chemoenzymatic catalysis: Clean chemistry in “dirty” water. *Chem Catal.* **2023**, *3*, 100458.
46. Lee, N. R.; Bikovtseva, A. A.; Cortes-Clerget, M.; Gallou, F.; Lipshutz, B. H., Carbonyl Iron Powder: A Reagent for Nitro Group Reductions under Aqueous Micellar Catalysis Conditions. *Org. Lett.* **2017**, *19*, 6518-6521.

47. Lee, N. R.; Gallou, F.; Lipshutz, B. H., SNAr Reactions in Aqueous Nanomicelles: From Milligrams to Grams with No Dipolar Aprotic Solvents Needed. *Org. Process Res. Dev.* **2017**, *21*, 218-221.

2.3 Appendix

General Information

All commercial reagents were used without further purification unless otherwise noted. The THF used for the preparation of NPs was distilled using a sodium benzophenone ketyl system. All other solvents were used as received, such as MeOH, EtOAc, hexanes, and Et₂O, unless otherwise noted, and purchased from Fisher Scientific. FeCl₃ (anhydrous, 98%) was purchased from Alfa Aesar (Lot number: D06Q37) and stored in an argon purged glove box. Methylmagnesium chloride was purchased from Sigma-Aldrich (product number: 189901) and was titrated precisely. Ligands were either purchased from Sigma-Aldrich, Combi-Block or received from Johnson Matthey. Palladium acetate was received from Johnson Matthey. Pd(*t*Bu₃P)₂ was purchased from Sigma-Aldrich. All palladium catalysts and ligands were stored in an argon purged glove box. K₃PO₄·H₂O was purchased from Sigma-Aldrich (≥95%, product number: 04249). DIPEA was purchased from Sigma-Aldrich (ReagentPlus®, ≥99%, product number: D125806). K₃PO₄ was purchased from Fisher Chemical (FCC, 97%, catalog number: 18-605-684). NaCl was purchased from Fisher Chemical (Crystalline/Certified ACS, catalog number: S271-500). Zinc powder was purchased from Alfa Aesar (~100 mesh, 99.9%, Lot number: Z21B027) and stored in an argon purged glove box. TMEDA was purchased from Sigma-Aldrich (≥99.5%, purified by redistillation, product number: 411019). A solution of 2 wt % TPGS-750-M/H₂O solution was prepared by dissolving TPGS-750-M in degassed HPLC grade water and was stored in Schlenk flask under argon. TPGS-750-M was made as previously described¹ and is available from Sigma-Aldrich (catalog number 733857). A standard 2 wt % aqueous solution of

TPGS-750-M was typically prepared on a 100 g scale by dissolving 2 g of the TPGS-750-M wax into 98 g of thoroughly degassed (steady stream of argon, minimum of 12 h bubbling time with stirring and heating). HPLC grade water in a Schlenk flask equipped with a stir bar and allowed to dissolve overnight with vigorous stirring under argon pressure (NOTE: Do not attempt to degas the aqueous phase with surfactant present; vigorous foaming will occur). The 2 wt % TPGS-750-M/H₂O solution, once prepared, was kept in a Schlenk flask. Thin layer chromatography (TLC) was done using Silica Gel 60 F254 plates (0.25 mm thick) purchased from Merck. Column chromatography was done in glass columns using Silica gel 60 (EMD, 40-63 μm) or with pre-packed 25-gram KP-Sil Biotage[®] SNAP Cartridges on the Biotage[®] Isolera One autocolumn. GC-MS data was recorded on an Agilent Technologies 7890A GC system coupled with Agilent Technologies 5975C mass spectrometer using HP-5MS column (30 m × 0.250 mm, 0.25 μ) purchased from Agilent Technologies. ¹H, ¹³C, and ¹⁹F NMR spectra were recorded at 25 °C on an Agilent Technologies 400 MHz, a Varian Unity Inova 500 MHz, Varian Unity Inova 600 MHz, Bruker Avance III HD 400 MHz or Bruker Avance NEO 500 MHz spectrometer in CDCl₃ with residual CHCl₃ (¹H = 7.26 ppm, ¹³C = 77.16 ppm) or in DMSO-d₆ with residual (CH₃)₂SO (¹H = 2.50 ppm, ¹³C = 39.52 ppm) as internal standards. Chemical shifts are reported in parts per million (ppm). NMR Data are reported as follows: chemical shift, multiplicity (s = singlet, d = doublet, dd = doublet of doublets, ddd = doublet of doublet of doublets, t = triplet, td = triplet of doublets, q = quartet, quin = quintet, m = multiplet), coupling constant (if applicable), and integration. Chemical shifts in ¹³C NMR spectra are reported in ppm on the δ scale from the central peak of residual CDCl₃ (77.16 ppm) or the central peak of DMSO-d₆ (39.52 ppm). High-resolution mass analyses (HRMS) were recorded on Waters GCT Premier GC TOF or

Agilent 6230 TOF LC/MS System. STEM images were obtained using ThermoFisher Talos G2 200X TEM/STEM w/ChemiSTEM EDS.

Procedures to synthesize different NPs

General procedure for NPs used in procedure A:

In an oven-dried 25 mL microwave reaction vial purged with argon, covered with a rubber septum containing a PTFE-coated magnetic stir bar, 250 mg FeCl₃ (1.54 mmol), 632 mg SPhos (1.54 mmol) and 4 mL dry THF were added under a stream of dry argon. The mixture was stirred for 15 min. While maintaining a dry atmosphere at rt, 3.1 mL of 1 M solution of MeMgCl in THF was very slowly (1 drop/2 sec) added to the reaction mixture. After complete addition of the Grignard reagent, the mixture was stirred for an additional 15 min at rt. THF were removed by rotary evaporator, and the solid-state Fe/SPhos NPs were transferred and stored in a glove box.

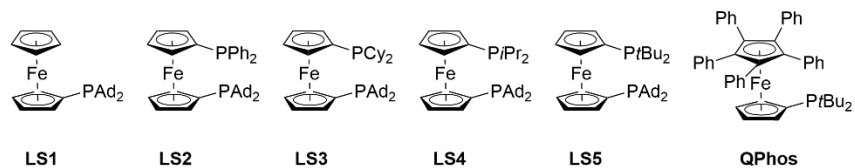
General procedure for NPs used in procedure B:

In an oven-dried 25 mL microwave reaction vial purged with argon, covered with a rubber septum containing a PTFE-coated magnetic stir bar, 250 mg FeCl₃ (1.54 mmol) and 3 mg Pd(OAc)₂ (0.0133 mmol) were added, 4 mL dry THF were added under a stream of dry argon. The mixture was stirred for 15 min. While maintaining a dry atmosphere at rt, 3.1 mL of 1 M solution of MeMgCl in THF was very slowly (1 drop/2 sec) added to the reaction mixture. After complete addition of the Grignard reagent, the mixture was stirred for an additional 15 min at rt. THF were removed by rotary evaporator, and the solid-state Fe/ppm Pd NPs were transferred and stored in glove box.

General procedure for NPs used in procedure C:

In an oven-dried 25 mL microwave reaction vial purged with argon, covered with a rubber septum containing a PTFE-coated magnetic stir bar, 250 mg FeCl_3 (1.54 mmol) and 4 mL dry THF were added under a stream of dry argon. The mixture was stirred for 15 min. While maintaining a dry atmosphere at rt, 3.1 mL of 1 M solution of MeMgCl in THF was very slowly (1 drop/2 sec) added to the reaction mixture. After complete addition of the Grignard reagent, the mixture was stirred for an additional 15 min at rt. THF were removed by rotary evaporator, and the solid-state Fe NPs were transferred and stored in glove box.

Optimization on ferrocene-based ligands on four different reactions



reaction type	product	Conversion with LS1 ^a	Conversion with LS2 ^a	Conversion with LS3 ^a	Conversion with LS4 ^a	Conversion with LS5 ^a	Conversion with QPhos ^a
Suzuki-Miyaura ^a		>95	<5	10	15	<5	86
Sonogashira ^b		<5	<5	<5	<5	<5	40
Mizoroki-Heck ^c		>95	>95	>95	>95	>95	80
		72	82	80	92	>95	-
Negishi ^d		<5	<5	<5	<5	<5	<5

^a Aryl bromide (0.2 mmol), Ar'-BR₂ (0.3 mmol), Fe NPs (8 mg, 5 % Fe NPs), Pd(OAc)₂ (500 ppm) in pot, ligand (5 mol %), K₃PO₄·H₂O (0.3 mmol), 2 wt % TPGS-750-M/H₂O (0.4 mL), 45 °C, 24 h;

^b Aryl bromide (0.2 mmol), alkyne (0.3 mmol), Fe NPs (8 mg, 5 % Fe NPs), Pd(OAc)₂ (500 ppm) in pot, ligand (5 mol %), DIPEA (0.4 mmol), 2 wt % TPGS-750-M/H₂O (0.4 mL), 45 °C, 24 h;

^c Aryl iodide (0.2 mmol), alkene (0.4 mmol), Fe NPs (2.8 mg, 5 % Fe NPs), 2500 ppm Pd(*t*Bu₃P)₂ in pot, ligand (2.5 mol %), K₃PO₄ (0.6 mmol), NaCl (1.2 mmol), 2 wt % TPGS-750-M/H₂O (0.4 mL), DMF (0.04 mL), 45 °C, 40 h;

^d Aryl bromide (0.2 mmol), alkyl bromide (0.6 mmol), Fe NPs (8 mg, 5 % Fe NPs), 2500 ppm Pd(OAc)₂ in pot, ligand (5 mol %), Zn powder (0.8 mmol), TMEDA (1.0 mmol), 2 wt % TPGS-750-M/H₂O (0.4 mL), 45 °C, 40 h;

^e Conversion based on ¹H NMR, 1,3,5-trimethoxy benzene as internal standard

Titration of MeMgCl in THF with LiCl/I₂

To an oven-dried 25 mL round bottom flask, anhydrous LiCl (424 mg, 10 mmol) was added under an argon atmosphere in the glovebox. The flask was sealed with a rubber septum, and 20 mL dry THF was added by syringe and the mixture was stirred at rt until the LiCl was completely dissolved, resulting in the formation of a 0.5 M solution of LiCl in THF.

A 10 mL microwave vial equipped with a magnetic stirring bar and a septum was heated with a heat gun under reduced pressure and cooled to rt under an argon atmosphere. In the glovebox, the dry microwave vial was charged with accurately weighed I₂ (127 mg, 0.5 mmol) and capped with a rubber septum. The saturated solution of LiCl in THF (2 mL) was added and stirring was started. After the iodine was completely dissolved, the resulting brown solution was cooled to 0 °C in an ice bath. Another 5 mL round bottom flask equipped with a magnetic stirring bar and a septum was heated with a heat gun under reduced pressure and cooled to rt under an argon atmosphere. To this round bottom flask, methyl magnesium chloride solution (from Sigma-Aldrich, catalog No. 189901; 3 mL) and dry THF (6 mL) were added by syringe and then stirred. To the vial with I₂, the methyl

magnesium chloride solution was added dropwise via a 1.00 mL syringe (0.01 mL graduation) until the brown color disappeared. The amount consumed contains 1 equiv of the methyl magnesium chloride relative to iodine. The MeMgCl solution was titrated five times.

General procedure for Suzuki-Miyaura coupling reactions

To a flame dried 1-dram vial equipped with an oven dried stir bar was added aryl bromide (0.2 mmol, 1 equiv), organoboron compound (0.3 mmol, 1.5 equiv) and $\text{K}_3\text{PO}_4 \cdot \text{H}_2\text{O}$ (69.2 mg, 0.3 mmol, 1.5 equiv). The vial was then transferred inside of a glove box. Fe NPs (8.0 mg, 5 mol % FeCl_3) and SPhos (4.1 mg, 5 mol %, or another ligand) was added into the vial in the glovebox. The vial was then sealed with a rubber septum inside of the glovebox. 500 ppm of $\text{Pd}(\text{OAc})_2$ was added as a stock solution in THF, followed by the addition of 0.4 mL 2 wt % TPGS-750-M/ H_2O solution by syringe and the mixture was stirred vigorously at 45 °C for 16 h (unless otherwise noted). Then EtOAc was added, and the mixture stirred gently for 2 min at rt. Stirring was then stopped and the organic layer was decanted via pipette after centrifugation. The same extraction procedure was repeated twice. The combined organic extracts were dried under reduced pressure and purified by flash chromatography over silica gel.

General procedure for Sonogashira coupling reactions

To a flame dried 1-dram vial equipped with an oven-dried stir bar was added aryl halide (0.2 mmol, 1 equiv). The vial was then transferred inside of a glove box. Fe NPs (8.0 mg, 5

mol % FeCl_3) and XPhos (2.8 mg, 3 mol %, or another ligand) was added into the vial in the glovebox. The vial was then sealed with a rubber septum inside of the glovebox. 500 ppm of $\text{Pd}(\text{OAc})_2$ was added as a stock solution in THF, followed by the addition of alkyne (0.4 mmol, 2.0 equiv), DIPEA (0.07 mL, 0.4 mmol, 2.0 equiv) and 0.4 mL 2 wt % TPGS-750-M/ H_2O solution by syringe and the mixture was stirred vigorously at 45 °C for 16 h (unless otherwise noted). Then EtOAc was added, and the mixture stirred gently for 2 min at rt. Stirring was then stopped and the organic layer was decanted via pipette after centrifugation. The same extraction procedure was repeated twice. The combined organic extracts were dried under reduced pressure and purified by flash chromatography over silica gel.

General procedure for Mizoroki-Heck coupling reactions

To a flame-dried 1-dram vial equipped with an oven dried stir bar was added aryl iodide (0.2 mmol, 1 equiv), alkene (if it is solid), NaCl (70.2 mg, 1.2 mmol, 6 equiv) and K_3PO_4 (127.4 mg, 0.6 mmol, 3 equiv). The vial was then transferred inside of a glove box. Fe NPs (2.8 mg, 1.8 mol % FeCl_3) and *t*Bu₃P (1.5 mg, 2.5 mol %; or another ligand) was added into the vial in the glovebox. The vial was then sealed with a rubber septum inside of the glovebox. 2500 ppm of $\text{Pd}(\text{tBu}_3\text{P})_2$ was added as a stock solution in DCM. The DCM was removed by vacuum and the vial was refilled with argon. The vial was then added 0.4 mL 2 wt % TPGS-750-M/ H_2O solution, alkene (if it is liquid) and 0.04 mL DMF by syringe and the mixture was stirred vigorously at 45 °C for 40 h (unless otherwise noted). Then EtOAc was added, and the mixture stirred gently for 2 min at rt. Stirring was then stopped and the organic layer was decanted via pipette after centrifugation. The same extraction procedure

was repeated twice. The combined organic extracts were dried under reduced pressure and purified by flash chromatography over silica gel.

General procedure for Negishi coupling reactions

To a flame-dried 1-dram vial equipped with an oven-dried stir bar was added aryl bromide (0.2 mmol, 1 equiv). The vial was then transferred inside of a glove box. Fe NPs (8.0 mg, 5 mol % FeCl_3), AmPhos (2.7 mg, 5 mol %; or another ligand) and zinc powder (52 mg, 0.8 mmol, 4 equiv) was added into the vial in the glovebox. The vial was then sealed with a rubber septum inside of the glovebox. 2500 ppm of $\text{Pd}(\text{OAc})_2$ was added as a stock solution in THF, followed by the addition of alkyl bromide (0.8 mmol, 4 equiv), TMEDA (0.15 mL, 1.0 mmol, 5 equiv) and 1.0 mL 2 wt % TPGS-750-M/ H_2O solution by syringe and the mixture was stirred vigorously at 45 °C for 40 h (unless otherwise noted). Then EtOAc was added, and the mixture stirred gently for 2 min at rt. Stirring was then stopped and the organic layer was decanted via pipette after centrifugation. The same extraction procedure was repeated twice. The combined organic extracts were dried under reduced pressure and purified by flash chromatography over silica gel.

STEM-EDS images for new Fe NPs with SPhos in 2 wt % TPGS-750-M/ H_2O solution

The Fe NPs (4 mg) and SPhos (4.1 mg, 0.01 mmol) was added to a vial in the glove box, and the vial was covered with a septum. 500 ppm $\text{Pd}(\text{OAc})_2$ (0.0225 mg, 0.0001 mmol) were added by stock solution in THF. 2 wt % TPGS-750-M/ H_2O (2 mL) was inserted into the vial via syringe and the mixture was stirred for 15 min.

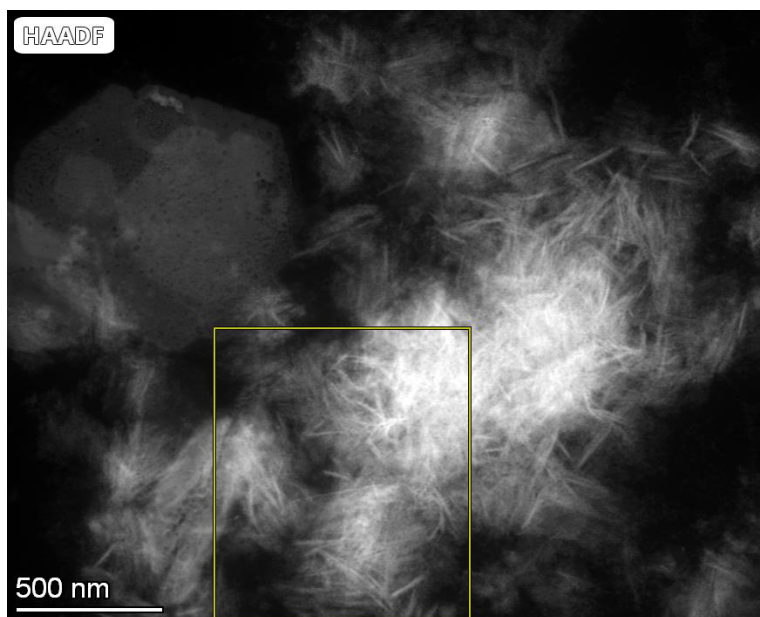


Figure S1. HAADF image showing new Fe NPs with SPhos in 2 wt % TPGS-750-M/H₂O in a 500 nm scale.

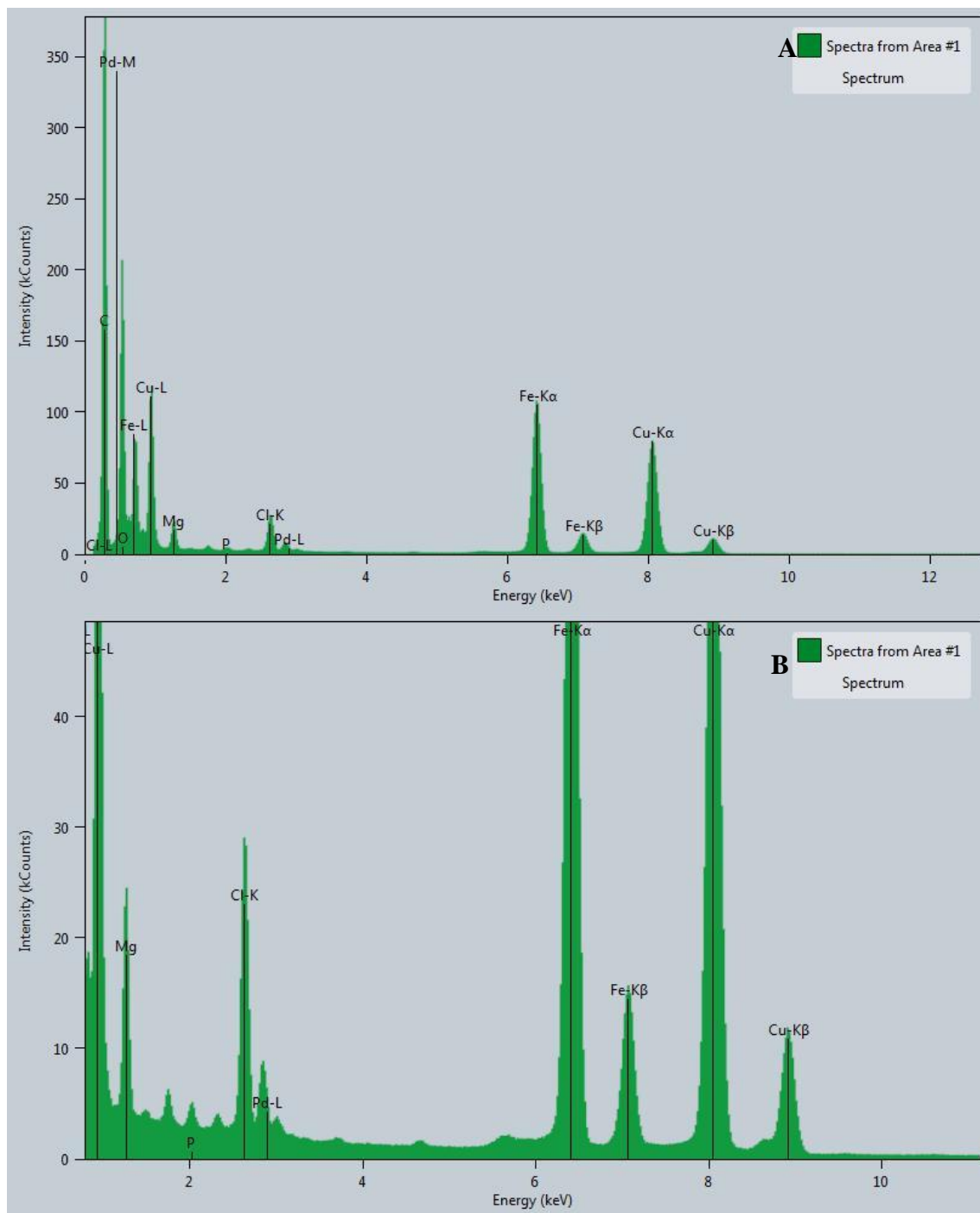


Figure S2. EDS analysis showing new Fe NPs with SPhos in 2 wt % TPGS-750-M/H₂O.

STEM-EDS images for original NPs with SPhos in 2 wt % TPGS-750-M/H₂O solution

The Fe/ppm Pd NPs were synthesized as reported.² The Fe/ppm Pd NPs (4 mg) was added to a vial in the glove box, and the vial was covered with a septum. 2 wt % TPGS-750-M/H₂O (2 mL) was inserted into the vial via syringe and the mixture was stirred for 15 min.

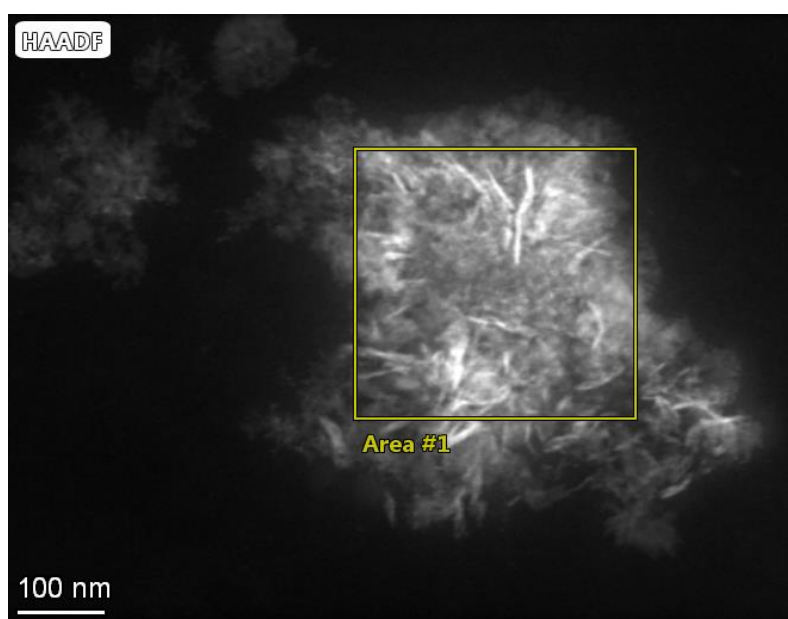


Figure S3. HAADF image showing original Fe/ppm Pd NPs with SPhos in 2 wt % TPGS-750-M/H₂O in a 100 nm scale.

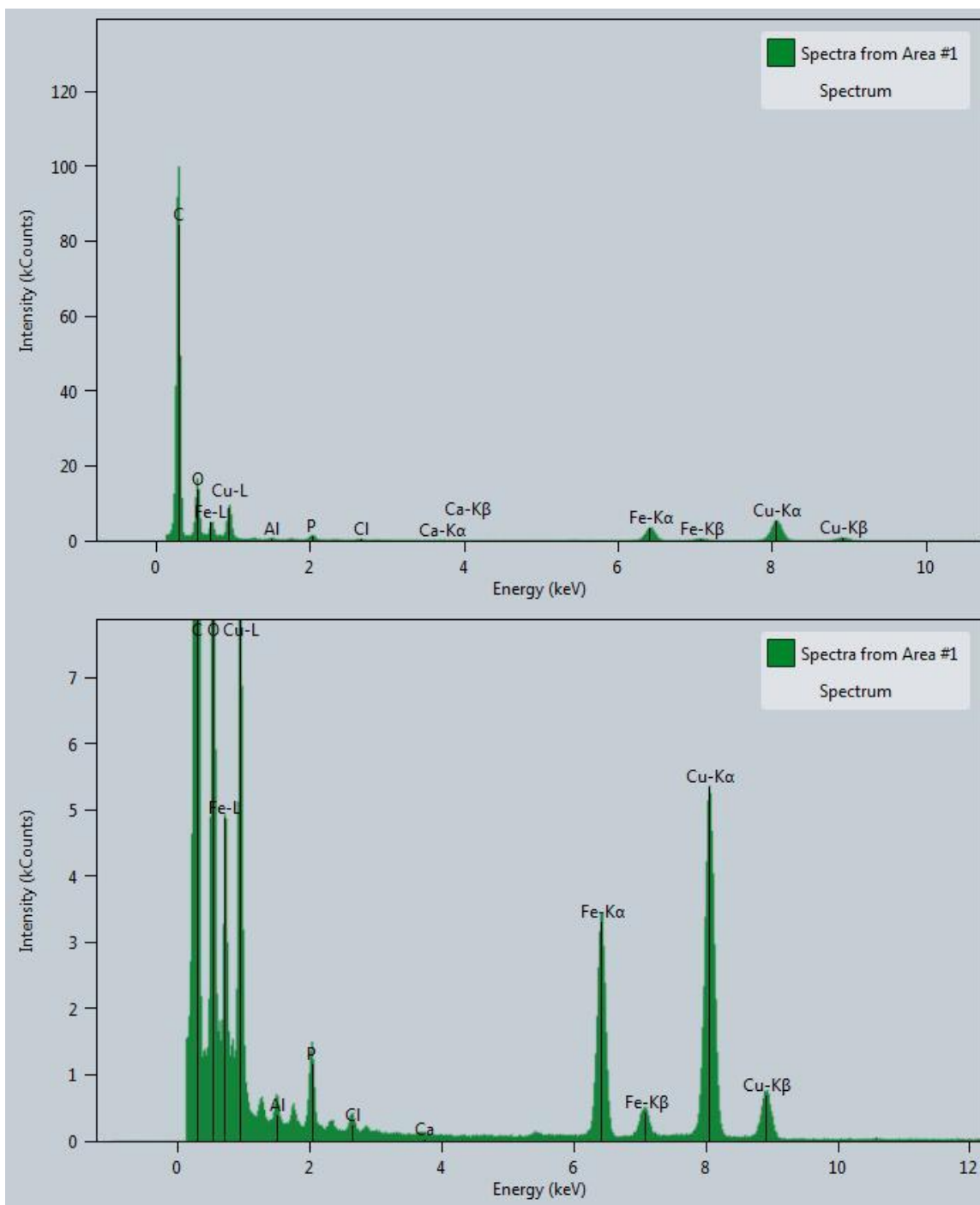
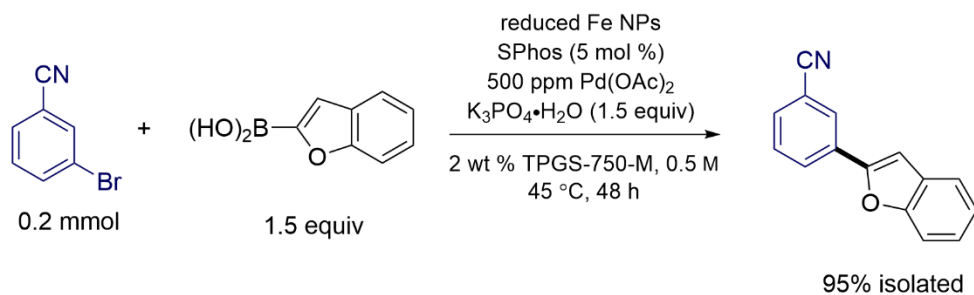


Figure S4. EDS analysis showing original Fe/ppm Pd NPs with SPhos in 2 wt % TPGS-750-M/H₂O.

E Factor evaluation



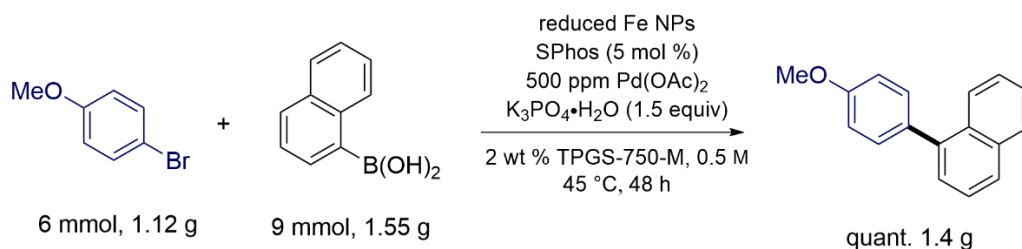
To a flame-dried 1-dram vial equipped with an oven-dried stir bar was added 3-bromobenzonitrile (36.4 mg, 0.2 mmol, 1 equiv), benzofuran-2-ylboronic acid (48.6 mg, 0.3 mmol, 1.5 equiv) and K₃PO₄·H₂O (69.2 mg, 0.3 mmol, 1.5 equiv). The vial was then transferred inside of a glove box. Fe NPs (8.0 mg, 5 mol % FeCl₃) and SPhos (4.1 mg, 5 mol %) was added into the vial in the glovebox. The vial was then sealed with a rubber septum inside of the glovebox. 500 ppm of Pd(OAc)₂ was added as a stock solution in THF, followed by the addition of 0.4 mL 2 wt % TPGS-750-M/H₂O solution by syringe and the mixture was stirred vigorously at 45 °C for 48 h. Stirring was then stopped and the liquid was decanted carefully via pipette after centrifugation. The solid were dried under reduced pressure and purified by flash chromatography over silica gel to get 3-(benzofuran-2-yl)benzonitrile (41.7 mg, 95 %) as a white solid.

E Factor calculation:

$$\begin{aligned}
 \text{E Factor (without water)} &= \frac{\text{mass of organic waste}}{\text{mass of product}} \\
 &= \frac{\text{mass of excess boronic acid}}{\text{mass of product}} \\
 &= \frac{16.2 \text{ mg}}{41.7 \text{ mg}} \\
 &= 0.39
 \end{aligned}$$

$$\begin{aligned}
 \text{E Factor (with water)} &= \frac{\text{mass of organic waste} + \text{mass of water}}{\text{mass of product}} \\
 &= \frac{\text{mass of excess boronic acid} + \text{mass of water}}{\text{mass of product}} \\
 &= \frac{16.2 \text{ mg} + 400 \text{ mg}}{41.7 \text{ mg}} \\
 &= 9.98
 \end{aligned}$$

Gram Scale Reaction

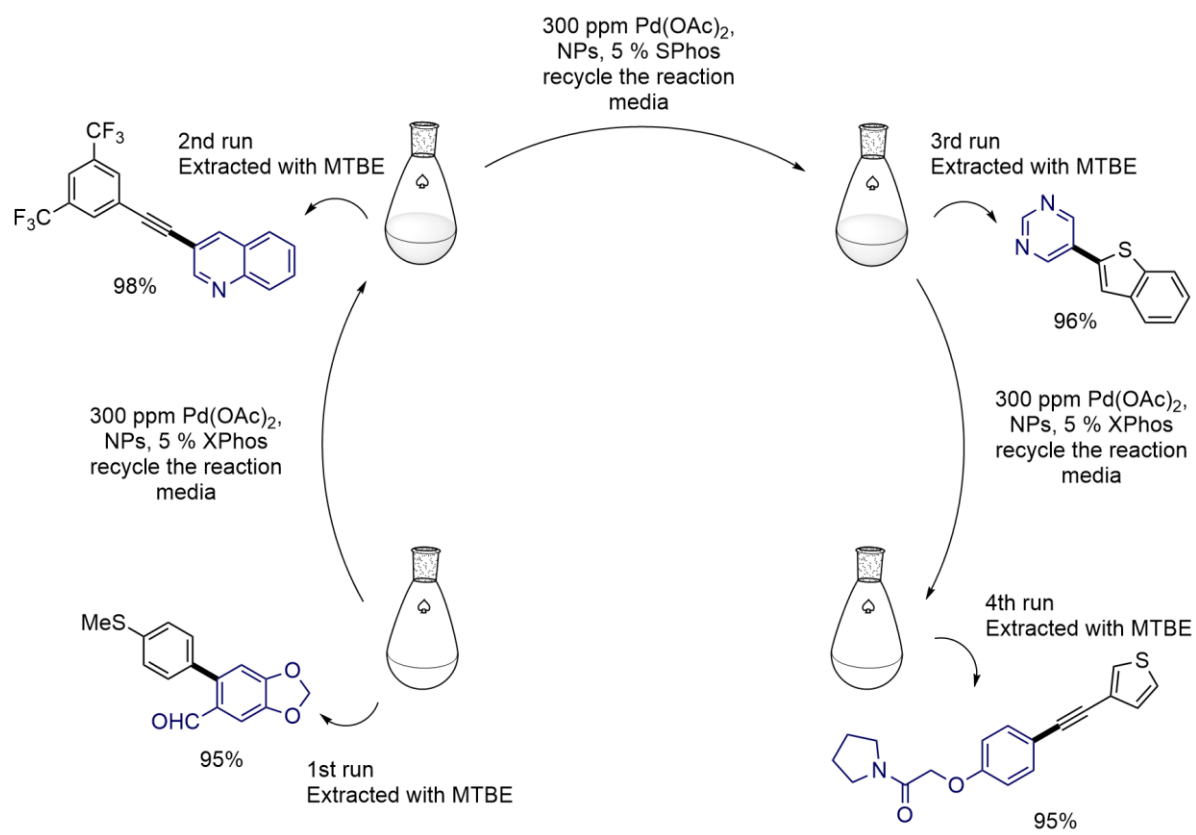


To an oven-dried 50 mL round bottom flask with an oven-dried stir bar was added naphthalen-1-ylboronic acid (1.55 g, 9 mmol, 1.5 equiv), $\text{K}_3\text{PO}_4 \cdot \text{H}_2\text{O}$ (2.08 g, 9 mmol, 1.5 equiv). The flask was then transferred inside of a glove box. Fe NPs (240 mg, 5 mol % FeCl_3) and SPhos (123 mg, 5 mol %) was added into the vial in the glovebox. The vial was then sealed with a rubber septum inside of the glovebox. 500 ppm of Pd(OAc)_2 was added as

a stock solution in THF, followed by the addition of 12 mL 2 wt % TPGS-750-M/H₂O solution by syringe and the mixture was stirred vigorously at 45 °C for 48 h. Then EtOAc was added, and the mixture stirred gently for 2 min at rt. Stirring was then stopped and the mixture were transferred into separatory funnel. The organic layer was collected. The same extraction procedure was repeated twice. The combined organic extracts were dried under reduced pressure and purified by flash chromatography over silica gel to get 1-(4-methoxyphenyl)naphthalene (1.4 g, quant) as a white solid.

Recycling reactions

Scheme S1, Recycling reactions of Suzuki-Miyuara coupling and Sonogashira couplings



1st run:

To a flame-dried 1-dram vial equipped with an oven-dried stir bar was added 6-bromobenzo[*d*][1,3]dioxole-5-carbaldehyde (0.2 mmol, 45.8 mg, 1 equiv), (4-(methylthio)phenyl)boronic acid (0.3 mmol, 50.4 mg, 1.5 equiv) and K₃PO₄·H₂O (69.2 mg, 0.3 mmol, 1.5 equiv). The vial was then transferred inside of a glove box. Fe NPs (8.0 mg, 5 mol % FeCl₃) and SPhos (4.1 mg, 5 mol %) was added into the vial in the glovebox. The vial was then sealed with a rubber septum inside of the glovebox. 500 ppm of Pd(OAc)₂ was added as a stock solution in THF, followed by the addition of 0.4 mL 2 wt % TPGS-750-M/H₂O solution by syringe and the mixture was stirred vigorously at 45 °C for 16 h. Then, 0.4 mL MTBE was added, and the mixture stirred gently for 2 min at rt. Stirring was then stopped and the organic layer was decanted via pipette after centrifugation. The same extraction procedure was repeated twice. The combined organic extracts were dried under reduced pressure and purified by flash chromatography over silica gel with Hex/EtOAc: 95/5 to obtain 6-(4-(methylthio)phenyl)benzo[*d*][1,3]dioxole-5-carbaldehyde. (51.7 mg, 95%).

2nd run:

To the same vial, Fe NPs (8 mg, 5 mol % FeCl₃), XPhos (2.8 mg, 3 mol %) were added under argon. The vial was then sealed with a rubber septum under an argon flow. Then, 3-bromoquinoline (27 μL, 0.2 mmol, 1 equiv), 1-ethynyl-3,5-bis(trifluoromethyl)benzene (0.07 mL, 0.4 mmol, 2 equiv), and DIPEA (0.07 mL, 0.4 mmol, 2 equiv) were added to the vial via syringe. 300 ppm of Pd(OAc)₂ was added as a stock solution in THF. The vial was then stirred vigorously at 45 °C for 16 h. Then, 0.4 mL MTBE was added, and the mixture

stirred gently for 2 min at rt. Stirring was then stopped and the organic layer was decanted via pipette after centrifugation. The same extraction procedure was repeated twice. The combined organic extracts were dried under reduced pressure and purified by flash chromatography over silica gel with hexanes/EtOAc : 95/5 to obtain 3-((3,5-bis(trifluoromethyl)phenyl)ethynyl)quinoline. (71.4 mg, 98%).

3rd run:

To the same vial, Fe NPs (8 mg, 5 mol % FeCl₃), SPhos (4.1 mg, 5 mol %), 5-bromopyrimidine (31.8 mg, 0.2 mmol, 1 equiv), benzo[*b*]thiophen-2-ylboronic acid (53.4 mg, 0.3 mmol, 1.5 equiv) and K₃PO₄·H₂O (69.2 mg, 0.3 mmol, 1.5 equiv) were added under argon. The vial was then sealed with a rubber septum under an argon flow. Then 300 ppm of Pd(OAc)₂ was added as a stock solution in THF. The vial was then stirred vigorously at 45 °C for 16 h. Then, 0.4 mL MTBE was added, and the mixture stirred gently for 2 min at rt. Stirring was then stopped and the organic layer was decanted via pipette after centrifugation. The same extraction procedure was repeated twice. The combined organic extracts were dried under reduced pressure and purified by flash chromatography over silica gel with hexanes/EtOAc:70/30 to 5-(benzo[*b*]thiophen-2-yl)pyrimidine. (40.3 mg, 95%).

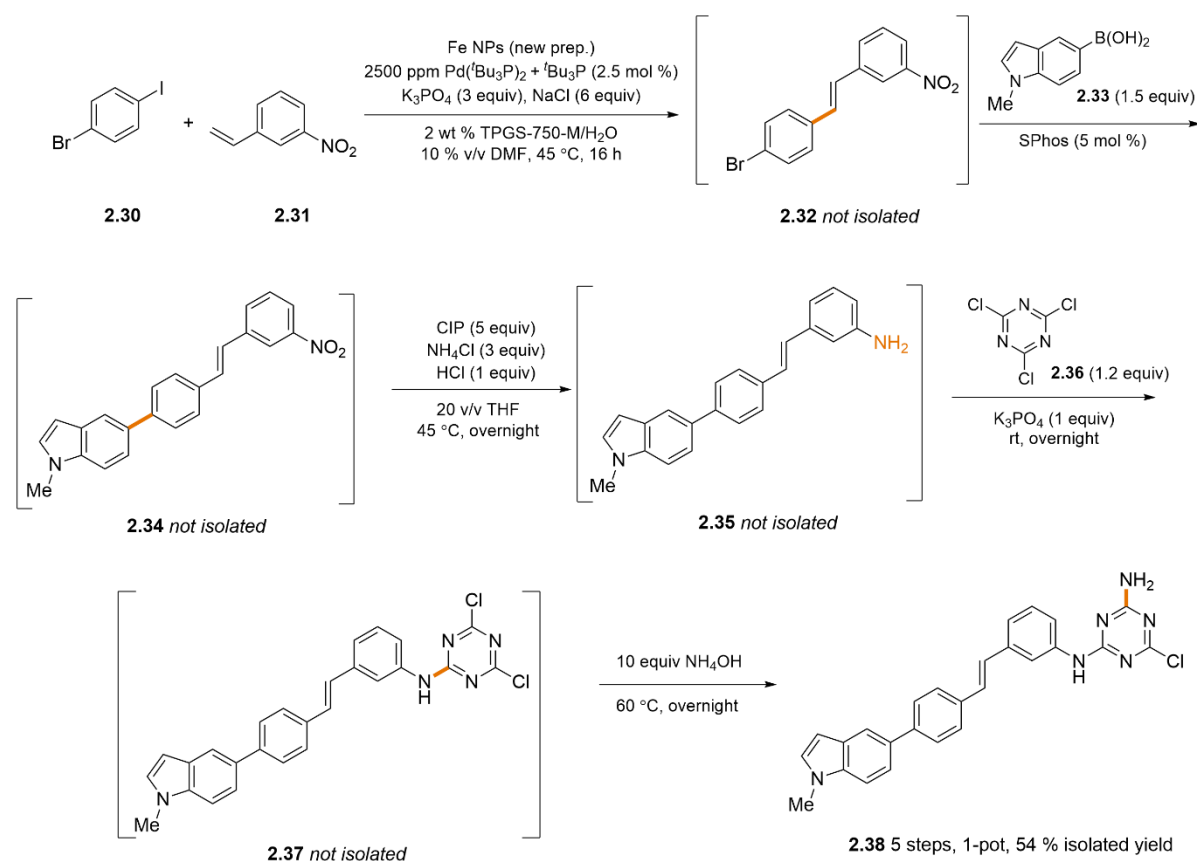
4th run:

To the same vial, Fe NPs (8 mg, 5 mol % FeCl₃), XPhos (2.8 mg, 3 mol %) and 2-(4-iodophenoxy)-1-(pyrrolidin-1-yl)ethan-1-one (66.2 mg, 0.2 mmol, 1 equiv) were added under argon. The vial was then sealed with a rubber septum under an argon flow. Then 3-ethynylthiophene (39 μL, 0.4 mmol, 2 equiv) and DIPEA (0.07 mL, 0.4 mmol, 2 equiv) were added to the vial via syringe. 300 ppm of Pd(OAc)₂ was added as a stock solution in

THF followed by 0.15 mL 2 wt % TPGS-750-M aqueous solution to maintain the solvent volume. The vial was then stirred vigorously at 45 °C for 16 h. Then, 0.4 mL MTBE was added, and the mixture stirred gently for 2 min at rt. Stirring was then stopped and the organic layer was decanted via pipette after centrifugation. The same extraction procedure was repeated twice. The combined organic extracts were dried under reduced pressure and purified by flash chromatography over silica gel with hexanes/EtOAc:75/25 to obtain 1-(pyrrolidin-1-yl)-2-(4-(thiophen-3-ylethynyl)phenoxy)ethan-1-one. (59.6 mg, 96%).

One-pot sequence of reactions

Scheme S2. One-Pot Reaction Sequence



Step 1: To a flame dried 1-dram vial equipped with an oven dried stir bar was added 1-bromo-4-iodobenzene (141.5 mg, 0.5 mmol), K_3PO_4 (318 mg, 1.5 mmol, 3 equiv), and NaCl (175.5 mg, 3.0 mmol, 6 equiv) and the vial was then transferred into a glove box to which was added $P(tBu)_3$ (2.5 mg, 0.0125 mmol, 2.5 mol %) inside of an argon-purged glove box. The vial was sealed with a rubber septum and removed from the glove box. Then, $Pd(tBu_3P)_2$ (0.64 mg, 0.00125 mmol, 2500 ppm) were added by stock solution in DCM. The DCM was removed by vacuum and the vial was refilled with argon. 1-Nitro-3-vinylbenzene (0.14 mL, 1.0 mmol, 2 equiv), DMF (0.1 mL) and 2 wt % TPGS-750-M/ H_2O (1.0 mL) was added to the vial via syringe and the vial were stirred vigorously under constant argon pressure at 45 °C for 16 h. The progress of the reaction was monitored by TLC.

Step 2: After complete consumption of starting material, the septum was removed. SPhos (10.3 mg, 0.025 mmol, 5 mol %) and (1-methyl-1H-indol-5-yl)boronic acid (131.3 mg, 0.75 mmol, 1.5 equiv) was added to the vial under argon flow. The vial was sealed with a rubber septum and stirred vigorously under constant argon pressure at 45 °C for overnight. The progress of the reaction was monitored by TLC.

Step 3: After complete consumption of starting material, the septum was removed. Carbonyl iron powder (CIP; 140 mg, 2.5 mmol, 5 equiv) and NH_4Cl (80.3 mg, 1.5 mmol, 3 equiv) were added to the vial under an argon flow. The vial was sealed with a rubber septum. 1 M HCl (0.5 mL, 0.5 mmol, 1 equiv) and THF (0.2 mL) were added via syringe and the contents of the vial were stirred vigorously under constant argon pressure at 45 °C for overnight. The progress of the reaction was monitored by TLC.

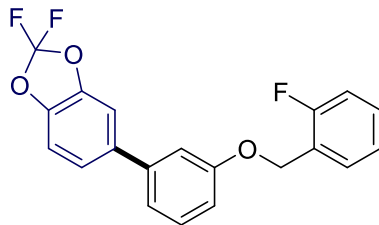
Step 4: After complete consumption of starting material, the septum was removed. 2,4,6-Trichloro-1,3,5-triazine (110 mg, 0.6 mmol, 1.2 equiv) and K_3PO_4 (106 mg, 0.5 mmol,

1 equiv) were added to the vial under an argon flow. The vial was sealed with a rubber septum and the contents stirred vigorously under constant argon pressure at rt overnight. The progress of the reaction was monitored by TLC.

Step 5: After complete consumption of starting material, the septum was removed. 28% NH₄OH aqueous solution (0.33 mL, 5 mmol, 10 equiv) was added via syringe and the contents of the vial were stirred vigorously under constant argon pressure at 60 °C for overnight. The reaction was then monitored by thin-layer chromatography until completion. Then, 2.0 mL EtOAc was added to the mixture after which it was stirred *gently* for 2 min at rt. Stirring was then stopped and the organic layer was decanted via a pipette after centrifugation. The same extraction procedure was repeated four times. The combined organic extracts were dried over anhydrous Na₂SO₄ and the solvent removed *in vacuo*, with the resulting crude material being purified by flash chromatography over silica gel with EtOAc/hexanes: 50/50 to afford (*E*)-6-chloro-*N*²-(3-(4-(1-methyl-1*H*-indol-5-yl)styryl)phenyl)-1,3,5-triazine-2,4-diamine (122.2 mg, 54% overall yield) as a red solid.

Analytical data

2,2-Difluoro-5-(3-((2-fluorobenzyl)oxy)phenyl)benzo[*d*][1,3]dioxole (2.1)



5-Bromo-2,2-difluorobenzo[*d*][1,3]dioxole (47.4 mg, 27 μL, 0.2 mmol), (3-((2-fluorobenzyl)oxy)phenyl)-boronic acid (121.8 mg, 0.3 mmol), Pd(OAc)₂ (0.0225 mg,

0.0001 mmol), SPhos (4.1 mg, 0.01 mmol), Fe NPs (8 mg, 5 mol % FeCl₃) and K₃PO₄·H₂O (69.2 mg, 0.3 mmol) in 0.4 mL 2 wt % TPGS-750-M/H₂O were reacted at 45 °C for 24 h yielding 68.1 mg (95%) of 2,2-difluoro-5-(3-((2-fluorobenzyl)oxy)phenyl)-benzo[d][1,3]dioxole as a yellow oil (hexanes/EtOAc: 90/10).

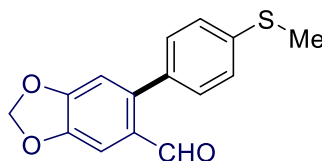
¹H NMR (400 MHz, chloroform-*d*) δ 7.35 – 7.28 (m, 4H), 7.25 (dd, *J* = 7.7, 2.1 Hz, 1H), 7.12 – 7.05 (m, 3H), 7.04 – 6.97 (m, 3H), 5.09 (s, 2H).

¹³C NMR (101 MHz, chloroform-*d*) δ 164.31, 161.86, 155.27, 143.66, 142.93, 139.64 (d, *J*_(C-F) = 8 Hz), 134.59, 131.07, 130.24 (d, *J*_(C-F) = 9 Hz), 130.11, 129.25, 124.99, 122.32 (d, *J*_(C-F) = 3 Hz), 121.81, 114.82 (d, *J*_(C-F) = 21.2 Hz), 113.88 (d, *J*_(C-F) = 22.2 Hz), 113.44, 111.15, 109.02, 69.92 (d, *J*_(C-F) = 2 Hz).

¹⁹F NMR (376 MHz, chloroform-*d*) δ -49.94, -112.70.

HRMS(EI): Calcd. for C₂₀H₁₃F₃O₃⁺: 358.0817 Found: 358.0816.

6-(4-(Methylthio)phenyl)benzo[d][1,3]dioxole-5-carbaldehyde (2.2)



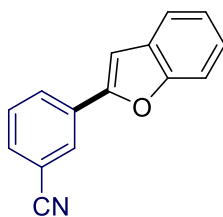
6-Bromobenzo[d][1,3]dioxole-5-carbaldehyde (45.8 mg, 0.2 mmol), (4-(methylthio)phenyl)boronic acid (50.4 mg, 0.3 mmol), Pd(OAc)₂ (0.0225 mg, 0.0001 mmol), SPhos (4.1 mg, 0.01 mmol), Fe NPs (8 mg, 5 mol % FeCl₃) and K₃PO₄·H₂O (69.2 mg, 0.3 mmol) in 0.4 mL 2 wt % TPGS-750-M/H₂O were reacted at 45 °C for 24 h yielding 50.8 mg (93%) of 6-(4-(methylthio)phenyl)benzo[d][1,3]dioxole-5-carbaldehyde as a white solid (hexanes/EtOAc : 90/10).

^1H NMR (400 MHz, chloroform-*d*) δ 9.75 (s, 1H), 7.45 (s, 1H), 7.31 (d, $J = 8.4$ Hz, 2H), 7.25 (d, $J = 8.4$ Hz, 2H), 6.81 (s, 1H), 6.08 (s, 2H), 2.53 (s, 3H).

^{13}C NMR (126 MHz, chloroform-*d*) δ 190.63, 152.25, 147.89, 143.12, 139.25, 134.17, 130.60, 128.93, 126.19, 110.24, 106.48, 102.23, 15.67.

Spectral data matched those previously reported.²

3-(Benzofuran-2-yl)benzonitrile (2.3)



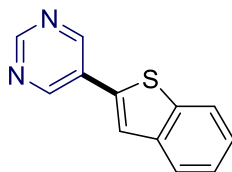
3-Bromobenzonitrile (36.4 mg, 0.2 mmol), benzofuran-2-MIDA boronate (81.9 mg, 0.3 mmol), Pd(OAc)₂ (0.0225 mg, 0.0001 mmol), SPhos (4.1 mg, 0.01 mmol), Fe NPs (8 mg, 5 mol % FeCl₃) and K₃PO₄·H₂O (69.2 mg, 0.3 mmol) in 0.4 mL 2 wt % TPGS-750-M/H₂O were reacted at 45 °C for 24 h yielding 42.0 mg (96%) of 3-(benzofuran-2-yl)benzonitrile as a white solid (hexanes/EtOAc : 95/5).

^1H NMR (400 MHz, chloroform-*d*) δ 7.98 (t, $J = 1.5$ Hz, 1H), 7.91 (dt, $J = 7.8, 1.5$ Hz, 1H), 7.83 (ddd, $J = 16.6, 6.8, 2.5$ Hz, 2H), 7.61 (m, 2H), 7.53 (t, $J = 7.8$ Hz, 1H), 7.42 – 7.34 (m, 2H).

^{13}C NMR (101 MHz, chloroform-*d*) δ 141.39, 140.44, 139.80, 135.77, 131.45, 130.67, 129.96, 129.89, 125.29, 125.06, 124.16, 122.53, 121.20, 118.60, 113.41.

Spectral data matched those previously reported.³

5-(Benzo[b]thiophen-2-yl)pyrimidine (2.4)



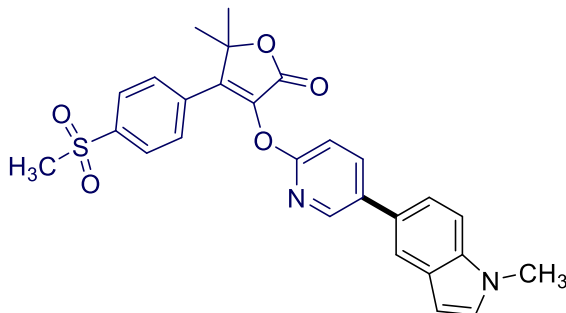
5-Bromopyrimidine (31.8 mg, 0.2 mmol), benzo[*b*]thiophen-2-ylboronic acid (53.4 mg, 0.3 mmol), Pd(OAc)₂ (0.0225 mg, 0.0001 mmol), SPhos (4.1 mg, 0.01 mmol), Fe NPs (8 mg, 5 mol % FeCl₃) and K₃PO₄·H₂O (69.2 mg, 0.3 mmol) in 0.4 mL 2 wt % TPGS-750-M/H₂O were reacted at 45 °C for 24 h yielding 42.6 mg (100%) of 5-(benzo[*b*]thiophen-2-yl)pyrimidine as a yellow solid (hexanes/EtOAc : 70/30).

¹H NMR (400 MHz, chloroform-*d*) δ 9.17 (s, 1H), 9.04 (s, 2H), 7.85 (ddd, *J* = 14.2, 6.6, 3.0 Hz, 2H), 7.65 (s, 1H), 7.44 – 7.35 (m, 2H).

¹³C NMR (126 MHz, chloroform-*d*) δ 157.92, 154.05, 140.21, 140.03, 136.20, 128.80, 125.60, 125.23, 124.27, 122.58, 122.05.

Spectral data matched those previously reported.⁴

5,5-Dimethyl-3-((5-(1-methyl-1H-indol-5-yl)pyridin-2-yl)oxy)-4-(4-(methylsulfonyl)phenyl)furan-2(5*H*)-one (2.5)



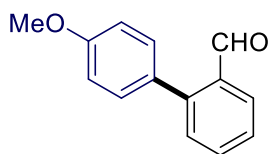
3-((5-Bromopyridin-2-yl)oxy)-5,5-dimethyl-4-(4-(methylsulfonyl)phenyl)furan-2(5H)-one (87.7 mg, 0.2 mmol), (1-methyl-1H-indol-5-yl)boronic acid (52.5 mg, 0.3 mmol), Pd(OAc)₂ (0.0338 mg, 0.00015 mmol), SPhos (4.1 mg, 0.01 mmol), Fe NPs (8 mg, 5 mol % FeCl₃) and K₃PO₄·H₂O (69.2 mg, 0.3 mmol) in 0.4 mL 2 wt % TPGS-750-M/H₂O were reacted at 55 °C for 48 h yielding 82.1 mg (84%) of 5,5-dimethyl-3-((5-(1-methyl-1H-indol-5-yl)pyridin-2-yl)oxy)-4-(4-(methylsulfonyl)phenyl)furan-2(5H)-one as a white solid (hexanes/EtOAc : 75/25).

¹H NMR (400 MHz, chloroform-*d*) δ 8.37 (d, *J* = 2.3 Hz, 1H), 8.01 (d, *J* = 8.5 Hz, 2H), 7.95 (dd, *J* = 8.5, 2.5 Hz, 1H), 7.80 (d, *J* = 8.5 Hz, 2H), 7.75 (s, 1H), 7.44 – 7.34 (m, 2H), 7.10 (d, *J* = 3.1 Hz, 1H), 7.06 (d, *J* = 8.5 Hz, 1H), 6.54 (d, *J* = 3.0 Hz, 1H), 3.83 (s, 3H), 3.06 (s, 3H), 1.79 (s, 6H).

¹³C NMR (101 MHz, chloroform-*d*) δ 165.97, 160.01, 148.24, 145.61, 141.31, 138.84, 138.07, 136.42, 135.08, 134.78, 129.84, 129.04, 129.02, 128.60, 127.92, 120.94, 119.36, 110.77, 109.83, 101.38, 84.36, 44.39, 32.98, 26.46.

HRMS(EI): Calcd. for C₂₇H₂₄N₂O₅SH⁺: 489.1484 Found: 489.1488.

4'-Methoxy-[1,1'-biphenyl]-2-carbaldehyde (2.6)



4-Bromoanisole (37.4 mg, 25 μL, 0.2 mmol), (2-formylphenyl)boronic acid (45.0 mg, 0.3 mmol), Pd(OAc)₂ (0.0225 mg, 0.0001 mmol), SPhos (4.1 mg, 0.01 mmol), Fe NPs (8 mg, 5 mol % FeCl₃) and K₃PO₄·H₂O (69.2 mg, 0.3 mmol) in 0.4 mL 2 wt % TPGS-750-M/H₂O

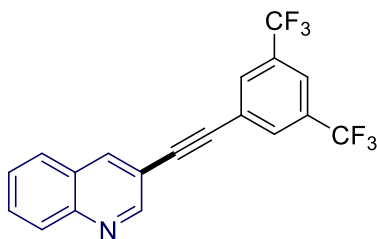
were reacted at 45 °C for 24 h yielding 42.0 mg (99%) 4'-methoxy-[1,1'-biphenyl]-2-carbaldehyde as a white solid (hexanes/EtOAc : 95/5).

¹H NMR (400 MHz, chloroform-*d*) δ 10.00 (s, 1H), 8.01 (d, *J* = 8.7 Hz, 1H), 7.62 (td, *J* = 7.5, 1.4 Hz, 1H), 7.50 – 7.41 (m, 2H), 7.31 (d, *J* = 8.7 Hz, 2H), 7.01 (d, *J* = 8.7 Hz, 2H), 3.88 (s, 3H).

¹³C NMR (126 MHz, chloroform-*d*) δ 192.83, 159.84, 145.80, 133.90, 133.67, 131.44, 130.93, 130.16, 127.76, 127.52, 114.08, 55.54.

Spectral data matched those previously reported.⁵

3-((3,5-bis(trifluoromethyl)phenyl)ethynyl)quinoline (2.7)



3-Bromoquinoline (47.4 mg, 27 μL, 0.2 mmol), 1-ethynyl-3,5-bis(trifluoromethyl)benzene (121.8 mg, 65 μL, 0.4 mmol), Pd(OAc)₂ (0.0225 mg, 0.0001 mmol), XPhos (2.9 mg, 0.006 mmol), Fe NPs (8 mg, 5 mol % FeCl₃) and DIPEA (51.7 mg, 0.07 mL, 0.4 mmol) in 0.4 mL 2 wt % TPGS-750-M/H₂O were reacted at 45 °C for 24 h yielding 73.1 mg (100%) of 3-((3,5-bis(trifluoromethyl)phenyl)ethynyl)quinoline as a yellow oil (hexanes/EtOAc : 80/20).

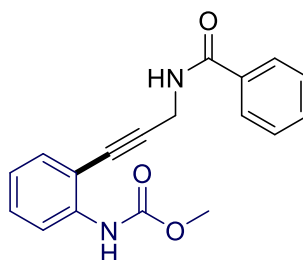
¹H NMR (600 MHz, chloroform-*d*) δ 9.01 (d, *J* = 2.1 Hz, 1H), 8.35 (d, *J* = 1.6 Hz, 1H), 8.12 (d, *J* = 8.4 Hz, 1H), 8.02 (s, 2H), 7.86 (s, 1H), 7.82 (d, *J* = 8.1 Hz, 1H), 7.79 – 7.74 (m, 1H), 7.60 (t, *J* = 7.3 Hz, 1H).

^{13}C NMR (126 MHz, chloroform-*d*) δ 151.82, 147.40, 139.21, 132.29 (q, $J_{\text{C-F}} = 34$ Hz), 131.70, 130.87, 129.66, 127.90, 127.21, 127.15, 125.14, 123.04 (q, $J_{\text{C-F}} = 274$ Hz), 122.21 (hept, $J_{\text{C-F}} = 4$ Hz), 116.16, 90.10, 89.43.

^{19}F NMR (376 MHz, chloroform-*d*) δ -63.14.

HRMS(EI): Calcd. for $\text{C}_{19}\text{H}_9\text{F}_6\text{NH}^+$: 366.0717 Found: 366.0722.

Methyl (2-(3-benzamidoprop-1-yn-1-yl)phenyl)carbamate (2.8)



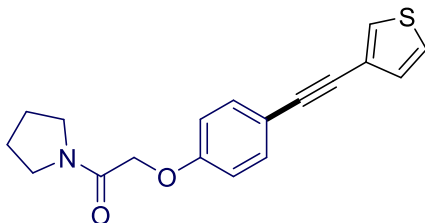
Methyl (2-bromophenyl)carbamate (46 mg, 0.2 mmol), *N*-(prop-2-yn-1-yl)benzamide (63.7 mg, 0.4 mmol), $\text{Pd}(\text{OAc})_2$ (0.0225 mg, 0.0001 mmol), XPhos (2.9 mg, 0.006 mmol), Fe NPs (8 mg, 5 mol % FeCl_3) and DIPEA (51.7 mg, 0.07 mL, 0.4 mmol) in 0.4 mL 2 wt % TPGS-750-M/ H_2O were reacted at 45 °C for 24 h yielding 51.6 mg (84%) of methyl (2-(3-benzamidoprop-1-yn-1-yl)phenyl)carbamate as a yellow oil (hexanes/ EtOAc : 70/30).

^1H NMR (400 MHz, chloroform-*d*) δ 8.12 (d, $J = 8.3$ Hz, 1H), 7.82 (d, $J = 7.3$ Hz, 2H), 7.52 (t, $J = 7.3$ Hz, 1H), 7.44 (t, $J = 7.4$ Hz, 3H), 7.38 – 7.28 (m, 2H), 6.97 (t, $J = 7.5$ Hz, 1H), 6.63 (br, 1H), 4.52 (d, $J = 5.3$ Hz, 2H), 3.76 (s, 3H).

^{13}C NMR (126 MHz, chloroform-*d*) δ 167.42, 153.89, 139.55, 133.88, 132.04, 131.99, 130.03, 128.77, 127.21, 122.62, 117.99, 110.87, 92.08, 79.02, 52.52, 30.82.

HRMS(EI): Calcd. for $\text{C}_{18}\text{H}_{16}\text{N}_2\text{O}_3\text{H}^+$: 309.1239 Found: 309.1244.

1-(Pyrrolidin-1-yl)-2-(4-(thiophen-3-ylethynyl)phenoxy)ethan-1-one (2.9)



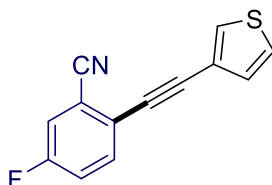
2-(4-Iodophenoxy)-1-(pyrrolidin-1-yl)ethan-1-one (66.2 mg, 0.2 mmol), 3-ethynylthiophene (43.3 mg, 39 μ L, 0.4 mmol), Pd(OAc)₂ (0.0225 mg, 0.0001 mmol), XPhos (2.9 mg, 0.006 mmol), Fe NPs (8 mg, 5 mol % FeCl₃) and DIPEA (51.7 mg, 0.07 mL, 0.4 mmol) in 0.4 mL 2 wt % TPGS-750-M/H₂O were reacted at 45 °C for 24 h yielding 62.4 mg (100%) of 1-(pyrrolidin-1-yl)-2-(4-(thiophen-3-ylethynyl)phenoxy)ethan-1-one as a yellow solid (hexanes/EtOAc : 70/30).

¹H NMR (400 MHz, chloroform-*d*) δ 7.48 (dd, *J* = 3.0, 1.1 Hz, 1H), 7.46 – 7.42 (m, 2H), 7.29 (dd, *J* = 5.0, 3.0 Hz, 1H), 7.17 (dd, *J* = 5.0, 1.1 Hz, 1H), 6.95 – 6.89 (m, 2H), 4.64 (s, 2H), 3.52 (td, *J* = 6.8, 4.6 Hz, 4H), 1.97 (p, *J* = 7.1, 6.6 Hz, 2H), 1.86 (p, *J* = 6.5 Hz, 2H).

¹³C NMR (101 MHz, chloroform-*d*) δ 166.30, 158.14, 133.19, 129.99, 128.31, 125.41, 122.62, 116.41, 114.86, 88.69, 83.57, 68.13, 46.39, 46.17, 26.41, 23.93.

HRMS(ED): Calcd. for C₁₈H₁₇NO₂SNa⁺: 334.0878 Found: 334.0894.

5-Fluoro-2-(thiophen-3-ylethynyl)benzonitrile (2.10)



2-Bromo-5-fluorobenzonitrile (40 mg, 0.2 mmol), 3-ethynylthiophene (43.3 mg, 39 μ L, 0.4 mmol), Pd(OAc)₂ (0.0225 mg, 0.0001 mmol), XPhos (2.9 mg, 0.006 mmol), Fe NPs (8 mg, 5 mol % FeCl₃) and DIPEA (51.7 mg, 0.07 mL, 0.4 mmol) in 0.4 mL 2 wt % TPGS-750-M/H₂O were reacted at 45 °C for 24 h yielding 43 mg (95%) of 5-fluoro-2-(thiophen-3-ylethynyl)benzonitrile as a yellow oil (hexanes/EtOAc : 90/10).

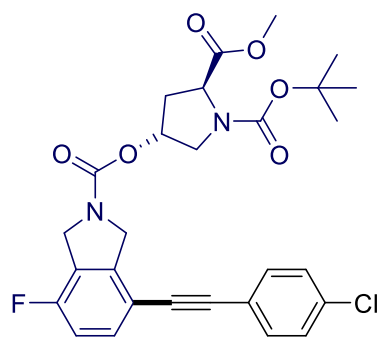
¹H NMR (400 MHz, chloroform-*d*) δ 7.64 (dd, *J* = 3.0, 1.2 Hz, 1H), 7.59 (dd, *J* = 8.8, 5.2 Hz, 1H), 7.36 (dd, *J* = 7.9, 2.6 Hz, 1H), 7.33 (dd, *J* = 5.0, 3.0 Hz, 1H), 7.31 – 7.26 (m, 1H), 7.25 (dd, *J* = 5.0, 1.2 Hz, 1H).

¹³C NMR (126 MHz, chloroform-*d*) δ 161.33 (d, *J*_(C-F) = 253.3 Hz), 134.19 (d, *J*_(C-F) = 8.8 Hz), 130.52, 129.95, 125.90, 123.89 (d, *J*_(C-F) = 3.8 Hz), 121.06, 120.57 (d, *J*_(C-F) = 21.4 Hz), 119.81 (d, *J*_(C-F) = 25.2 Hz), 116.72 (d, *J*_(C-F) = 10.1 Hz), 116.52 (d, *J*_(C-F) = 2.5 Hz), 91.13, 84.30.

¹⁹F NMR (376 MHz, chloroform-*d*) δ -108.80.

HRMS(ED): Calcd. for C₁₃H₆FNSNa⁺: 250.0103 Found: 250.0110.

1-(*t*-Butyl) 2-methyl (2*S*,4*R*)-4-((4-((4-chlorophenyl)ethynyl)-7-fluoroisindoline-2-carbonyl)oxy)pyrrolidine-1,2-dicarboxylate (2.11)



1-(*t*-Butyl)-2-methyl-(2*S*,4*R*)-4-((4-bromo-7-fluoroisindoline-2-carbonyloxy)pyrrolidine-1,2-dicarboxylate (97.5 mg, 0.2 mmol), 1-chloro-4-ethynylbenzene (54.6 mg, 0.4 mmol), Pd(OAc)₂ (0.0338 mg, 0.00015 mmol), XPhos (2.9 mg, 0.006 mmol), Fe NPs (8 mg, 5 mol % FeCl₃), and DIPEA (51.7 mg, 0.07 mL, 0.4 mmol) in 0.4 mL 2 wt % TPGS-750-M/H₂O were reacted at 55 °C for 48 h yielding 88 mg (81%) of 1-(*t*-butyl)-2-methyl-(2*S*,4*R*)-4-(((4-((4-chlorophenyl)ethynyl)-7-fluoroisindoline-2-carbonyloxy) pyrrolidine-1,2-dicarboxylate (hexanes/EtOAc : 75/25).

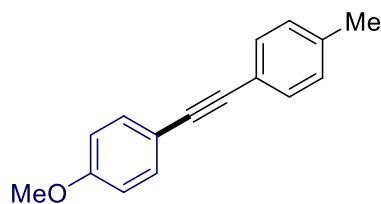
¹H NMR (400 MHz, chloroform-*d*) δ 7.50 (d, *J* = 3.6 Hz, 1H), 7.44 (m, 2H), 7.40 – 7.31 (m, 2H), 7.04 – 6.94 (m, 1H), 5.34 (s, 1H), 4.84 (d, *J* = 17.6 Hz, 2H), 4.76 (m, 2H), 4.44 (m, *J* = 35.7, 7.6 Hz, 1H), 3.76 (m, 5H), 2.56 – 2.41 (m, 1H), 2.25 (m, 1H), 1.44 (m, 9H).

¹³C NMR (126 MHz, chloroform-*d*) δ 173.28, 173.00, 158.78, 158.62, 156.77, 156.62, 154.55, 154.52, 153.95, 153.92, 153.86, 142.39, 142.35, 134.93, 133.33, 133.28, 133.02, 132.98, 131.73, 128.96, 128.95, 123.99, 123.84, 121.23, 121.18, 115.17, 115.07, 115.01, 114.91, 92.35, 86.14, 80.76, 80.69, 74.13, 74.06, 73.39, 73.37, 58.21, 57.78, 53.57, 53.11, 52.85, 52.54, 52.34, 50.45, 50.01, 37.12, 36.12, 36.08, 28.51, 28.39.

¹⁹F NMR (376 MHz, chloroform-*d*) δ -114.97, -115.07, -115.30, -115.51.

HRMS(EI): Calcd. for C₂₈H₂₈ClFN₂O₆Na⁺: 565.1517 Found: 565.1520.

1-Methoxy-4-(*p*-tolylethynyl)benzene (2.12)



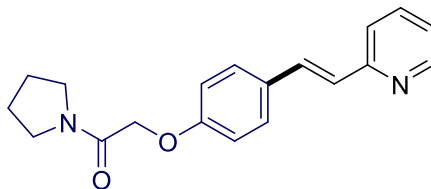
1-Bromoanisole (37.4 mg, 25 μ L, 0.2 mmol), 1-ethynyl-4-methylbenzene (46.5 mg, 51 μ L, 0.4 mmol), Pd(OAc)₂ (0.0225 mg, 0.0001 mmol), XPhos (2.9 mg, 0.006 mmol), Fe NPs (8 mg, 5 mol % FeCl₃), and DIPEA (51.7 mg, 0.07 mL, 0.4 mmol) in 0.4 mL 2 wt % TPGS-750-M/H₂O were reacted at 45 °C for 24 h yielding 42.8 mg (96%) of 1-methoxy-4-(p-tolylethynyl)benzene as a yellow crystal (hexanes/EtOAc : 97/3).

¹H NMR (500 MHz, chloroform-*d*) δ 7.46 (d, *J* = 8.9 Hz, 2H), 7.40 (d, *J* = 8.1 Hz, 2H), 7.14 (d, *J* = 7.9 Hz, 2H), 6.87 (d, *J* = 8.8 Hz, 2H), 3.83 (s, 3H), 2.36 (s, 3H).

¹³C NMR (126 MHz, chloroform-*d*) δ 159.63, 138.16, 133.12, 131.48, 129.22, 120.64, 115.75, 114.11, 88.79, 88.33, 55.45, 21.64.

Spectral data matched those previously reported.⁶

(*E*)-2-(4-(2-(pyridin-2-yl)vinyl)phenoxy)-1-(pyrrolidin-1-yl)ethan-1-one (2.13)



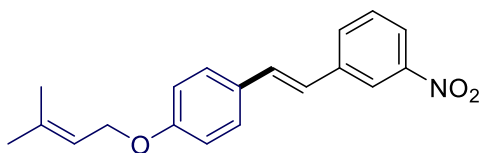
2-(4-Iodophenoxy)-1-(pyrrolidin-1-yl)ethan-1-one (66.2 mg, 0.2 mmol), 2-vinylpyridine (42 mg, 43 μ L, 0.4 mmol), Pd(*t*Bu₃P)₂ (0.26 mg, 0.0005 mmol), *t*Bu₃P (1 mg, 0.005 mmol), Fe NPs (2.8 mg, 1.8 mol % FeCl₃), K₃PO₄ (127.4 mg, 0.6 mmol), and NaCl (70.2 mg, 1.2 mmol) in 0.4 mL 2 wt % TPGS-750-M/H₂O with 0.04 mL DMF were reacted at 45 °C for 40 h yielding 61.7 mg (100%) of (*E*)-2-(4-(2-(pyridin-2-yl)vinyl)phenoxy)-1-(pyrrolidin-1-yl)ethan-1-one as a yellow solid (hexanes/EtOAc : 60/40).

^1H NMR (500 MHz, chloroform-*d*) δ 8.56 (d, $J = 4.6$ Hz, 1H), 7.64 – 7.58 (m, 1H), 7.55 (d, $J = 16.1$ Hz, 1H), 7.49 (d, $J = 8.7$ Hz, 2H), 7.33 (d, $J = 7.9$ Hz, 1H), 7.12 – 7.06 (m, 1H), 7.02 (d, $J = 16.1$ Hz, 1H), 6.93 (d, $J = 8.6$ Hz, 2H), 4.62 (s, 2H), 3.50 (q, $J = 6.8$ Hz, 4H), 1.94 (p, $J = 6.8$ Hz, 2H), 1.82 (p, $J = 6.8$ Hz, 2H).

^{13}C NMR (126 MHz, chloroform-*d*) δ 166.36, 158.35, 155.88, 149.64, 136.59, 132.14, 130.31, 128.55, 126.29, 121.92, 121.84, 114.97, 68.06, 46.28, 46.07, 26.31, 23.85.

HRMS(EI): Calcd. for $\text{C}_{19}\text{H}_{20}\text{N}_2\text{O}_2\text{H}^+$: 309.1603 Found: 309.1601.

(*E*)-1-(4-((3-Methylbut-2-en-1-yl)oxy)styryl)-3-nitrobenzene (2.14)



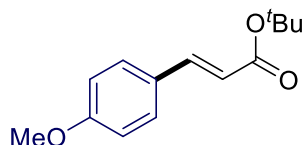
1-Iodo-4-((3-methylbut-2-en-1-yl)oxy)benzene (57.6 mg, 0.2 mmol), 1-nitro-3-vinylbenzene (59.7 mg, 56 μL , 0.4 mmol), $\text{Pd}(t\text{Bu}_3\text{P})_2$ (0.26 mg, 0.0005 mmol), $t\text{Bu}_3\text{P}$ (1 mg, 0.005 mmol), Fe NPs (2.8 mg, 1.8 mol % FeCl_3), K_3PO_4 (127.4 mg, 0.6 mmol) and NaCl (70.2 mg, 1.2 mmol) in 0.4 mL 2 wt % TPGS-750-M/ H_2O with 0.04 mL DMF were reacted at 45 $^\circ\text{C}$ for 40 h yielding 54.3 mg (88%) of (*E*)-1-(4-((3-methylbut-2-en-1-yl)oxy)styryl)-3-nitrobenzene as a yellow solid (hexanes/ EtOAc : 90/10).

^1H NMR (500 MHz, chloroform-*d*) δ 8.33 (t, $J = 1.8$ Hz, 1H), 8.06 (ddd, $J = 8.1, 2.1, 0.8$ Hz, 1H), 7.76 (d, $J = 7.8$ Hz, 1H), 7.49 (m, 3H), 7.18 (d, $J = 16.3$ Hz, 1H), 6.99 (d, $J = 16.3$ Hz, 1H), 6.94 (d, $J = 8.7$ Hz, 2H), 5.51 (tt, $J = 6.7, 1.3$ Hz, 1H), 4.55 (d, $J = 6.7$ Hz, 2H), 1.81 (s, 3H), 1.76 (s, 3H).

^{13}C NMR (126 MHz, chloroform-*d*) δ 159.45, 148.87, 139.70, 138.64, 132.12, 131.47, 129.62, 129.07, 128.26, 123.96, 121.69, 120.70, 119.56, 115.15, 65.01, 25.98, 18.37.

HRMS(EI): Calcd. for $\text{C}_{19}\text{H}_{19}\text{NO}_3\text{Na}^+$: 332.1263 Found: 332.1259.

***t*-Butyl (*E*)-3-(4-methoxyphenyl)acrylate (2.15)**



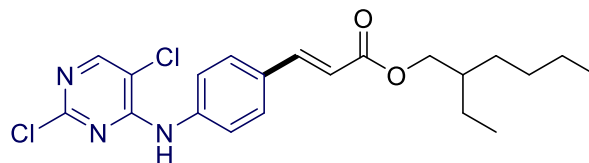
4-Iodoanisole (46.8 mg, 0.2 mmol), *t*-butyl acrylate (51.3 mg, 59 μL , 0.4 mmol), $\text{Pd}(t\text{Bu}_3\text{P})_2$ (0.26 mg, 0.0005 mmol), $t\text{Bu}_3\text{P}$ (1 mg, 0.005 mmol), Fe NPs (2.8 mg, 1.8 mol % FeCl_3), K_3PO_4 (127.4 mg, 0.6 mmol), and NaCl (70.2 mg, 1.2 mmol) in 0.4 mL 2 wt % TPGS-750-M/ H_2O with 0.04 mL DMF were reacted at 45 $^\circ\text{C}$ for 40 h yielding 46.9 mg (100%) of *t*-butyl (*E*)-3-(4-methoxyphenyl)acrylate as a white solid (hexanes/ EtOAc : 90/10).

^1H NMR (400 MHz, chloroform-*d*) δ 7.54 (d, $J = 15.9$ Hz, 1H), 7.45 (d, $J = 8.7$ Hz, 2H), 6.89 (d, $J = 8.8$ Hz, 2H), 6.24 (d, $J = 15.9$ Hz, 1H), 3.83 (s, 3H), 1.53 (s, 9H).

^{13}C NMR (126 MHz, chloroform-*d*) δ 166.83, 161.26, 143.34, 129.69, 127.55, 117.86, 114.39, 80.36, 55.49, 28.38.

Spectral data matched those previously reported.⁷

2-Ethylhexyl (*E*)-3-(4-((2,5-dichloropyrimidin-4-yl)amino)phenyl)acrylate (2.16)



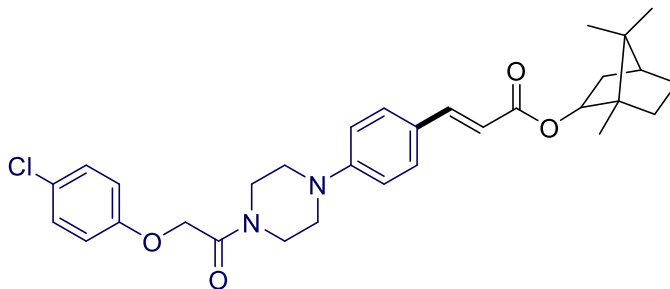
2,5-Dichloro-*N*-(4-iodophenyl)pyrimidin-4-amine (73.2 mg, 0.2 mmol), 2-ethylhexyl acrylate (73.7 mg, 83 μ L, 0.4 mmol), Pd(*t*Bu₃P)₂ (0.26 mg, 0.0005 mmol), *t*Bu₃P (1 mg, 0.005 mmol), Fe NPs (2.8 mg, 1.8 mol % FeCl₃), K₃PO₄ (127.4 mg, 0.6 mmol), and NaCl (70.2 mg, 1.2 mmol) in 0.4 mL 2 wt % TPGS-750-M/H₂O with 0.04 mL DMF were reacted at 45 °C for 40 h yielding 80.3 mg (95%) of 2-ethylhexyl (*E*)-3-(4-((2,5-dichloropyrimidin-4-yl)amino)phenyl)acrylate as a yellow oil (hexanes/EtOAc : 50/50).

¹H NMR (400 MHz, chloroform-*d*) δ 8.22 (s, 1H), 7.72 – 7.59 (m, 3H), 7.55 (d, *J* = 8.6 Hz, 2H), 7.38 (s, 1H), 6.40 (d, *J* = 16.0 Hz, 1H), 4.22 – 4.03 (m, 2H), 1.65 (m, 1H), 1.47 – 1.27 (m, 8H), 0.91 (m, 6H).

¹³C NMR (126 MHz, chloroform-*d*) δ 167.32, 158.30, 156.17, 155.04, 143.53, 138.71, 131.14, 129.15, 120.98, 117.94, 114.09, 67.14, 38.98, 30.58, 29.07, 23.97, 23.10, 14.19, 11.15.

HRMS(ESI): Calcd. for C₂₁H₂₅Cl₂N₃O₂Na⁺: 444.1222 Found: 444.1222.

(1*R*,4*S*)-1,7,7-Trimethylbicyclo[2.2.1]heptan-2-yl **(*E*)-3-(4-(4-(2-(4-chlorophenoxy)-acetyl)piperazin-1-yl)phenyl)acrylate (2.17)**



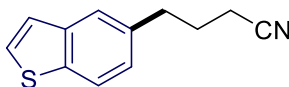
2-(4-Chlorophenoxy)-1-(4-(4-iodophenyl)piperazin-1-yl)ethan-1-one (91.3 mg, 0.2 mmol), (1*R*,4*S*)-1,7,7-trimethylbicyclo[2.2.1]heptan-2-yl acrylate (83.3 mg, 85 μ L, 0.4 mmol), Pd(*t*Bu₃P)₂ (0.26 mg, 0.0005 mmol), *t*Bu₃P (1 mg, 0.005 mmol), Fe NPs (2.8 mg, 1.8 mol % FeCl₃), K₃PO₄ (127.4 mg, 0.6 mmol) and NaCl (70.2 mg, 1.2 mmol) in 0.4 mL 2 wt % TPGS-750-M/H₂O with 0.04 mL DMF were reacted at 45 °C for 40 h yielding 106.3 mg (99%) of (1*R*,4*S*)-1,7,7-trimethylbicyclo[2.2.1]heptan-2-yl (*E*)-3-(4-(4-(2-(4-chlorophenoxy)acetyl)piperazin-1-yl)phenyl)acrylate as a yellow oil (hexanes/EtOAc : 60/40).

¹H NMR (500 MHz, chloroform-*d*) δ 7.55 (d, *J* = 15.9 Hz, 1H), 7.43 (d, *J* = 8.7 Hz, 2H), 7.24 (d, *J* = 8.9 Hz, 2H), 6.89 (d, *J* = 8.9 Hz, 2H), 6.85 (d, *J* = 8.7 Hz, 2H), 6.25 (d, *J* = 15.9 Hz, 1H), 4.78 (dd, *J* = 7.3, 4.1 Hz, 1H), 4.71 (s, 2H), 3.75 (d, *J* = 19.0 Hz, 4H), 3.33 – 3.18 (m, 4H), 1.89 – 1.66 (m, 4H), 1.57 (td, *J* = 12.2, 4.0 Hz, 1H), 1.27 – 1.03 (m, 5H), 0.87 (m, 6H).

¹³C NMR (126 MHz, chloroform-*d*) δ 167.06, 166.30, 156.43, 151.86, 143.89, 129.68, 129.60, 126.86, 126.21, 116.00, 115.83, 115.62, 80.91, 68.02, 48.95, 48.67, 48.15, 47.06, 45.17, 45.08, 41.87, 38.98, 33.85, 27.17, 20.26, 20.12, 11.61.

HRMS(ED): Calcd. for C₃₁H₃₇ClN₂O₄Na⁺: 559.2339 Found: 559.2338.

4-(Benzo[*b*]thiophen-5-yl)butanenitrile (2.18)



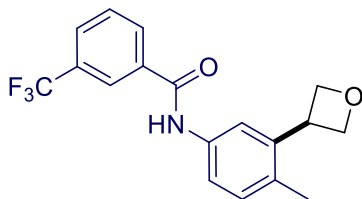
5-Bromobenzo[*b*]thiophene (42.6 mg, 0.2 mmol), 4-bromobutanenitrile (118.4 mg, 80 μ L, 0.8 mmol), Pd(OAc)₂ (0.11 mg, 0.0005 mmol), AmPhos (2.7 mg, 0.01 mmol), Fe NPs (8 mg, 5 mol % FeCl₃), Zn powder (52 mg, 0.8 mmol) and TMEDA (116.2 mg, 0.15 mL, 1.0 mmol) in 1.0 mL 2 wt % TPGS-750-M/H₂O were reacted at 45 °C for 40 h yielding 38.5 mg (96%) of 4-(benzo[*b*]thiophen-5-yl)butanenitrile as a yellow oil (hexanes/EtOAc : 90/10).

¹H NMR (400 MHz, chloroform-*d*) δ 7.82 (d, *J* = 8.3 Hz, 1H), 7.67 – 7.61 (m, 1H), 7.45 (d, *J* = 5.4 Hz, 1H), 7.30 (d, *J* = 5.4 Hz, 1H), 7.18 (dd, *J* = 8.3, 1.4 Hz, 1H), 2.91 (t, *J* = 7.4 Hz, 2H), 2.33 (t, *J* = 7.1 Hz, 2H), 2.04 (p, *J* = 7.2 Hz, 2H).

¹³C NMR (126 MHz, chloroform-*d*) δ 140.12, 138.04, 135.86, 127.05, 125.09, 123.65, 123.31, 122.75, 119.63, 34.33, 27.25, 16.41.

HRMS(ED): Calcd. for C₁₂H₁₁NSNa⁺: 224.0510 Found: 224.0510.

N-(4-Methyl-3-(oxetan-3-yl)phenyl)-3-(trifluoromethyl)benzamide (2.19)



N-(3-Bromo-4-methylphenyl)-3-(trifluoromethyl)benzamide (71.6 mg, 0.2 mmol), 3-bromooxetane (109.6 mg, 62 μ L, 0.8 mmol), Pd(OAc)₂ (0.11 mg, 0.0005 mmol), AmPhos

(2.7 mg, 0.01 mmol), Fe NPs (8 mg, 5 mol % FeCl₃), Zn powder (52 mg, 0.8 mmol) and TMEDA (116.2 mg, 0.15 mL, 1.0 mmol) in 1.0 mL 2 wt % TPGS-750-M/H₂O were reacted at 45 °C for 40 h yielding 50.6 mg (76%) of *N*-(4-methyl-3-(oxetan-3-yl)phenyl)-3-(trifluoromethyl)benzamide as a white powder (hexanes/EtOAc : 70/30).

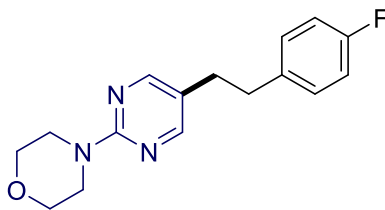
¹H NMR (400 MHz, DMSO-*d*₆) δ 10.43 (s, 1H), 8.35 – 8.24 (m, 2H), 7.96 (d, *J* = 7.7 Hz, 1H), 7.84 – 7.74 (m, 2H), 7.69 – 7.61 (m, 1H), 7.15 (d, *J* = 8.2 Hz, 1H), 4.96 (dd, *J* = 8.3, 5.7 Hz, 2H), 4.73 – 4.63 (m, 2H), 4.48 (q, *J* = 7.8 Hz, 1H), 2.09 (s, 3H).

¹³C NMR (126 MHz, DMSO-*d*₆) δ 163.83, 139.61, 137.06, 135.82, 131.80, 131.08, 130.18, 129.73, 129.22 (q, *J*_(C-F) = 32.8 Hz), 128.11 (q, *J*_(C-F) = 3.8 Hz), 124.21 (q, *J*_(C-F) = 3.8 Hz), 124.04 (q, *J*_(C-F) = 273.4 Hz), 118.68, 117.83, 76.15, 36.70, 18.42.

¹⁹F NMR (376 MHz, DMSO-*d*₆) δ -61.09.

HRMS(EI): Calcd. for C₁₈H₁₆F₃NO₂H⁺: 336.1211 Found: 336.1208.

4-(5-(4-Fluorophenethyl)pyrimidin-2-yl)morpholine (2.20)



4-(5-Bromopyrimidin-2-yl)morpholine (48.8 mg, 0.2 mmol), 1-(2-bromoethyl)-4-fluorobenzene (162.4 mg, 0.11 mL, 0.8 mmol), Pd(OAc)₂ (0.11 mg, 0.0005 mmol), AmPhos (2.7 mg, 0.01 mmol), Fe NPs (8 mg, 5 mol % FeCl₃), Zn powder (52 mg, 0.8 mmol), and TMEDA (116.2 mg, 0.15 mL, 1.0 mmol) in 1.0 mL 2 wt % TPGS-750-M/H₂O were reacted

at 45 °C for 40 h yielding 48.7 mg (76%) of 4-(5-(4-fluorophenethyl)pyrimidin-2-yl)morpholine as a yellow oil (hexanes/EtOAc : 70/30).

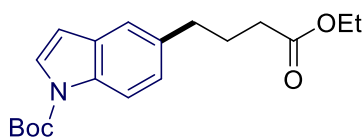
¹H NMR (400 MHz, chloroform-*d*) δ 8.07 (s, 2H), 7.08 (ddd, *J* = 8.3, 5.3, 2.5 Hz, 2H), 7.00 – 6.92 (m, 2H), 3.75 (m, 8H), 2.82 (t, *J* = 7.2 Hz, 2H), 2.72 (t, *J* = 7.2 Hz, 2H).

¹³C NMR (126 MHz, chloroform-*d*) δ 162.56, 161.34 (d, *J*_(C-F) = 55.4 Hz), 157.71, 136.37 (d, *J*_(C-F) = 3.8 Hz), 130.05 (d, *J*_(C-F) = 7.6 Hz), 122.42, 115.41 (d, *J*_(C-F) = 21.4 Hz), 66.96, 44.53, 36.84, 31.61.

¹⁹F NMR (376 MHz, chloroform-*d*) δ -117.04.

HRMS(ESI): Calcd. for C₁₆H₁₈FN₃OH⁺: 288.1512 Found: 288.1526.

***t*-Butyl 5-(4-ethoxy-4-oxobutyl)-1*H*-indole-1-carboxylate (2.21)**



t-Butyl 5-bromo-1*H*-indole-1-carboxylate (59.2 mg, 0.2 mmol), ethyl 4-bromobutanoate (156 mg, 0.8 mmol), Pd(OAc)₂ (0.11 mg, 0.0005 mmol), AmPhos (2.7 mg, 0.01 mmol), Fe NPs (8 mg, 5 mol % FeCl₃), Zn powder (52 mg, 0.8 mmol) and TMEDA (116.2 mg, 0.15 mL, 1.0 mmol) in 1.0 mL 2 wt % TPGS-750-M/H₂O were reacted at 45 °C for 40 h yielding 56.9 mg (86%) of *t*-butyl 5-(4-ethoxy-4-oxobutyl)-1*H*-indole-1-carboxylate as a yellow oil (hexanes/EtOAc : 90/10).

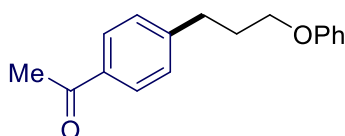
¹H NMR (600 MHz, chloroform-*d*) δ 8.14 – 7.91 (br, 1H), 7.60 – 7.50 (m, 1H), 7.37 – 7.34 (m, 1H), 7.13 (dd, *J* = 8.5, 1.6 Hz, 1H), 6.51 (d, *J* = 3.6 Hz, 1H), 4.12 (q, *J* = 7.1 Hz,

2H), 2.74 (t, $J = 7.5$ Hz, 2H), 2.32 (t, $J = 7.5$ Hz, 2H), 1.99 (p, $J = 7.5$ Hz, 2H), 1.67 (s, 9H), 1.25 (t, $J = 7.1$ Hz, 3H).

^{13}C NMR (126 MHz, chloroform-*d*) δ 173.77, 149.96, 135.91, 133.86, 130.93, 126.19, 125.12, 120.58, 115.10, 107.24, 83.67, 60.39, 35.15, 33.79, 28.35, 27.16, 14.40.

Spectral data matched those previously reported.⁸

1-(4-(3-Phenoxypropyl)phenyl)ethan-1-one (2.22)



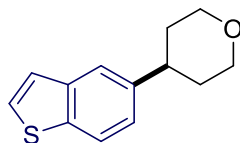
1-(4-Bromophenyl)ethan-1-one (40 mg, 0.2 mmol), (3-bromopropoxy)benzene (172 mg, 0.13 mL, 0.8 mmol), Pd(OAc)₂ (0.11 mg, 0.0005 mmol), AmPhos (2.7 mg, 0.01 mmol), Fe NPs (8 mg, 5 mol % FeCl₃), Zn powder (52 mg, 0.8 mmol), and TMEDA (116.2 mg, 0.15 mL, 1.0 mmol) in 1.0 mL 2 wt % TPGS-750-M/H₂O were reacted at 45 °C for 40 h yielding 41.1 mg (81%) of 1-(4-(3-phenoxypropyl)phenyl)ethan-1-one as a yellow oil (hexanes/EtOAc : 90/10).

^1H NMR (500 MHz, chloroform-*d*) δ 7.89 (d, $J = 8.2$ Hz, 2H), 7.33 – 7.26 (m, 4H), 6.95 (t, $J = 7.3$ Hz, 1H), 6.89 (d, $J = 7.8$ Hz, 2H), 3.96 (t, $J = 6.2$ Hz, 2H), 2.92 – 2.84 (m, 2H), 2.59 (s, 3H), 2.13 (m, 2H).

^{13}C NMR (126 MHz, chloroform-*d*) δ 198.00, 159.02, 147.55, 135.35, 129.61, 128.90, 128.76, 120.87, 114.63, 66.63, 32.38, 30.66, 26.72.

Spectral data matched those previously reported.⁸

4-(Benzo[*b*]thiophen-5-yl)tetrahydro-2*H*-pyran (2.23)



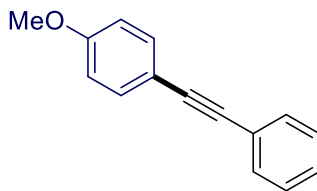
5-Bromobenzo[*b*]thiophene (42.6 mg, 0.2 mmol), 4-bromotetrahydro-2*H*-pyran (132 mg, 0.06 mL, 0.8 mmol), Pd(OAc)₂ (0.11 mg, 0.0005 mmol), AmPhos (2.7 mg, 0.01 mmol), Fe NPs (8 mg, 5 mol % FeCl₃), Zn powder (52 mg, 0.8 mmol) and TMEDA (116.2 mg, 0.15 mL, 1.0 mmol) in 1.0 mL 2 wt % TPGS-750-M/H₂O were reacted at 45 °C for 40 h yielding 36.1 mg (83%) of 4-(benzo[*b*]thiophen-5-yl)tetrahydro-2*H*-pyran as a yellow oil (hexanes/EtOAc : 90/10).

¹H NMR (400 MHz, chloroform-*d*) δ 7.83 (d, *J* = 8.3 Hz, 1H), 7.68 (s, 1H), 7.44 (d, *J* = 5.4 Hz, 1H), 7.31 (d, *J* = 5.4 Hz, 1H), 7.24 (dd, *J* = 8.4, 1.3 Hz, 1H), 4.12 (dd, *J* = 11.1, 3.7 Hz, 2H), 3.57 (td, *J* = 11.6, 2.3 Hz, 2H), 2.88 (tt, *J* = 11.6, 4.1 Hz, 1H), 1.97 – 1.79 (m, 4H).

¹³C NMR (126 MHz, chloroform-*d*) δ 142.28, 140.09, 137.85, 126.83, 123.89, 123.85, 122.58, 121.36, 68.58, 41.68, 34.41.

HRMS(EI): Calcd. for C₁₃H₁₄O⁺: 219.0844 Found: 219.0853.

1-Methoxy-4-(phenylethynyl)benzene (2.24)



1-Bromoanisole (37.4 mg, 25 μL, 0.2 mmol), ethynylbenzene (40.9 mg, 44 μL, 0.4 mmol), Pd(OAc)₂ (0.0225 mg, 0.0001 mmol), XPhos (2.9 mg, 0.006 mmol), Fe NPs (8 mg,

5 mol % FeCl₃) and DIPEA (51.7 mg, 0.07 mL, 0.4 mmol) in 0.4 mL 2 wt % TPGS-750-M/H₂O were reacted at 45 °C for 24 h yielding 39.6 mg (95%) of 1-methoxy-4-(phenylethynyl)benzene as a yellow crystal (hexanes/EtOAc : 97/3).

¹H NMR (400 MHz, chloroform-*d*) δ 7.57 – 7.45 (m, 4H), 7.39 – 7.29 (m, 3H), 6.96 – 6.84 (m, 2H), 3.83 (s, 3H).

¹³C NMR (126 MHz, chloroform-*d*) δ 159.76, 133.19, 131.59, 128.44, 128.07, 123.74, 115.52, 114.14, 89.51, 88.20, 55.44.

Spectral data matched those previously reported.⁹

Pyrrolidin-1-yl(4-(thiophen-3-yl)phenyl)methanone (2.25)



(4-Bromophenyl)(pyrrolidin-1-yl)methanone (50.8 mg, 0.2 mmol), thiophen-3-ylboronic acid (50.4 mg, 0.3 mmol), Pd(OAc)₂ (0.0225 mg, 0.0001 mmol), LS1 (FcPAd₂) (4.9 mg, 0.01 mmol), Fe NPs (8 mg, 5 mol % FeCl₃) and K₃PO₄·H₂O (69.2 mg, 0.3 mmol) in 0.4 mL 2 wt % TPGS-750-M/H₂O were reacted at 45 °C for 24 h yielding 48.8 mg (95%) of pyrrolidin-1-yl(4-(thiophen-3-yl)phenyl)methanone as a white solid (hexanes/EtOAc : 80/20).

¹H NMR (400 MHz, chloroform-*d*) δ 7.65 – 7.53 (m, 4H), 7.49 (t, *J* = 2.0 Hz, 1H), 7.39 (d, *J* = 2.0 Hz, 2H), 3.65 (t, *J* = 6.8 Hz, 2H), 3.47 (t, *J* = 6.4 Hz, 2H), 1.91 (ddt, *J* = 34.2, 13.0, 6.5 Hz, 4H).

^{13}C NMR (126 MHz, chloroform-*d*) δ 169.48, 141.56, 137.27, 135.79, 127.92, 126.60, 126.26, 126.21, 121.15, 49.74, 46.35, 26.53, 24.53.

HRMS(EI): Calcd. for $\text{C}_{15}\text{H}_{15}\text{NOSNa}^+$: 280.0772 Found: 280.0769.

2-Fluoro-4-(6-formylbenzo[*d*][1,3]dioxol-5-yl)benzonitrile (2.26)



6-Bromobenzo[*d*][1,3]dioxole-5-carbaldehyde (45.8 mg, 0.2 mmol), (4-cyano-3-fluorophenyl)boronic acid (49.5 mg, 0.3 mmol), $\text{Pd}(\text{OAc})_2$ (0.0225 mg, 0.0001 mmol), LS1 (FcPAd_2) (4.9 mg, 0.01 mmol), Fe NPs (8 mg, 5 mol % FeCl_3) and $\text{K}_3\text{PO}_4 \cdot \text{H}_2\text{O}$ (69.2 mg, 0.3 mmol) in 0.4 mL 2 wt % TPGS-750-M/ H_2O were reacted at 45 °C for 24 h yielding 27.4 mg (51%) of 2-fluoro-4-(6-formylbenzo[*d*][1,3]dioxol-5-yl)benzonitrile as a yellow oil (hexanes/EtOAc : 90/10).

^1H NMR (400 MHz, chloroform-*d*) δ 9.72 (s, 1H), 7.71 (t, $J = 7.3$ Hz, 1H), 7.49 (s, 1H), 7.26 – 7.21 (m, 2H), 6.80 (s, 1H), 6.14 (s, 2H).

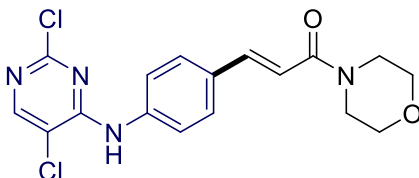
^{13}C NMR (126 MHz, chloroform-*d*) δ 188.99, 162.89 (d, $J_{\text{C-F}} = 261.2$ Hz), 152.59, 149.08, 145.37 (d, $J_{\text{C-F}} = 8.1$ Hz), 139.65 (d, $J_{\text{C-F}} = 1.8$ Hz), 133.47, 128.97, 126.80 (d, $J_{\text{C-F}} = 3.4$ Hz), 118.16 (d, $J_{\text{C-F}} = 20.1$ Hz), 113.65, 109.95, 107.36, 102.75, 101.39 (d, $J_{\text{C-F}} = 15.5$ Hz).

^{19}F NMR (376 MHz, chloroform-*d*) δ -105.49.

HRMS(EI): Calcd. for $\text{C}_{15}\text{H}_8\text{FNO}_3\text{H}^+$: 270.0566 Found: 270.0561.

(E)-3-(4-((2,5-Dichloropyrimidin-4-yl)amino)phenyl)-1-morpholinoprop-2-en-1-one

(2.27)



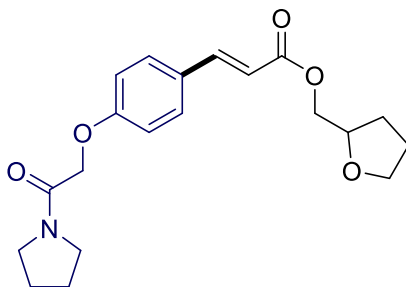
2,5-Dichloro-*N*-(4-iodophenyl)pyrimidin-4-amine (73.2 mg, 0.2 mmol), 1-morpholinoprop-2-en-1-one (56.5 mg, 0.4 mmol), Pd(*t*Bu₃P)₂ (0.26 mg, 0.0005 mmol), LS2 (FcPAd₂PtBu₂) (4.0 mg, 0.005 mmol), Fe NPs (2.8 mg, 1.8 mol % FeCl₃), K₃PO₄ (127.4 mg, 0.6 mmol) and NaCl (70.2 mg, 1.2 mmol) in 0.4 mL 2 wt % TPGS-750-M/H₂O with 0.04 mL DMF were reacted at 45 °C for 40 h yielding 69.5 mg (92%) of (*E*)-3-(4-((2,5-dichloropyrimidin-4-yl)amino)phenyl)-1-morpholinoprop-2-en-1-one as a yellow oil (hexanes/ EtOAc : 50/50).

¹H NMR (500 MHz, chloroform-*d*) δ 8.23 (s, 1H), 7.70 – 7.65 (m, 3H), 7.56 (d, *J* = 8.5 Hz, 2H), 7.37 (s, 1H), 6.81 (d, *J* = 15.4 Hz, 1H), 3.70 (m, 8H).

¹³C NMR (126 MHz, chloroform-*d*) δ 165.66, 158.32, 156.24, 155.04, 142.38, 138.30, 131.88, 128.88, 121.08, 116.15, 114.08, 66.99, 46.77, 41.71, 29.82.

Spectral data matched those previously reported.¹⁰

(Tetrahydrofuran-2-yl)methyl (*E*)-3-(4-(2-oxo-2-(pyrrolidin-1-yl)ethoxy)phenyl)acrylate (2.28)



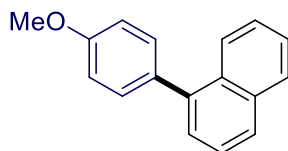
2-(4-Iodophenoxy)-1-(pyrrolidin-1-yl)ethan-1-one (66.2 mg, 0.2 mmol), (tetrahydrofuran-2-yl)methyl acrylate (62.5 mg, 59 μ L, 0.4 mmol), Pd(*t*Bu₃P)₂ (0.26 mg, 0.0005 mmol), LS2 (FcPAD₂P*t*Bu₂) (4.0 mg, 0.005 mmol), Fe NPs (2.8 mg, 1.8 mol % FeCl₃), K₃PO₄ (127.4 mg, 0.6 mmol) and NaCl (70.2 mg, 1.2 mmol) in 0.4 mL 2 wt % TPGS-750-M/H₂O with 0.04 mL DMF were reacted at 45 °C for 40 h yielding 63.9 mg (89%) of (tetrahydrofuran-2-yl)methyl (*E*)-3-(4-(2-oxo-2-(pyrrolidin-1-yl)ethoxy)phenyl)acrylate as a yellow oil (hexanes/EtOAc : 80/20).

¹H NMR (400 MHz, chloroform-*d*) δ 7.63 (d, *J* = 16.0 Hz, 1H), 7.44 (d, *J* = 8.7 Hz, 2H), 6.93 (d, *J* = 8.7 Hz, 2H), 6.34 (d, *J* = 16.0 Hz, 1H), 4.63 (s, 2H), 4.27 (dd, *J* = 11.2, 3.2 Hz, 1H), 4.17 (qd, *J* = 6.9, 3.3 Hz, 1H), 4.09 (dd, *J* = 11.1, 6.9 Hz, 1H), 3.90 (q, *J* = 6.8 Hz, 1H), 3.80 (q, *J* = 7.9, 7.5 Hz, 1H), 3.49 (q, *J* = 6.6 Hz, 4H), 1.92 (m, 7H), 1.63 (dq, *J* = 11.9, 7.2 Hz, 1H).

¹³C NMR (126 MHz, chloroform-*d*) δ 167.26, 166.08, 159.89, 144.61, 129.90, 128.03, 115.90, 115.12, 76.76, 68.58, 67.93, 66.60, 46.32, 46.07, 28.12, 26.35, 25.78, 23.89.

HRMS(ED): Calcd. for C₂₀H₂₅NO₅H⁺: 360.1811 Found: 360.1797.

1-(4-Methoxyphenyl)naphthalene (2.29)



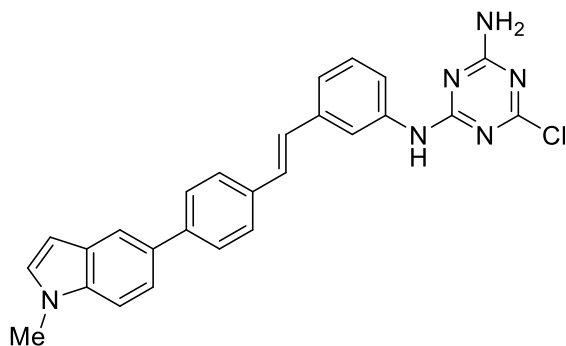
Following the procedure for a gram-scale reaction.

^1H NMR (400 MHz, chloroform-*d*) δ 7.98 – 7.89 (m, 2H), 7.85 (d, $J = 8.2$ Hz, 1H), 7.56 – 7.47 (m, 2H), 7.44 (m, 4H), 7.09 – 7.02 (m, 2H), 3.91 (s, 3H).

^{13}C NMR (101 MHz, chloroform-*d*) δ 159.09, 140.05, 133.98, 133.27, 131.97, 131.25, 128.40, 127.47, 127.05, 126.21, 126.06, 125.84, 125.54, 113.86, 55.50.

Spectral data matched those previously reported.¹¹

(*E*)-6-Chloro-*N*²-(3-(4-(1-methyl-1*H*-indol-5-yl)styryl)phenyl)-1,3,5-triazine-2,4-diamine (2.30)



Following the procedure for the one-pot sequence.

^1H NMR (400 MHz, DMSO-*d*₆) δ 9.98 (s, 1H), 8.00 (s, 1H), 7.91 – 7.84 (m, 1H), 7.75 – 7.59 (m, 6H), 7.59 – 7.54 (m, 1H), 7.51 (s, 2H), 7.36 (d, $J = 3.0$ Hz, 1H), 7.32 (m, 2H), 7.25 (s, 2H), 6.49 (d, $J = 3.1$ Hz, 1H), 3.82 (s, 3H).

^{13}C NMR (126 MHz, DMSO- d_6) δ 168.42, 166.96, 164.05, 140.92, 139.36, 137.58, 136.10, 134.95, 130.84, 130.44, 128.90, 128.65, 128.32, 127.96, 127.11, 126.83, 121.12, 120.21, 119.70, 118.43, 118.25, 110.17, 100.88, 32.59.

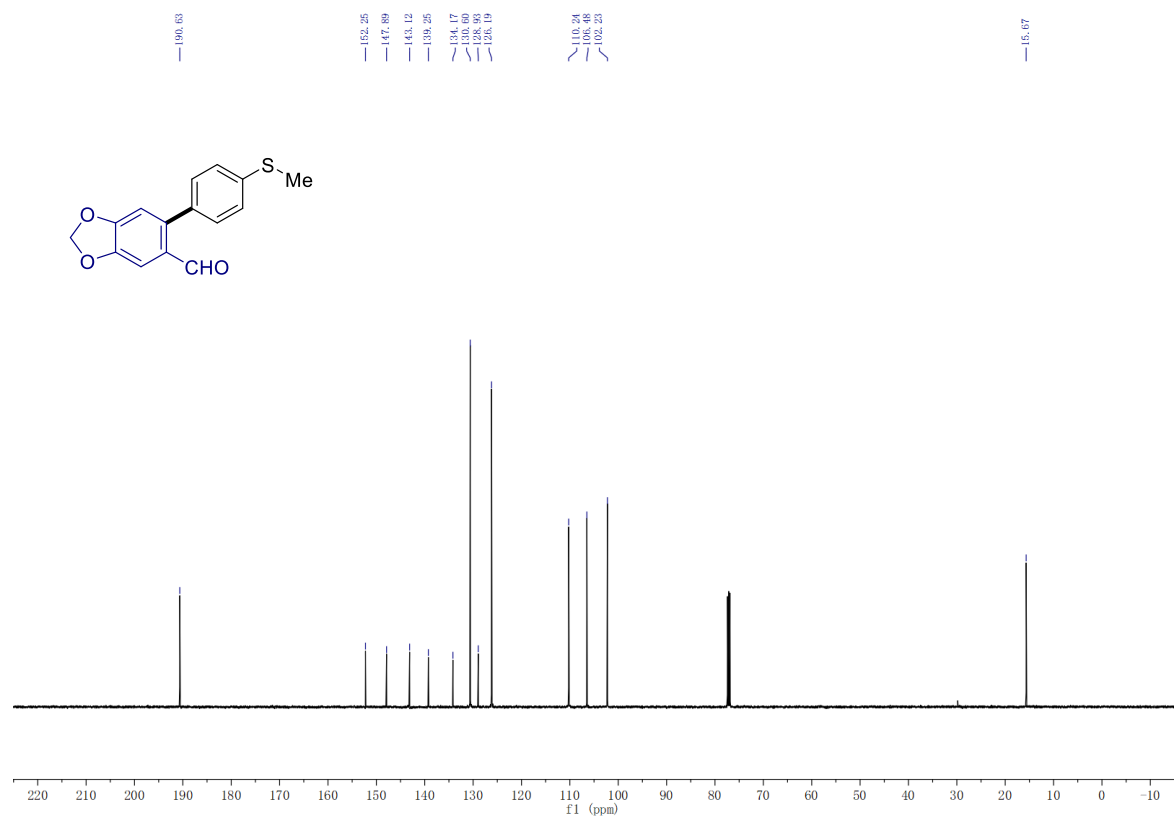
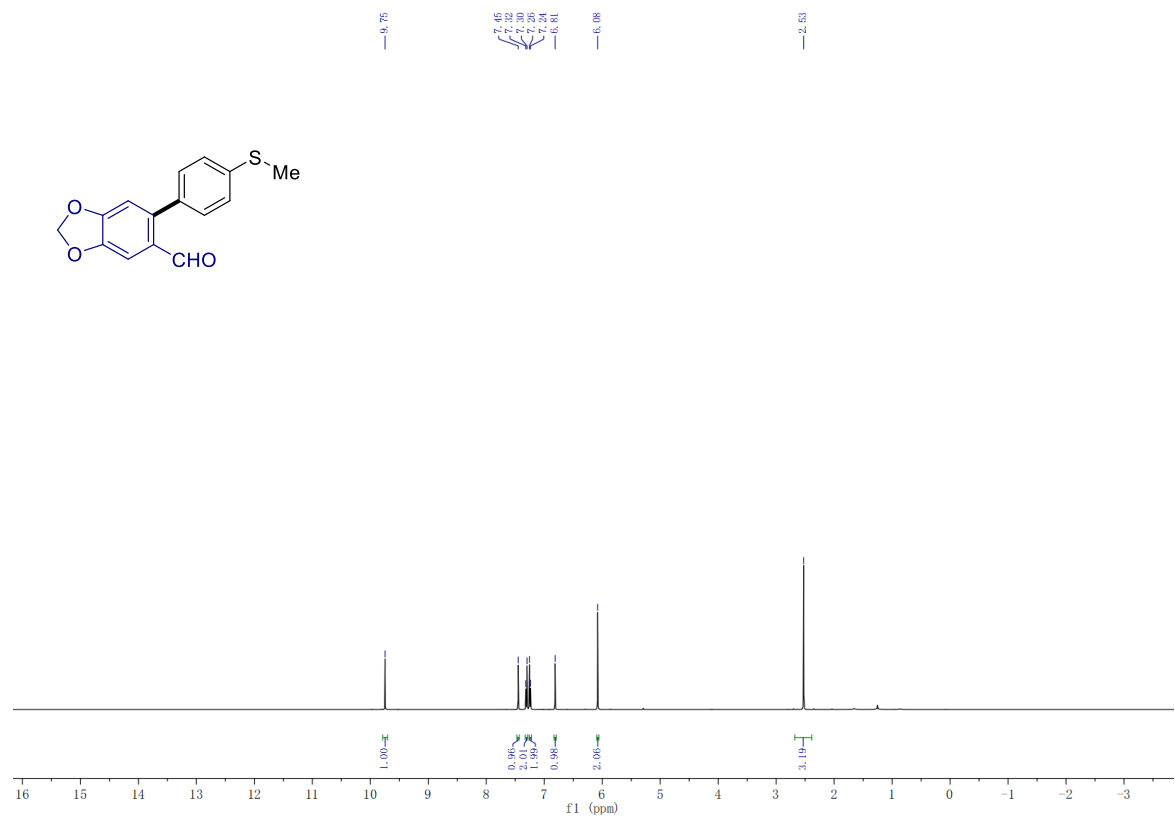
HRMS(ED): Calcd. for $\text{C}_{26}\text{H}_{21}\text{ClN}_6\text{H}^+$: 453.1595 Found: 453.1616

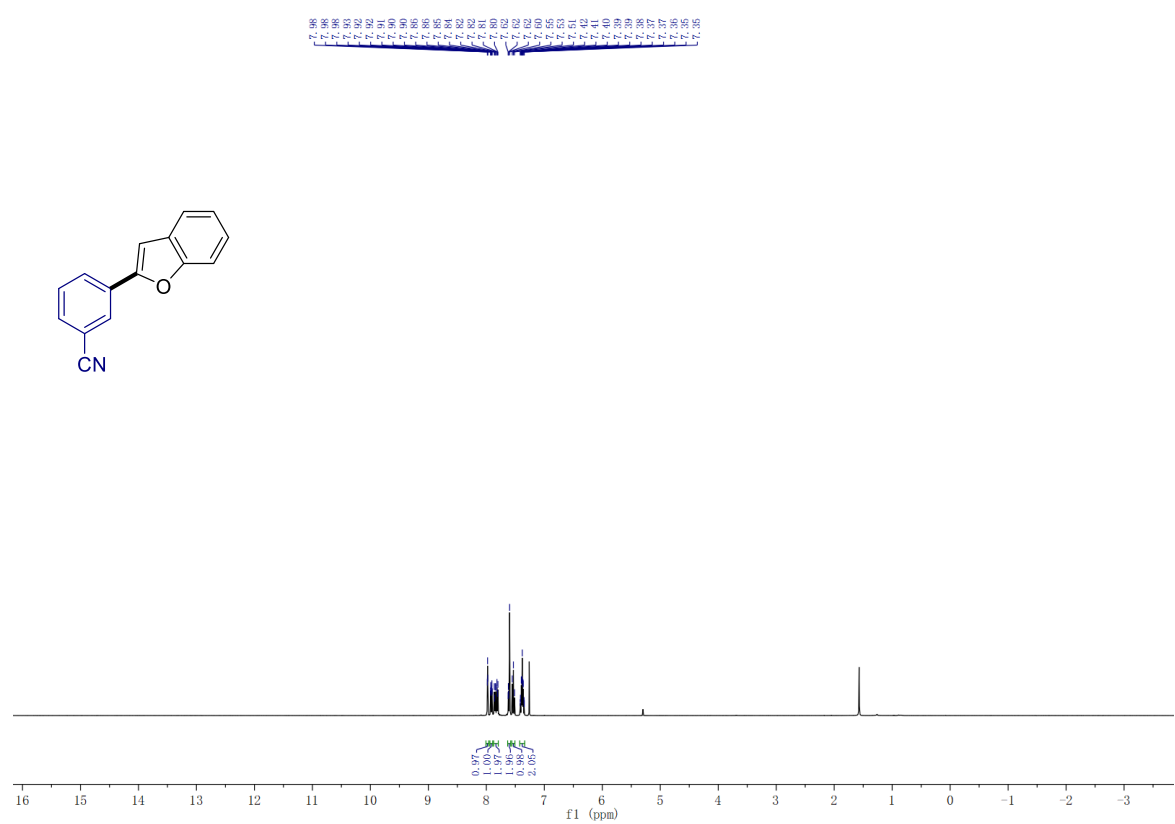
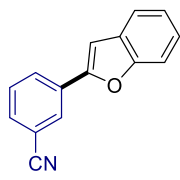
References

1. Lipshutz, B. H.; Ghorai, S.; Abela, A. R.; Moser, R.; Nishikata, T.; Duplais, C.; Krasovskiy, A.; Gaston, R. D.; Gadwood, R. C., TPGS-750-M: A Second-Generation Amphiphile for Metal-Catalyzed Cross-Couplings in Water at Room Temperature. *J. Org. Chem.* **2011**, *76*, 4379-4391.
2. Khanapure, S. P.; Garvey, D. S.; Young, D. V.; Ezawa, M.; Earl, R. A.; Gaston, R. D.; Fang, X.; Murty, M.; Martino, A.; Shumway, M.; Trocha, M.; Marek, P.; Tam, S. W.; Janero, D. R.; Letts, L. G., Synthesis and Structure–Activity Relationship of Novel, Highly Potent Metharyl and Methcycloalkyl Cyclooxygenase-2 (COX-2) Selective Inhibitors. *J. Med. Chem.* **2003**, *46*, 5484-5504.
3. Chakrabarty, I.; Akram, M. O.; Biswas, S.; Patil, N. T., Visible light mediated desilylative C(sp 2)–C(sp 2) cross-coupling reactions of arylsilanes with aryldiazonium salts under Au(i)/Au(iii) catalysis. *Chem. Commun.* **2018**, *54*, 7223-7226.
4. Ge, S.; Hartwig, J. F., Highly Reactive, Single-Component Nickel Catalyst Precursor for Suzuki–Miyaura Cross-Coupling of Heteroaryl Boronic Acids with Heteroaryl Halides. *Angew. Chem., Int. Ed.* **2012**, *51*, 12837-12841.
5. Fu, H.-Y.; Xu, N.; Pan, Y.-M.; Lu, X.-L.; Xia, M., Emission behaviours of novel V- and X-shaped fluorophores in response to pH and force stimuli. *Phys. Chem. Chem. Phys.* **2017**, *19*, 11563-11570.

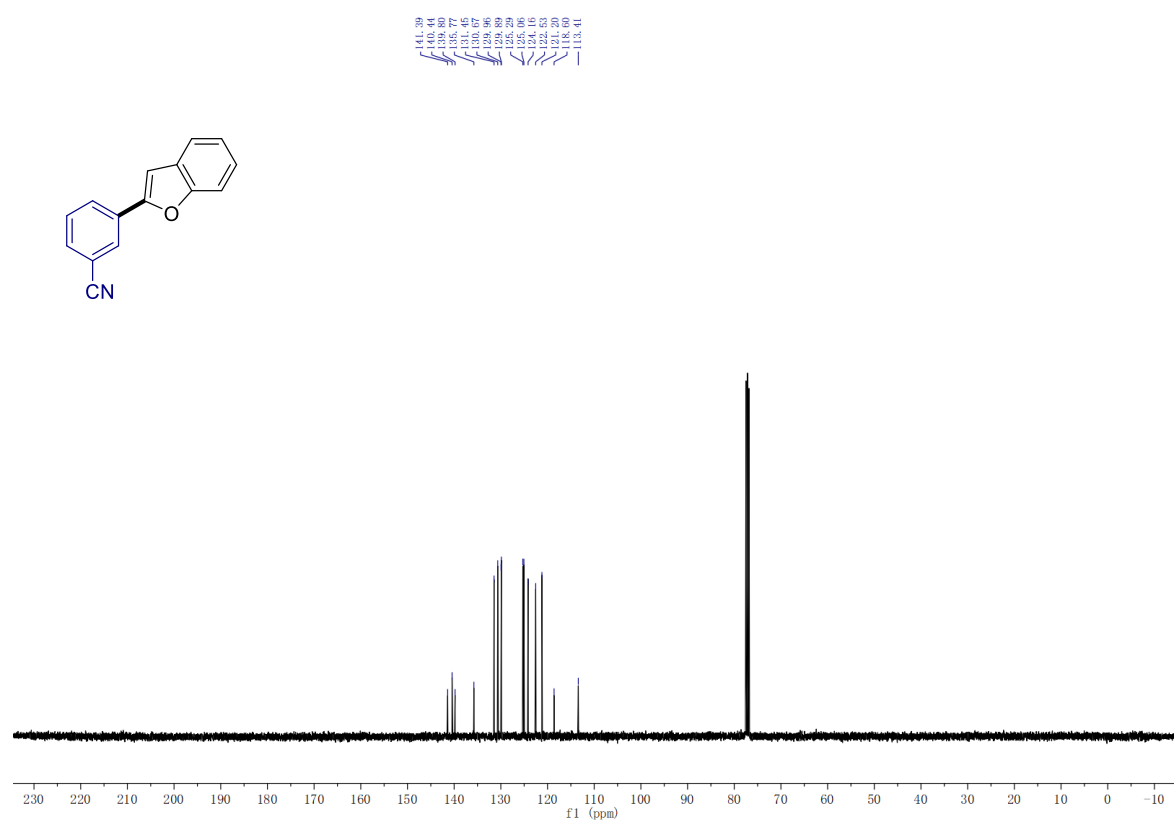
6. Mandali, P. K.; Chand, D. K., Palladium nanoparticles catalyzed Sonogashira reactions for the one-pot synthesis of symmetrical and unsymmetrical diarylacetylenes. *Catal. Commun.* **2014**, *47*, 40-44.
7. Lauer, M. G.; Thompson, M. K.; Shaughnessy, K. H., Controlling Olefin Isomerization in the Heck Reaction with Neopentyl Phosphine Ligands. *J. Org. Chem.* **2014**, *79*, 10837-10848.
8. Hu, Y.; Wong, M. J.; Lipshutz, B. H., ppm Pd-Containing Nanoparticles as Catalysts for Negishi Couplings ... in Water. *Angew. Chem., Int. Ed.* **2022**, *61*, e202209784.
9. Nie, X.; Liu, S.; Zong, Y.; Sun, P.; Bao, J., Facile synthesis of substituted alkynes by nano-palladium catalyzed oxidative cross-coupling reaction of arylboronic acids with terminal alkynes. *J. Organomet. Chem.* **2011**, *696*, 1570-1573.
10. Pang, H.; Hu, Y.; Yu, J.; Gallou, F.; Lipshutz, B. H., Water-Sculpting of a Heterogeneous Nanoparticle Precatalyst for Mizoroki–Heck Couplings under Aqueous Micellar Catalysis Conditions. *J. Am. Chem. Soc.* **2021**, *143*, 3373-3382.
11. Gu, Z.-S.; Shao, L.-X.; Lu, J.-M., NHC–Pd(II)–Im (NHC = N-heterocyclic carbene; Im = 1-methylimidazole) complex catalyzed Hiyama reaction of aryl chlorides with aryltrimethoxysilanes. *J. Organomet. Chem.* **2012**, *700*, 132-134.

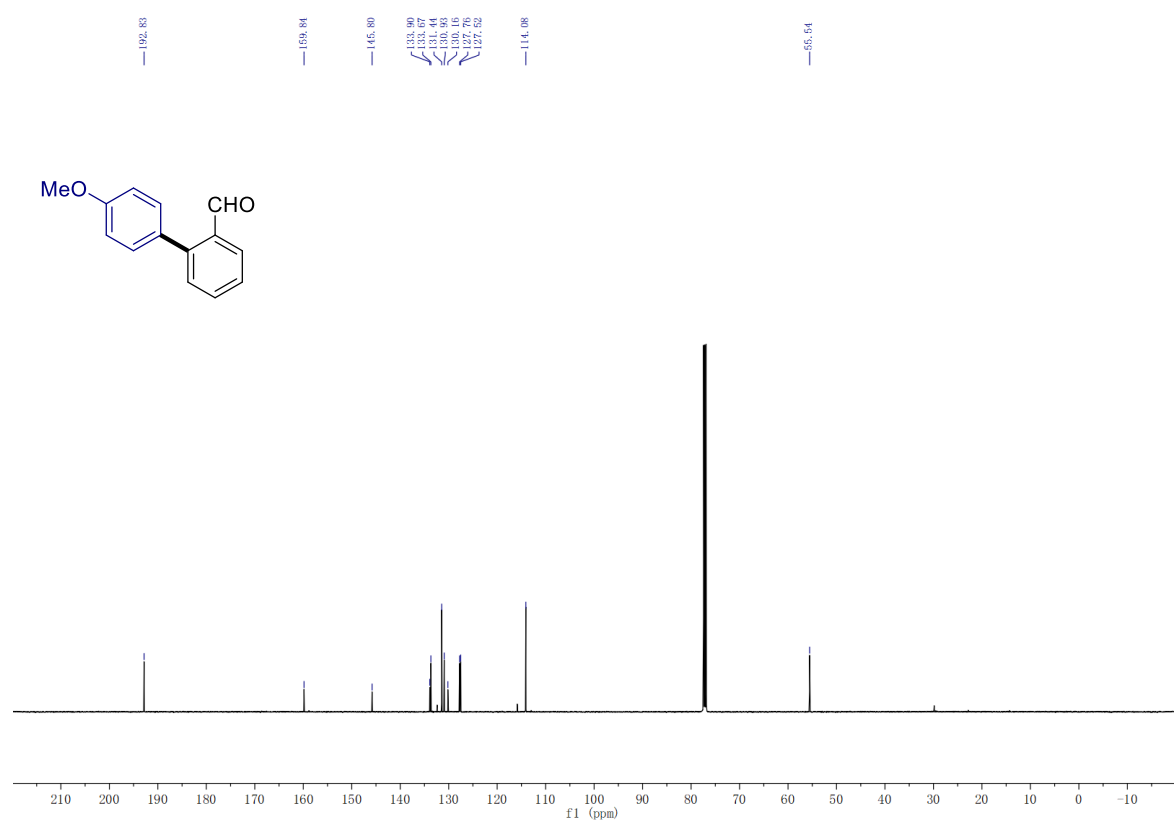
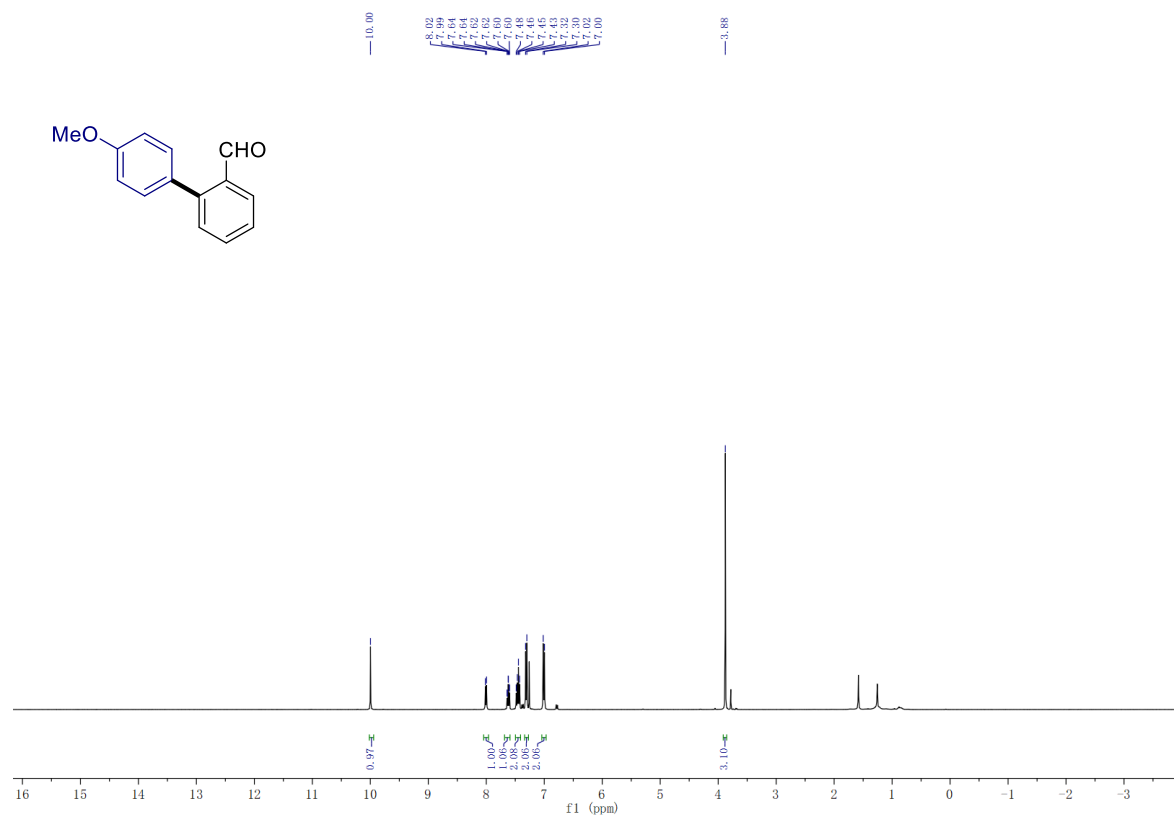


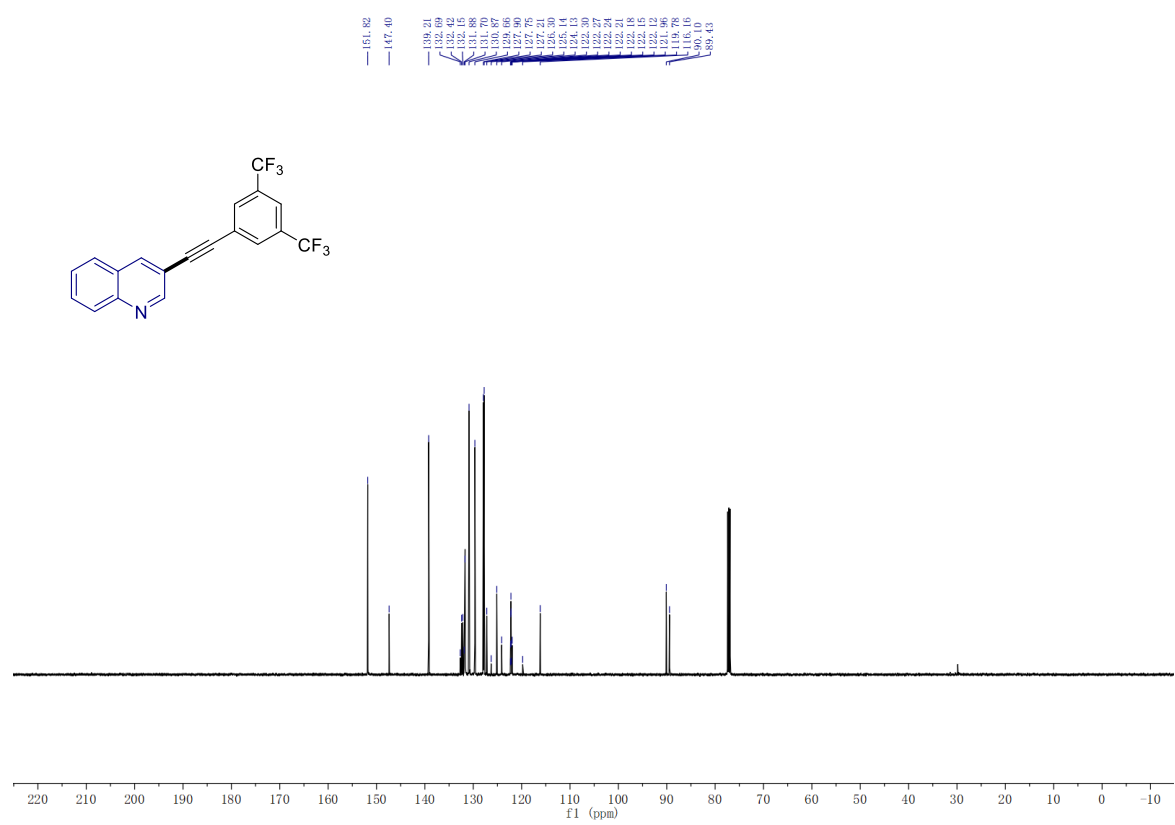
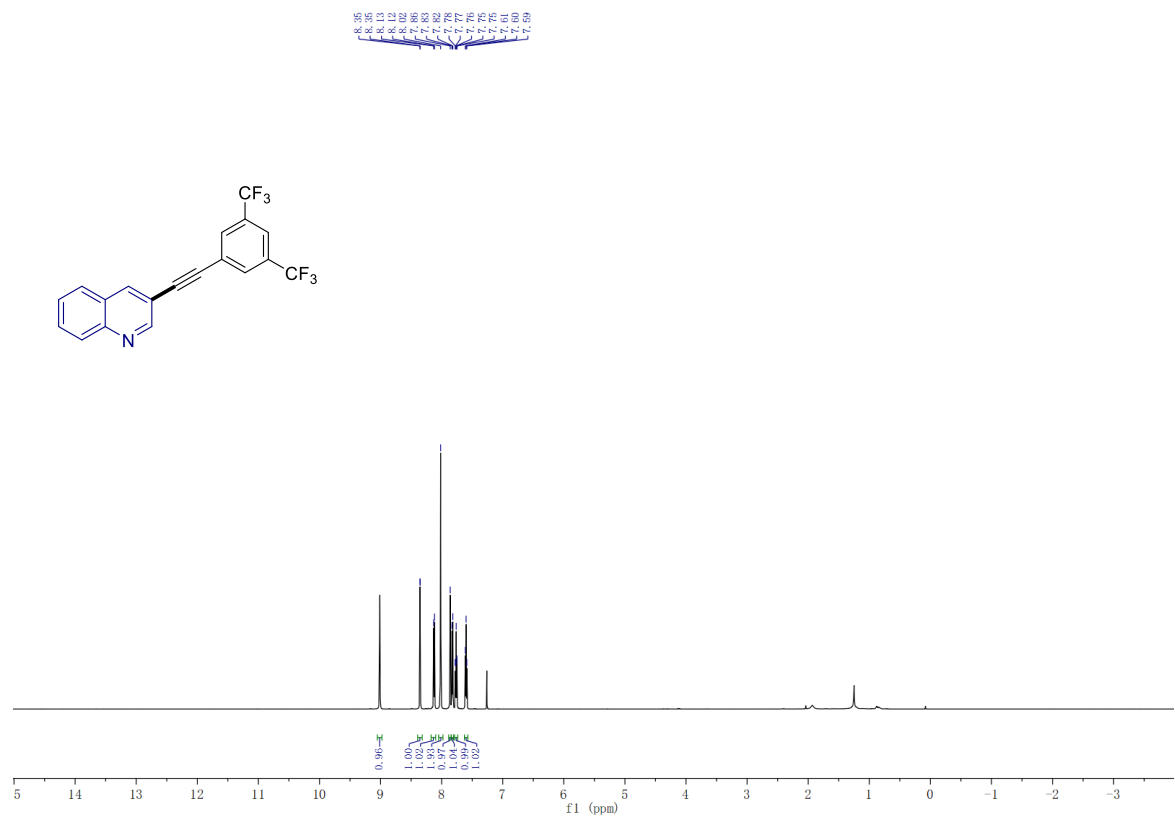


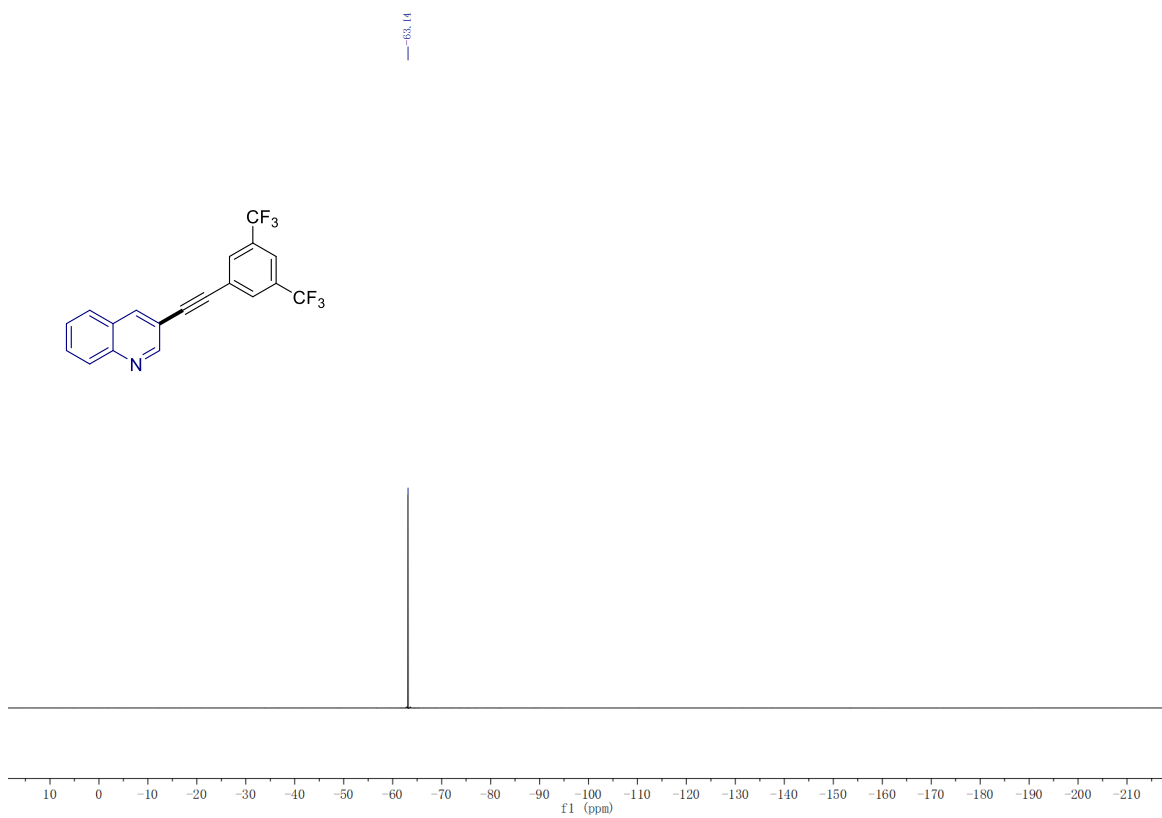


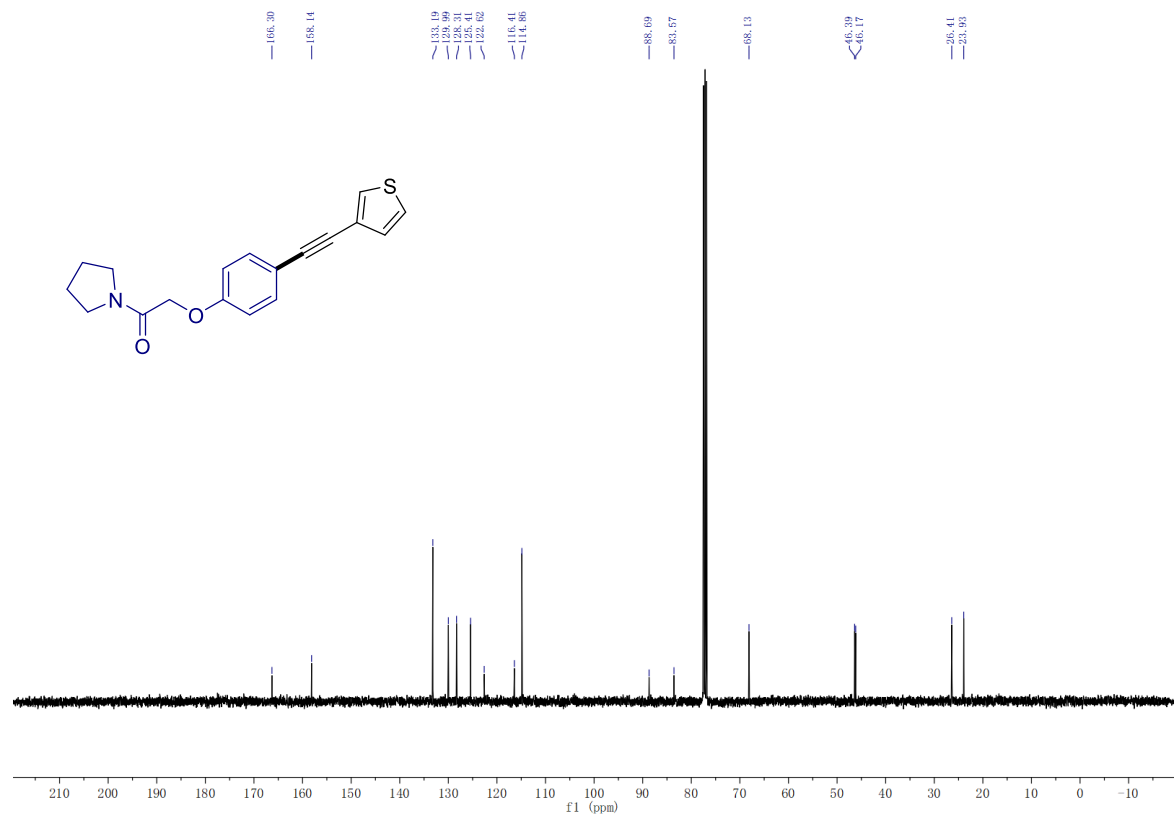
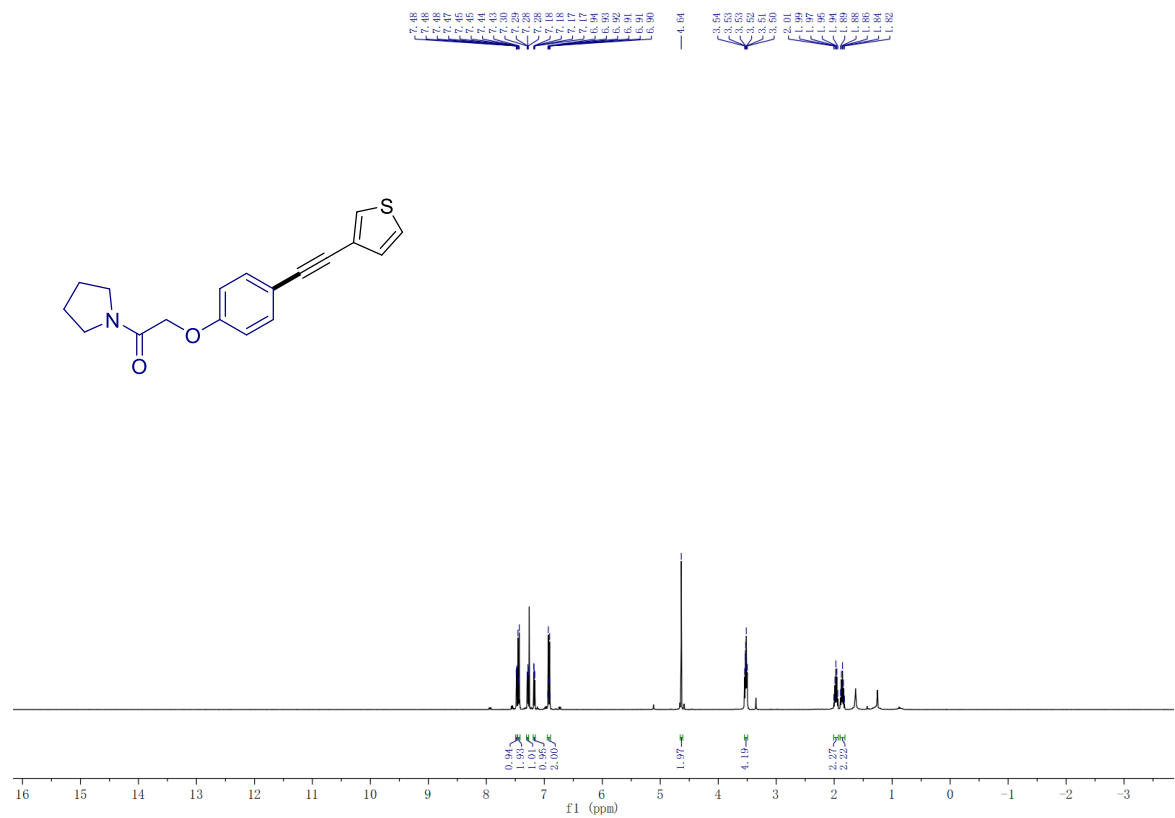
8.06, 7.98, 7.96, 7.95, 7.93, 7.92, 7.91, 7.90, 7.89, 7.88, 7.87, 7.86, 7.85, 7.84, 7.83, 7.82, 7.81, 7.80, 7.79, 7.78, 7.77, 7.76, 7.75, 7.74, 7.73, 7.72, 7.71, 7.70, 7.69, 7.68, 7.67, 7.66, 7.65, 7.64, 7.63, 7.62, 7.61, 7.60, 7.59, 7.58, 7.57, 7.56, 7.55, 7.54, 7.53, 7.52, 7.51, 7.50, 7.49, 7.48, 7.47, 7.46, 7.45, 7.44, 7.43, 7.42, 7.41, 7.40, 7.39, 7.38, 7.37, 7.36, 7.35, 7.34, 7.33, 7.32, 7.31, 7.30, 7.29, 7.28, 7.27, 7.26, 7.25, 7.24, 7.23, 7.22, 7.21, 7.20, 7.19, 7.18, 7.17, 7.16, 7.15, 7.14, 7.13, 7.12, 7.11, 7.10, 7.09, 7.08, 7.07, 7.06, 7.05, 7.04, 7.03, 7.02, 7.01, 7.00, 6.99, 6.98, 6.97, 6.96, 6.95, 6.94, 6.93, 6.92, 6.91, 6.90, 6.89, 6.88, 6.87, 6.86, 6.85, 6.84, 6.83, 6.82, 6.81, 6.80, 6.79, 6.78, 6.77, 6.76, 6.75, 6.74, 6.73, 6.72, 6.71, 6.70, 6.69, 6.68, 6.67, 6.66, 6.65, 6.64, 6.63, 6.62, 6.61, 6.60, 6.59, 6.58, 6.57, 6.56, 6.55, 6.54, 6.53, 6.52, 6.51, 6.50, 6.49, 6.48, 6.47, 6.46, 6.45, 6.44, 6.43, 6.42, 6.41, 6.40, 6.39, 6.38, 6.37, 6.36, 6.35, 6.34, 6.33, 6.32, 6.31, 6.30, 6.29, 6.28, 6.27, 6.26, 6.25, 6.24, 6.23, 6.22, 6.21, 6.20, 6.19, 6.18, 6.17, 6.16, 6.15, 6.14, 6.13, 6.12, 6.11, 6.10, 6.09, 6.08, 6.07, 6.06, 6.05, 6.04, 6.03, 6.02, 6.01, 6.00, 5.99, 5.98, 5.97, 5.96, 5.95, 5.94, 5.93, 5.92, 5.91, 5.90, 5.89, 5.88, 5.87, 5.86, 5.85, 5.84, 5.83, 5.82, 5.81, 5.80, 5.79, 5.78, 5.77, 5.76, 5.75, 5.74, 5.73, 5.72, 5.71, 5.70, 5.69, 5.68, 5.67, 5.66, 5.65, 5.64, 5.63, 5.62, 5.61, 5.60, 5.59, 5.58, 5.57, 5.56, 5.55, 5.54, 5.53, 5.52, 5.51, 5.50, 5.49, 5.48, 5.47, 5.46, 5.45, 5.44, 5.43, 5.42, 5.41, 5.40, 5.39, 5.38, 5.37, 5.36, 5.35, 5.34, 5.33, 5.32, 5.31, 5.30, 5.29, 5.28, 5.27, 5.26, 5.25, 5.24, 5.23, 5.22, 5.21, 5.20, 5.19, 5.18, 5.17, 5.16, 5.15, 5.14, 5.13, 5.12, 5.11, 5.10, 5.09, 5.08, 5.07, 5.06, 5.05, 5.04, 5.03, 5.02, 5.01, 5.00, 4.99, 4.98, 4.97, 4.96, 4.95, 4.94, 4.93, 4.92, 4.91, 4.90, 4.89, 4.88, 4.87, 4.86, 4.85, 4.84, 4.83, 4.82, 4.81, 4.80, 4.79, 4.78, 4.77, 4.76, 4.75, 4.74, 4.73, 4.72, 4.71, 4.70, 4.69, 4.68, 4.67, 4.66, 4.65, 4.64, 4.63, 4.62, 4.61, 4.60, 4.59, 4.58, 4.57, 4.56, 4.55, 4.54, 4.53, 4.52, 4.51, 4.50, 4.49, 4.48, 4.47, 4.46, 4.45, 4.44, 4.43, 4.42, 4.41, 4.40, 4.39, 4.38, 4.37, 4.36, 4.35, 4.34, 4.33, 4.32, 4.31, 4.30, 4.29, 4.28, 4.27, 4.26, 4.25, 4.24, 4.23, 4.22, 4.21, 4.20, 4.19, 4.18, 4.17, 4.16, 4.15, 4.14, 4.13, 4.12, 4.11, 4.10, 4.09, 4.08, 4.07, 4.06, 4.05, 4.04, 4.03, 4.02, 4.01, 4.00, 3.99, 3.98, 3.97, 3.96, 3.95, 3.94, 3.93, 3.92, 3.91, 3.90, 3.89, 3.88, 3.87, 3.86, 3.85, 3.84, 3.83, 3.82, 3.81, 3.80, 3.79, 3.78, 3.77, 3.76, 3.75, 3.74, 3.73, 3.72, 3.71, 3.70, 3.69, 3.68, 3.67, 3.66, 3.65, 3.64, 3.63, 3.62, 3.61, 3.60, 3.59, 3.58, 3.57, 3.56, 3.55, 3.54, 3.53, 3.52, 3.51, 3.50, 3.49, 3.48, 3.47, 3.46, 3.45, 3.44, 3.43, 3.42, 3.41, 3.40, 3.39, 3.38, 3.37, 3.36, 3.35, 3.34, 3.33, 3.32, 3.31, 3.30, 3.29, 3.28, 3.27, 3.26, 3.25, 3.24, 3.23, 3.22, 3.21, 3.20, 3.19, 3.18, 3.17, 3.16, 3.15, 3.14, 3.13, 3.12, 3.11, 3.10, 3.09, 3.08, 3.07, 3.06, 3.05, 3.04, 3.03, 3.02, 3.01, 3.00, 2.99, 2.98, 2.97, 2.96, 2.95, 2.94, 2.93, 2.92, 2.91, 2.90, 2.89, 2.88, 2.87, 2.86, 2.85, 2.84, 2.83, 2.82, 2.81, 2.80, 2.79, 2.78, 2.77, 2.76, 2.75, 2.74, 2.73, 2.72, 2.71, 2.70, 2.69, 2.68, 2.67, 2.66, 2.65, 2.64, 2.63, 2.62, 2.61, 2.60, 2.59, 2.58, 2.57, 2.56, 2.55, 2.54, 2.53, 2.52, 2.51, 2.50, 2.49, 2.48, 2.47, 2.46, 2.45, 2.44, 2.43, 2.42, 2.41, 2.40, 2.39, 2.38, 2.37, 2.36, 2.35, 2.34, 2.33, 2.32, 2.31, 2.30, 2.29, 2.28, 2.27, 2.26, 2.25, 2.24, 2.23, 2.22, 2.21, 2.20, 2.19, 2.18, 2.17, 2.16, 2.15, 2.14, 2.13, 2.12, 2.11, 2.10, 2.09, 2.08, 2.07, 2.06, 2.05, 2.04, 2.03, 2.02, 2.01, 2.00, 1.99, 1.98, 1.97, 1.96, 1.95, 1.94, 1.93, 1.92, 1.91, 1.90, 1.89, 1.88, 1.87, 1.86, 1.85, 1.84, 1.83, 1.82, 1.81, 1.80, 1.79, 1.78, 1.77, 1.76, 1.75, 1.74, 1.73, 1.72, 1.71, 1.70, 1.69, 1.68, 1.67, 1.66, 1.65, 1.64, 1.63, 1.62, 1.61, 1.60, 1.59, 1.58, 1.57, 1.56, 1.55, 1.54, 1.53, 1.52, 1.51, 1.50, 1.49, 1.48, 1.47, 1.46, 1.45, 1.44, 1.43, 1.42, 1.41, 1.40, 1.39, 1.38, 1.37, 1.36, 1.35, 1.34, 1.33, 1.32, 1.31, 1.30, 1.29, 1.28, 1.27, 1.26, 1.25, 1.24, 1.23, 1.22, 1.21, 1.20, 1.19, 1.18, 1.17, 1.16, 1.15, 1.14, 1.13, 1.12, 1.11, 1.10, 1.09, 1.08, 1.07, 1.06, 1.05, 1.04, 1.03, 1.02, 1.01, 1.00, 0.99, 0.98, 0.97, 0.96, 0.95, 0.94, 0.93, 0.92, 0.91, 0.90, 0.89, 0.88, 0.87, 0.86, 0.85, 0.84, 0.83, 0.82, 0.81, 0.80, 0.79, 0.78, 0.77, 0.76, 0.75, 0.74, 0.73, 0.72, 0.71, 0.70, 0.69, 0.68, 0.67, 0.66, 0.65, 0.64, 0.63, 0.62, 0.61, 0.60, 0.59, 0.58, 0.57, 0.56, 0.55, 0.54, 0.53, 0.52, 0.51, 0.50, 0.49, 0.48, 0.47, 0.46, 0.45, 0.44, 0.43, 0.42, 0.41, 0.40, 0.39, 0.38, 0.37, 0.36, 0.35, 0.34, 0.33, 0.32, 0.31, 0.30, 0.29, 0.28, 0.27, 0.26, 0.25, 0.24, 0.23, 0.22, 0.21, 0.20, 0.19, 0.18, 0.17, 0.16, 0.15, 0.14, 0.13, 0.12, 0.11, 0.10, 0.09, 0.08, 0.07, 0.06, 0.05, 0.04, 0.03, 0.02, 0.01, 0.00, -0.01, -0.02, -0.03, -0.04, -0.05, -0.06, -0.07, -0.08, -0.09, -0.10, -0.11, -0.12, -0.13, -0.14, -0.15, -0.16, -0.17, -0.18, -0.19, -0.20, -0.21, -0.22, -0.23, -0.24, -0.25, -0.26, -0.27, -0.28, -0.29, -0.30, -0.31, -0.32, -0.33, -0.34, -0.35, -0.36, -0.37, -0.38, -0.39, -0.40, -0.41, -0.42, -0.43, -0.44, -0.45, -0.46, -0.47, -0.48, -0.49, -0.50, -0.51, -0.52, -0.53, -0.54, -0.55, -0.56, -0.57, -0.58, -0.59, -0.60, -0.61, -0.62, -0.63, -0.64, -0.65, -0.66, -0.67, -0.68, -0.69, -0.70, -0.71, -0.72, -0.73, -0.74, -0.75, -0.76, -0.77, -0.78, -0.79, -0.80, -0.81, -0.82, -0.83, -0.84, -0.85, -0.86, -0.87, -0.88, -0.89, -0.90, -0.91, -0.92, -0.93, -0.94, -0.95, -0.96, -0.97, -0.98, -0.99, -1.00, -1.01, -1.02, -1.03, -1.04, -1.05, -1.06, -1.07, -1.08, -1.09, -1.10, -1.11, -1.12, -1.13, -1.14, -1.15, -1.16, -1.17, -1.18, -1.19, -1.20, -1.21, -1.22, -1.23, -1.24, -1.25, -1.26, -1.27, -1.28, -1.29, -1.30, -1.31, -1.32, -1.33, -1.34, -1.35, -1.36, -1.37, -1.38, -1.39, -1.40, -1.41, -1.42, -1.43, -1.44, -1.45, -1.46, -1.47, -1.48, -1.49, -1.50, -1.51, -1.52, -1.53, -1.54, -1.55, -1.56, -1.57, -1.58, -1.59, -1.60, -1.61, -1.62, -1.63, -1.64, -1.65, -1.66, -1.67, -1.68, -1.69, -1.70, -1.71, -1.72, -1.73, -1.74, -1.75, -1.76, -1.77, -1.78, -1.79, -1.80, -1.81, -1.82, -1.83, -1.84, -1.85, -1.86, -1.87, -1.88, -1.89, -1.90, -1.91, -1.92, -1.93, -1.94, -1.95, -1.96, -1.97, -1.98, -1.99, -2.00, -2.01, -2.02, -2.03, -2.04, -2.05, -2.06, -2.07, -2.08, -2.09, -2.10, -2.11, -2.12, -2.13, -2.14, -2.15, -2.16, -2.17, -2.18, -2.19, -2.20, -2.21, -2.22, -2.23, -2.24, -2.25, -2.26, -2.27, -2.28, -2.29, -2.30, -2.31, -2.32, -2.33, -2.34, -2.35, -2.36, -2.37, -2.38, -2.39, -2.40, -2.41, -2.42, -2.43, -2.44, -2.45, -2.46, -2.47, -2.48, -2.49, -2.50, -2.51, -2.52, -2.53, -2.54, -2.55, -2.56, -2.57, -2.58, -2.59, -2.60, -2.61, -2.62, -2.63, -2.64, -2.65, -2.66, -2.67, -2.68, -2.69, -2.70, -2.71, -2.72, -2.73, -2.74, -2.75, -2.76, -2.77, -2.78, -2.79, -2.80, -2.81, -2.82, -2.83, -2.84, -2.85, -2.86, -2.87, -2.88, -2.89, -2.90, -2.91, -2.92, -2.93, -2.94, -2.95, -2.96, -2.97, -2.98, -2.99, -3.00, -3.01, -3.02, -3.03, -3.04, -3.05, -3.06, -3.07, -3.08, -3.09, -3.10, -3.11, -3.12, -3.13, -3.14, -3.15, -3.16, -3.17, -3.18, -3.19, -3.20, -3.21, -3.22, -3.23, -3.24, -3.25, -3.26, -3.27, -3.28, -3.29, -3.30, -3.31, -3.32, -3.33, -3.34, -3.35, -3.36, -3.37, -3.38, -3.39, -3.40, -3.41, -3.42, -3.43, -3.44, -3.45, -3.46, -3.47, -3.48, -3.49, -3.50, -3.51, -3.52, -3.53, -3.54, -3.55, -3.56, -3.57, -3.58, -3.59, -3.60, -3.61, -3.62, -3.63, -3.64, -3.65, -3.66, -3.67, -3.68, -3.69, -3.70, -3.71, -3.72, -3.73, -3.74, -3.75, -3.76, -3.77, -3.78, -3.79, -3.80, -3.81, -3.82, -3.83, -3.84, -3.85, -3.86, -3.87, -3.88, -3.89, -3.90, -3.91, -3.92, -3.93, -3.94, -3.95, -3.96, -3.97, -3.98, -3.99, -4.00, -4.01, -4.02, -4.03, -4.04, -4.05, -4.06, -4.07, -4.08, -4.09, -4.10, -4.11, -4.12, -4.13, -4.14, -4.15, -4.16, -4.17, -4.18, -4.19, -4.20, -4.21, -4.22, -4.23, -4.24, -4.25, -4.26, -4.27, -4.28, -4.29, -4.30, -4.31, -4.32, -4.33, -4.34, -4.35, -4.36, -4.37, -4.38, -4.39, -4.40, -4.41, -4.42, -4.43, -4.44, -4.45, -4.46, -4.47, -4.48, -4.49, -4.50, -4.51, -4.52, -4.53, -4.54, -4.55, -4.56, -4.57, -4.58, -4.59, -4.60, -4.61, -4.62, -4.63, -4.64, -4.65, -4.66, -4.67, -4.68, -4.69, -4.70, -4.71, -4.72, -4.73, -4.74, -4.75, -4.76, -4.77, -4.78, -4.79, -4.80, -4.81, -4.82, -4.83, -4.84, -4.85, -4.86, -4.87, -4.88, -4.89, -4.90, -4.91, -4.92, -4.93, -4.94, -4.95, -4.96, -4.97, -4.98, -4.99, -5.00, -5.01, -5.02, -5.03, -5.04, -5.05, -5.06, -5.07, -5.08, -5.09, -5.10, -5.11, -5.12, -5.13, -5.14, -5.15, -5.16, -5.17, -5.18, -5.19, -5.20, -5.21, -5.22, -5.23, -5.24, -5.25, -5.26, -5.27, -5.28, -5.29, -5.30, -5.31, -5.32, -5.33, -5.34, -5.35, -5.36, -5.37, -5.38, -5.39, -5.40, -5.41, -5.42, -5.43, -5.44, -5.45, -5.46, -5.47, -5.48, -5.49, -5.50, -5.51, -5.52, -5.53, -5.54, -5.55, -5.56, -5.57, -5.58, -5.59, -5.60, -5.61, -5.62, -5.63, -5.64, -5.65, -5.66, -5.67, -5.68, -5.69, -5.70, -5.71, -5.72, -5.73, -5.74, -5.75, -5.76, -5.77, -5.78, -5.79, -5.80, -5.81, -5.82, -5.83, -5.84, -5.85, -5.86, -5.87, -5.88, -5.89, -5.90, -5.91, -5.92, -5.93, -5.94, -5.95, -5.96, -5.97, -5.98, -5.99, -6.00, -6.01, -6.02, -6.03, -6.04, -6.05, -6.06, -6.07, -6.08, -6.09, -6.10, -6.11, -6.12, -6.13, -6.14, -6.15, -6.16, -6.17, -6.18, -6.19, -6.20, -6.21, -6.22, -6.23, -6.24, -6.25, -6.26, -6.27, -6.28, -6.29, -6.30, -6.31, -6.32, -6.33, -6.34, -6.35, -6.36, -6.37, -6.38, -6.39, -6.40, -6.41, -6.42, -6.43, -6.44, -6.45, -6.46, -6.47, -6.48, -6.49, -6.50, -6.51, -6.52, -6.53, -6.54, -6.55, -6.56, -6.57, -6.58, -6.59, -6.60, -6.61, -6.62, -6.63, -6.64, -6.65, -6.66, -6.67, -6.68, -6.69, -6.70, -6.71, -6.72, -6.73, -6.74, -6.75, -6.76, -6.77, -6.78, -6.79, -6.80, -6.81, -6.82, -6.83, -6.84, -6.85, -6.86, -6.87, -6.88, -6.89, -6.90, -6.91, -6.92, -6.93, -6.94, -6.95, -6.96, -6.97, -6.98, -6.99, -7.00, -7.01, -7.02, -7.03, -7.04, -7.05, -7.06, -7.07, -7.08, -7.09, -7.10, -7.11, -7.12, -7.13, -7.14, -7.15, -7.16, -7.17, -7.18, -7.19, -7.20, -7.21, -7.22, -7.23, -7.24, -7.25, -7.26, -7.27, -7.28, -7.29, -7.30, -7.31, -7.32, -7.33, -7.34, -7.35, -7.36, -7.37, -7.38, -7.39, -7.40, -7.41, -7.42, -7.43, -7.44, -7.45, -7.46, -7.47, -7.48, -7.49, -7.50, -7.51, -7.52, -7.53, -7.54, -7.55, -7.56, -7.57, -7.58, -7.59, -7.60, -7.61, -7.62, -7.63, -7.64, -7.65, -7.66, -7.67, -7.68, -7.69, -7.70, -7.71, -7.72, -7.73, -7.74, -7.75, -7.76, -7.77, -7.78, -7.79, -7.80, -7.81, -7.82, -7.83, -7.84, -7.85, -7.86, -7.87, -7.88, -7.89, -7.90, -7.91, -7.92, -7.93, -7.94, -7.95, -7.96, -7.97, -7.98, -7.99, -8.00, -8.01, -8.02, -8.03, -8.04, -8.05, -8.06, -8.07, -8.08, -8.09, -8.10, -8.11, -8.12, -8.13, -8.14, -8.15, -8.16, -8.17, -8.18, -8.19, -8.20, -8.21, -8.22, -8.23, -8.24, -8.25, -8.26, -8.27, -8.28, -8.29, -8.30, -8.31, -8.32, -8.33, -8.34, -8.35, -8.36, -8.37, -8.38, -8.39, -8.40, -8.41, -8.42, -8.43, -8.44, -8.45, -8.46, -8.47, -8.48, -8.49, -8.50, -8.51, -8.52, -8.53, -8.54, -8.55, -8.56, -8.57, -8.58, -8.59, -8.60, -8.61, -8.62, -8.63, -8.64, -8.65, -8.66, -8.67, -8.68, -8.69, -8.70, -8.71, -8.72, -8.73, -8.74, -8.75, -8.76, -8.77, -8.78, -8.79, -8.80, -8.81, -8.82, -8.83, -8.84, -8.85, -8.86, -8.87, -8.88, -8.89, -8.90, -8.91, -8.92, -8.93, -8.94, -8.95, -8.96, -8.97, -8.98, -8.99, -9.00, -9.01, -9.02, -9.03, -9.04, -9.05, -9.06, -9.07, -9.08, -9.09, -9.10, -9.11, -9.12, -9.13, -9.14, -9.15, -9.16, -9.17, -9.18, -9.19, -9.20, -9.21, -9.22, -9.23, -9.24, -9.25, -9.26, -9.27, -9.28, -9.29, -9.30, -9.31, -9.32, -9.33, -9.34, -9.35, -9.36, -9.37, -9.38, -9.39, -9.40, -9.41, -9.42, -9.43, -9.44, -9.45, -9.46, -9.47, -9.48, -9.49, -9.50, -9.51, -9.52, -9.53, -9.54, -9.55, -9.56, -9.57, -9.58, -9.59, -9.60, -9.61, -9.62, -9.63, -9.64, -9.65, -9.66, -9.67, -9.68, -9.69, -9.70, -9.71, -9.72, -9.73, -9.74, -9.75, -9.76, -9.77, -9.78, -9.79, -9.80, -9.81, -9.82, -9.83, -9.84, -9.85, -9.86, -9.87, -9.88, -9.89, -9.90, -9.91, -9.92, -9.93, -9.94, -9.95, -9.96, -9.97, -9.98, -9.99, -10.00.

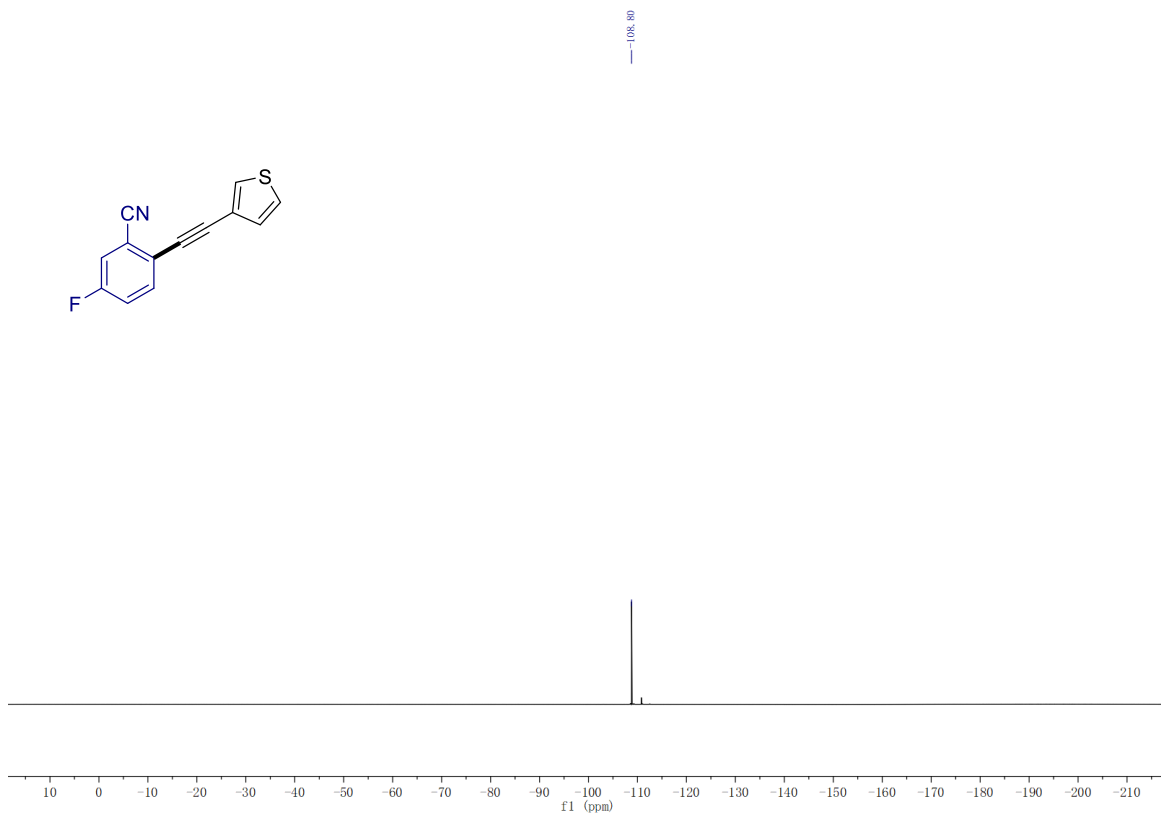
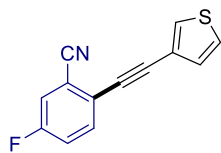


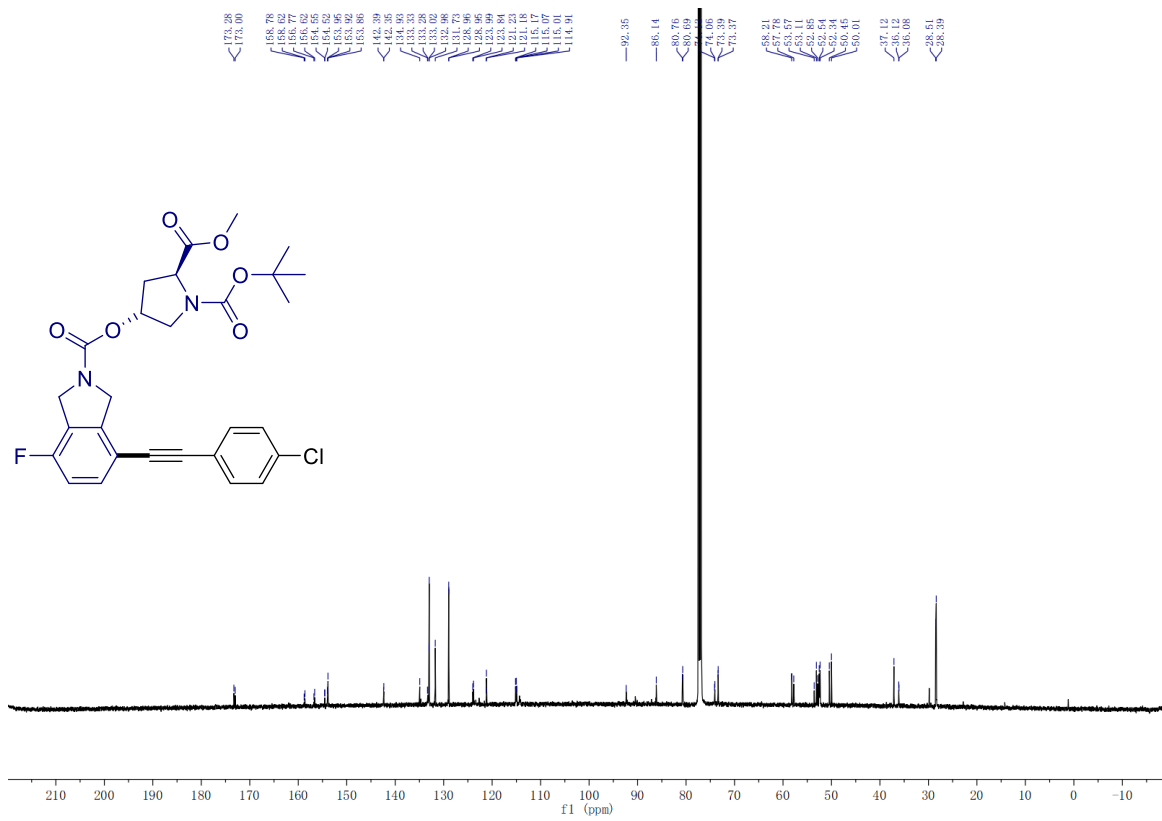
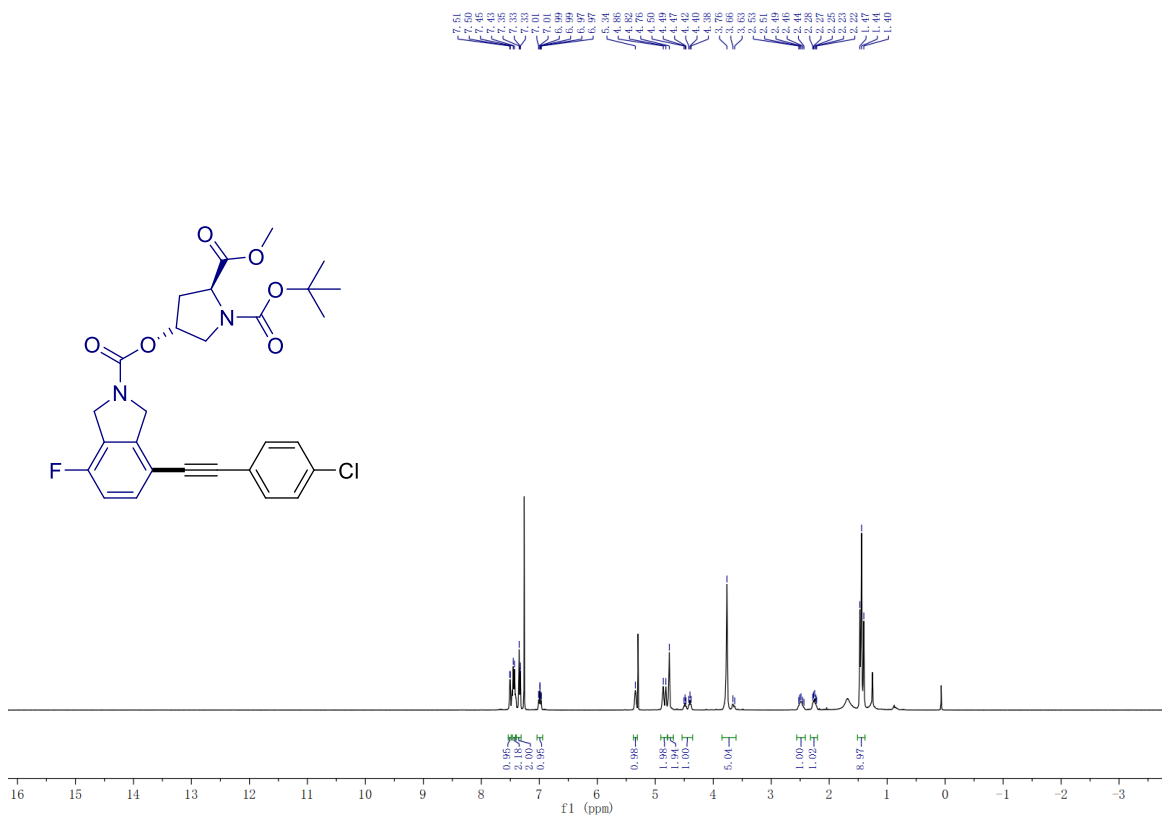


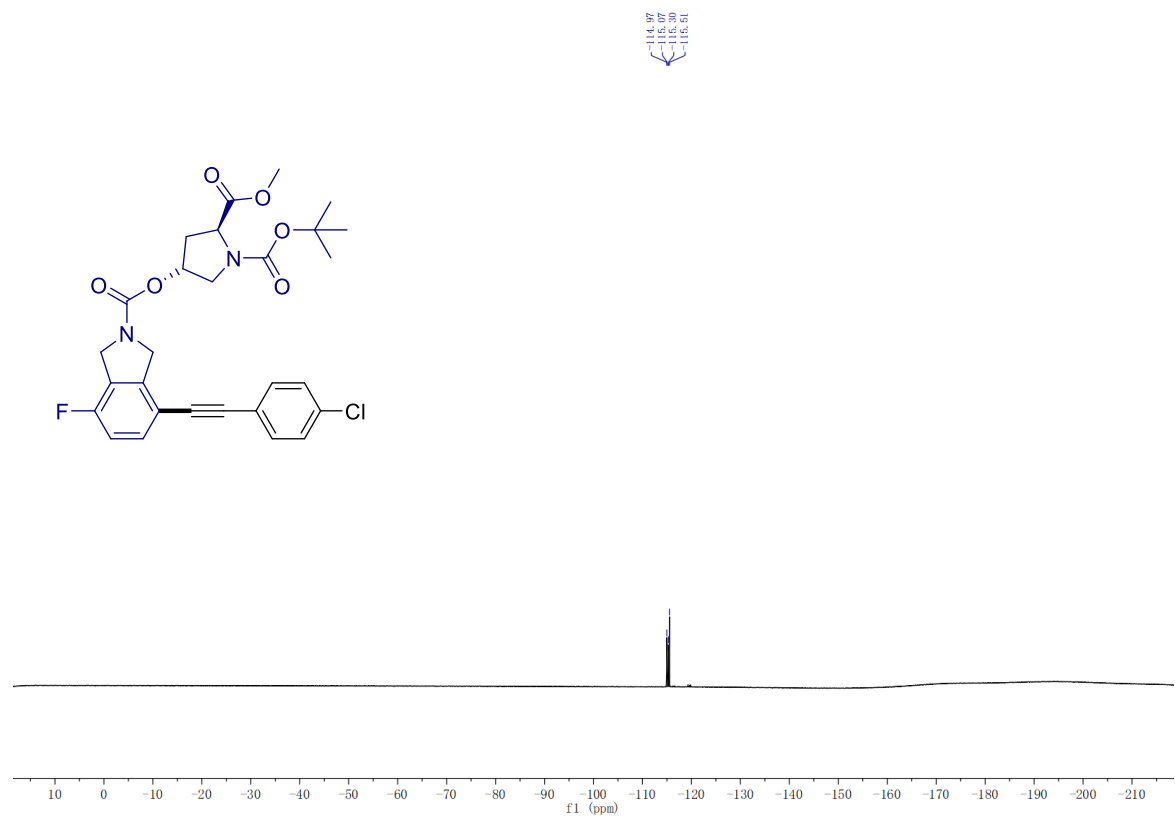


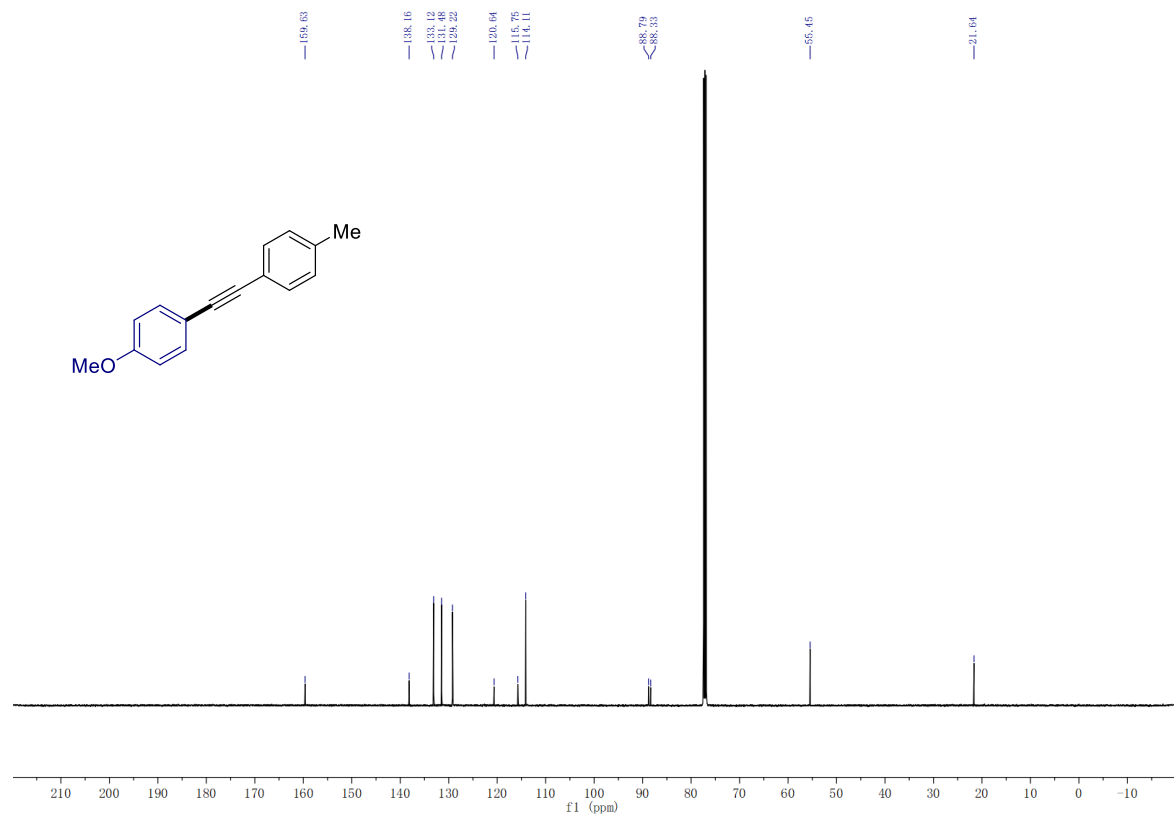
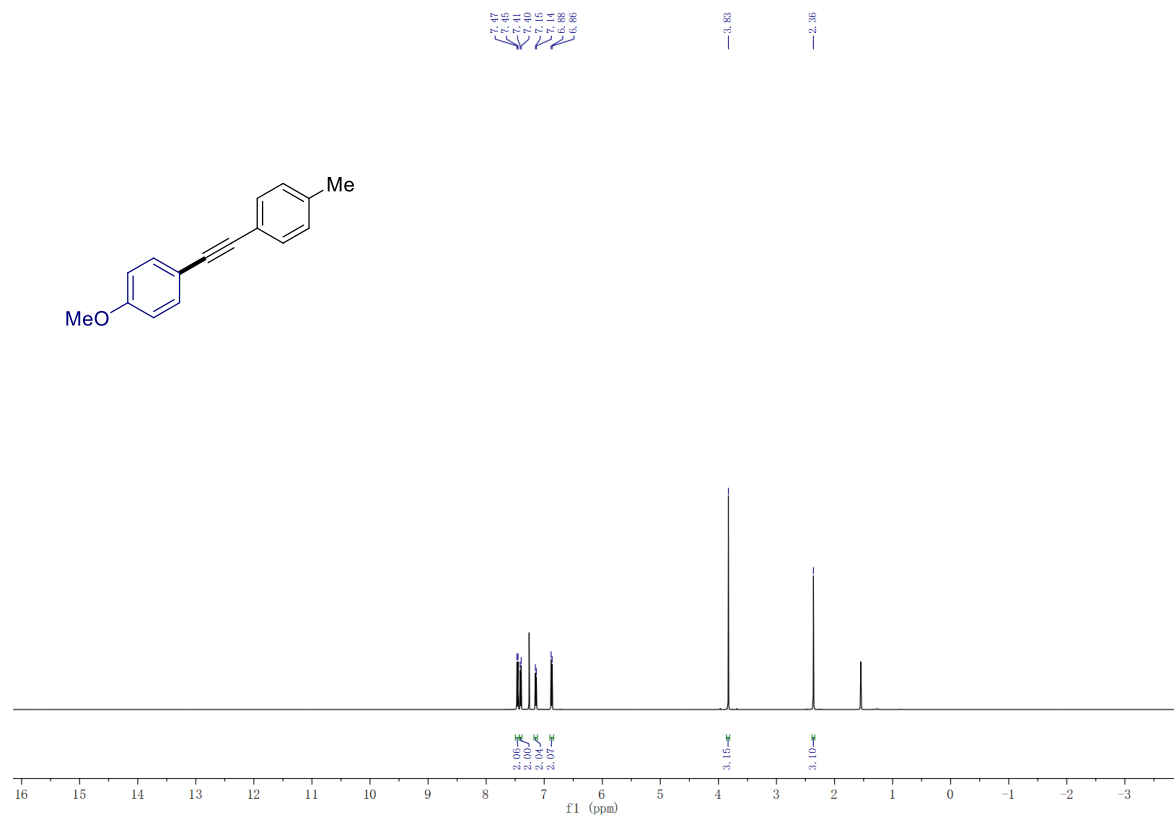


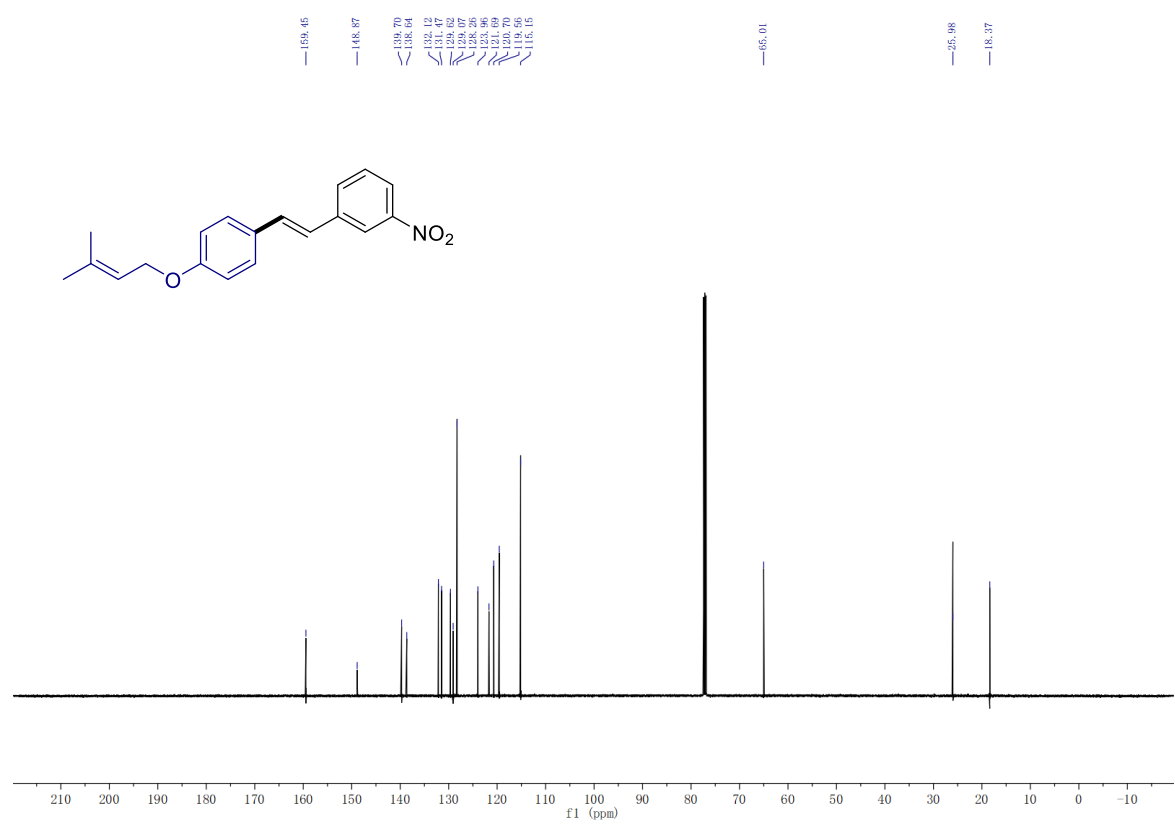
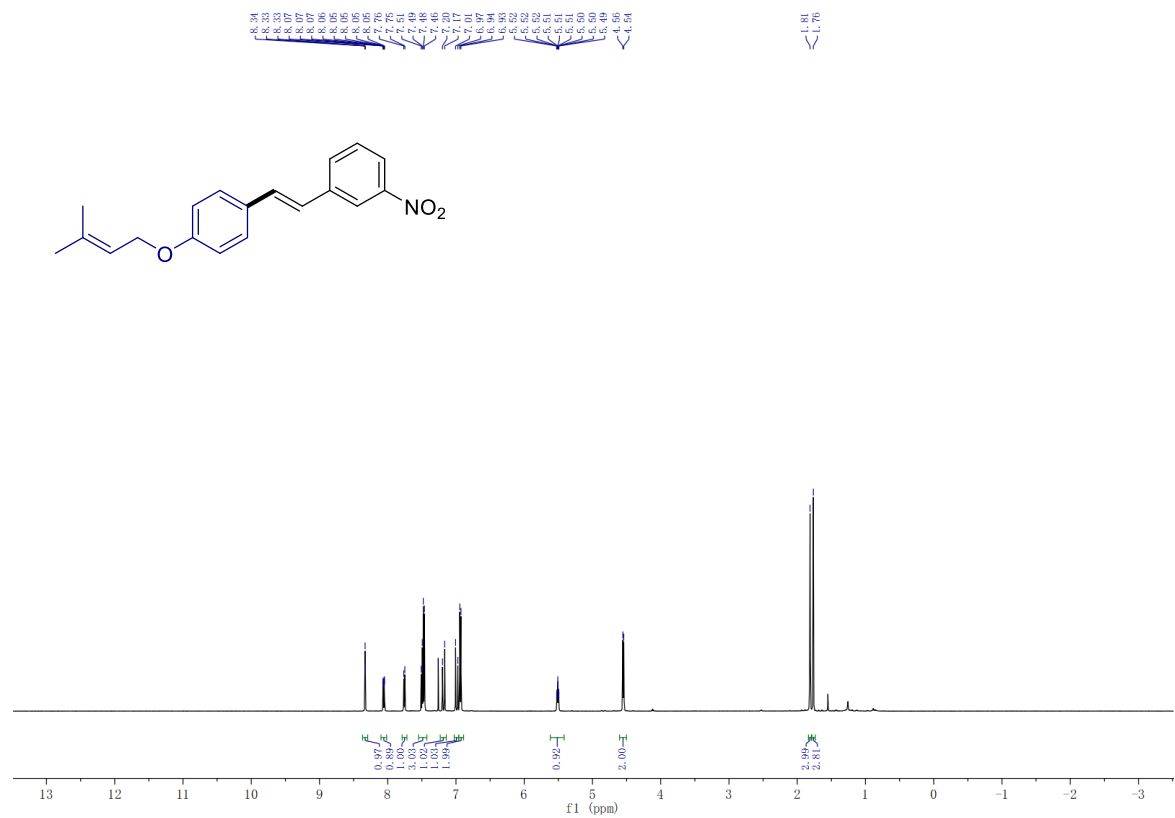


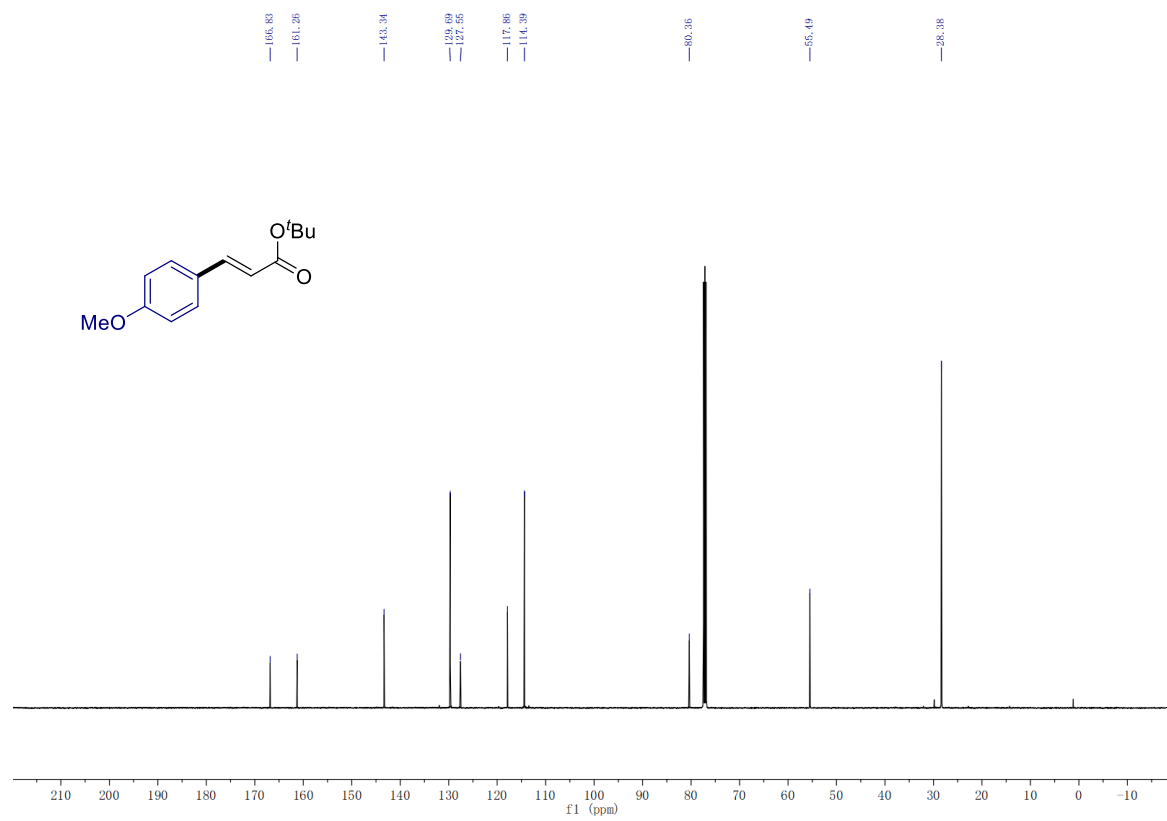
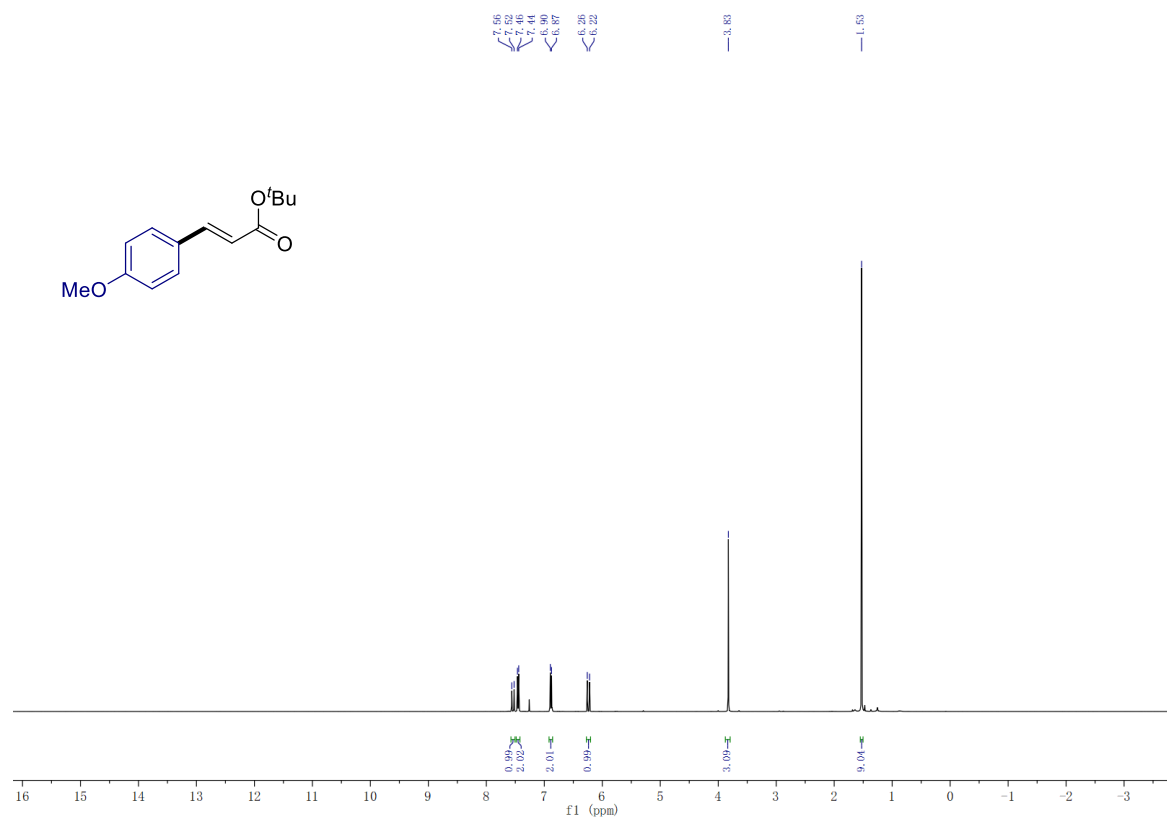


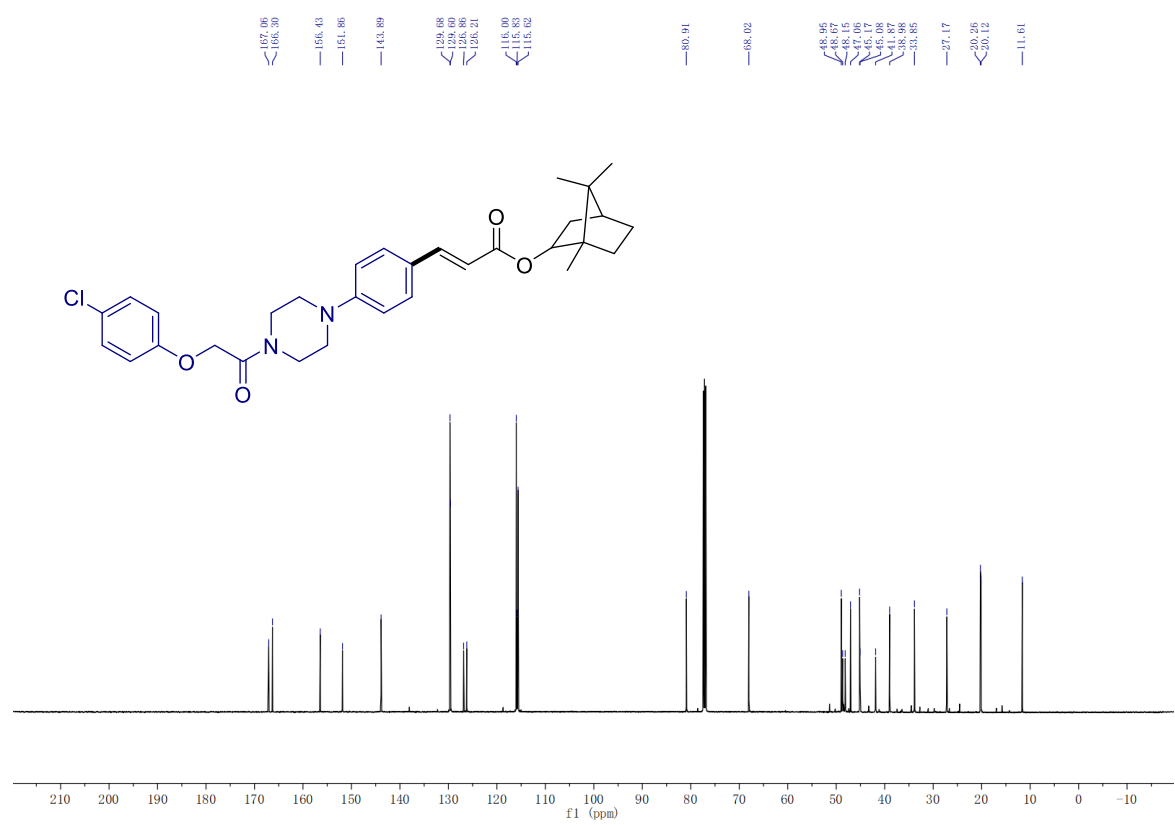
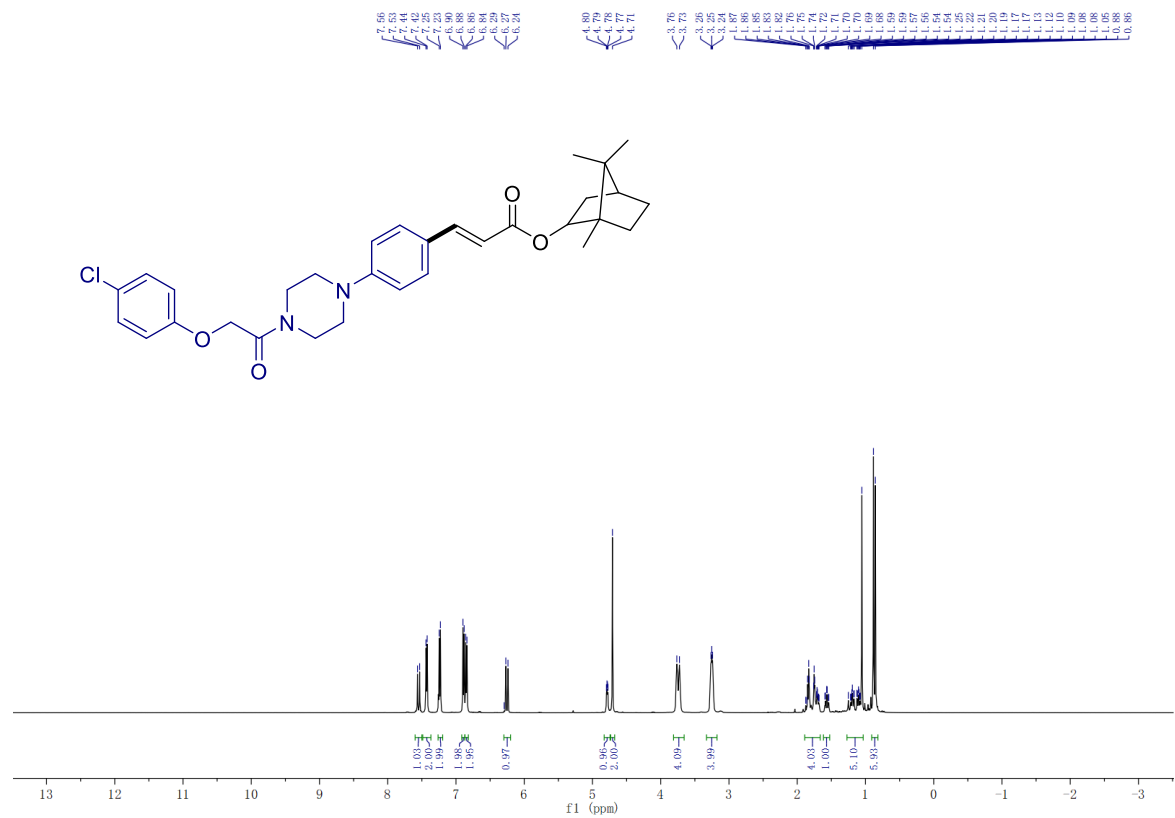


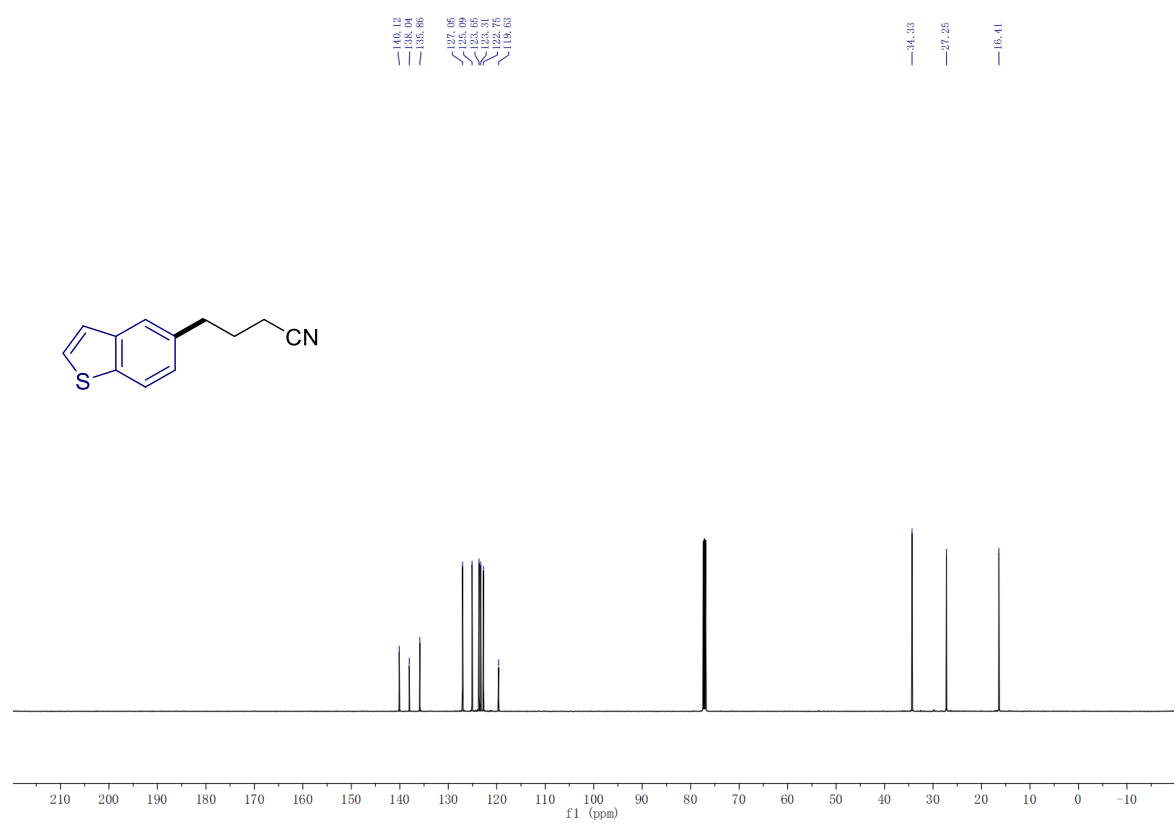
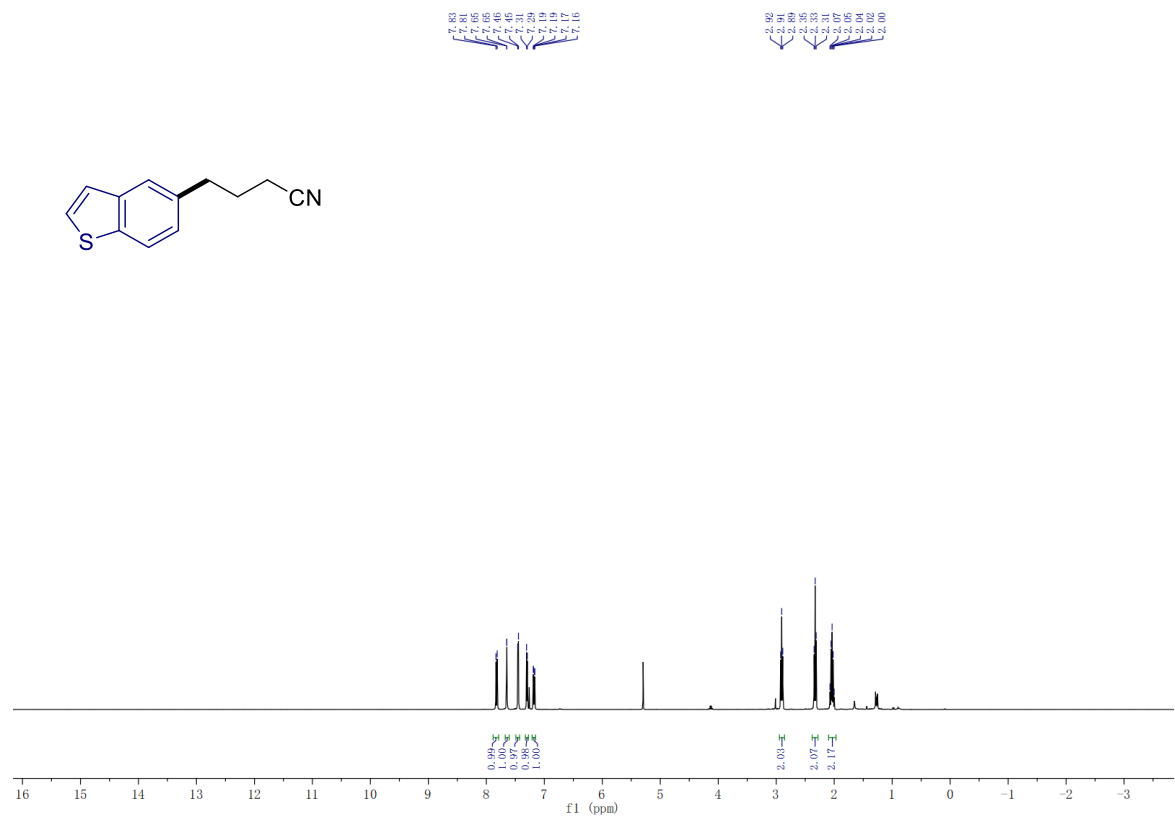


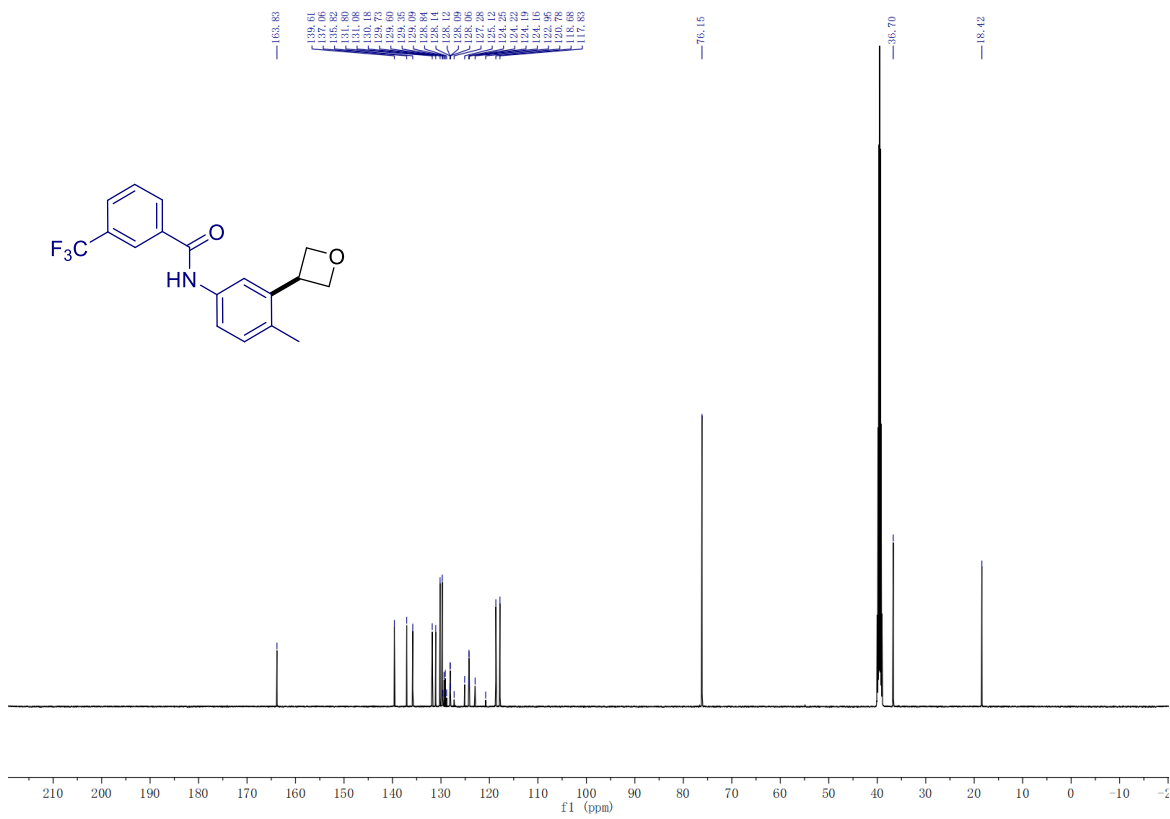
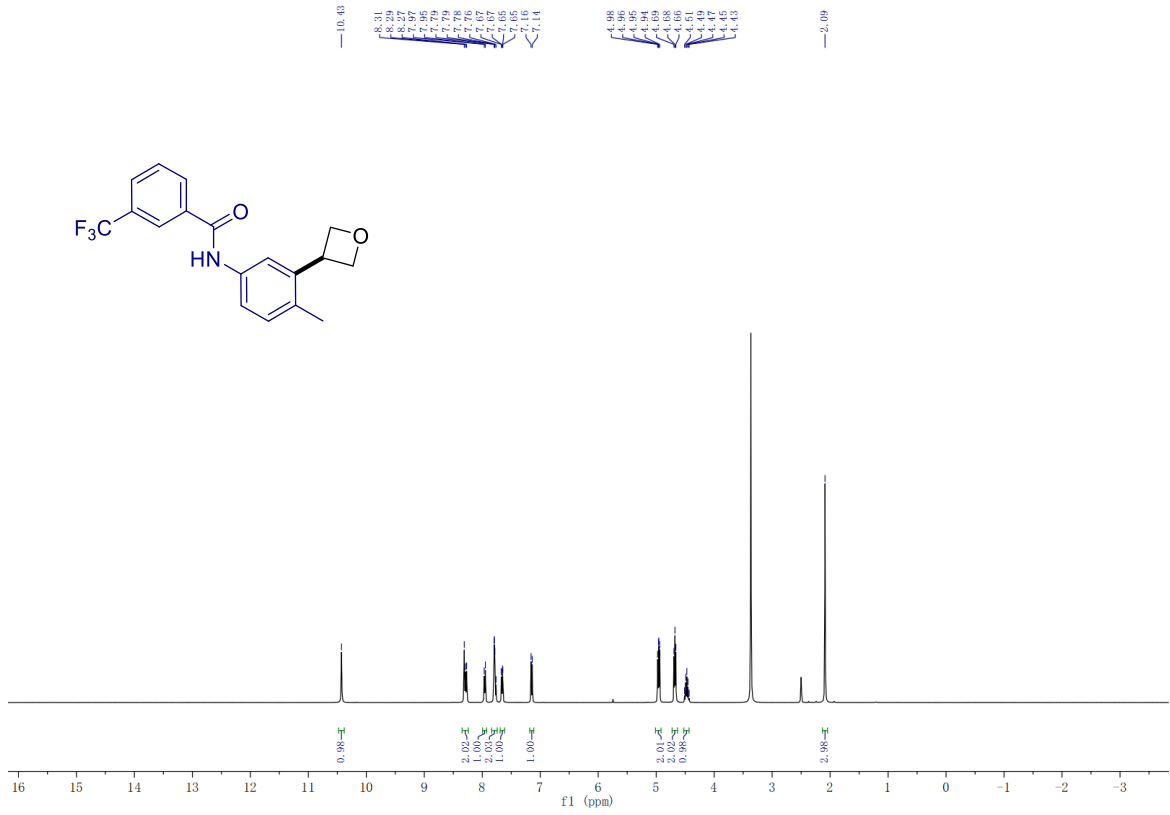


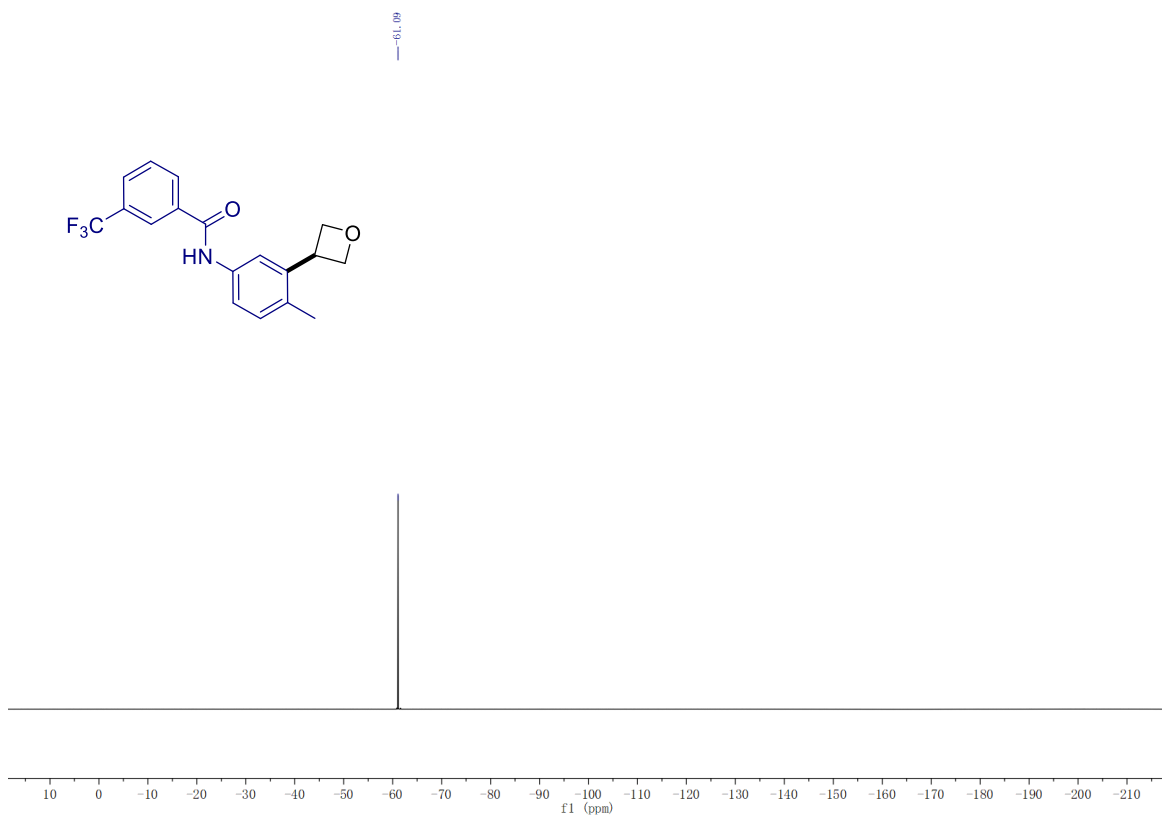


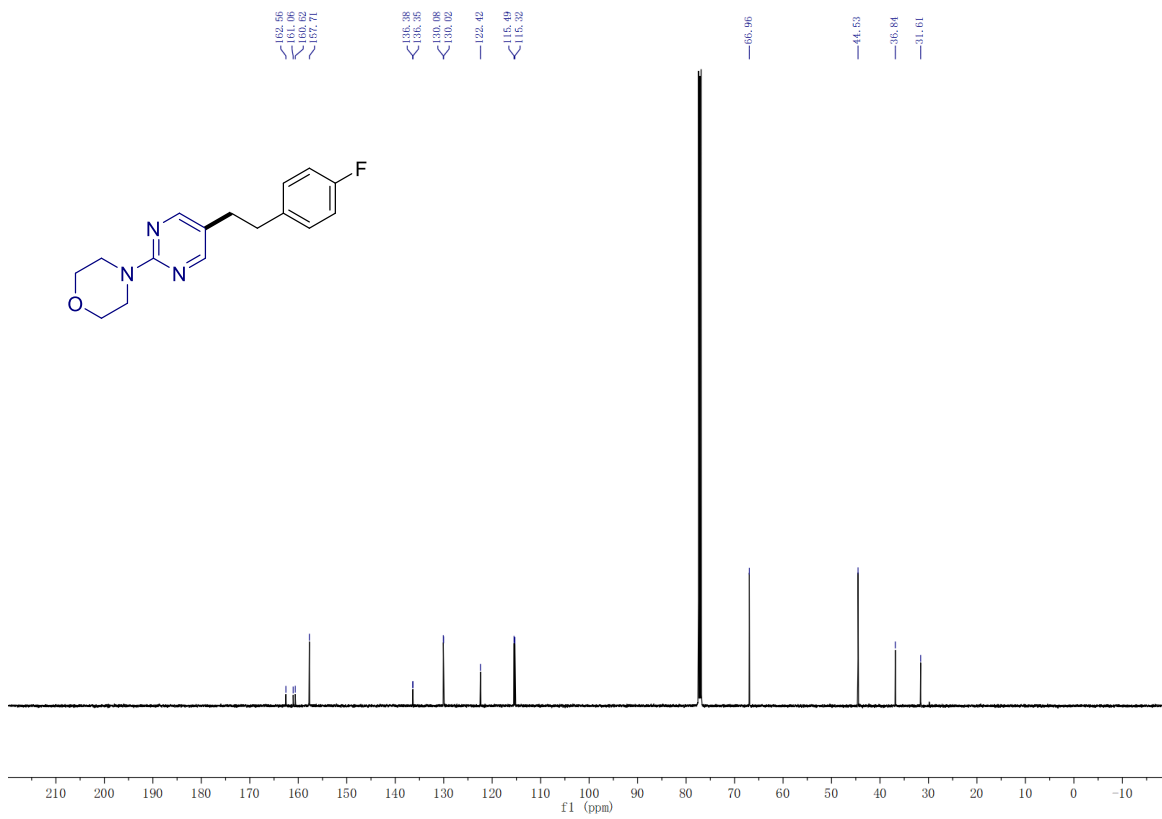
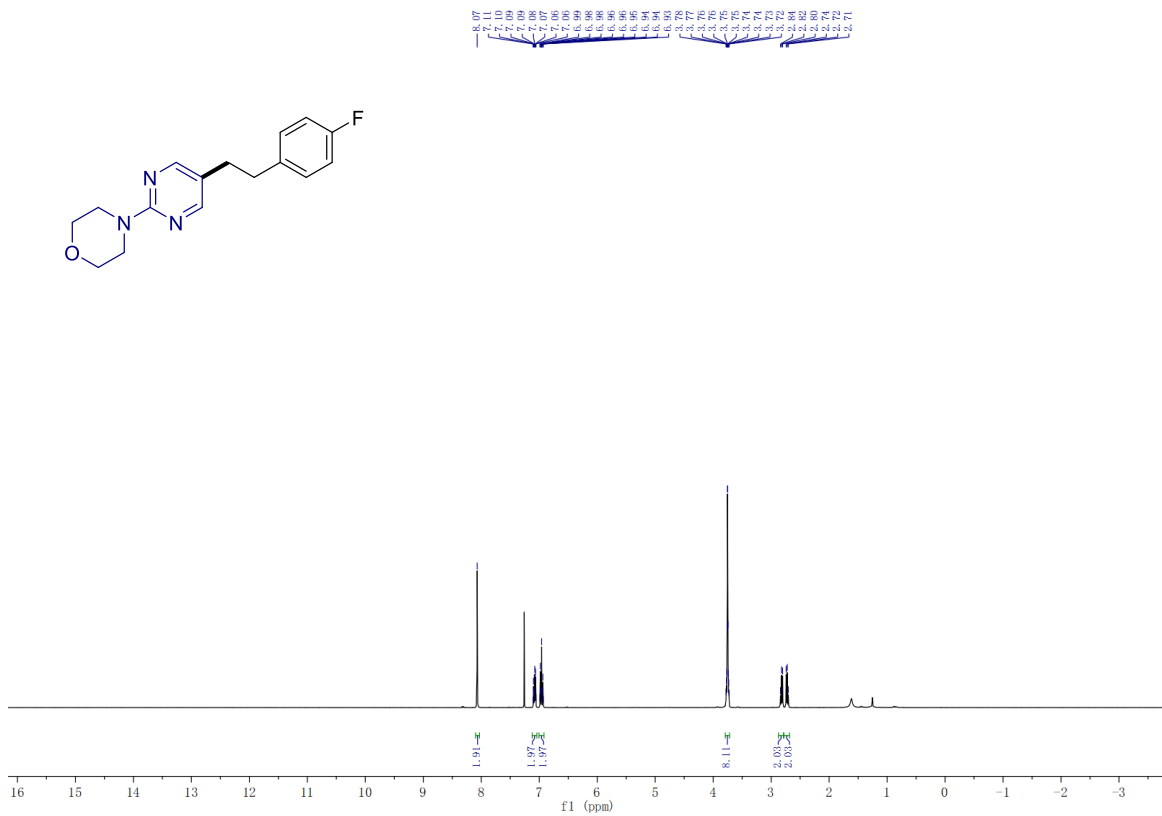
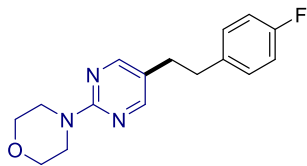


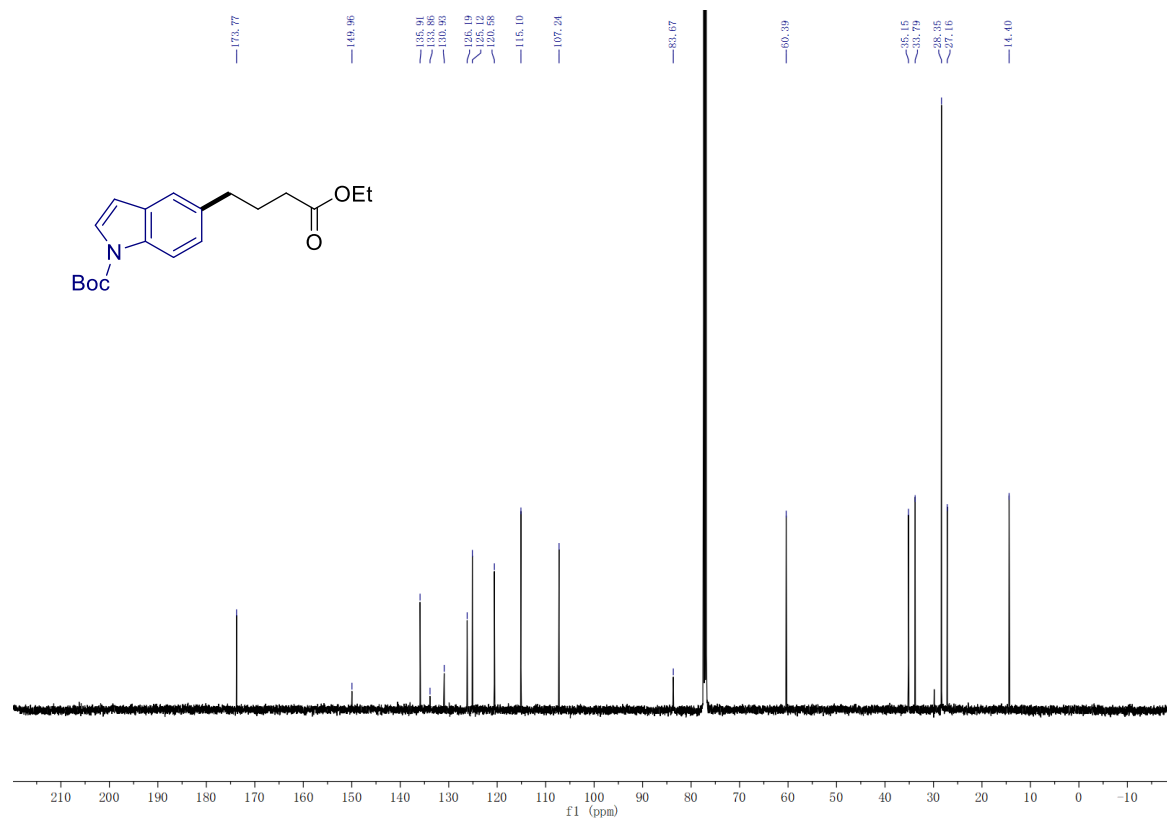
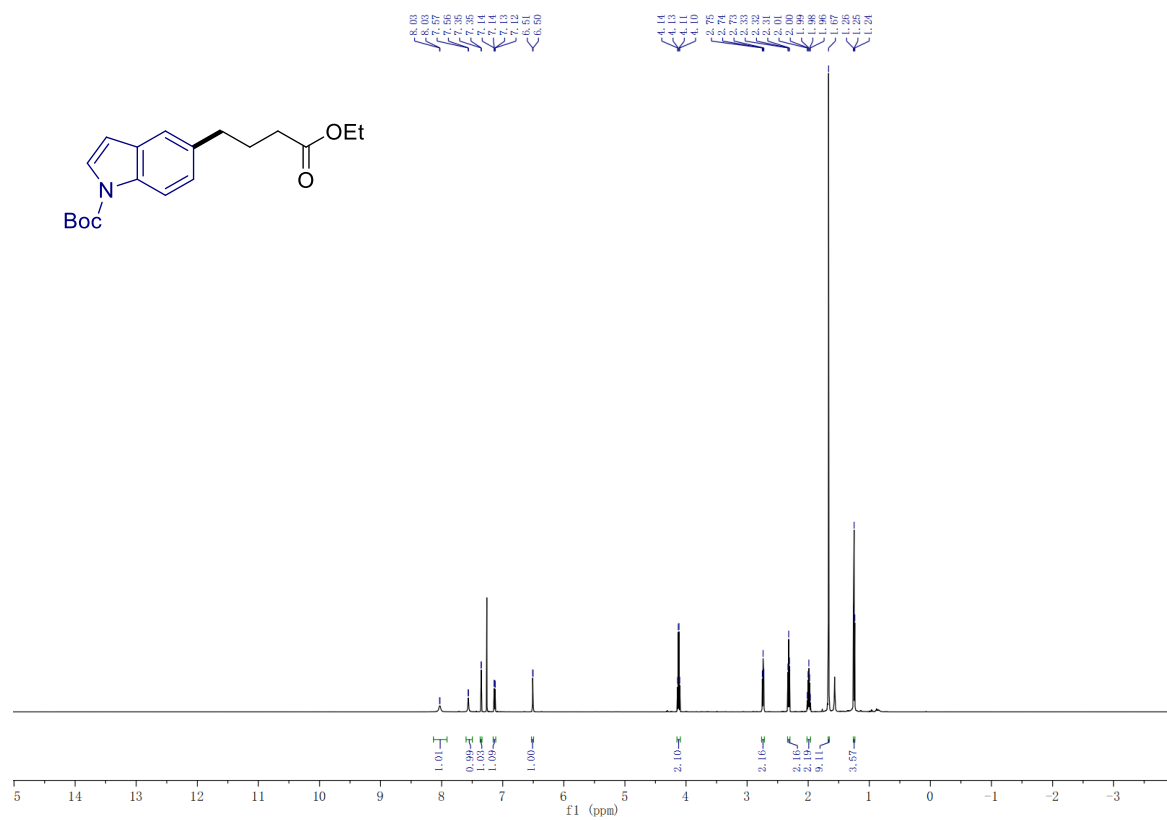


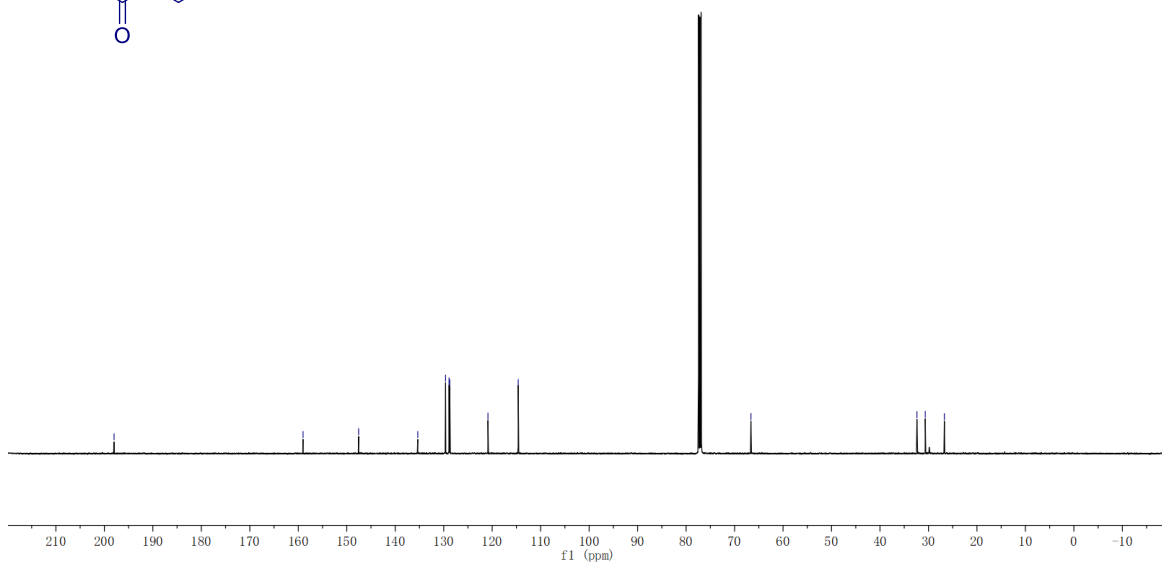
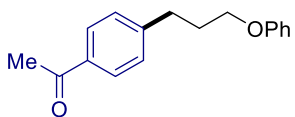
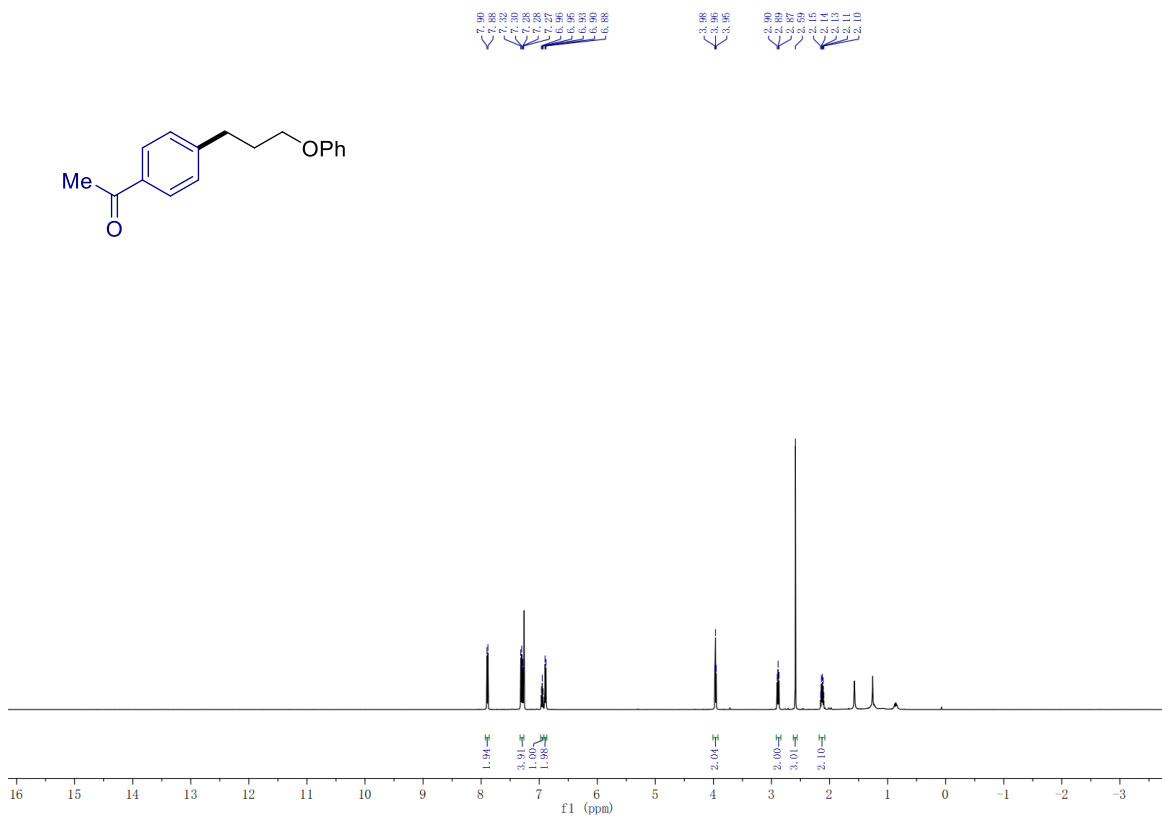
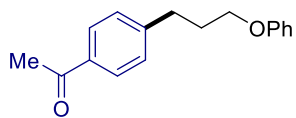


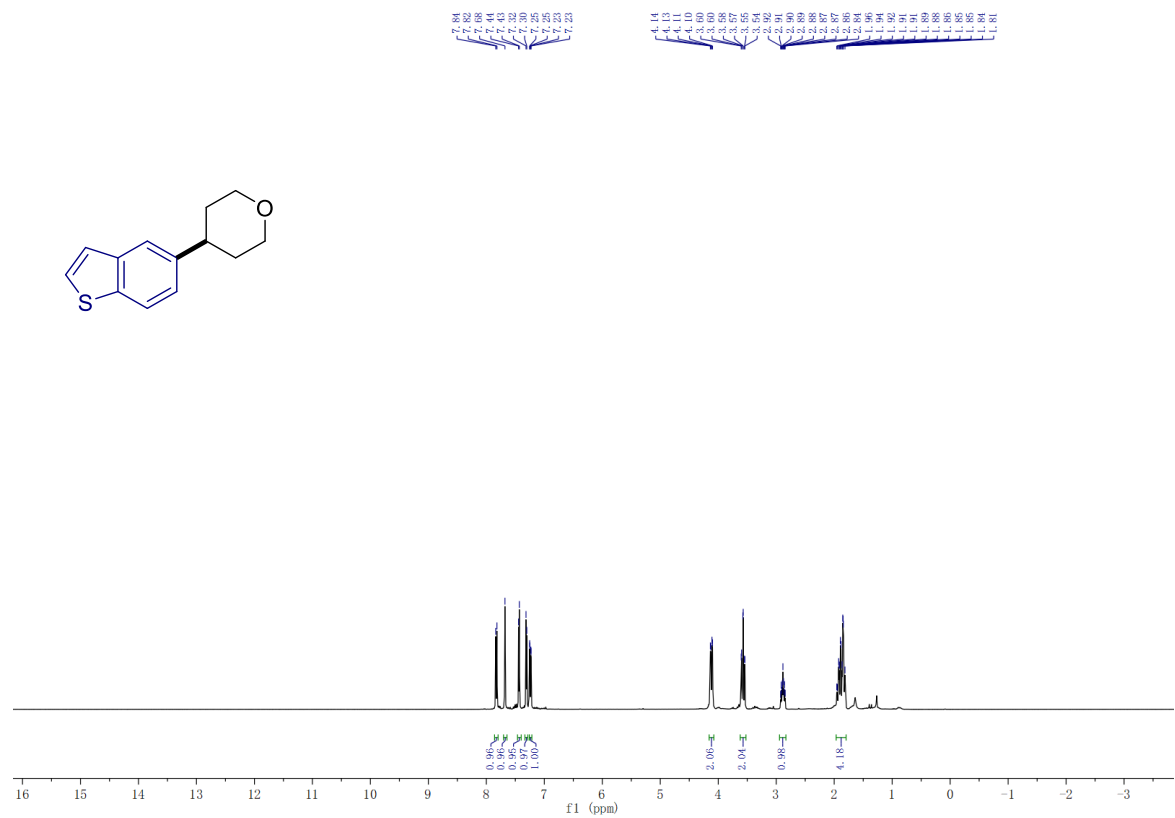




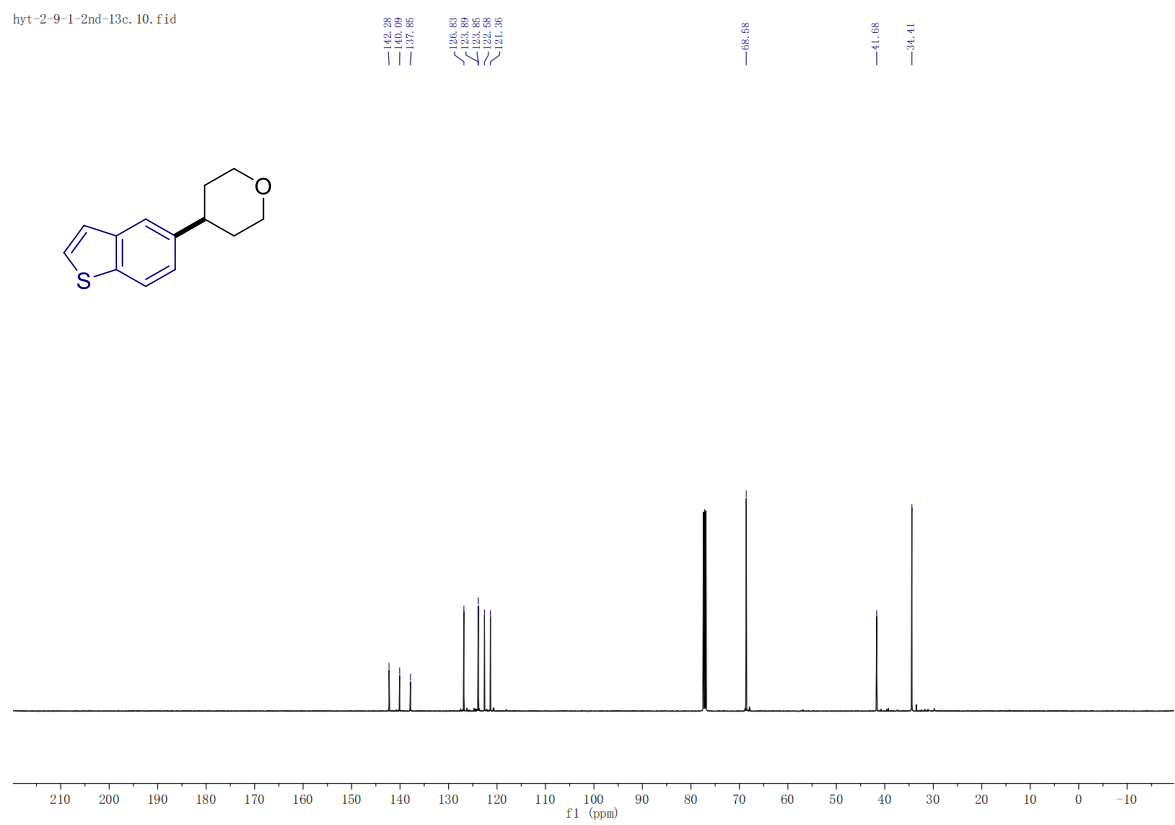


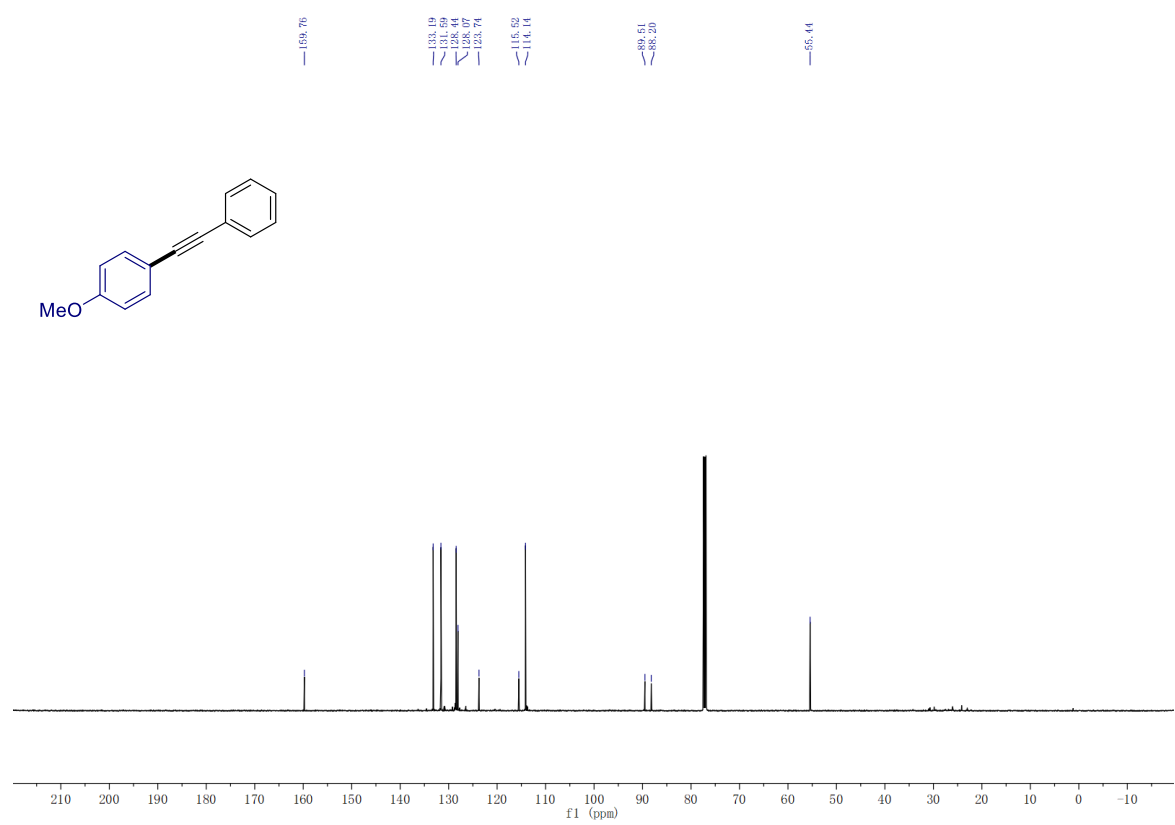
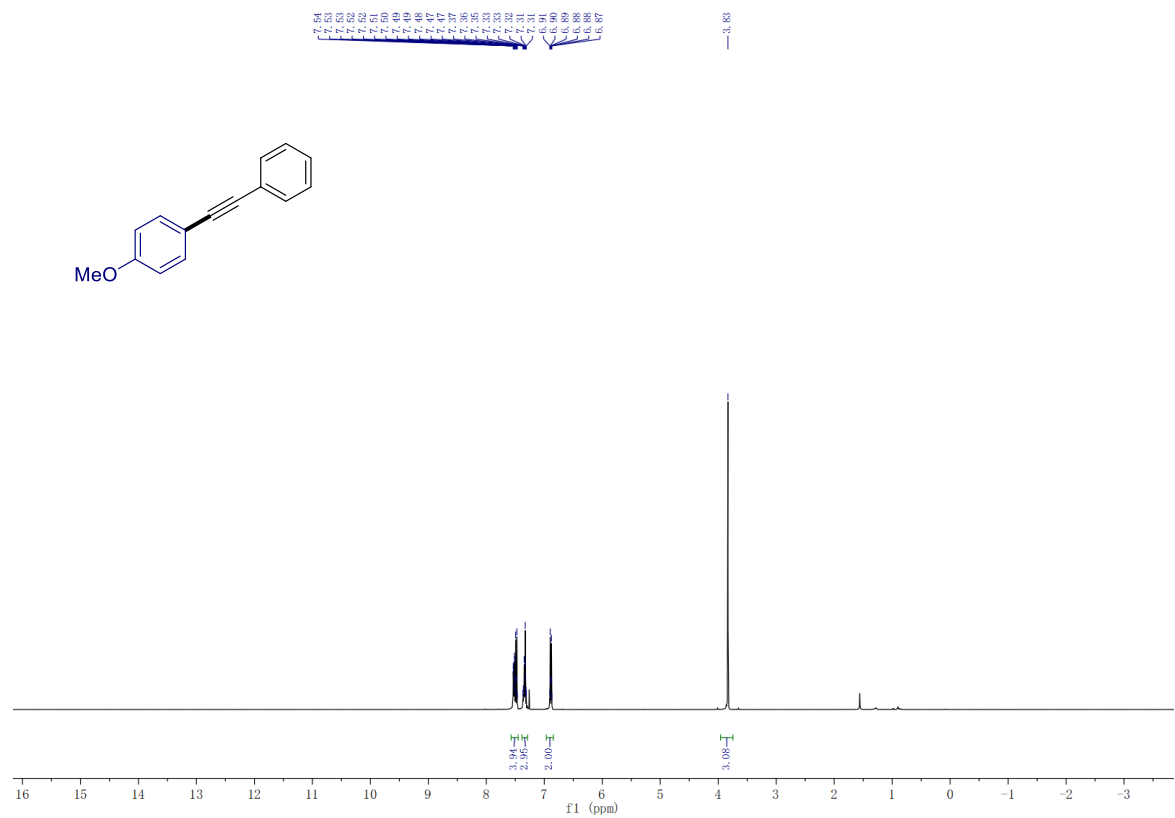


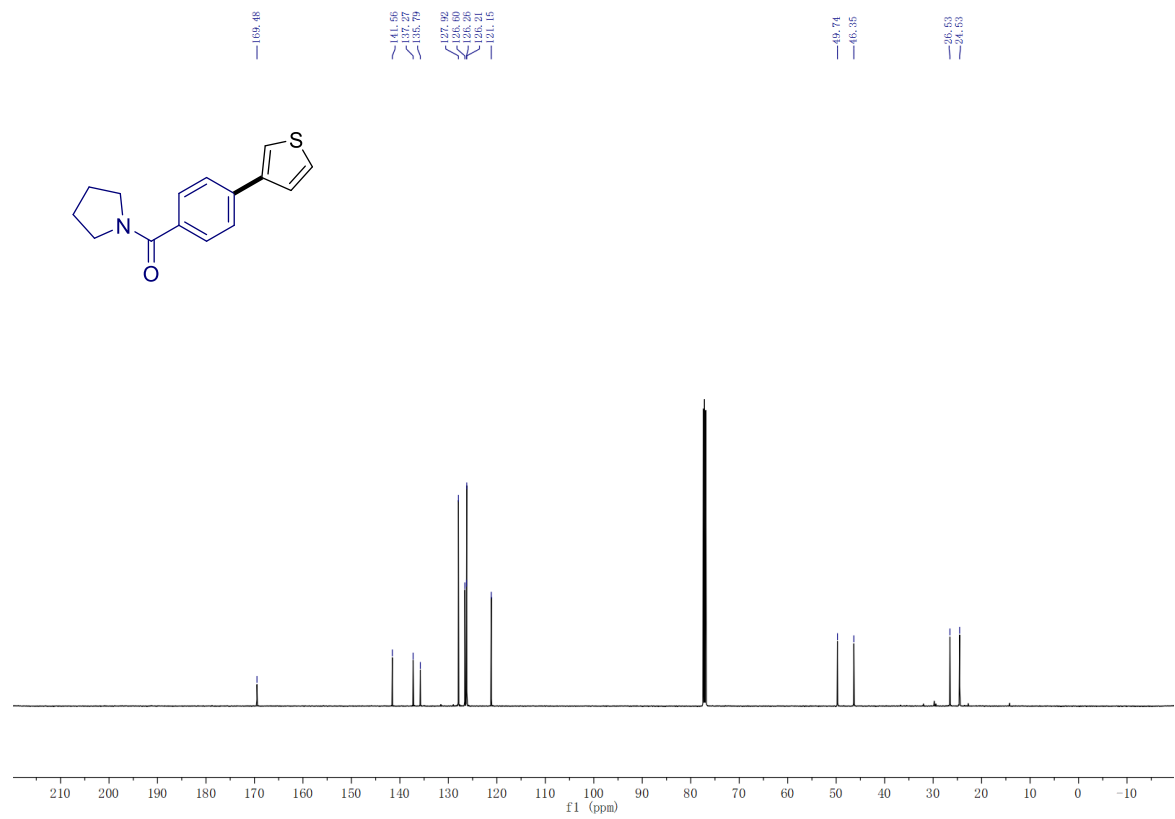
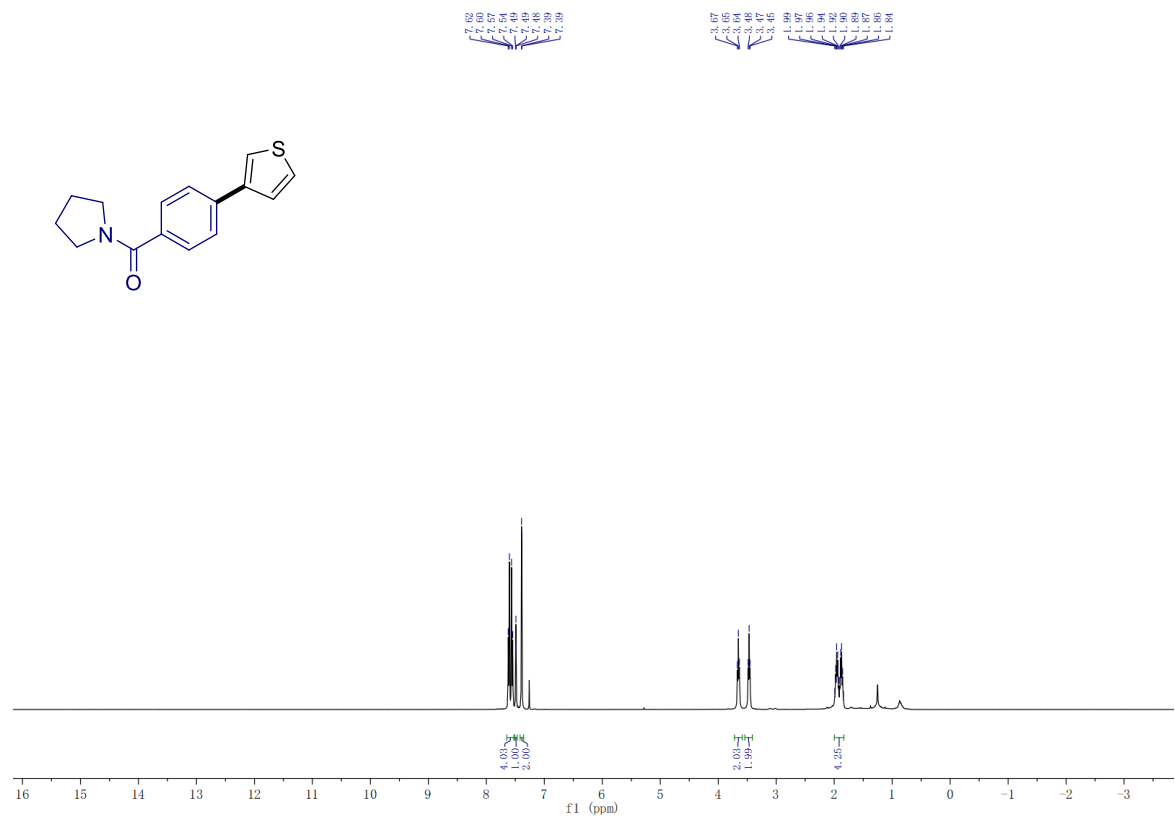


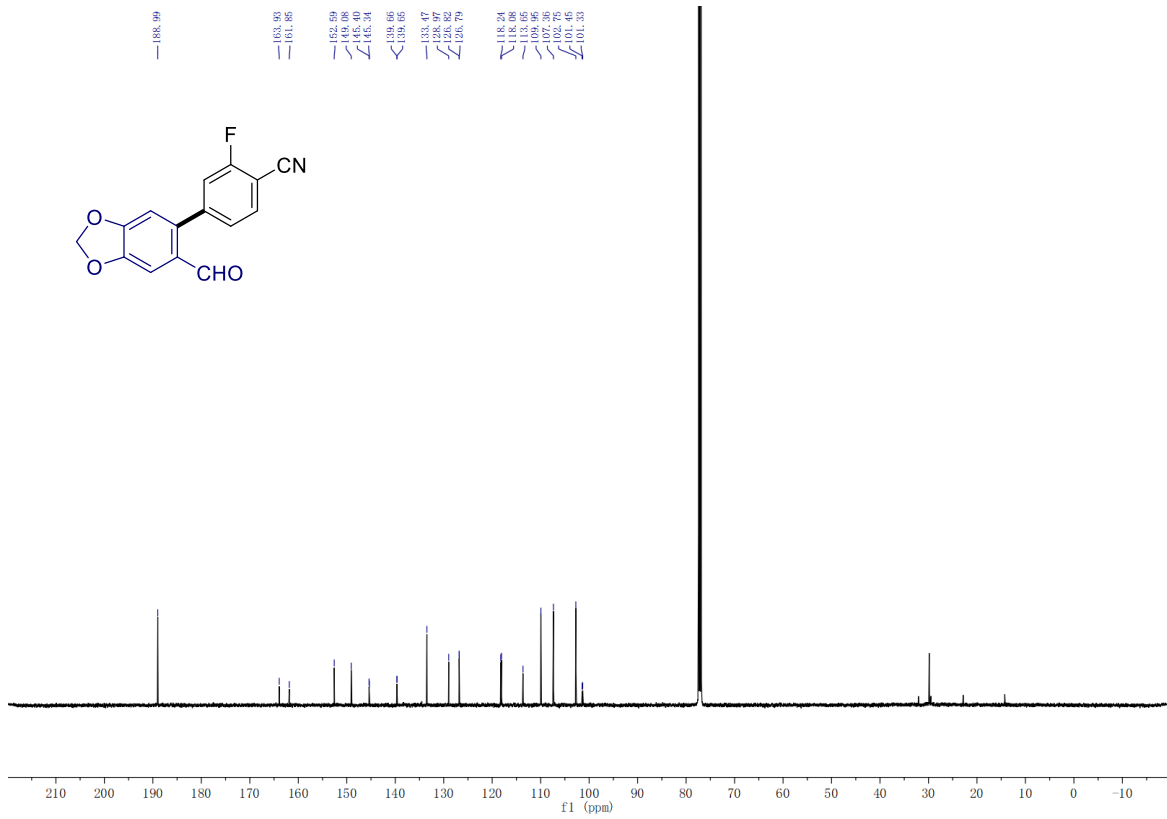
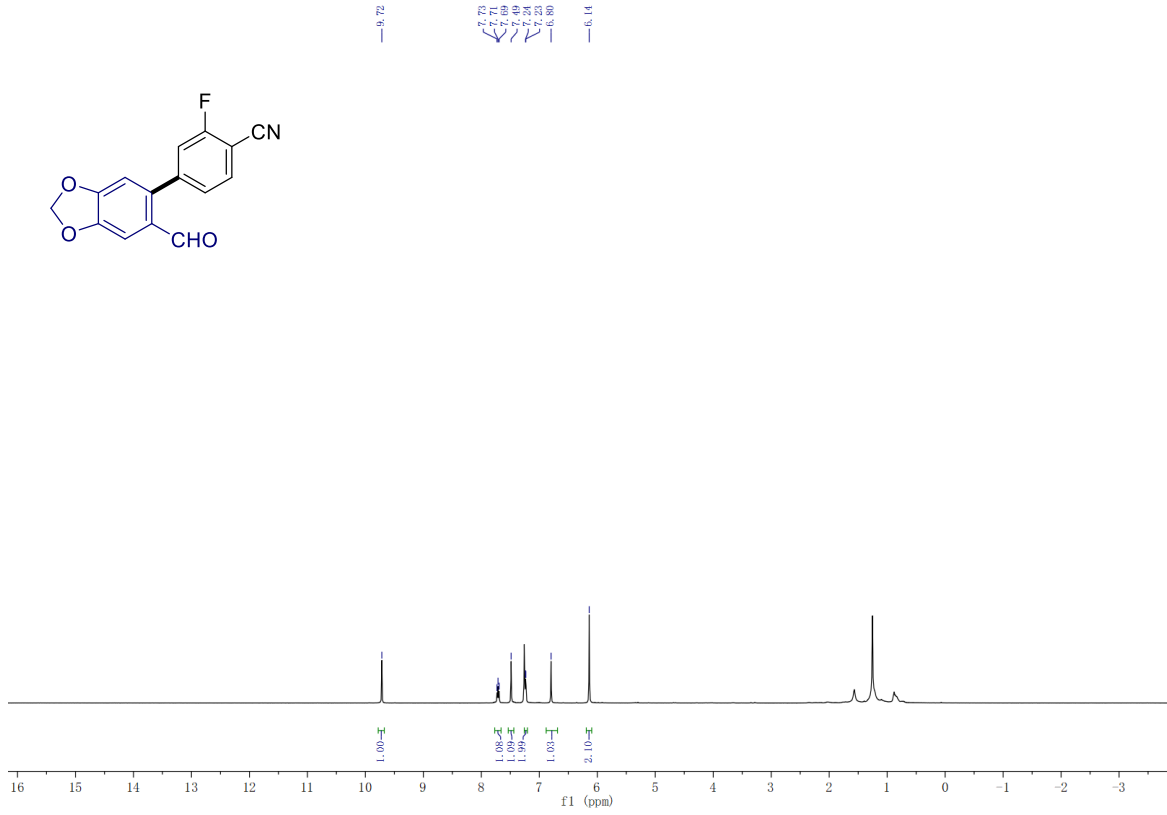
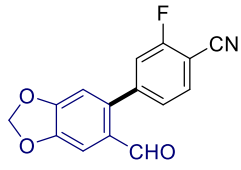


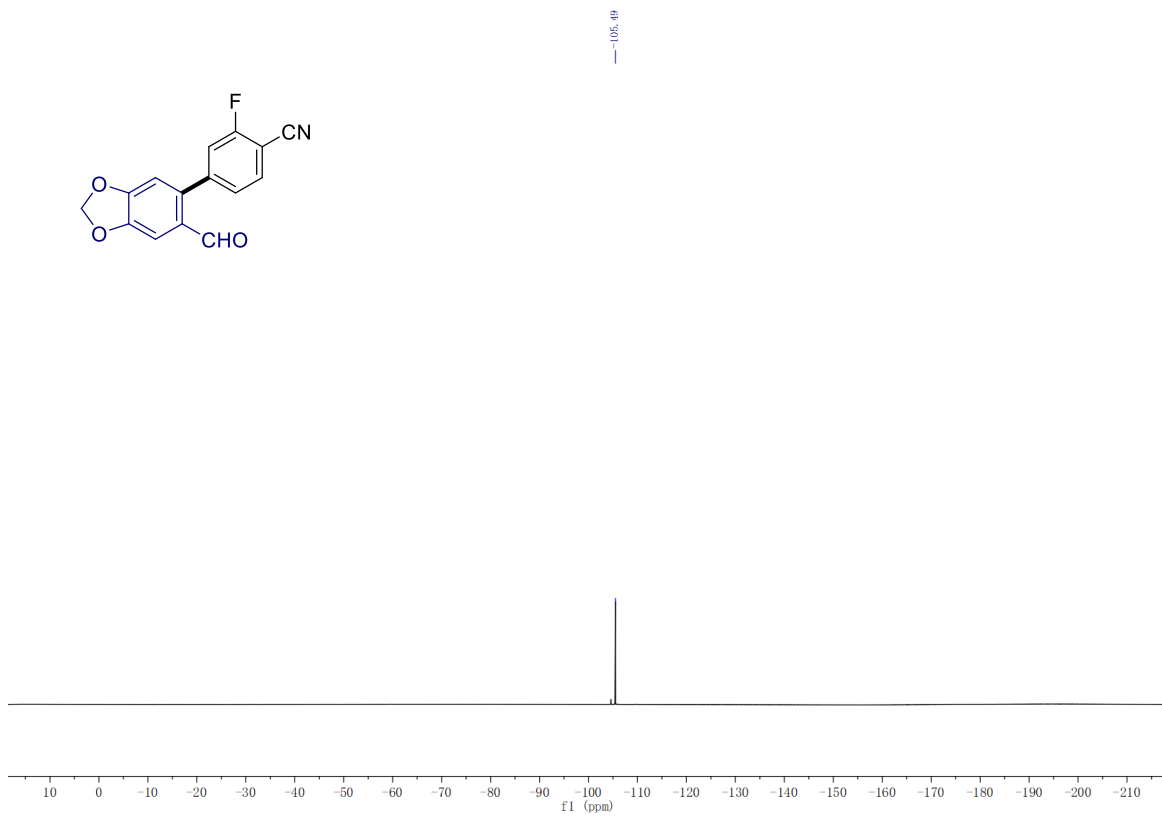
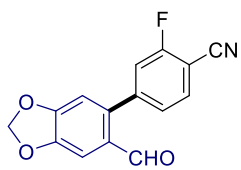
hyt-2-9-1-2nd-13c. 10. fid

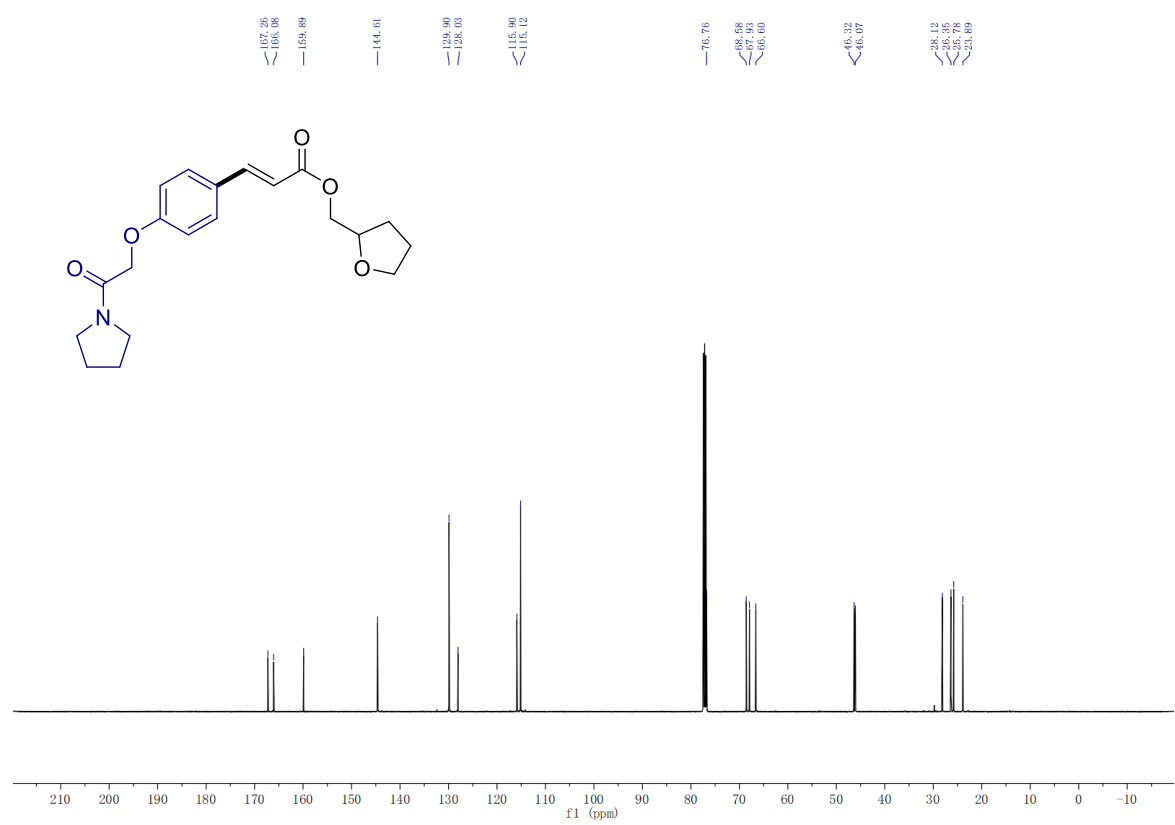
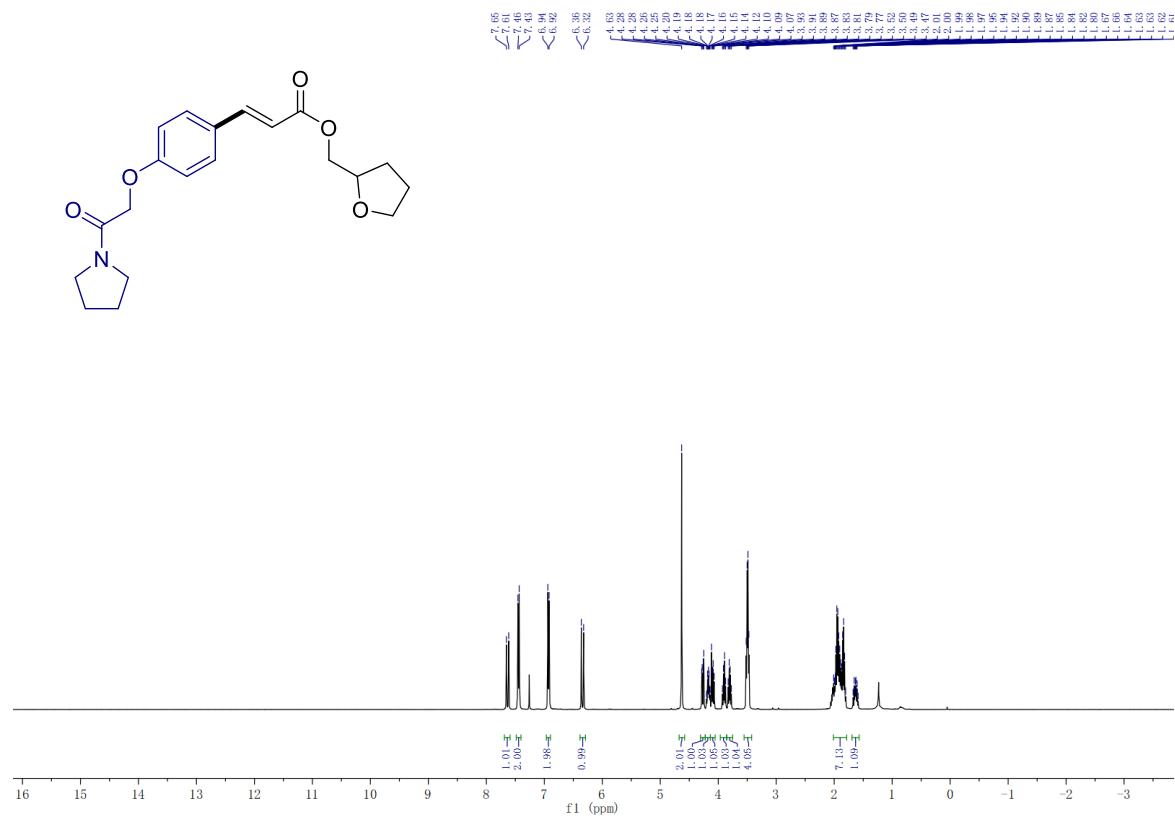


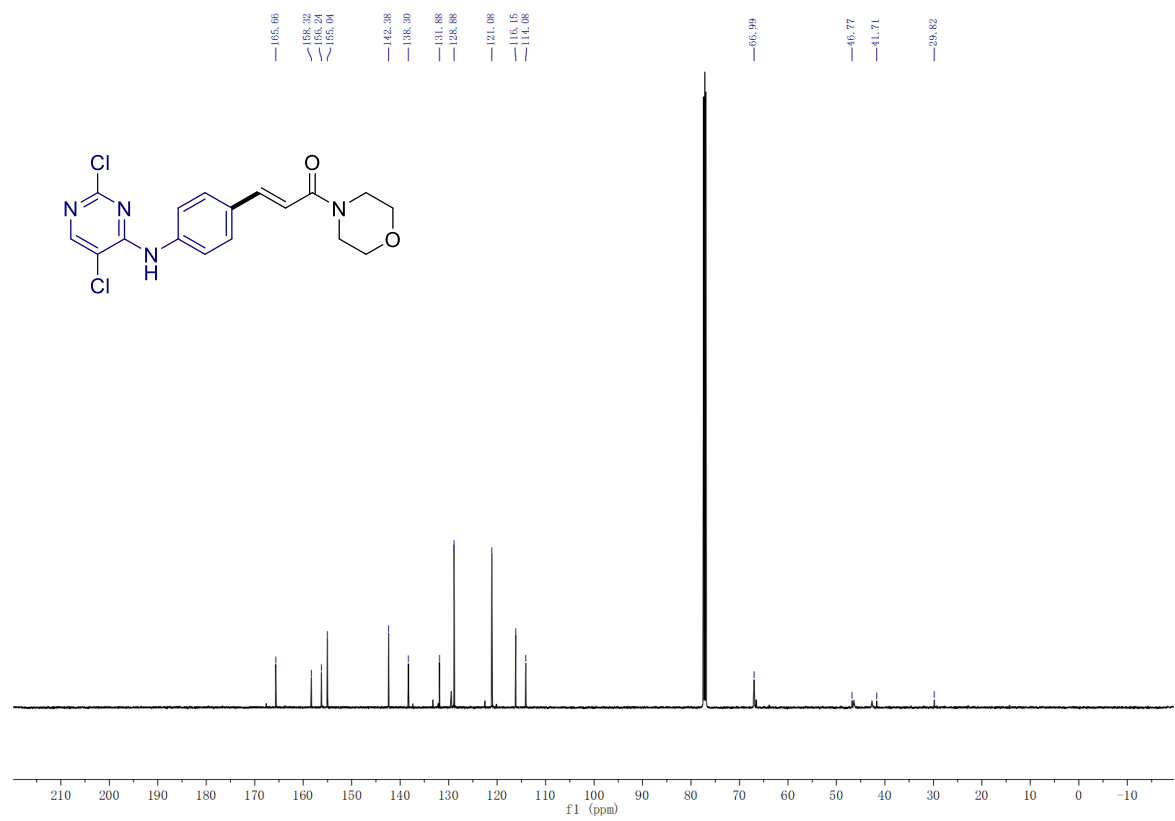
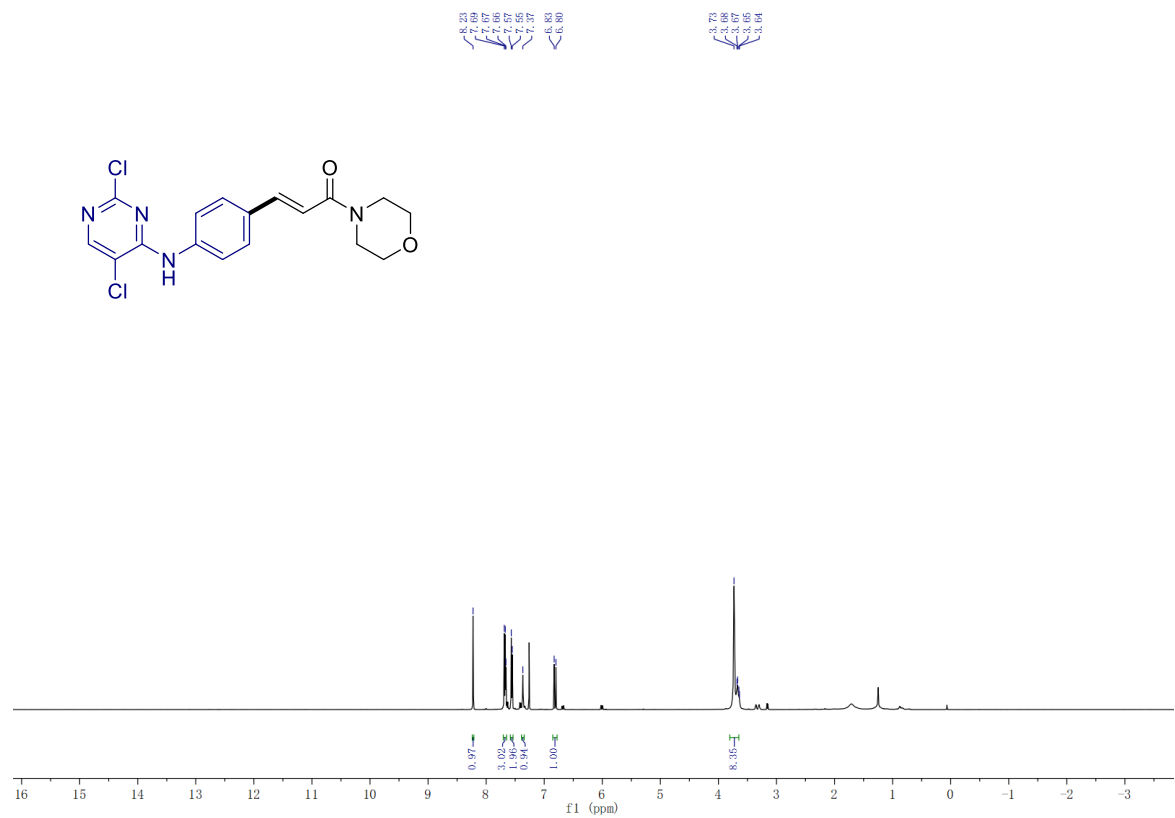












3. Efforts towards using Dipyridyldithiocarbonate (DPDTC) as an Environmentally Responsible Reagent for Ketone Synthesis via Fukuyama Reactions in Water

3.1 Background Introduction

Ketones, a fundamental functional group, play important roles in the field of organic chemistry. Ketone-containing compounds are extensively found in a diverse range of molecules, including natural products,^{1,2} pharmaceuticals,³ agrochemicals,⁴ organic electronics,⁵ fragrances,^{6,7} and polymers.^{8,9} For example, ketones constitute the core structural element in numerous small-molecule drugs, such as Warfarin (anticoagulant), Topsentin (antitumor), Lanperisone (muscle relaxant), Prasterone (DHEA), Amfenac (anti-inflammatory), and Ocina-plon (anxiolytic), as shown in Figure 1. Moreover, ketones are frequently used as versatile precursors in the synthesis of heterocycles¹⁰ and natural products,^{11,12} given that they could be easily converted into imines or enamines. Beyond their traditional use in organic synthesis, ketones also serve as key precursors in enzymatic catalysis leading to chiral amines and alcohols.^{13,14}

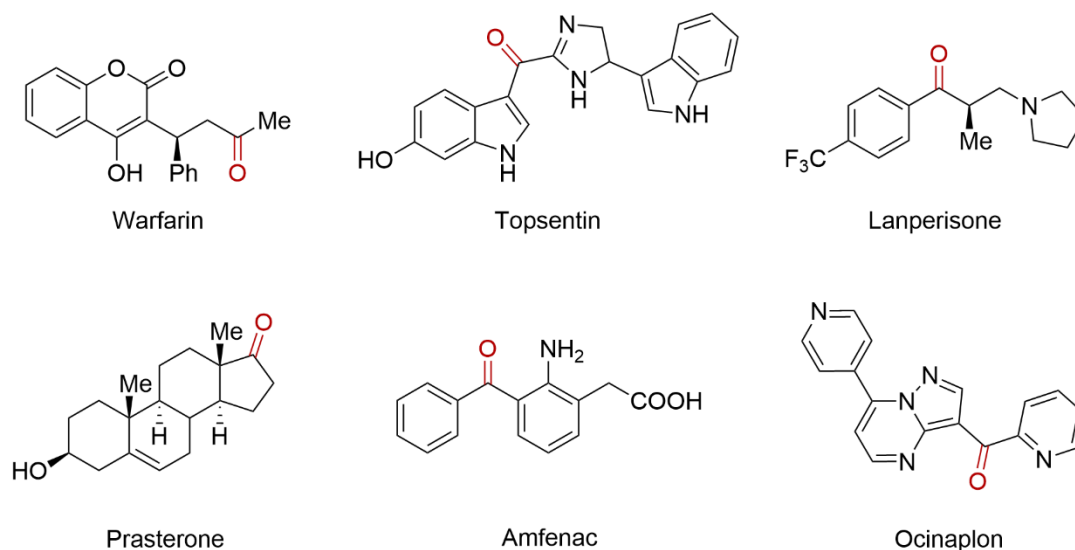
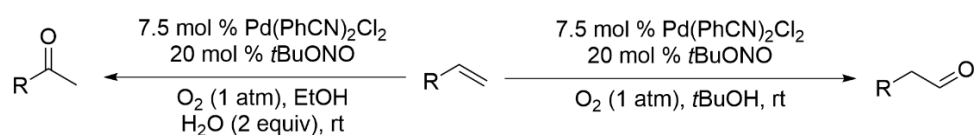


Figure 1. Examples of ketone-containing small-molecule drugs

While ketones are crucial in organic synthesis, a general and robust method for their synthesis has not yet been established. The conventional methodologies for ketone synthesis include: 1) oxidation of secondary alcohols using stoichiometric amounts of oxidants such as KMnO_4 , CrO_3 , or PCC;¹⁵ 2) Friedel-Crafts acylation catalyzed by Lewis acids such as AlCl_3 , TiCl_4 or FeCl_3 ;¹⁶ 3) nucleophilic addition of organometallic reagents, like organolithium, organomagnesium (Grignard reagent), or organozinc reagent to Weinreb amides;¹⁷ 4) cross coupling reactions catalyzed by palladium or nickel;¹⁸ 5) decarboxylative addition with nitriles or esters.¹⁹

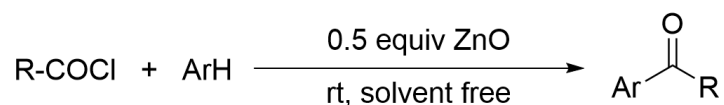
A common industrial method for synthesizing ketones or aldehydes is the use of Pd or Ni to catalyze the oxidation of alkenes, a process known as the Wacker Process. Traditionally, Wacker oxidation occurs in wet DMF and typically follows Markovnikov's rule, resulting in ketones as the primary products. However, there is significant research interest in achieving anti-Markovnikov selective oxidation for the direct synthesis of aldehydes, which is considered highly desirable. In 2018, the Kang group reported controlling the regioselectivity of Wacker oxidation within the same catalytic system.²⁰ They developed a method for regioselectivity-controllable aerobic Wacker oxidation that under room temperature and does not require copper or silver. A catalytic amount of tert-butyl nitrite was used as a simple organic redox co-catalyst. Notably, they found that by switching the solvent from ethanol/water to tert-butanol, the selectivity of the oxidation on the terminal alkene can be altered from ketone to aldehyde.

Scheme 1. Kang's work for regioselectivity controlled Wacker oxidation



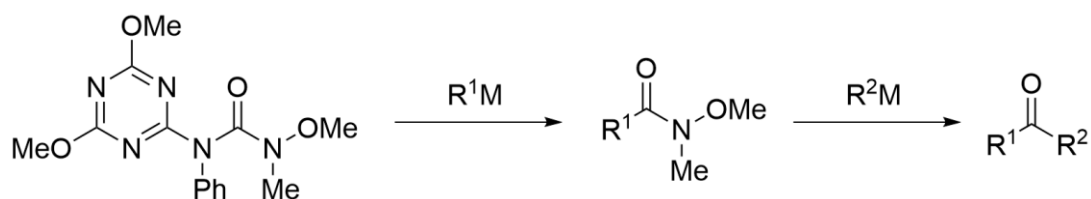
Friedel-Crafts acylation is a pivotal transformation in organic synthesis. Typically, this reaction involves the electrophilic substitution of an aromatic compound with an acylating agent, facilitated by more than one equivalent of an acid catalyst such as anhydrous AlCl_3 , which complexes with the ketone product. However, the catalysts used in this traditional method are not easily recoverable or recyclable, and the reaction generally requires high temperatures. Addressing these limitations, in 2004, the Sharghi group introduced a simple, economical, and efficient alternative using zinc oxide (ZnO) as a novel catalyst.²¹ They developed a highly efficient, solvent-free protocol for the Friedel-Crafts acylation of aromatic compounds using non-toxic and inexpensive ZnO powder. This environmentally friendly and safe method offers several advantages: a straightforward reaction setup that does not require specialized equipment, mild reaction conditions, high yields, significantly reduced reaction times, and the complete elimination of solvents.

Scheme 2. Sharghi's work for F-C acylation under mild, solvent free condition



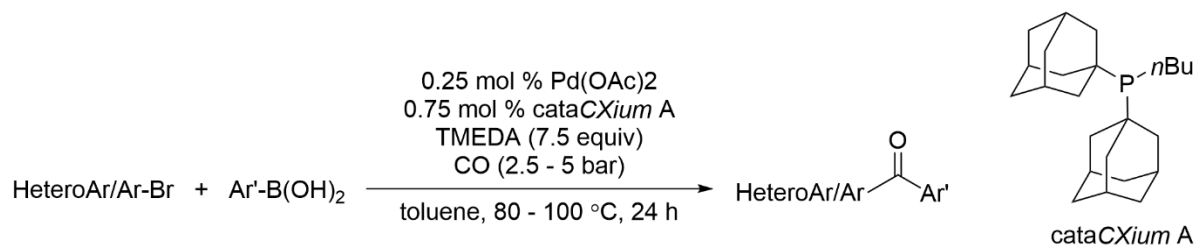
Using chelation to limit the second Grignard addition to a ketone is a widely used method for synthesizing ketones by Grignard reagents. In 2022, the Hirao group reported a novel approach for synthesizing unsymmetrical ketones through double chelation-controlled sequential substitution of N-triazinylamide/Weinreb Amide by organometallic reagents.¹⁷ A key finding in their research was the activation of the carbonyl group by a 2,4-dimethoxy-1,3,5-triazinyl (DMT)-amino group, which effectively prevents overaddition. This characteristic of the DMT-amino group is analogous to the function of the Weinreb amide, yet exhibits higher reactivity. The reactant in their study, featuring a DMT-amino group alongside a Weinreb amide group, functioned as a synthetic equivalent of the dicationic carbonyl group. Remarkably, this reactant underwent sequential nucleophilic substitution with diverse organometallic reagents, successfully yielding unsymmetrical ketones without producing any detectable tertiary alcohols. This new protocol presents a valuable tool for complex synthetic applications in organic chemistry.

Scheme 3. Hirao's work for the synthesis of asymmetric ketone with DMT-amino group and Weinreb amide



The awarding of the 2010 Nobel Prize in Chemistry for Pd-catalyzed cross-coupling reactions underscored their critical role in organic synthesis. It is also used in carbonylation processes. In 2008, the Beller group reported a general synthesis of diaryl ketones, utilizing a three-component cross-coupling method that combines aryl and heteroaryl bromides, carbon monoxide, and boronic acids.²² This reaction provides efficient access to a variety of biologically active compounds, exemplified by the two-step preparation of Suprofen. Noteworthy attributes of this catalyst include its high selectivity and enhanced reactivity. Additionally, the system is easy to handle due to its air-stable nature. It's important to note that the scope of carbonylation extends beyond ketone synthesis, as it is also extensively employed in the production of amides, aldehydes, carboxylic acids, and esters.

Scheme 4. Beller's work for using carbonylation to synthesize diaryl ketone



Although these reactions have been successfully applied to the synthesis of several target molecules, they each have certain drawbacks. These include low levels of regioselectivity, the use of highly toxic stoichiometric oxidants, challenges associated with functional group compatibility, and the generation of large amounts of organic waste. In brief, they have been developed in a traditional sense, and for the most part, under unsustainable reaction conditions.²⁴

Among the reactions mentioned previously, the Fukuyama reaction has captured our interest due to its significant role in synthetic organic chemistry, distinguished by its high chemoselectivity, mild reaction conditions, and reliance on less toxic reagents.²⁵ Notably, this method is compatible with sensitive functional groups, including ketones, esters, sulfides, and aldehydes. The remarkable reactivity and selectivity of the Fukuyama reaction can be attributed to the rapid transmetalation rate of organozinc reagents, compared to the nucleophilic addition of zinc reagents to other functional groups that might be present. Despite its numerous synthetic applications, the mechanism of the Fukuyama reaction remains insufficiently explored. The proposed mechanism for a conventional Pd-catalyzed Fukuyama is presented in Figure 2.

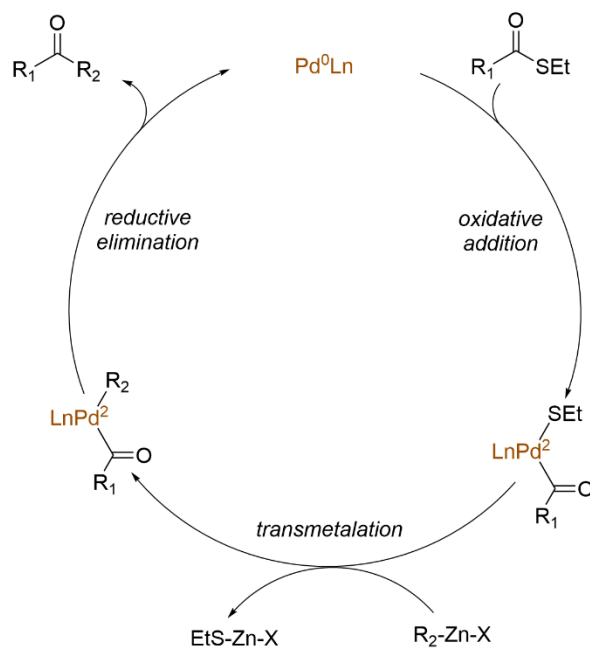


Figure 2. Proposed mechanism for the conventional Pd-catalyzed Fukuyama reaction

Originally developed as a chelation group akin to the Weinreb amide, the 2-*S*-pyridyl group by the Fukuyama group to achieve a novel reduction. In 1990, they reported the reduction of ethyl thioesters to corresponding aldehydes using triethylsilane and Pd/C. In a significant expansion of this methodology in 1998, the same group demonstrated the applicability of thioesters in cross-coupling reactions. Utilizing 5 mol % of $\text{Pd}(\text{PPh}_3)_2\text{Cl}_2$ as a catalyst, they successfully coupled thioesters with organozinc reagents, yielding ketone products within a timeframe ranging from 5 minutes to 2 hours.²⁶ This reaction has since gained considerable significance in synthetic organic chemistry, particularly due to its high chemoselectivity, mild reaction conditions, and the employment of less toxic reagents.

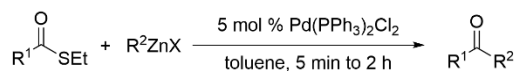
In 2012, the Weix group published a study detailing a novel method for synthesizing functionalized dialkyl ketones from carboxylic acid derivatives and alkyl halides.²⁷ While

most of the cases in their work utilized acyl chlorides as the carboxylic acid derivatives, they notably reported three cases where ketones were synthesized from thioesters. A key aspect of their methodology was the use of Zn or Mn in combination with alkyl iodide, as opposed to the more commonly used organozinc iodide. This approach suggested that the Ni/Zn catalytic system could facilitate the reaction through an alternative mechanism involving the generation of radicals, thereby broadening the understanding and potential optimization of this catalytic system in organic synthesis.

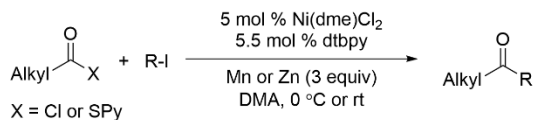
Professor Tohru Fukuyama's initial focus on developing novel methodologies for the synthesis of natural products has led to significant contributions in organic synthesis, particularly with the development of the Fukuyama reaction. In 2016, the Kishi group made a notable advancement in this area by reporting a method for in situ generation of organozinc reagents, which they subsequently utilized in the synthesis of ketones.²⁸ Their work involved a comprehensive investigation of the reactivity of organozinc reagent formation and the Fukuyama reaction. They provided two distinct conditions for the formation of zinc reagents and three different conditions for the Fukuyama reaction. Furthermore, they developed a one-pot method for synthesizing ketones, demonstrating its effectiveness for late-stage coupling in the convergent synthesis of complex molecules. This methodology was exemplified in their synthesis of a precursor containing all the carbon atoms of Eribulin, highlighting the method's utility and versatility in crafting complex molecular structures.

Scheme 6. Representative cases for Fukuyama reaction

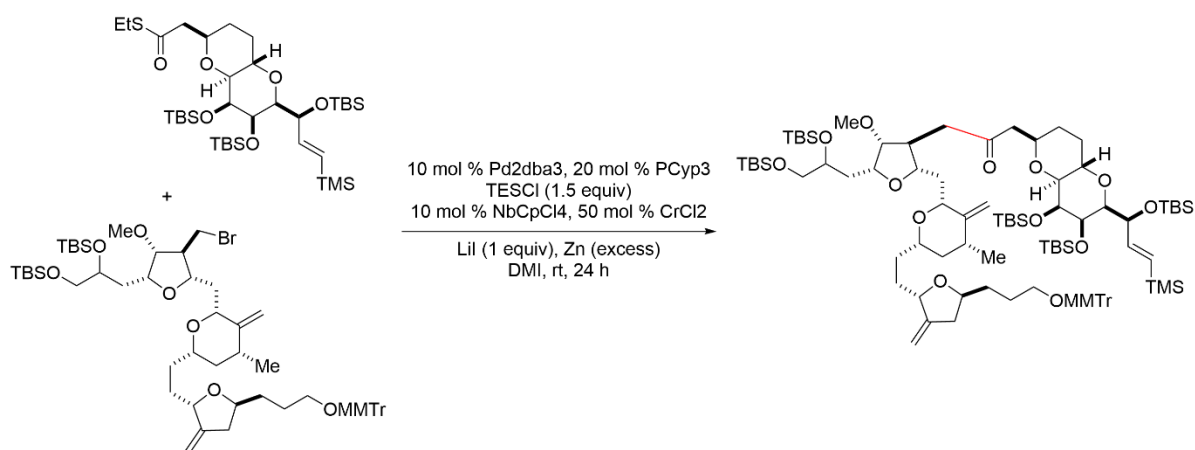
1) First Fukuyama reaction reported in 1998



2) Weix's work for synthesis ketones from carboxylic acid derivatives



3) Kishi's work for one-pot ketone synthesis ketones



Although the Fukuyama reaction offers distinct advantages in synthesis, it still has its limitations and drawbacks in terms of applications. A notable challenge is the additional step required for the synthesis and purification of the intermediate thioester, akin to the process using a Weinreb amide. It also needs an extra step to generate the organozinc reagent, especially given the limited commercial availability of these reagents. Additionally, the use of ethanethiol for synthesizing ethyl thioesters is problematic due to its strong and unpleasant odor, potentially restricting its large-scale industrial application.²⁹ Lastly, the traditional Fukuyama reaction typically employs organic solvents such as THF, toluene, or

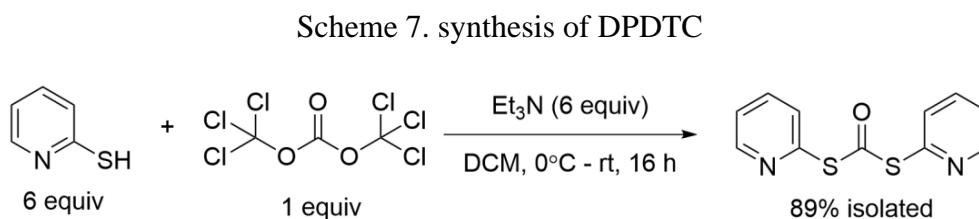
1,3-dimethyl-2-imidazolidinone (DMI), which translates into a large amount of organic waste.²⁰

Our group has recently developed a little-explored carboxylic acid activating reagent, dipyridyldithiocarbonate (DPDTC).³⁰ This reagent has been successfully utilized to transform carboxylic acids into thioesters that can subsequently be reduced to aldehydes or alcohols,³¹ or which can undergo reactions with thiols, alcohols, or amines to synthesize thioesters, esters, or amides, respectively.^{30,32} A notable advantage of both DPDTC and 2-mercaptopyridine, the precursor in DPDTC synthesis, is their lack of odor, possibly due to their non-volatile nature and thione resonance. Additionally, our group has developed a Negishi reaction in water that employs *in situ*-formed organozinc reagents from alkyl bromides/iodides and zinc.^{33,34} While organozinc reagents and thioesters are typically sensitive to water, leading to proto-quenching and hydrolysis, the addition of the designer surfactant TPGS-750-M offers new opportunities for their use.³⁵ The feasibility of a one-pot process involving *in situ*-generated organozinc reagents together with freshly prepared thioesters in water has inspired us to refine the Fukuyama reaction into a greener, simpler, and more universally applicable method.

3.2 Results and discussion

DPDTC synthesis and purification

Since DPDTC is needed as the activating reagent for a carboxylic acid, a robust procedure to synthesize DPDTC on a large scale has been developed. Initially, testing on a smaller scale, the synthesis involves combining one equivalent of solid, easy-to-handle triphosgene with six equivalents of 2-mercaptopyridine in DCM, using triethylamine as base. As shown in Scheme 7, this approach produced DPDTC with an isolated yield of 89%, after being purified by column chromatography.



The method for large-scale purification of DPDTC was subsequently explored. As shown in Figure 3, the reaction mixture turned into an orange-colored slurry containing solid salts after 16 hours. These salts, potentially ammonium chloride resulting from triethylamine, has good solubility in DCM, posing challenges for subsequent purification steps. Various solvents, including EtOAc, DCM, Et₂O, MTBE, and methanol, were evaluated for their solubilization of salt impurities and DPDTC. Et₂O emerged as the most ideal, demonstrating minimal solubility for the salt impurities while efficiently solubilizing DPDTC. Based on these findings, the solvent was switched to Et₂O, followed by filtration of the reaction mixture to enhance removal of salt impurities.

Following the elimination of salt impurities, the predominant impurities identified were unreacted 2-mercaptopyridine and its corresponding disulfide derivative. Further work-up with various extraction conditions revealed that washing with saturated Na_2CO_3 aqueous solution was most effective in removing 2-mercaptopyridine. The use of more basic solutions, such as NaOH aqueous solution, was avoided to prevent hydrolysis of DPDTC. The disulfide impurity, on the other hand, proved resistant to extraction under these conditions. Nonetheless, its amount could be significantly reduced by conducting the reaction under an argon atmosphere. Alternatively, it could be removed in subsequent trituration.

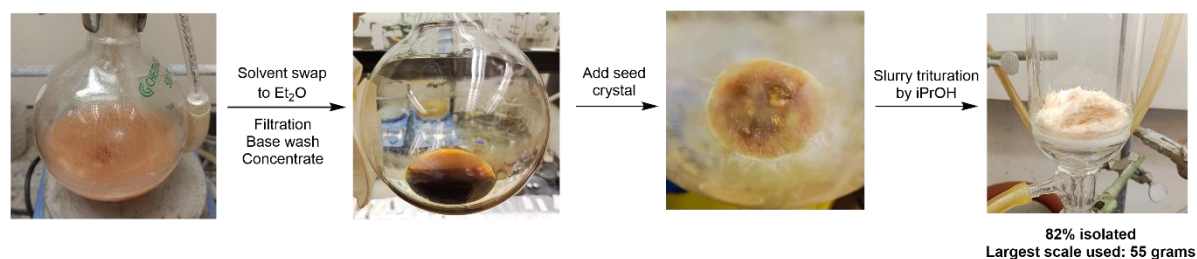


Figure 3. Large scale purification of DPDTC

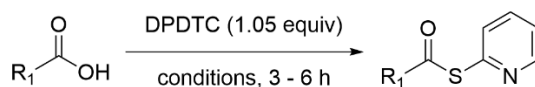
After solvent removal, the process yielded a sticky yellow oil as the crude product. Given that DPDTC is solid at room temperature, recrystallization and trituration were initially selected for purification. Nonetheless, the resultant oil proved challenging to completely solidify, persisting as a liquid or semi-solid state even after extended vacuum exposure overnight or subsequent solvent exchanges. This difficulty in solidification was likely due to the minimal amounts of solvent trapped within the mixture. A breakthrough was achieved by introducing seed crystals into the mixture, which facilitated solidification of the oil within one minute. Subsequently, the solid crude product was obtained by further

removing of residual solvent under vacuum. As the final purification step, *i*-PrOH was employed in minimal quantities for trituration, resulting in the isolation of a pale-yellow solid as the pure product. This method proved to be efficient, yielding an 82% of the target compound, with the largest batch processed amounting to 55 grams.

Thioester formation

As shown in Table 1, three different conditions using 1.1 equivalents of DPDTC were evaluated for synthesizing thioesters from carboxylic acids: 1) a neat reaction at 60 °C; 2) with 10 mol % DMAP in 2 M EtOAc at 60 °C; 3) with 10 mol % DMAP in 2 M EtOAc at room temperature. Extensive testing across various carboxylic acids revealed that the first set of conditions; *i.e.*, conducting the reaction in a neat environment consistently yielded the highest conversion for most carboxylic acids. However, for those carboxylic acids that do not melt and lead to blockage of the stir bar, the third set of conditions proved more effective, enhancing solubility, and consequently improving the yield.

Table 1. Various reaction conditions for thioester synthesis

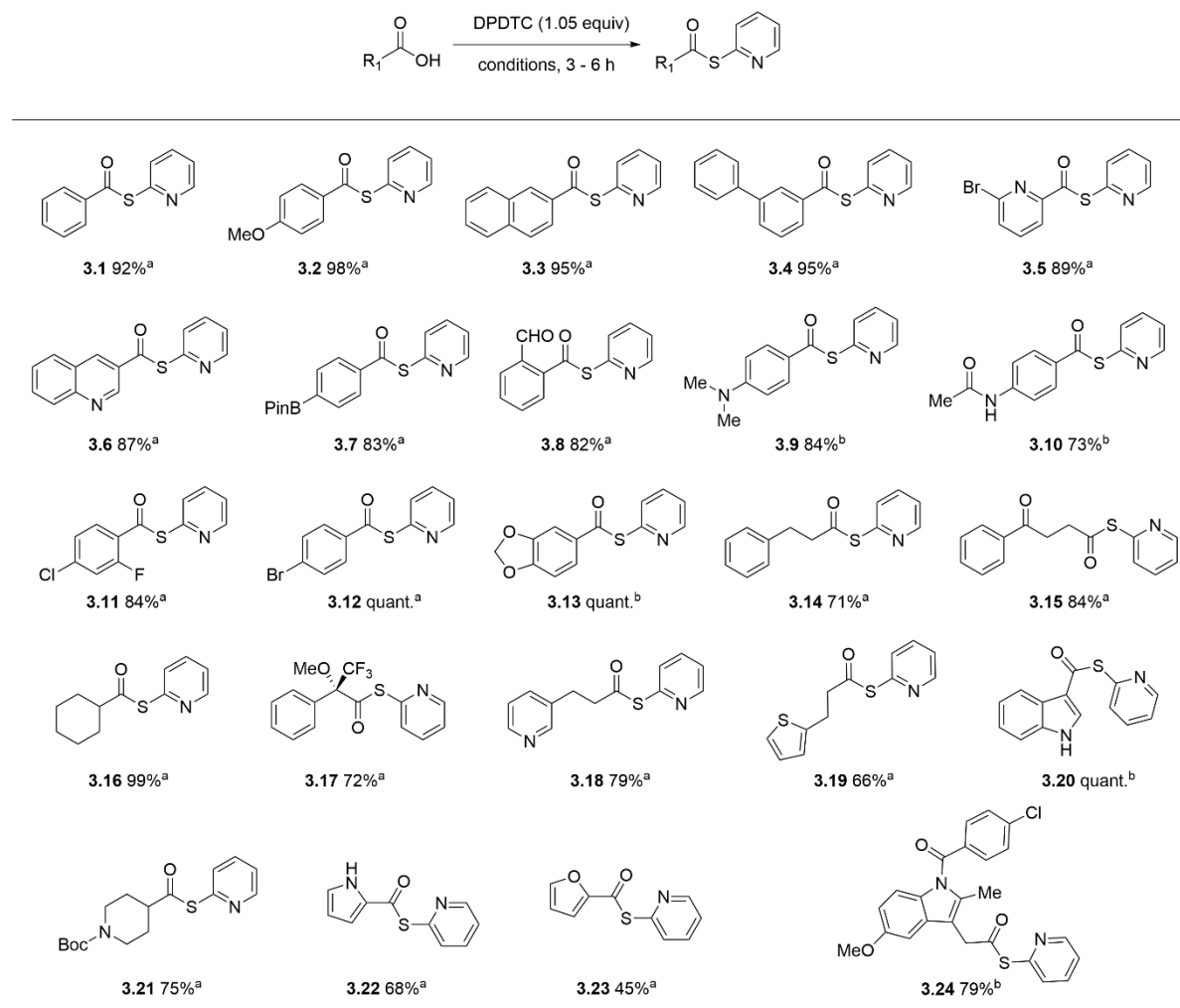


Entry	Conditions	Results
1	neat, 60 °C	Suitable for most carboxylic acids
2	10 mol % DMAP, in 2 M EtOAc, 60 °C	Gives moderate yield
3	10 mol % DMAP, in 2 M EtOAc, rt	Suitable for carboxylic acid which doesn't melt

The utilization of DPDTC for thioester synthesis has been demonstrated to be highly effective and broadly applicable. As shown in Table 2, various of carboxylic acids were successfully converted into thioesters with excellent yields. The reaction exhibited

remarkable tolerance to the presence of various functional groups, including aldehydes, halides, amides, amines, and the presence of a Bpin residue, as well as heterocyclic compounds such as pyridine, thiophene, and pyrrole. Notably, the thioester derived from the drug molecule indomethacin was isolated with an impressive yield of 79%.

Table 2. Thioesters synthesized from carboxylic acids.



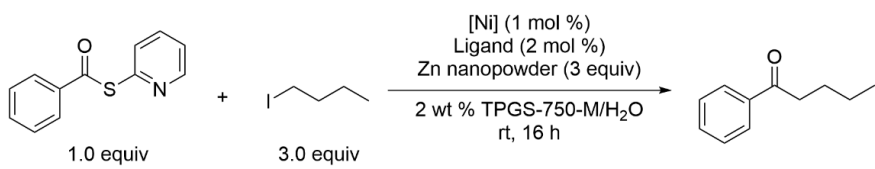
^a Carboxylic acid (2 mmol), DPDTC (2.1 mmol, 521.0 mg), 60 °C, 3 - 6 h;

^b Carboxylic acid (2 mmol), DPDTC (2.1 mmol, 521.0 mg), DMAP (0.2 mmol, 24.4 mg), EtOAc (1 mL), rt, 3 - 6 h.

Optimization of Fukuyama reaction conditions

The initial optimization results using nickel salts and ligands are shown in Table 3. Employing 1 mol % Ni(acac)₂ as the catalyst without any ligand, together with 1.0 equivalent of *S*-(pyridin-2-yl)benzothioate, 3.0 equivalents of iodobutane, and 3.0 equivalents of Zn nanopowder in a 2 wt % TPGS-750-M aqueous solution, yielded the desired product in 35% yield.

Table 3. Screening of nickel salts and ligands



Entry ^a	Nickel salt	Ligand	Yield ^b
1	Ni(acac) ₂	-	35
2	Ni(acac) ₂	1,10-phenanthroline	74
3	Ni(COD) ₂	1,10-phenanthroline	78
4	NiCl ₂ (PCy) ₃	1,10-phenanthroline	27
5	NiCl ₂ (PPh ₃) ₂	1,10-phenanthroline	18
6	NiCl ₂ (glyme)	1,10-phenanthroline	73
7	NiBr ₂ (glyme)	1,10-phenanthroline	78(76)
8	NiBr ₂ (dimethoxyethyl ether)	1,10-phenanthroline	68
9	NiCl ₂ (dppp)	1,10-phenanthroline	11
10	NiCl ₂ (dppe)	1,10-phenanthroline	18
11	NiCl ₂ (FcPCy ₂)	1,10-phenanthroline	8
12	NiCl ₂ (FcPPh ₂)	1,10-phenanthroline	16
13	NiBr ₂ (glyme)	3,4,7,8-tetramethyl-1,10-phenanthroline	82
14	NiBr ₂ (glyme)	4,7-dichloro-1,10-phenanthroline	85
15	NiBr ₂ (glyme)	4,7-diphenyl-1,10-phenanthroline	85
16	NiBr ₂ (glyme)	4,7-dimethoxy-1,10-phenanthroline	36
17	NiBr₂(glyme)	1,1'-bipyridine	85 (84)
18	NiBr ₂ (glyme)	4,4'-tertbutyl-1,1'-bipyridine	79

^a *S*-(pyridin-2-yl)benzothioate (0.4 mmol), 1-iodobutane (1.2 mmol), Ni salt (1 mol %), ligand (2 mol %), Zn nanopowder (1.2 mmol), 2 wt % TPGS-750-M/H₂O (1 mL), rt, 16 h;

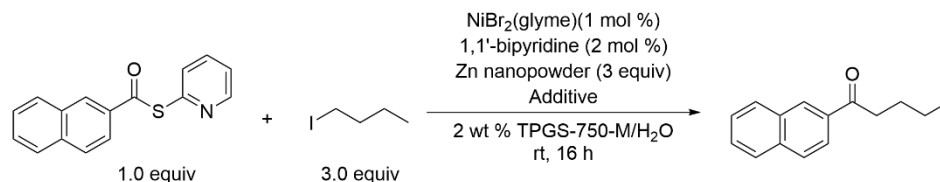
^b Isolated yield.

Introducing 2 mol % 1,10-phenanthroline as a ligand enhanced the yield to 74%. Further experimentation with various nickel salts combined with 1,10-phenanthroline as ligand was conducted. Notably, as shown in entries 4, 5, 9, 10, 11, and 12, pre-ligated nickel with a phosphine ligand resulted in yields lower than 30%. Ni(COD)₂ and NiBr₂(glyme) emerged as the most effective catalysts, producing a 78% yield of the desired ketone product. Subsequent screening of different ligands revealed that various substituted phenanthrolines did not significantly enhance the yield. Consequently, 1,1'-pyridine (entry 17) was selected for future reactions due to its comparable reactivity and cost-effectiveness.

However, it was found that the conditions that worked for the previous thioester were not generally applicable. Under the same conditions, when the starting material was switched to *S*-(pyridin-2-yl) naphthalene-2-carbothioate, the yield decreased to 61%. Additional optimization involving temperature, surfactants, and catalyst loading were explored, but none significantly enhanced the reaction (see the Table in the SI). The addition of various additives, however, did impact the reaction. Initially, a cuprous salt was intentionally added as a scavenger of the byproduct, 2-mercaptopyridine, to prevent potential catalyst poisoning. This approach improved the yield to 74% (entry 14). Interestingly, increasing the amount of cuprous salt (entries 13-16) did not substantially benefit the reaction. Moreover, adding an extra equivalent of 2-mercaptopyridine had no effect on the reaction (entry 2). This led us to hypothesize that cuprous acetate might not act as a scavenger of 2-mercaptopyridine but as a Lewis acid, activating the carbonyl group. Subsequent screening of various Lewis acids identified 0.75 equivalents of ZnCl₂·TMEDA as the most effective, achieving a 95% yield. Notably, using one equivalent of ZnCl₂ resulted in only a 61% yield (entry 28), possibly due to the hydrolysis of ZnCl₂ to Zn(OH)₂,

which lacks an activating effect (entry 29). Further, the addition of an extra equivalent of TMEDA reduced the yield to 20% (entry 18), indicating that the reaction did not benefit from the TMEDA-Zn coordination effect. Instead, TMEDA likely acted as a base, leading to hydrolysis of the thioester.

Table 4. Optimization of additives



Entry ^a	Additive	Yield ^b	Entry	Additive	Yield
1	none	61	16	200 mol % Cu(OAc)	73
2	1 equiv 2-mercaptopyridine	63	17	50 mol % MgCl ₂	71
3	3 equiv Lil	49	18	1 equiv TMEDA	20
4	10 mol % Co(acac) ₂	21	19	10 mol % Sc(OTf) ₃	73
5	10 mol % Cu(acac) ₂	22	20	10 mol % Bi(OTf) ₃	12
6	10 mol % MnPc	31	21	50 mol % Sc(OTf) ₃	67
7	10 mol % Mn(acac) ₃	11	22	100 mol % Sc(OTf) ₃	21
8	10 mol % Cu(OAc)	67	23	1 equiv ZnCl ₂ ·TMEDA	81
9	10 mol % CuI	62	24	0.25 equiv ZnCl ₂ ·TMEDA	82
10	10 mol % CuCN	64	25	0.5 equiv ZnCl ₂ ·TMEDA	92
11	10 mol % Cu(OTf)(CH ₃ CN) ₄	58	26	0.75 equiv ZnCl₂·TMEDA	95 (92)
12	10 mol % CuCl	64	27	2.0 equiv ZnCl ₂ ·TMEDA	61
13	30 mol % Cu(OAc)	68	28	1 equiv ZnCl ₂	61
14	50 mol % Cu(OAc)	74	29	1 equiv Zn(OH) ₂	16
15	100 mol % Cu(OAc)	44			

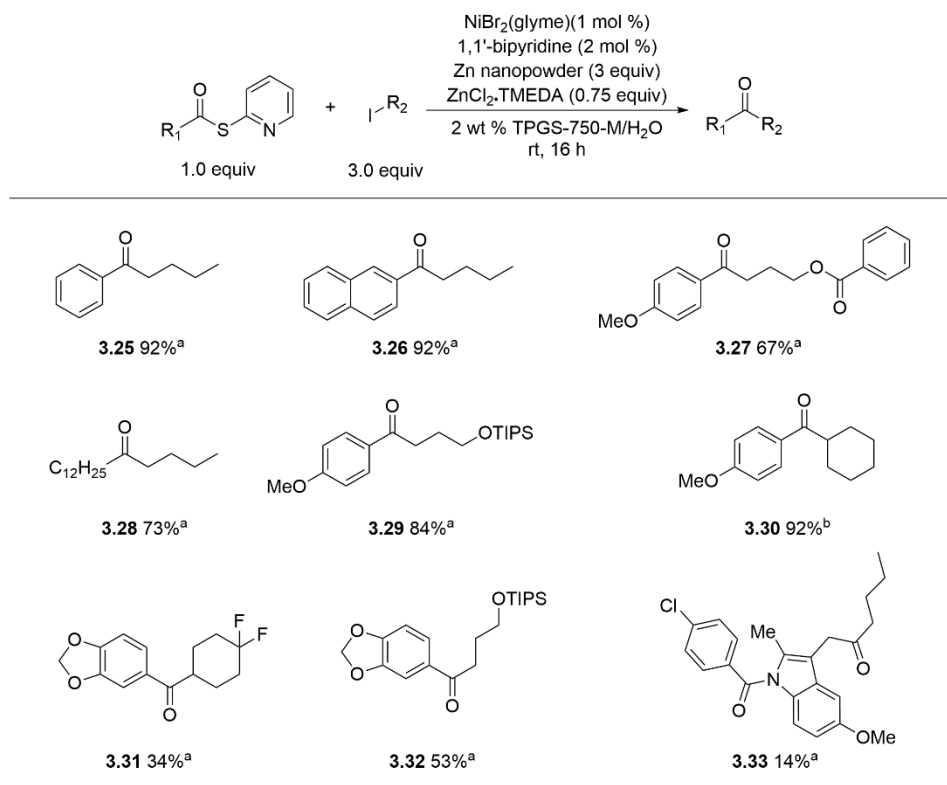
^a *S*-(pyridin-2-yl) naphthalene-2-carbothioate (0.4 mmol), 1-iodobutane (1.2 mmol), NiBr₂(glyme) (1 mol %), 1,1'-bipyridine (2 mol %), Zn nanopowder (1.2 mmol), additives, 2 wt % TPGS-750-M/H₂O (1 mL), rt, 16 h;

^b Isolated yield.

Substrate scope

With the optimized conditions established, a series of reactions involving different thioesters and alkyl iodides were performed to assess generality. These reactions demonstrated notable success, showing tolerance for methoxy groups (**3.27**, **3.29**, **3.30**, **3.33**), ester groups (**3.27**), and TIPS groups (**3.29**). Compounds containing heterocycles, such as benzo[*d*][1,3]dioxole (**3.31**, **3.32**) and indomethacin (**3.33**), gave lower yield outcomes. Both aliphatic thioesters (**3.28**) and secondary alkyl iodides (**3.30**) were well accommodated, resulting in moderate-to-good yields.

Table 5. Substrate scope

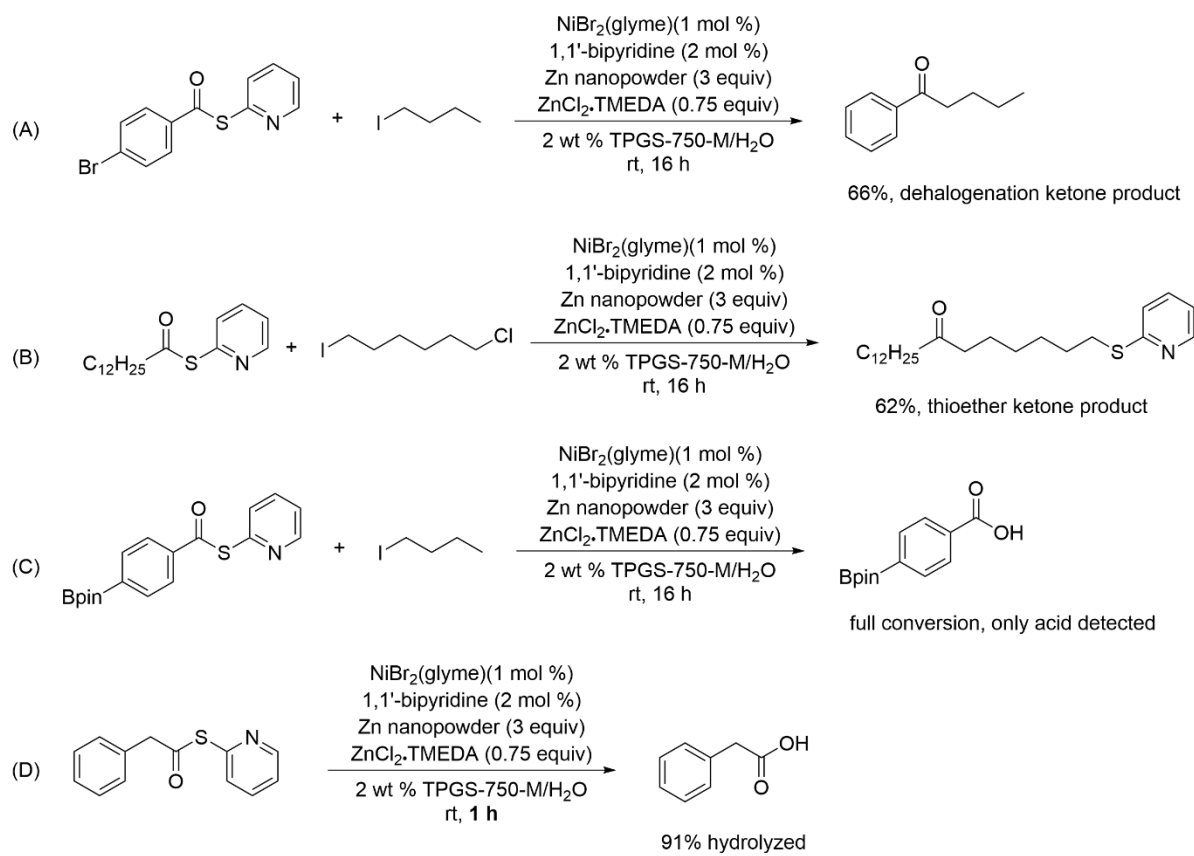


^a Thioester (0.4 mmol), alkyl iodide (1.2 mmol), NiBr₂(glyme) (1 mol %), 1,1'-bipyridine (2 mol %), Zn nanopowder (1.2 mmol), ZnCl₂·TMEDA (0.3 mmol), 2 wt % TPGS-750-M/H₂O (1 mL), rt, 16 h;

^b Reaction performed in pure water, with 2 mol % NiBr₂(glyme) and 4 mol % 1,1'-bipyridine.

Despite some successful examples, the reaction exhibits certain limitations. As shown in Scheme 8A, the nickel hydride generated *in situ* effectively catalyzes the dehalogenation reaction. It has been observed that aryl bromides or chlorides tend to yield ketone products accompanied by dehalogenation. Additionally, a byproduct of the reaction, 2-mercaptopyridine, acts as a relatively potent nucleophile. This is observed in Scheme 8B, where alkyl chlorides, serving as an electrophile, undergo substitution to form thioethers under the reaction conditions. Lastly, the conditions demonstrate enhanced reactivity with electron-rich compounds. In contrast, electron-deficient aromatic thioesters or benzylic thioesters rapidly undergo hydrolysis in water, as shown in Schemes 8C and 8D.

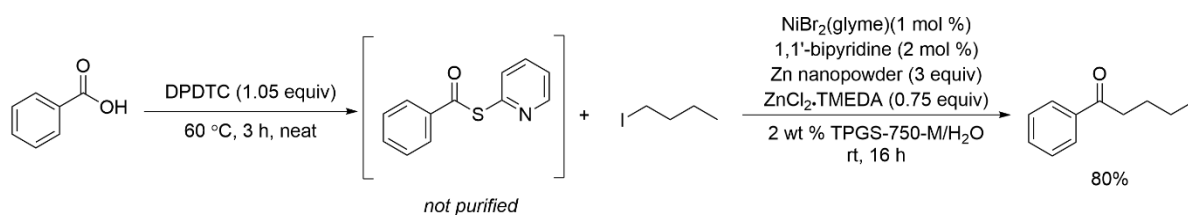
Scheme 8, Limitations with the condition



One-pot reaction test

A one-pot reaction sequence, starting with carboxylic acid and ending in ketone formation, was evaluated. As shown in Scheme 9, this one-pot approach yielded the desired ketone product with an 80% isolated yield. This yield is slightly lower than that obtained when starting from the thioester, the difference likely attributable to inefficient mixing due to the viscosity of the crude product formed in the first step. This mixing issue could potentially be solved by the addition of a co-solvent.

Scheme 9. One-pot reaction test for Fukuyama reaction in water



Conclusion

In conclusion, this work focuses on optimizing and developing the initial substrate scope for a safe, effective, and green one-pot method to synthesize ketones from carboxylic acids. This process involves the use of a readily formed thioester intermediate and an in-situ generated organozinc reagent. Both the potential and limitations of this reaction have been thoroughly investigated, providing a robust reference for future research projects in similar areas.

References

1. McDaniel, R.; Thamchaipenet, A.; Gustafsson, C.; Fu, H.; Betlach, M.; Betlach, M.; Ashley, G., Multiple genetic modifications of the erythromycin polyketide synthase to produce a library of novel “unnatural” natural products. *Proc. Natl. Acad. Sci.* **1999**, *96*, 1846-1851.
2. O’Keefe, B. M.; Simmons, N.; Martin, S. F., Facile access to sterically hindered aryl ketones via carbonylative cross-coupling: application to the total synthesis of luteolin. *Tetrahedron* **2011**, *67*, 4344-4351.
3. Romines, K. R.; Freeman, G. A.; Schaller, L. T.; Cowan, J. R.; Gonzales, S. S.; Tidwell, J. H.; Andrews, C. W.; Stammers, D. K.; Hazen, R. J.; Ferris, R. G.; Short, S. A.; Chan, J. H.; Boone, L. R., Structure–Activity Relationship Studies of Novel Benzophenones Leading to the Discovery of a Potent, Next Generation HIV Nonnucleoside Reverse Transcriptase Inhibitor. *J. Med. Chem.* **2006**, *49*, 727-739.
4. Zhu, J.; Dhammi, A.; van Kretschmar, J. B.; Vargo, E. L.; Apperson, C. S.; Michael Roe, R., Novel use of aliphatic n-methyl ketones as a fumigant and alternative to methyl bromide for insect control. *Pest Manag. Sci.* **2018**, *74*, 648-657.
5. Sharmoukh, W.; Ko, K. C.; Noh, C.; Lee, J. Y.; Son, S. U., Designed Synthesis of Multi-Electrochromic Systems Bearing Diaryl Ketone and Isophthalates. *J. Org. Chem.* **2010**, *75*, 6708-6711.
6. Tan, Y.; Siebert, K. J., Quantitative Structure–Activity Relationship Modeling of Alcohol, Ester, Aldehyde, and Ketone Flavor Thresholds in Beer from Molecular Features. *J. Agric. Food Chem.* **2004**, *52*, 3057-3064.
7. Guo, H.; Chang, S.; Jia, L.; Wang, Z.; Zhang, Q.; Zhang, G., Advances in the synthesis and applications of raspberry ketone: A review. *Flavour Fragr. J.* **2021**, *36*, 615-625.
8. Wang, J.; Mathias, L. J., A polymerizable photosensitizer and its photopolymerization kinetics. *Polym. Int.* **2005**, *54*, 1537-1542.

9. Maeyama, K.; Yamashita, K.; Saito, H.; Aikawa, S.; Yoshida, Y., Synthesis of aromatic poly(ether ketone)s bearing optically active macrocycles through Suzuki coupling polymerization. *Polym. J.* **2012**, *44*, 315-320.
10. Joule, J. A.; Mills, K., *Heterocyclic Chemistry. 4th Edition*. Blackwell Science: Oxford, 2000.
11. Hagiwara, H., Aspects in the Total Syntheses of Higher Terpenoids Starting From Wieland–Miescher Ketone and Its Derivative: A Review. *Nat. Prod. Commun.* **2020**, *15*, 1934578X20925340.
12. Foley, D. J.; Waldmann, H., Ketones as strategic building blocks for the synthesis of natural product-inspired compounds. *Chem. Soc. Rev.* **2022**, *51*, 4094-4120.
13. Gröger, H.; Gallou, F.; Lipshutz, B. H., Where Chemocatalysis Meets Biocatalysis: In Water. *Chem. Rev.* **2023**, *123*, 5262-5296.
14. Lipshutz, B. H., Nanomicelle-enabled chemoenzymatic catalysis: Clean chemistry in “dirty” water. *Chem. Catal.* **2023**, *3*, 100458.
15. Muzart, J., Chromium-catalyzed oxidations in organic synthesis. *Chem. Rev.* **1992**, *92*, 113-140.
16. Heravi, M. M.; Zadsirjan, V.; Saedi, P.; Momeni, T., Applications of Friedel–Crafts reactions in total synthesis of natural products. *RSC Adv.* **2018**, *8*, 40061-40163.
17. Hirao, S.; Saeki, R.; Takahashi, T.; Iwai, K.; Nishiwaki, N.; Ohga, Y., Synthesis of Unsymmetrical Ketones Using Chelation-Controlled Sequential Substitution of N-Triazinylamide/Weinreb Amide by Organometallic Reagents. *ACS Omega* **2022**, *7*, 48476-48483.
18. Karakaya, I.; Rizwan, K.; Munir, S., Transition-Metal Catalyzed Coupling Reactions for the Synthesis of (Het)aryl Ketones: An Approach from their Synthesis to Biological Perspectives. *ChemistrySelect* **2023**, *8*, e202204005.
19. Rahaman, A.; Chauhan, S. S.; Bhadra, S., Recent advances in catalytic decarboxylative transformations of carboxylic acid groups attached to a non-aromatic sp² or sp carbon. *Org. Biomol. Chem.* **2023**, *21*, 5691-5724.

20. Hu, K.-F.; Ning, X.-S.; Qu, J.-P.; Kang, Y.-B., Tuning Regioselectivity of Wacker Oxidation in One Catalytic System: Small Change Makes Big Step. *J. Org. Chem.* **2018**, *83*, 11327-11332.
21. Sarvari, M. H.; Sharghi, H., Reactions on a Solid Surface. A Simple, Economical and Efficient Friedel–Crafts Acylation Reaction over Zinc Oxide (ZnO) as a New Catalyst. *J. Org. Chem.* **2004**, *69*, 6953-6956.
22. Neumann, H.; Brennführer, A.; Beller, M., A General Synthesis of Diarylketones by Means of a Three-Component Cross-Coupling of Aryl and Heteroaryl Bromides, Carbon Monoxide, and Boronic acids. *Chem. Eur. J.* **2008**, *14*, 3645-3652.
23. Ni, S.; Padial, N. M.; Kingston, C.; Vantourout, J. C.; Schmitt, D. C.; Edwards, J. T.; Kruszyk, M. M.; Merchant, R. R.; Mykhailiuk, P. K.; Sanchez, B. B.; Yang, S.; Perry, M. A.; Gallego, G. M.; Mousseau, J. J.; Collins, M. R.; Cherney, R. J.; Lebed, P. S.; Chen, J. S.; Qin, T.; Baran, P. S., A Radical Approach to Anionic Chemistry: Synthesis of Ketones, Alcohols, and Amines. *J. Am. Chem. Soc.* **2019**, *141*, 6726-6739.
24. Sheldon, R. A., Metrics of Green Chemistry and Sustainability: Past, Present, and Future. *ACS Sustain. Chem. Eng.* **2018**, *6*, 32-48.
25. Sikandar, S.; Zahoor, A. F.; Naheed, S.; Parveen, B.; Ali, K. G.; Akhtar, R., Fukuyama reduction, Fukuyama coupling and Fukuyama–Mitsunobu alkylation: recent developments and synthetic applications. *Mol. Divers.* **2022**, *26*, 589-628.
26. Tokuyama, H.; Yokoshima, S.; Yamashita, T.; Fukuyama, T., A novel ketone synthesis by a palladium-catalyzed reaction of thiol esters and organozinc reagents. *Tetrahedron Lett.* **1998**, *39*, 3189-3192.
27. Wotal, A. C.; Weix, D. J., Synthesis of Functionalized Dialkyl Ketones from Carboxylic Acid Derivatives and Alkyl Halides. *Org. Lett.* **2012**, *14*, 1476-1479.

28. Lee, J. H.; Kishi, Y., One-Pot Ketone Synthesis with Alkylzinc Halides Prepared from Alkyl Halides via a Single Electron Transfer (SET) Process: New Extension of Fukuyama Ketone Synthesis. *J. Am. Chem. Soc.* **2016**, *138*, 7178-7186.
29. Amoores, J. E.; Hautala, E., Odor as an aid to chemical safety: Odor thresholds compared with threshold limit values and volatilities for 214 industrial chemicals in air and water dilution. *J. Appl. Toxicol.* **1983**, *3*, 272-290.
30. Freiberg, Kaitlyn M.; Kavthe, R. D.; Thomas, R. M.; Fialho, D. M.; Dee, P.; Scurria, M.; Lipshutz, B. H., Direct formation of amide/peptide bonds from carboxylic acids: no traditional coupling reagents, 1-pot, and green. *Chem. Sci.* **2023**, *14*, 3462-3469.
31. Iyer, K. S.; Nelson, C.; Lipshutz, B. H., Facile, green, and functional group-tolerant reductions of carboxylic acids...in, or with, water. *Green Chem.* **2023**, *25*, 2663-2671.
32. Freiberg, K. M.; Ghiglietti, E.; Scurria, M.; Lipshutz, B. H., Use of dipyridyldithiocarbonate (DPDTC) as an environmentally responsible reagent leading to esters and thioesters under green chemistry conditions. *Green Chem.* **2023**, *25*, 9941-9947.
33. Krasovskiy, A.; Duplais, C.; Lipshutz, B. H., Zn-Mediated, Pd-Catalyzed Cross-Couplings in Water at Room Temperature Without Prior Formation of Organozinc Reagents. *J. Am. Chem. Soc.* **2009**, *131*, 15592-15593.
34. Hu, Y.; Wong, M. J.; Lipshutz, B. H., ppm Pd-Containing Nanoparticles as Catalysts for Negishi Couplings ... in Water. *Angew. Chem., Int. Ed.* **2022**, *61*, e202209784.
35. Lipshutz, B. H.; Ghorai, S.; Abela, A. R.; Moser, R.; Nishikata, T.; Duplais, C.; Krasovskiy, A.; Gaston, R. D.; Gadwood, R. C., TPGS-750-M: A Second-Generation Amphiphile for Metal-Catalyzed Cross-Couplings in Water at Room Temperature. *J. Org. Chem.* **2011**, *76*, 4379-4391.

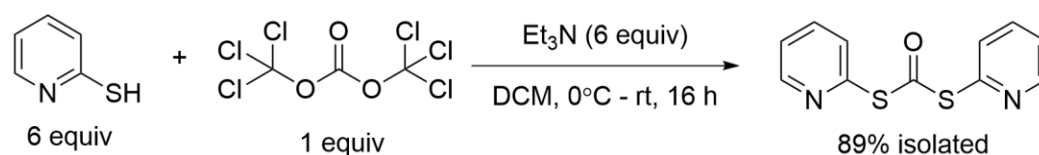
3.3 Appendix

General Information

All commercial reagents were used without further purification unless otherwise noted. All solvents were used as received, such as MeOH, EtOAc, hexanes, iPrOH, and Et₂O, unless otherwise noted, and purchased from Fisher Scientific. 2-Pyridinethiol (97%, Catalog No.: PY-7722) was purchased from CombiBlock. Triphosgene (98%, Product number: T1467) was purchased from TCI and stored under 4 °C. Nickel salt and ligands were purchased from Sigma-Aldrich, Combi-Block and TCI. All nickel catalysts tested were stored in an argon purged glove box. NiBr₂(glyme) (98%, Catalog No.: QH-4240) was purchased from CombiBlock. ZnCl₂·TMEDA was purchased from CombiBlock (98%, Catalog No.: QH-6590). Zinc nanopowder (40-60 nm avg. part. size, ≥99% trace metals basis, Product No. 578002) was purchased from Sigma Aldrich and stored in an argon purged glove box. A solution of 2 wt % TPGS-750-M/H₂O solution was prepared by dissolving TPGS-750-M in degassed HPLC grade water and was stored in Schlenk flask under argon. TPGS-750-M was made as previously described and is available from Sigma-Aldrich (catalog number 733857). A standard 2 wt % aqueous solution of TPGS-750-M was typically prepared on a 100 g scale by dissolving 2 g of the TPGS-750-M wax into 98 g of thoroughly degassed (steady stream of argon, minimum of 12 h bubbling time with stirring and heating). HPLC grade water in a Schlenk flask equipped with a stir bar and allowed to dissolve overnight with vigorous stirring under argon pressure (NOTE: Do not attempt to degas the aqueous phase with surfactant present; vigorous foaming will occur). The 2 wt % TPGS-750-M/H₂O solution, once prepared, was kept in a Schlenk flask. Thin layer

chromatography (TLC) was done using Silica Gel 60 F254 plates (0.25 mm thick) purchased from Merck. Column chromatography was done in glass columns using Silica gel 60 (EMD, 40-63 μm). ^1H , ^{13}C , and ^{19}F NMR spectra were recorded at 25 $^\circ\text{C}$ on an Agilent Technologies 400 MHz, a Varian Unity Inova 500 MHz, Varian Unity Inova 600 MHz, Bruker Avance III HD 400 MHz or Bruker Avance NEO 500 MHz spectrometer in CDCl_3 with residual CHCl_3 (^1H = 7.26 ppm, ^{13}C = 77.16 ppm) or in DMSO-d_6 with residual $(\text{CH}_3)_2\text{SO}$ (^1H = 2.50 ppm, ^{13}C = 39.52 ppm) as internal standards. Chemical shifts are reported in parts per million (ppm). NMR Data are reported as follows: chemical shift, multiplicity (s = singlet, d = doublet, dd = doublet of doublets, ddd = doublet of doublet of doublets, t = triplet, td = triplet of doublets, q = quartet, quin = quintet, m = multiplet), coupling constant (if applicable), and integration. Chemical shifts in ^{13}C NMR spectra are reported in ppm on the δ scale from the central peak of residual CDCl_3 (77.16 ppm) or the central peak of DMSO-d_6 (39.52 ppm).

DPDTC synthesis and purification



To a flame-dried 250 mL round-bottom flask (RBF) equipped with a PTFE-coated magnetic stir bar was added 2-mercaptopyridine (6 equiv, 60 mmol, 6.67 g) and DCM (100 mL) then the flask was sealed with a rubber septum. Et_3N (6 equiv, 60 mmol, 8.3 mL) was added via syringe and the solution was stirred until all components were fully dissolved. The reaction was cooled down to 0 $^\circ\text{C}$ in ice bath. A solution of triphosgene (1 equiv, 10 mmol,

2.97 g) in DCM (12.5 mL) was added to the RBF slowly. Upon full addition, triethylammonium chloride was observed to precipitate. The reaction was allowed to warm to rt and stir overnight.

Upon completion, the reaction mixture was firstly filtered to remove the undissolved ammonium chloride. Then DCM was removed via vacuum and diethyl ether (100 mL) was added to dissolve the DPDTC. The solution was filtered again to remove the ammonium chloride to the maximum extent. The resulting diethyl ether solution was washed with saturated aqueous Na₂CO₃ solution (100 mL × 3) to remove the 2-mercaptopyridine. Then the organic phase was dried over anhydrous Na₂SO₄ and concentrated *in vacuo* to a crude oil.

A seed crystal of DPDTC was added to the crude oil to facilitate the solidification of the oil. The resultant solid was mechanically pulverized into powder and subjected to high vacuum for 1 h to ensure dryness. Minimal amount of *i*-PrOH (5 mL × 2) was added to conduct the trituration. The semi-solid was thoroughly mixed and filtered to yield the DPDTC as a pile yellow powder (6.11 g, 82%).

Thioester formation

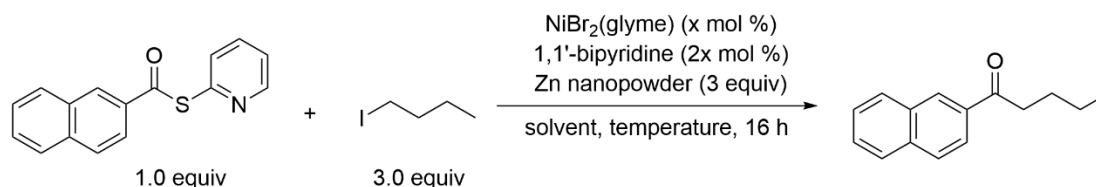
Condition 1: To a flame-dried 2-dram vial equipped with a PTFE-coated magnetic stir bar was added carboxylic acid (1 equiv, 5 mmol) and DPDTC (1.05 equiv, 5.15 mmol, 1.28 g) then the vial was sealed with a rubber septum. An argon needle was introduced to ensure the CO₂ emission. The reaction was stirred under 60 ° C for 3–6 h. Upon completion, DCM was added to dissolve the crude product. Column chromatography or recrystallization was then carried out to obtain the pure thioester.

Condition 2: To a flame-dried 2-dram vial equipped with a PTFE-coated magnetic stir bar was added carboxylic acid (1 equiv, 5 mmol), DPDTC (1.05 equiv, 5.15 mmol, 1.28 g), DMAP (0.5 mmol, 0.1 equiv, 61.09 mg), and EtOAc (2.5 mL) then the vial was sealed with a rubber septum. An argon needle was introduced to ensure the CO₂ emission. The reaction was stirred under 60 °C for 3–6 h. Upon completion, EtOAc was added to dissolve the crude product. Column chromatography or recrystallization was then carried out to obtain the pure thioester.

Condition 3: The same as Condition 2, except the reaction was conducted at rt.

Fukuyama reaction optimization

Table S1. Optimization of catalyst loading, temperature and solvent



Entry ^a	Catalyst Loading	Temperature	Solvent	Yield ^b
1	1 mol % NiBr ₂ (glyme)	rt	2 wt % TPGS-750-M/H ₂ O	61
2	2 mol % NiBr ₂ (glyme)	rt	2 wt % TPGS-750-M/H ₂ O	68
3	10 mol % NiBr ₂ (glyme)	rt	2 wt % TPGS-750-M/H ₂ O	49
4	1 mol % NiBr ₂ (glyme)	45 °C	2 wt % TPGS-750-M/H ₂ O	62
5	1 mol % NiBr ₂ (glyme)	55 °C	2 wt % TPGS-750-M/H ₂ O	58
6	1 mol % NiBr ₂ (glyme)	rt	2 wt % Solutol HS 15/H ₂ O	62
7	1 mol % NiBr ₂ (glyme)	rt	2 wt % MC-1/H ₂ O	72
8	1 mol % NiBr ₂ (glyme)	rt	2 wt % Triton X-100/H ₂ O	63
9	1 mol % NiBr ₂ (glyme)	rt	2 wt % Savie/H ₂ O	70
10	1 mol % NiBr ₂ (glyme)	rt	2 wt % PTS-600/H ₂ O	73
11	1 mol % NiBr ₂ (glyme)	rt	4 wt % Brij-30/H ₂ O	64
12	1 mol % NiBr ₂ (glyme)	rt	degassed water	65
13	1 mol % NiBr ₂ (glyme)	rt	in 2M EtOAc	34

^a *S*-(pyridin-2-yl) naphthalene-2-carbothioate (0.4 mmol), 1-iodobutane (1.2 mmol), NiBr₂(glyme), 1,1'-bipyridine, Zn nanopowder (1.2 mmol), solvent (1 mL), 16 h;

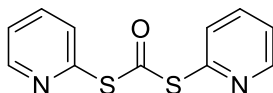
^b Yield based on ¹H NMR, 1,3,5-trimethoxybenzene as internal standard.

General procedure for the Fukuyama reaction

To a flame-dried 1-dram vial equipped with an oven dried stir bar was added thioester (0.4 mmol), alkyl iodide (if it is a solid, 1.2 mmol), bipyridine (2 mol %, 0.008 mmol, 1.3 mg), and ZnCl₂·TMEDA (0.75 equiv, 0.3 mmol, 75 mg). The vial was then transferred to an argon purged glovebox. NiBr₂(glyme) (1 mol %, 0.004 mmol, 1.2 mg) and zinc nanopowder (3 equiv, 1.2 mmol, 78 mg) were added inside of a glove box. The vial was then sealed with a rubber septum inside of the glovebox. A 2 wt % TPGS-750-M/H₂O solution and alkyl iodide (if it is a liquid, 1.2 mmol) were added to the vial by syringe and the mixture was stirred (450 rpm) at rt for 16 h. Upon completion, EtOAc (4 mL) was added, and the mixture was stirred gently for 2 min at rt. Stirring was then stopped and the organic layer was decanted via pipette after centrifugation. The same extraction procedure was repeated twice. The combined organic extracts were dried under reduced pressure and purified by flash chromatography over silica gel.

Analytical data

***S,S*-di(pyridin-2-yl) carbonodithioate**

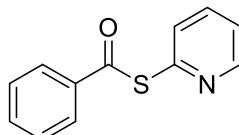


Following the DPDTC synthesis procedure.

^1H NMR (400 MHz, chloroform-*d*) δ 8.62 (ddd, $J = 4.9, 1.9, 0.9$ Hz, 2H), 7.74 (td, $J = 7.6, 1.9$ Hz, 2H), 7.68 (dt, $J = 7.9, 1.2$ Hz, 2H), 7.31 (ddd, $J = 7.3, 4.9, 1.4$ Hz, 2H).

^{13}C NMR (101 MHz, chloroform-*d*) δ 185.80, 150.74, 150.73, 137.56, 130.58, 124.22.

***S*-(Pyridin-2-yl) benzothioate**

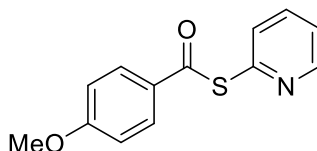


Following the thioester synthesis Condition 1.

^1H NMR (400 MHz, chloroform-*d*) δ 8.68 (ddd, $J = 4.9, 1.9, 0.9$ Hz, 1H), 8.02 (m, 2H), 7.79 (td, $J = 7.6, 1.9$ Hz, 1H), 7.73 (m, 1H), 7.65 – 7.59 (m, 1H), 7.53 – 7.46 (m, 2H), 7.34 (ddd, $J = 7.3, 4.9, 1.2$ Hz, 1H).

^{13}C NMR (101 MHz, chloroform-*d*) δ 189.50, 151.50, 150.68, 137.31, 136.71, 134.05, 131.00, 128.97, 127.72, 123.78.

***S*-(Pyridin-2-yl) 4-methoxybenzothioate**

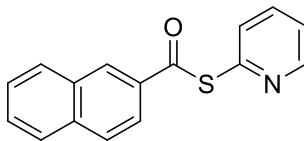


Following the thioester synthesis Condition 1.

^1H NMR (500 MHz, chloroform-*d*) δ 8.67 (m, 1H), 8.04 – 7.97 (m, 2H), 7.82 – 7.75 (m, 1H), 7.73 (m, 1H), 7.36 – 7.30 (m, 1H), 6.97 (m, 2H), 3.89 (s, 3H).

^{13}C NMR (126 MHz, chloroform-*d*) δ 187.87, 164.35, 151.81, 150.59, 137.23, 131.08, 130.01, 129.44, 123.64, 114.16, 55.72.

S-(Pyridin-2-yl) naphthalene-2-carbothioate

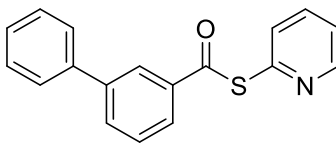


Following the thioester synthesis Condition 1.

^1H NMR (400 MHz, chloroform-*d*) δ 8.74 – 8.69 (m, 1H), 8.64 – 8.60 (m, 1H), 8.05 – 7.98 (m, 2H), 7.91 (m, 2H), 7.85 – 7.76 (m, 2H), 7.67 – 7.55 (m, 2H), 7.36 (ddd, $J = 6.7, 4.8, 1.6$ Hz, 1H).

^{13}C NMR (126 MHz, chloroform-*d*) δ 189.41, 151.57, 150.70, 137.37, 136.15, 134.00, 132.59, 131.07, 129.84, 129.46, 128.96, 128.91, 128.01, 127.23, 123.82, 123.34.

S-(Pyridin-2-yl) [1,1'-biphenyl]-3-carbothioate

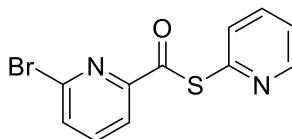


Following the thioester synthesis Condition 1.

^1H NMR (400 MHz, chloroform-*d*) δ 8.73 – 8.66 (m, 1H), 8.24 (t, $J = 1.7$ Hz, 1H), 8.00 (dt, $J = 7.8, 1.3$ Hz, 1H), 7.87 – 7.78 (m, 2H), 7.76 (m, 1H), 7.66 – 7.61 (m, 2H), 7.57 (t, $J = 7.8$ Hz, 1H), 7.48 (m, 2H), 7.43 – 7.38 (m, 1H), 7.35 (ddd, $J = 7.0, 4.9, 1.2$ Hz, 1H).

^{13}C NMR (126 MHz, chloroform-*d*) δ 189.56, 151.47, 150.72, 142.17, 139.93, 137.36, 137.30, 132.67, 131.01, 129.46, 129.14, 128.13, 127.35, 126.50, 126.34, 123.84.

S-(Pyridin-2-yl) 6-bromopyridine-2-carbothioate

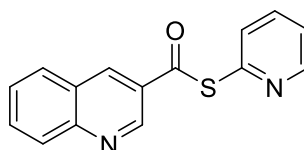


Following the thioester synthesis Condition 1.

^1H NMR (500 MHz, chloroform-*d*) δ 8.75 – 8.65 (m, 1H), 7.93 – 7.87 (m, 1H), 7.78 (td, $J = 7.7, 1.8$ Hz, 1H), 7.75 – 7.70 (m, 2H), 7.68 (m, 1H), 7.34 (dd, $J = 7.5, 4.9$ Hz, 1H).

^{13}C NMR (126 MHz, chloroform-*d*) δ 190.37, 152.40, 151.84, 150.87, 141.59, 139.62, 137.30, 133.09, 130.82, 123.82, 119.65.

S-(Pyridin-2-yl) quinoline-3-carbothioate

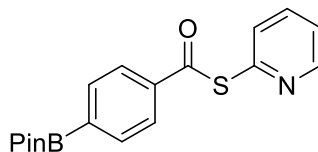


Following the thioester synthesis Condition 1.

^1H NMR (500 MHz, chloroform-*d*) δ 9.42 (d, $J = 2.3$ Hz, 1H), 8.83 (d, $J = 2.1$ Hz, 1H), 8.71 (ddd, $J = 4.8, 1.8, 0.8$ Hz, 1H), 8.18 (d, $J = 8.5$ Hz, 1H), 8.00 – 7.96 (m, 1H), 7.87 (m, 1H), 7.83 (td, $J = 7.6, 1.9$ Hz, 1H), 7.78 (dt, $J = 7.9, 0.9$ Hz, 1H), 7.69 – 7.64 (m, 1H), 7.38 (ddd, $J = 7.4, 4.8, 1.2$ Hz, 1H).

^{13}C NMR (126 MHz, chloroform-*d*) δ 188.09, 150.87, 150.60, 150.40, 147.90, 137.51, 136.82, 132.54, 131.03, 129.72, 129.56, 129.31, 128.02, 126.87, 124.12.

S-(Pyridin-2-yl) 4-(4,4,5,5-tetramethyl-1,3,2-dioxaborolan-2-yl)benzothioate S-(pyridin-2-yl)



Following the thioester synthesis Condition 1.

^1H NMR (400 MHz, chloroform-*d*) δ 8.72 – 8.64 (m, 1H), 7.99 (d, $J = 8.2$ Hz, 2H), 7.91 (d, $J = 8.2$ Hz, 2H), 7.79 (td, $J = 7.6, 1.8$ Hz, 1H), 7.73 (m, 1H), 7.34 (ddd, $J = 7.3, 4.9, 1.1$ Hz, 1H), 1.36 (s, 12H).

^{13}C NMR (126 MHz, chloroform-*d*) δ 189.73, 151.46, 150.70, 138.63, 137.32, 135.24, 131.00, 126.69, 123.81, 84.45, 25.02.

***S*-(Pyridin-2-yl) 2-formylbenzothioate**

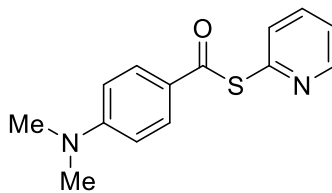


Following the thioester synthesis Condition 1.

^1H NMR (400 MHz, chloroform-*d*) δ 8.54 (ddd, $J = 4.9, 1.8, 0.9$ Hz, 1H), 7.94 (d, $J = 7.7$ Hz, 1H), 7.76 – 7.71 (m, 2H), 7.69 – 7.65 (m, 1H), 7.65 – 7.59 (m, 2H), 7.36 (dt, $J = 8.0, 0.9$ Hz, 1H), 7.16 (ddd, $J = 7.4, 4.9, 1.0$ Hz, 1H).

^{13}C NMR (126 MHz, chloroform-*d*) δ 169.36, 155.28, 150.00, 146.25, 137.16, 134.57, 130.33, 126.59, 125.89, 123.58, 123.48, 121.60, 83.12.

***S*-(Pyridin-2-yl) 4-(dimethylamino)benzothioate**

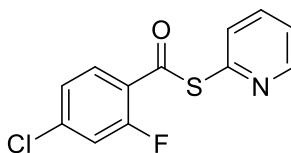


Following the thioester synthesis Condition 2.

^1H NMR (400 MHz, chloroform-*d*) δ 8.65 (dt, $J = 4.9, 1.4$ Hz, 1H), 7.96 – 7.89 (m, 2H), 7.75 (m, 2H), 7.29 (ddd, $J = 5.5, 4.9, 2.9$ Hz, 1H), 6.69 – 6.64 (m, 2H), 3.08 (s, 6H).

^{13}C NMR (126 MHz, chloroform-*d*) δ 186.76, 154.17, 152.62, 150.32, 137.06, 131.11, 130.00, 123.94, 123.27, 110.88, 40.20.

S-(Pyridin-2-yl) 4-chloro-2-fluorobenzothioate



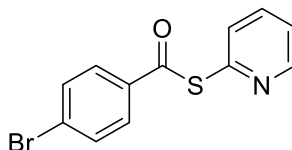
Following the thioester synthesis Condition 1.

^1H NMR (400 MHz, chloroform-*d*) δ 8.69 (ddd, $J = 4.8, 1.8, 0.8$ Hz, 1H), 7.87 (m, 1H), 7.80 (td, $J = 7.7, 1.9$ Hz, 1H), 7.72 (dt, $J = 7.9, 1.0$ Hz, 1H), 7.36 (ddd, $J = 7.5, 4.8, 1.2$ Hz, 1H), 7.28 – 7.22 (m, 2H).

^{13}C NMR (126 MHz, chloroform-*d*) δ 185.49, 161.60, 159.52, 150.80, 140.63 (d, $J_{\text{C-F}} = 10.4$ Hz), 137.47, 131.03, 130.96 (d, $J_{\text{C-F}} = 2.3$ Hz), 125.19 (d, $J_{\text{C-F}} = 3.7$ Hz), 124.13, 123.72 (d, $J_{\text{C-F}} = 11.4$ Hz), 117.96 (d, $J_{\text{C-F}} = 25.6$ Hz).

^{19}F NMR (471 MHz, chloroform-*d*) δ -107.12 (dd, $J = 10.0, 7.8$ Hz).

S-(Pyridin-2-yl) 4-bromobenzothioate

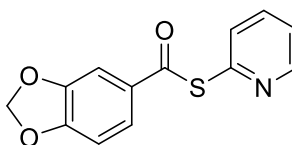


Following the thioester synthesis Condition 1.

^1H NMR (400 MHz, chloroform-*d*) δ 8.68 (ddd, $J = 4.8, 1.8, 0.8$ Hz, 1H), 7.91 – 7.85 (m, 2H), 7.79 (td, $J = 7.7, 1.9$ Hz, 1H), 7.71 (dt, $J = 7.9, 1.0$ Hz, 1H), 7.68 – 7.61 (m, 2H), 7.35 (ddd, $J = 7.5, 4.8, 1.2$ Hz, 1H).

^{13}C NMR (126 MHz, chloroform-*d*) δ 188.35, 150.73, 150.51, 137.15, 135.20, 132.04, 130.73, 128.95, 128.86, 123.70.

***S*-(Pyridin-2-yl) benzo[d][1,3]dioxole-5-carbothioate**

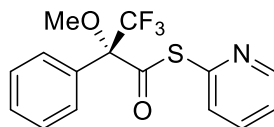


Following the thioester synthesis Condition 2.

^1H NMR (400 MHz, chloroform-*d*) δ 8.65 (ddd, $J = 4.8, 1.8, 0.8$ Hz, 1H), 7.76 (td, $J = 7.7, 1.9$ Hz, 1H), 7.72 – 7.64 (m, 2H), 7.43 (d, $J = 1.8$ Hz, 1H), 7.31 (ddd, $J = 7.4, 4.9, 1.3$ Hz, 1H), 6.87 (d, $J = 8.2$ Hz, 1H), 6.05 (s, 2H).

^{13}C NMR (126 MHz, chloroform-*d*) δ 187.57, 152.59, 151.56, 150.56, 148.33, 137.20, 131.03, 130.98, 124.02, 123.66, 108.28, 107.50, 102.20.

***S*-(Pyridin-2-yl) (*R*)-3,3,3-trifluoro-2-methoxy-2-phenylpropanethioate**



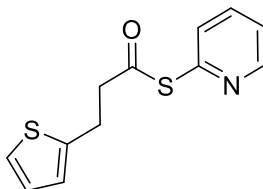
Following the thioester synthesis Condition 1.

^1H NMR (400 MHz, chloroform-*d*) δ 8.65 (ddd, $J = 4.8, 1.9, 0.8$ Hz, 1H), 7.75 (td, $J = 7.7, 1.9$ Hz, 1H), 7.64 – 7.60 (m, 2H), 7.57 (dt, $J = 7.9, 1.0$ Hz, 1H), 7.44 (m, 3H), 7.31 (ddd, $J = 7.5, 4.8, 1.1$ Hz, 1H), 3.67 (q, $J = 1.7$ Hz, 3H).

^{13}C NMR (126 MHz, chloroform-*d*) δ 195.26, 150.82, 137.39, 131.81, 130.77, 130.04, 128.88, 127.60, 127.59, 124.00, 123.13 (q, $J_{\text{C-F}} = 291.0$ Hz), 87.98 (q, $J_{\text{C-F}} = 26.4$ Hz), 56.04.

^{19}F NMR (471 MHz, chloroform-*d*) δ -68.85.

S-(Pyridin-2-yl) 3-(thiophen-2-yl)propanethioate

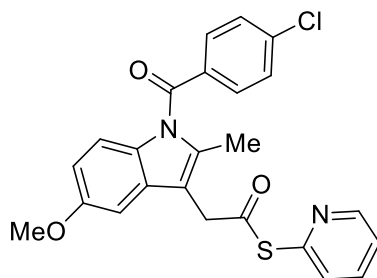


Following the thioester synthesis Condition 1.

^1H NMR (400 MHz, chloroform-*d*) δ 8.62 (ddd, $J = 4.8, 1.9, 0.8$ Hz, 1H), 7.74 (td, $J = 7.7, 1.9$ Hz, 1H), 7.61 (dt, $J = 7.9, 1.0$ Hz, 1H), 7.32 – 7.27 (m, 2H), 6.28 (dd, $J = 3.1, 1.9$ Hz, 1H), 6.06 (m, 1H), 3.06 (m, 4H).

^{13}C NMR (126 MHz, chloroform-*d*) δ 195.40, 153.37, 151.37, 150.54, 141.57, 137.35, 130.31, 123.74, 110.42, 105.93, 42.43, 23.68.

S-(Pyridin-2-yl) 2-(1-(4-chlorobenzoyl)-5-methoxy-2-methyl-1H-indol-3-yl)ethanethioate

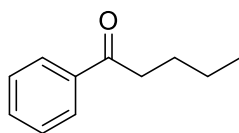


Following the thioester synthesis Condition 2.

^1H NMR (400 MHz, chloroform-*d*) δ 8.60 (ddd, $J = 4.8, 1.8, 0.8$ Hz, 1H), 7.75 – 7.65 (m, 3H), 7.58 (dt, $J = 7.9, 0.9$ Hz, 1H), 7.51 – 7.45 (m, 2H), 7.29 – 7.25 (m, 1H), 6.98 (d, $J = 2.5$ Hz, 1H), 6.89 (d, $J = 9.0$ Hz, 1H), 6.69 (dd, $J = 9.0, 2.5$ Hz, 1H), 4.00 (s, 2H), 3.84 (s, 3H), 2.45 (s, 3H).

^{13}C NMR (126 MHz, chloroform-*d*) δ 194.50, 168.41, 156.33, 151.67, 150.54, 139.57, 137.27, 137.21, 133.80, 131.38, 131.01, 130.55, 130.21, 129.30, 123.70, 115.15, 112.13, 111.43, 101.24, 55.86, 39.71, 13.66.

1-Phenylpentan-1-one

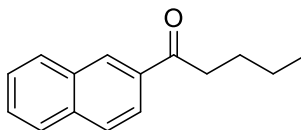


Following the general Fukuyama reaction procedure.

^1H NMR (500 MHz, chloroform-*d*) δ 8.04 – 7.91 (m, 2H), 7.61 – 7.50 (m, 1H), 7.46 (m, 2H), 3.01 – 2.92 (m, 2H), 1.73 (p, $J = 7.5$ Hz, 2H), 1.44 – 1.39 (m, 2H), 0.96 (t, $J = 7.3$ Hz, 3H).

^{13}C NMR (126 MHz, chloroform-*d*) δ 200.77, 137.26, 133.00, 128.69, 128.20, 38.49, 26.64, 22.64, 14.08.

1-(Naphthalen-2-yl)pentan-1-one

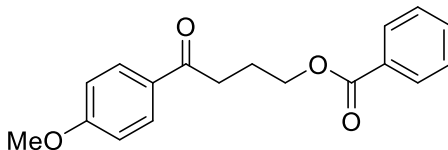


Following the general Fukuyama reaction procedure.

^1H NMR (400 MHz, chloroform-*d*) δ 8.48 (m, 1H), 8.04 (dd, $J = 8.6, 1.7$ Hz, 1H), 7.97 (m, 1H), 7.94 – 7.85 (m, 2H), 7.63 – 7.53 (m, 2H), 3.16 – 3.05 (m, 2H), 1.79 (p, $J = 7.5$ Hz, 2H), 1.50 – 1.42 (m, 2H), 0.99 (t, $J = 7.3$ Hz, 3H).

^{13}C NMR (126 MHz, chloroform-*d*) δ 200.60, 135.53, 134.46, 132.58, 129.62, 129.55, 128.41, 128.34, 127.78, 126.72, 124.00, 38.44, 26.68, 22.56, 14.00.

4-(4-Methoxyphenyl)-4-oxobutyl benzoate

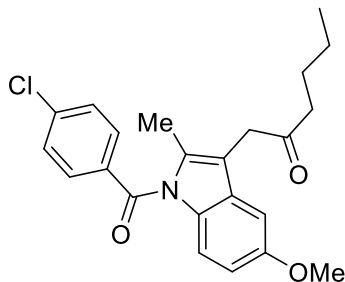


Following the general Fukuyama reaction procedure.

^1H NMR (400 MHz, chloroform-*d*) δ 8.03 (m, 2H), 7.99 – 7.92 (m, 2H), 7.59 – 7.52 (m, 1H), 7.43 (m, 2H), 6.96 – 6.89 (m, 2H), 4.43 (t, $J = 6.3$ Hz, 2H), 3.87 (s, 3H), 3.11 (t, $J = 7.2$ Hz, 2H), 2.24 (p, $J = 6.7$ Hz, 2H).

^{13}C NMR (126 MHz, chloroform-*d*) δ 197.79, 166.72, 163.65, 133.06, 130.44, 130.40, 130.07, 129.71, 128.50, 113.89, 64.55, 55.62, 34.74, 23.67.

1-(1-(4-Chlorobenzoyl)-5-methoxy-2-methyl-1H-indol-3-yl)hexan-2-one



Following the general Fukuyama reaction procedure.

^1H NMR (400 MHz, chloroform-*d*) δ 7.66 (d, $J = 8.5$ Hz, 2H), 7.47 (d, $J = 8.5$ Hz, 2H), 6.91 – 6.83 (m, 2H), 6.67 (dd, $J = 9.1, 2.4$ Hz, 1H), 3.82 (s, 3H), 3.69 (s, 2H), 2.47 (t, $J = 7.4$ Hz, 2H), 2.37 (s, 3H), 1.56 (m, 2H), 1.31 – 1.24 (m, 3H), 0.87 (t, $J = 7.3$ Hz, 3H).

^{13}C NMR (126 MHz, chloroform-*d*) δ 207.89, 168.30, 156.12, 139.31, 135.80, 133.90, 131.18, 130.90, 130.76, 129.16, 115.04, 112.92, 111.65, 101.22, 55.73, 41.38, 39.05, 25.90, 22.27, 13.85, 13.45.

